# Exploratory Analysis of the Impact of Ventilation on Strip Mall Fires

Craig Weinschenk
Robin Zevotek

UL Firefighter Safety Research Institute
Columbia, MD 20145

UNDERWRITERS
LABORATORIES™

# Exploratory Analysis of the Impact of Ventilation on Strip Mall Fires

Craig Weinschenk
Robin Zevotek

UL Firefighter Safety Research Institute
Columbia, MD 21045

April 17, 2020

UNDERWRITERS
LABORATORIES™



Underwriters Laboratories Inc.
*Terrence Brady, President*

UL Firefighter Safety Research Institute
*Steve Kerber, Director*

In no event shall UL be responsible to anyone for whatever use or non-use is made of the information contained in this Report and in no event shall UL, its employees, or its agents incur any obligation or liability for damages including, but not limited to, consequential damage arising out of or in connection with the use or inability to use the information contained in this Report. Information conveyed by this Report applies only to the specimens actually involved in these tests. UL has not established a factory Follow-Up Service Program to determine the conformance of subsequently produced material, nor has any provision been made to apply any registered mark of UL to such material. The issuance of this Report in no way implies Listing, Classification or Recognition by UL and does not authorize the use of UL Listing, Classification or Recognition Marks or other reference to UL on or in connection with the product or system.

# Acknowledgments

The authors would also like to acknowledge the fire service technical panel who volunteered their time in support of this series of experiments. The panel was established to review the test plan, analyze the results and develop the tactical considerations found in this report. Without the tireless effort from the individuals below, this work would not be nearly as impactful to the American fire service.

Fire Service Technical Panel

| Name | Department |
| --- | --- |
| Christopher Byrne | Colorado Springs Fire Department |
| Tony Carroll | District of Columbia Fire and EMS Department |
| Chad Christensen | Los Angeles County Fire Department |
| Shea Chwialkowski | Richfield Fire Department |
| Danny Doyle | Pittsburgh Fire Department |
| Brad French | Dayton Fire Department |
| Russell Gardner | Sacramento Metropolitan Fire Department |
| Scott Gray | Seattle Fire Department |
| David Guercio | Baltimore City Fire Department |
| Greg Hubbard | Orange County Fire Rescue |
| Curt Isakson | Escambia County Fire Rescue |
| Cody Johnson | Homer Volunteer Fire Department |
| Frank Leeb | Fire Department of New York |
| Dennis LeGear | Oakland Fire Department |
| Stephan Lopez | Dallas Fire-Rescue |
| Ray McCormack | Fire Department of New York |
| James Mendoza | San Jose Fire Department |
| Nicholas Papa | City of New Britain Fire Department |
| Joe Pronesti | Elyria Fire Department |
| Richard Riley | Kentland Volunteer Fire Department |
| Andrew Ruiz | Los Angeles Fire Department |
| Terrence Sheppard | Chicago Fire Department |
| Eric Staggs | City of Spokane Fire Department |
| Chris Stewart | Phoenix Fire Department |

# Contents

# List of Figures

# List of Tables

# List of Abbreviations

| | |
|---|---|
| AFG | Assistance to Firefighters Grant Program |
| BDP | Bi-directional probe |
| CFM | Cubic feet per minute |
| DHS | Department of Homeland Security |
| FEMA | Federal Emergency Management Agency |
| FPRF | Fire Protection Research Foundation |
| FDS | Fire Dynamics Simulator |
| FDNY | Fire Department of New York |
| HRR | Heat release rate |
| GPM | Gallons per minute |
| LODD | Line of duty death |
| NFPA | National Fire Protection Association |
| NIOSH | National Institute of Occupational Health |
| NIST | National Institute of Standards and Technology |
| NYU | New York University |
| OSB | Oriented strand board |
| PVC | Polyvinyl chloride |
| TYP | Typical |
| UL FSRI | UL Firefighter Safety Research Institute |

# Abstract

A majority of the existing full-scale research with the fire service was primarily designed to study and quantify the impact of tactics on the residential fireground. This project went beyond previous research by specifically conducting experiments in a commercial structure. Seven full-scale experiments were completed in four units of an twelve-unit acquired strip mall that was slated for demolition. These experiments were designed to analyze the impact of horizontal and vertical ventilation on ventilation-limited fires within the test units.

Beginning with a baseline case of no intentional fire service ventilation, three experiments focused on additional horizontal ventilation and three experiments focused on the combination of additional horizontal and vertical ventilation. The control variables included the ventilation method, total ventilation area provided, and timing relative to water application.

The volume of the strip mall units were larger than a typical residential compartment. A representative fuel load was chosen sufficient to generate ventilation-limited conditions within the unit for the duration of each respective experiment. As a result, providing ventilation (via horizontal or vertical methods) without suppression resulted in an increase in the heat release rate of the fire and a corresponding rise in temperature. When suppression was conducted simultaneously with horizontal and vertical ventilation, there were no measured increases in unit temperature or pressure during suppression. While some elements of these experiments (e.g. unit volume and wind) resulted in increased variability, the lessons learned highlighted the importance of having a systematic approach to the implementation of tactics. These results were consistent with concurrent research in single-family home fires.

# 1    Introduction

The purpose of this study is to improve fire service knowledge of fire dynamics and provide a better understanding of how suppression and ventilation coordinated on the fireground in an acquired commercial structure. This project expands on previous studies led by the UL Firefighter Safety Research Institute (FSRI) that examined the inherently coupled nature of fire service tactics and fire behavior in residential structures [1–4].

Strip malls are often single-story buildings separated into individual retail, office, or assembly occupancies. These are commonly Type-I or -II construction and may or may not incorporate a common attic space. To maximize construction efficiency, the units are narrow and deep with the access and egress limited to the front and rear. The retail nature of the businesses can lead to large quantities of flammable materials in large open spaces that allow for maximum flexibility to configure contents based on the individual use. In the event of a fire, this combination of large quantities of materials with limited access and egress presents a unique challenge to the fire service.

The National Institute of Occupational Health (NIOSH) investigates firefighter LODDs under the Fire Fighter Fatality Investigation Program. A search of the reports between 2001 and 2017 yielded four incidents each where a firefighter lost their life. The fatalities were attributed to roof collapse, fire progression, and the firefighter running out of air. Although each incident lists several contributing factors, all occurred in strip malls where interior firefighting was taking place. The recommendations all include the need to understand how the building construction impacts both fire dynamics and collapse hazards [5–9].

The National Institute of Standards and Technology (NIST) conducted two full-scale experiments in a warehouse in Phoenix, Arizona to better understand structural collapse [10]. The building was single-story, ordinary constriction with a peaked roof composed of rolled roofing material laid over 2 in. (51 mm) by 8 in. (200 mm) boards supported on wood trusses. The footprint of the warehouse was 135 ft (41 m) by 50 ft (15 m) and was divided in half by a purpose-built firewall to allow for two experiments within the space. The fuel load for the first experiment consisted of four stacks of ten wood pallets while the second experiment had three stacks of ten pallets. Each stack of pallets had a mass of approximately 360 lb (163 kg). In both experiments, the roof collapsed in under 25 min after ignition [10]. Researchers at NIST along with Harvey Mudd College also conducted experiments in three shopping mall units [11]. The roof system consisted of a metal deck supported by lightweight open-web steel trusses. The primary fuel in these experiments was wood pallets and ventilation was provided by the front door left open. In each of the experiments, the roof was loaded with 55 gal water barrels. In the two experiments where the roof did not collapse, there were four barrels. In the third experiment, with a twelve barrel load, the roof collapsed in 7 min [11].

Recent research conducted by UL FSRI was designed to evaluate the effectiveness of various firefighting tactics in residential structures. Research on the impact of horizontal ventilation, vertical ventilation, and positive pressure ventilation (PPV) all found that residential fires are limited by

the amount of oxygen, providing ventilation increased fire size. Studies focusing on fire attack, attic fires, and basement fires found that applying water decreased fire sizes and did not adversely impact firefighter or occupant safety [1–4, 12, 13]. Additional research by NIST into the use of PPV in high-rise fires and educational occupancies found PPV could be used to effectively control the spread of smoke and heat in those occupancy types [14, 15].

With a relative lack of research in buildings larger than single family residences, specifically strip malls, firefighting trade literature has primarily been based on the experience of those who wrote the given article. The available literature often compares the hazards in these larger buildings to common residential occupancies. The primary difference cited is the increase in fuel load, corresponding to a larger fire size. The articles also state that the larger fire sizes necessitate the delivery of higher flow rates for suppression. Additionally, access and egress problems, collapse hazards, a potentially higher occupant load, and multiple exposures all make fires in strip malls more challenging [16–19].

## 1.1 Objectives

Limited research has been conducted on fires in strip mall occupancies, resulting in a knowledge gap the fire service attempts to fill with experience. The fire service's existing experience is predominantly in residential type occupancies, which results in the use of residential style tactics on non-residential style buildings. With the increased fuel loading, open space, and access challenges, these tactics may not be as effective. Therefore, this project was designed to achieve the following goals:

- Expand the body of knowledge relating to fire dynamics in larger compartment fires.

- Evaluate the impact of horizontal ventilation in strip malls.

- Evaluate the impact of vertical ventilation in strip malls.

The main objective of this project was to characterize the impact of fire service ventilation on strip mall fires. The choice of ventilation and suppression operations for each experiment were determined with assistance from the fire service technical panel. Suppression was performed by the members of the Fairborn, Ohio Fire Department and their mutual aid organizations under the direction of research staff.

The safety of the personnel conducting suppression operations was paramount. In instances where fire exposure to the unprotected metal roof structure was anticipated, suppression was designed to occur from the exterior. The data acquired during experiments provided the research staff with real-time conditions on the interior, and cameras provided views of interior and exterior conditions. Two safety officers, one from the research team and one from the fire department, provided oversight during the experiments to ensure all aspects of the safety plan were implemented.

# 2   Experimental Setup

The use of an acquired structure for these experiments added variables such as unit layout, unit access, ventilation area, and weather; variables that are also part of actual fire responses. The following sections describe the units used within the strip mall, the instrumentation used to quantify the fire dynamics, and the primary and ignition fuel packages.

## 2.1   Experimental Structure

The Skyway Shopping Plaza located at 1067-1090 Kauffman Ave in Fairborn, Ohio, which was scheduled for demolition, was acquired for use in this project by the Fairborn Fire Department. An aerial view is presented in Figure 2.1. The shopping plaza contained a 12 unit strip mall constructed in 1970. The building was a Type II-B construction with unprotected, non-combustible, structural elements. The load bearing walls were masonry block (see Figure 2.2a), with a corrugated metal built-up roof, supported by open web steel bar joists (see Figure 2.2b). The built-up roof was comprised of a layer of approximately 2 in. (5 cm) rigid foam insulation secured to the metal deck with screws. The rigid foam insulation was covered with a layer of rubber, sealed at the seams with tar. The units had gypsum-encased steel support columns at the midpoint of the depth that supported a steel beam. The roof structure was separated into two sections of open web steel bar joists, one in the front and one in the rear. Images of the front, sides, and rear of the structure are presented in Figure 2.3.

Figure 2.1: Aerial image of the Skyway Plaza shopping center [20]. Side A of each store front faces the parking lot in the lower portion of the image.

(a) Masonry Block Wall                    (b) Roof Structure
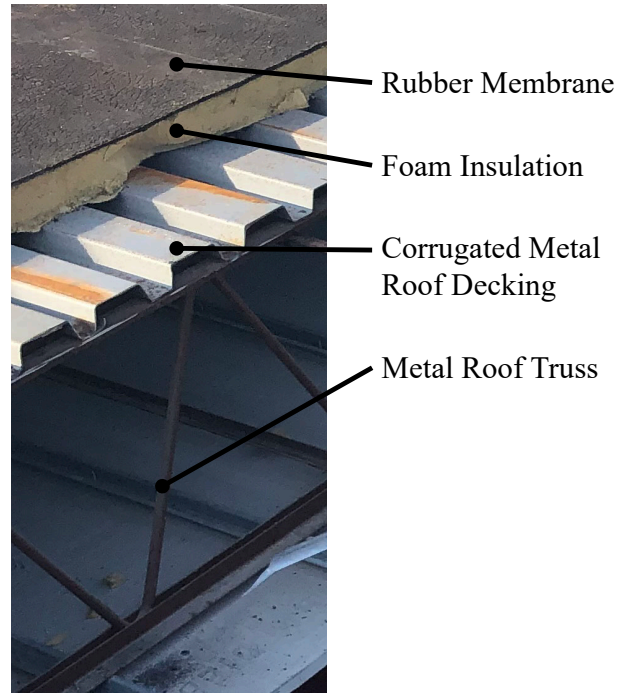
Figure 2.2: Images of the construction features found in the strip mall.

The strip mall contained a grocery store (unit 1090) and several smaller mercantile and office type occupancies (units 1067–1088). Units 1082–1090 were not utilized for this project. Unit 1090 had significant deterioration to the roof, and units 1082–1088 contained asbestos floor tiles.

(a) Side A (Front)


(b) Side B


(c) Side C (Access Road)


(d) Side C (Example of Typical Rear of Units)


(e) Side D

Figure 2.3: Images of the exterior of the Skyway Plaza shopping center in Fairborn, Ohio, utilized for these experiments.

The remainder of the units were instrumented for use as either fire units or exposure units. Sepa-

rations between units were a mix of masonry fire walls and rated partitions. The rated partitions were constructed of metal studs lined on both sides with two layers of 5/8 in. gypsum wall board. The fronts of the units were brick with large plate-glass window panes set in aluminum frames and a main entry door. The rear of the units were masonry block with a steel exit door in a steel frame. The width of the units used varied from 20 ft (12.2 m) to 30 ft (9.1 m) wide, and the depth varied between 70 ft (21.3 m) and 80 ft (24.4 m) deep. The site plan for the strip mall with individual unit square footages and use appear in Figure 2.4.
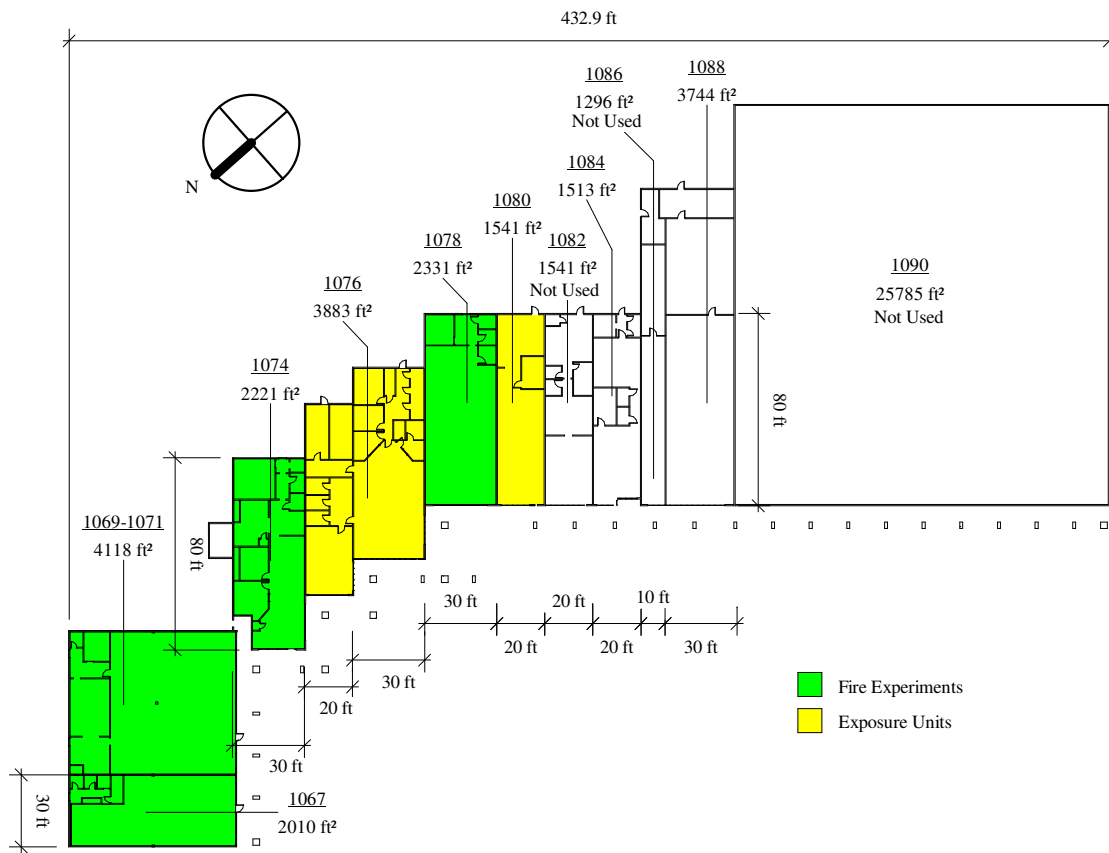


Figure 2.4: Site plan of the Skyway Plaza Shopping Center, including designations of the units used.

## 2.1.1 Unit 1078 - Experiments 1 and 2

Unit 1078 was utilized as the fire unit for Experiments 1 and 2. The unit was 80.0 ft (24.4 m) deep by 30.0 ft (9.3 m) wide. A detailed dimensioned drawing of the unit is presented in Figure 2.5. The roof deck was 14.0 ft (4.3 m) above the finished floor level. Acoustical ceiling tiles in an aluminum lattice frame (typical drop ceiling) were installed in each room at the elevations noted in Figure 2.5. The load bearing walls on side A and side C were concrete block with wood furring strips covered with two layers of 3/8 in. gypsum wall board. The non load bearing separation walls on side B and side D were concrete block with wood furring strips covered with two layers of 3/8 in. gypsum

wall board. The interior walls were constructed using 2x4 wood studs, with two layers of 3/8 in. gypsum wall board. The floor was a mixture of tile and carpet. Images from the interior of the unit are presented in Figure 2.6.



Figure 2.5: Floor plan of unit 1078 utilized for Experiments 1 and 2.

The unit was furnished with 90 group A commodity boxes stacked three high in rows of five stacks each, with a separation of 6 in. (15.2 cm) between stacks. The rows were configured to represent the aisles inside a retail-type occupancy with 4 ft (1.2 m) aisles between rows. The first three rows started 25 ft (7.6 m) back from the front wall. The rear three rows were separated from the front rows by a 4 ft (1.2 m) cross aisle. The configuration of the fuel package is illustrated in Figure 2.5, and images are presented in Figure 2.6.

9

Figure 2.6: Images from the interior of unit 1078 looking toward side C from front entry (left), and looking toward side C from the door to rear spaces (right)

The unit had two exterior access doors, one in the front and one in the rear. The front door was an aluminum frame with a single glass panel, and the rear door was a steel door in steel frame. The rear door was secured shut during both experiments via a 2x4 stud held in place by 2x4 wood stud brackets. The front door was closed for Experiment 1 and open for the duration of Experiment 2.

The front wall had a series of double-pane glass windows and aluminum panels, both in aluminum frames. Figure 2.7 illustrates the configuration and dimensions of the glass and aluminum panels and presents an image of the front elevation.
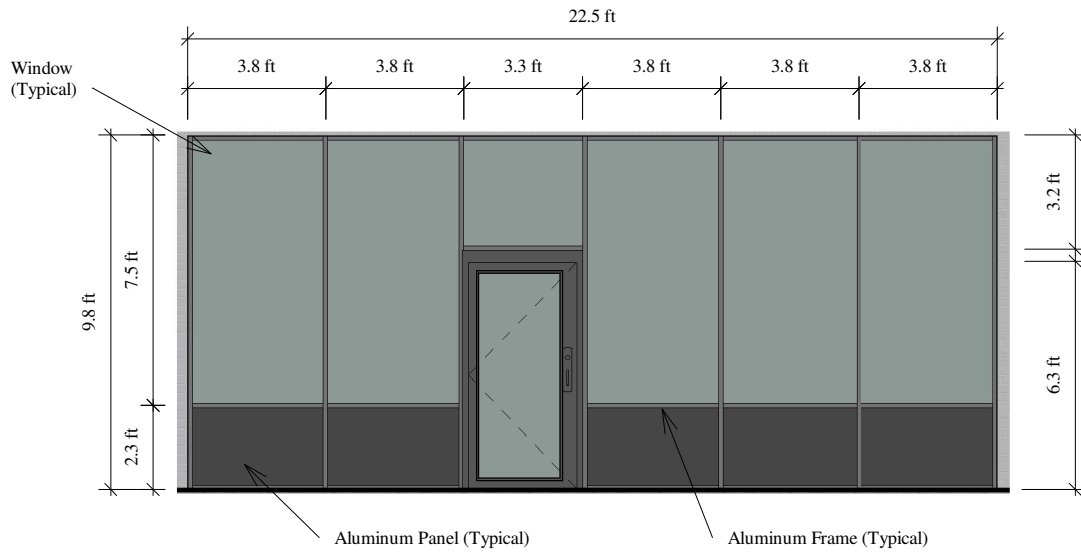
(a) Front Glass Illustration



(b) Front Elevation Photo

Figure 2.7: Image and dimensioned illustration of the front window wall in unit 1078.

Units 1076 and 1078 were utilized as the side B and side D exposure occupancies for Experiments 1 and 2. They were both separated from Unit 1078 with a masonry block fire wall that protruded up through the roof. The fire walls were covered on the fire unit side with furring strips and two layers of 3/8 in. gypsum wall board. On the exposure unit side they were covered with one layer of 3/8 in. gypsum wall board. No penetrations existed through the fire walls. Figure 2.8 illustrates the orientation of the exposures, the basic interior layouts, the dimensions of each occupancy and a schedule of the entry/doors.

| Door Schedule | | | | |
|---|---|---|---|---|
| Label | Door Material | Frame Material | Position Exp 1 | Position Exp 2 |
| 1 | Glass/Aluminum | Aluminum | Closed | Closed |
| 2 | Glass/Aluminum | Aluminum | Open | Open |
| 3 | Glass/Aluminum | Aluminum | Closed | Open |
| 4 | Glass/Aluminum | Aluminum | Open | Open |
| 5 | Steel | Steel | Closed | Closed |
| 6 | Steel | Steel | Closed | Closed |
| 7 | Steel | Steel | Closed | Closed |
| 8 | Steel | Steel | Closed | Closed |

All doors were 6.3 ft by 3 ft

KEY PLAN

1074 1076 1078 1080 1082 1084 1086-1088 1090

1069 -1071

1067

1078
2331 ft²

1080
1541 ft²

1076
3883 ft²
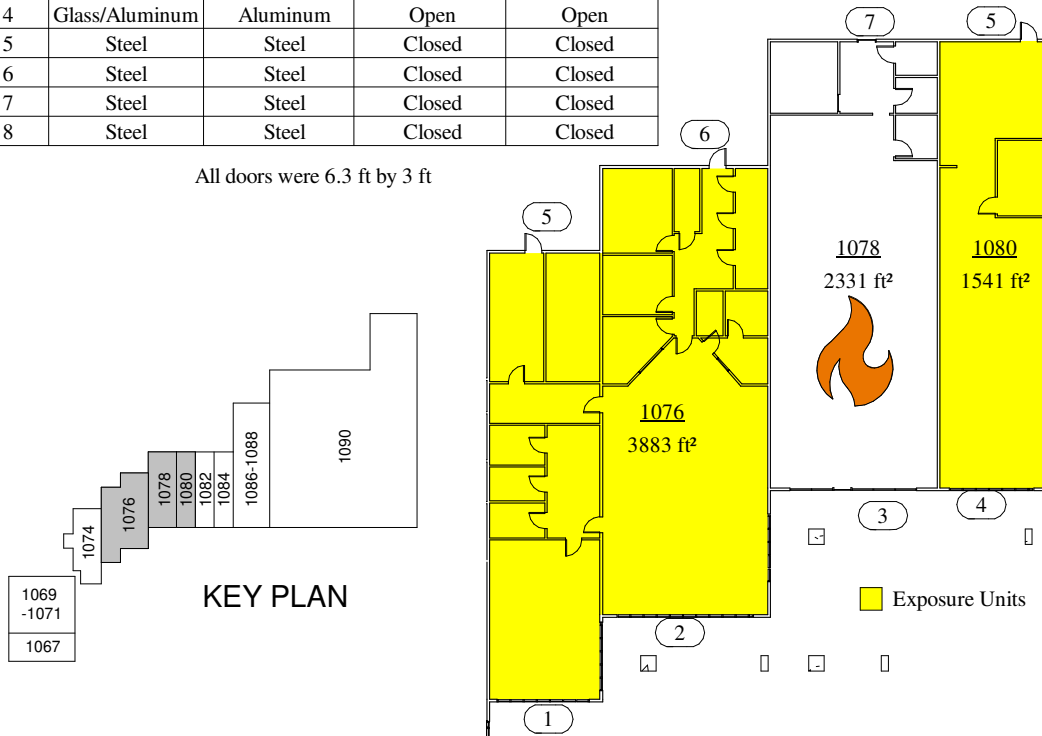
Exposure Units

Figure 2.8: Floor plan of units 1076, 1078, and 1080.

The exposure units had front glass windows and doors with rear exit doors similar to the fire unit. Unit 1076 was a double unit with two front access doors and four large window sections. These units were utilized as an exposure volume during Experiment 1 and 2. The exposure volume is defined as the volume of the unit(s) that has a common wall with the fire unit. None of the windows in the exposure units were utilized as ventilation. Figure 2.9 presents images of the front entrance of both units.

(a) Unit 1076 Entrance 1       (b) Unit 1076 Entrance 2       (c) Unit 1080 Entrance

Figure 2.9: Images of the front entrances to units 1076 and 1080.

## 2.1.2  Unit 1074 - Experiment 3

Unit 1074 was utilized as the fire unit for Experiment 3. The unit was 80.0 ft (24.4 m) deep by 30.0 ft (9.3 m) wide. A floor plan of the unit along with the ceiling heights, floor coverings, and the sizes of the doors appears in Figure 2.10. The roof deck was 14.0 ft (4.3 m) above the finished floor level. Acoustical ceiling tiles in an aluminum lattice frame (typical drop ceiling) were installed in each room at the elevations noted in Figure 2.10. The side A, side B, and side C exterior walls were concrete block with wood furring strips covered with two layers of 3/8 in. gypsum wall board. The separation between Unit 1074 and Unit 1076 on side D was a metal stud wall with two layers of 1/2 in. gypsum wall board on each side. The interior walls were constructed using 2x4 wood studs, with two layers of 3/8 in. gypsum wall board. The floor was a mixture of tile and carpet. The windows and door on the delta side were covered on the interior with 1/2 in. gypsum wall board. Images from the interior of the unit are presented in Figure 2.11.

Figure 2.10: Floor plan of unit 1074 utilized for Experiment 3.

The unit was furnished with 90 group A commodity boxes stacked three high in rows of five stacks each, with a separation of 6 in. (15.2 cm) between stacks. The rows were configured to represent the aisles of a retail type occupancy with 4 ft (1.2 m) aisles between rows. The first three rows started 25 ft (7.6 m) back from the front wall. The rear three rows were separated from the front rows by a 4 ft (1.2 m) cross aisle. The configuration of the fuel package is illustrated in Figure 2.10 and images are presented in Figure 2.11.

Figure 2.11: Interior images from unit 1074, looking toward side C from front entry (left), and toward side C from the door to rear spaces (right).

The unit had two exterior access doors, one in the front and one in the rear. The front door was in the set of windows on side D, which did not match the configuration of other units. To allow for direct comparison to other experiments, the door on side D was covered with wood framing and 3/8 in. gypsum wall board for the experiment, and a section of the side A windows was removed and replaced with a 2x4 framed wood opening. The areas outside the door opening were covered with 7/16 in. oriented strand board (OSB). The rear door was a steel door in steel frame. The rear door was secured shut during the experiment via a 2x4 stud held in place by 2x4 wood stud brackets. The front opening remained uncovered for the duration of the experiment.

The front wall had a series of double pane glass windows and aluminum panels, both in aluminum frames. Figure 2.12 illustrates the configuration and dimensions of the glass and aluminum panels as well as presents an image of the front elevation.
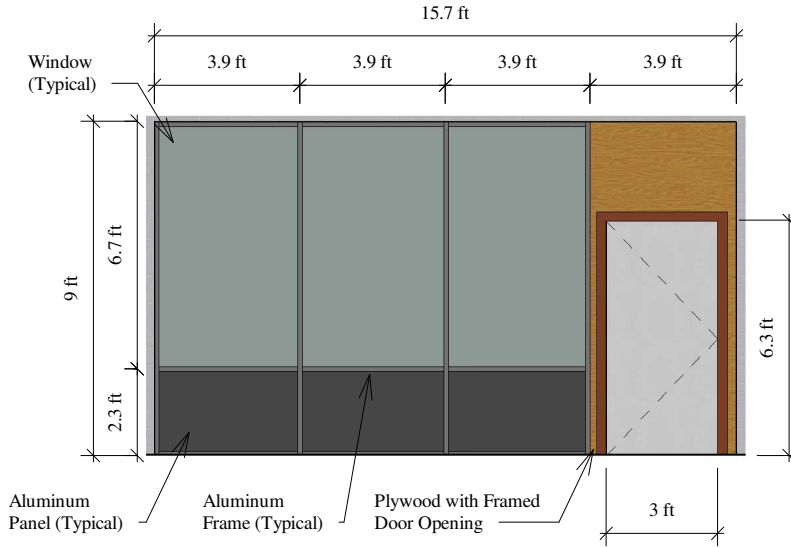
(a) Front Glass Illustration



(b) Front Elevation Photo

Figure 2.12: Image and dimensioned illustration of front window wall in unit 1074.

To limit fire spread from the roof of Unit 1074 to the roof of the side D exposure (Unit 1076) a section of the rubber membrane and foam insulation was removed from the roof of Unit 1076. The approximately 4 ft (1.2 m) wide section that was removed was located on the Unit 1076 side of the fire separation and continued the depth of the unit.

### 2.1.3   Unit 1069–1071 - Experiment 4

Unit 1069–1071 was utilized as the fire unit for Experiment 4. The unit was 70.0 ft (21.3 m) deep by 60.0 ft (18.3 m) wide. A floor plan of the unit, along with the ceiling heights, floor coverings, and the sizes and types of doors, appears in Figure 2.13. The roof deck was 15.0 ft (4.6 m) above the finished floor level. Acoustical ceiling tiles in an aluminum lattice frame (typical drop ceiling) were installed in each room at the elevations noted in Figure 2.13. The side A, side C, and side D exterior walls were concrete block with wood furring strips covered with two layers of 3/8 in. gypsum wall board. The separation between unit 1069–1071 and unit 1067, the side B exposure, was a metal stud wall with two layers of 5/8 in. gypsum wall board on each side. The interior walls were constructed using 2x4 wood studs, with two layers of 3/8 in. gypsum wall board. The floor was a mixture of tile, concrete, and carpet. The windows and door in the AD corner were covered on the exterior with 1/2 in. gypsum wall board. Images from the interior of the unit are presented in Figure 2.14.
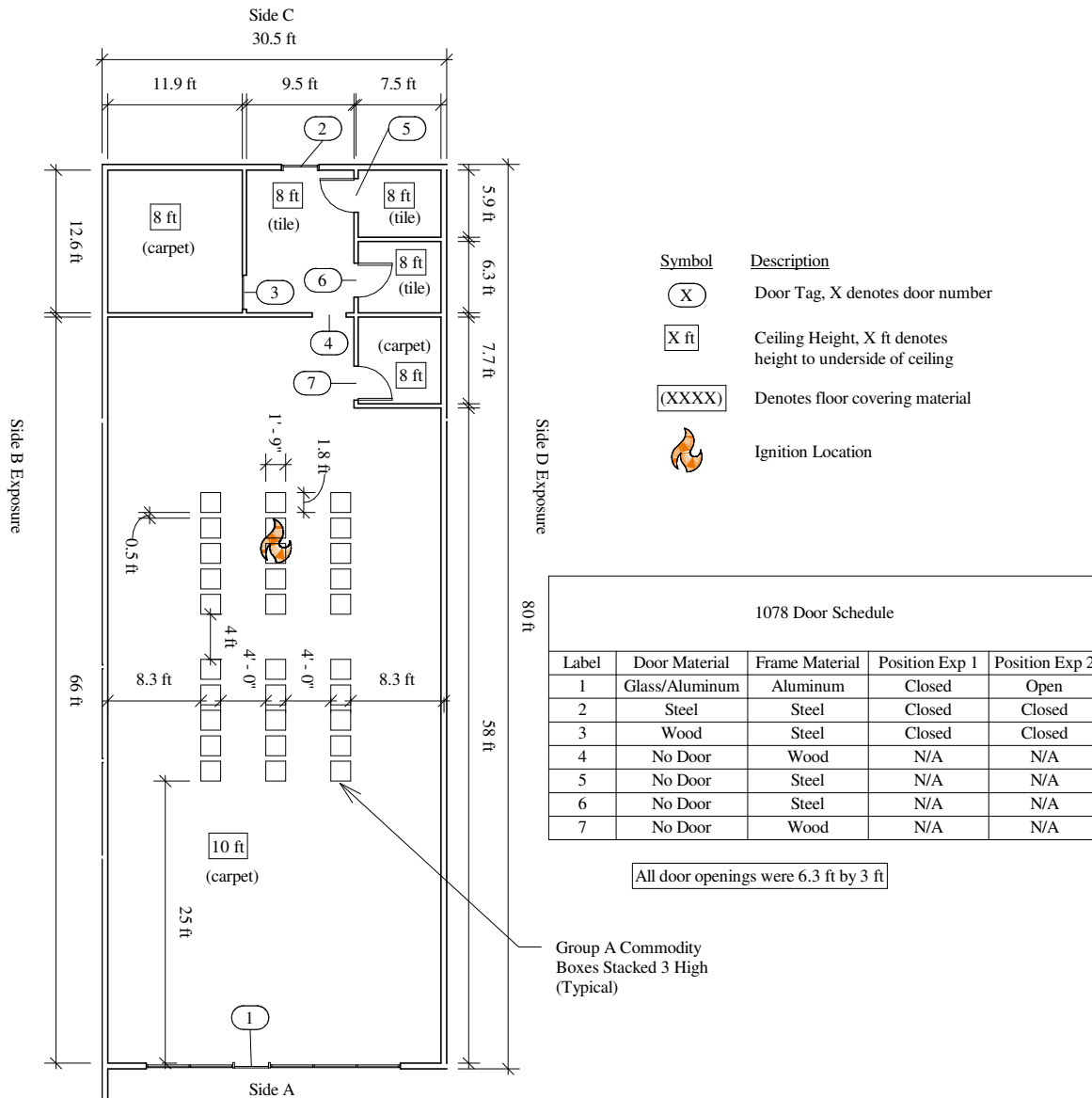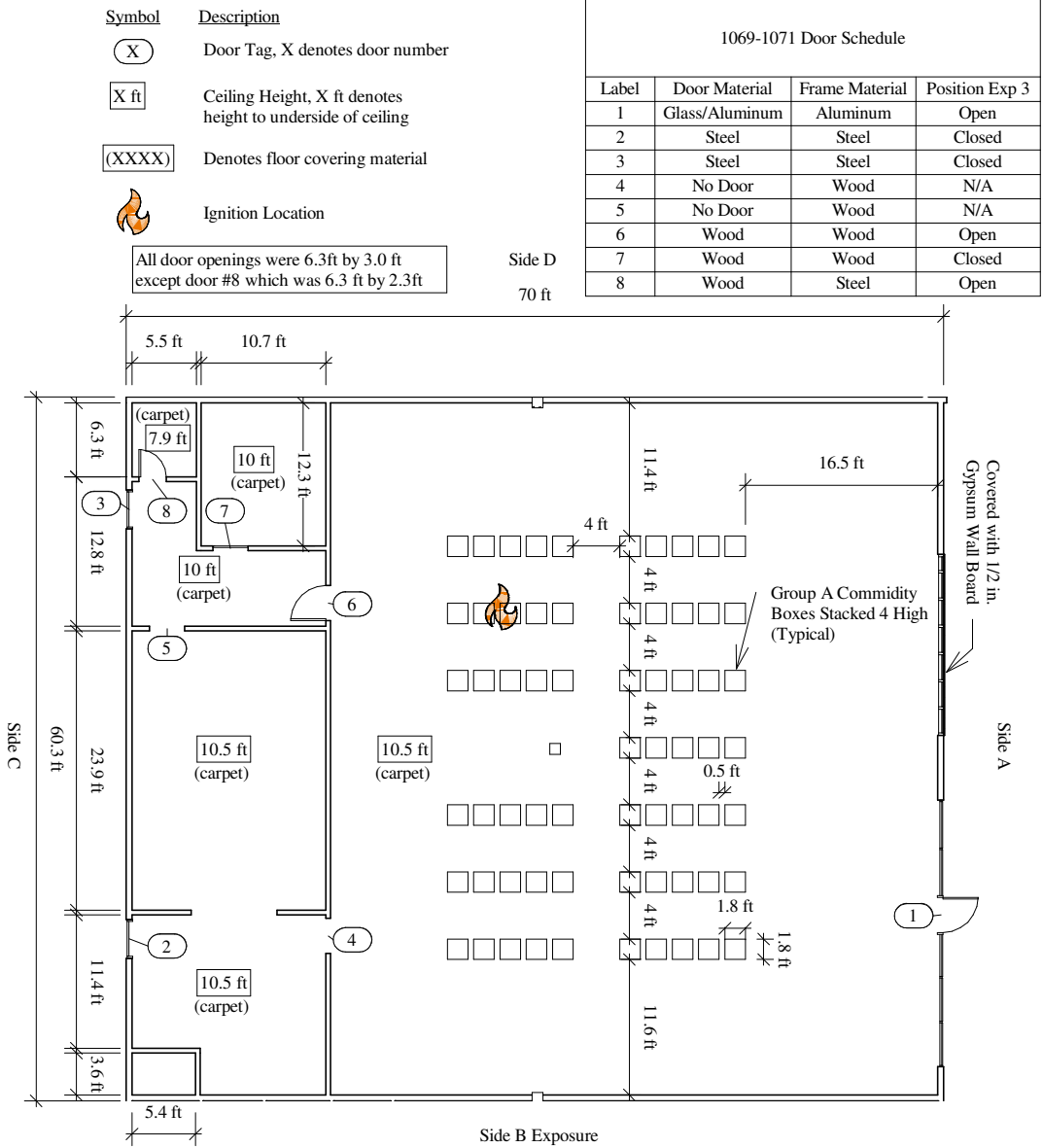
Figure 2.13: Floor plan of unit 1069–1071 utilized for Experiment 4.

The unit was furnished with 260 group A commodity boxes stacked four high in rows of five stacks each, with a separation of 6 in. (15.2 cm) between stacks. The rows were configured to represent the aisles inside a retail type occupancy, with 4 ft (1.2 m) aisles between rows. The front rows started 16 ft 6 in. (5.0 m) off the front wall. The front rows were separated from the rear rows by a 4 ft (1.2 m) cross aisle. The configuration of the fuel package is illustrated in Figure 2.13 and presented in Figure 2.14.

Figure 2.14: Images of the interior of unit 1069–1071. Looking toward the AB corner from the front entry door (left), and looking toward the CD corner from the front entry door (right).

The unit had four exterior access doors, two in the front and two in the rear. The front door in the AB corner was utilized as the main entrance for the experiment. The front door in the AD corner was covered from the exterior with 1/2 in. gypsum wall board. The two rear doors were steel in steel frames. The rear doors were secured shut via their door latches during the experiment.

The front wall had two sets of double-pane glass windows and aluminum panels, both in aluminum frames. The set in the AD corner was covered with 1/2 in. gypsum wall board from the exterior. The set in the AB corner remained uncovered. Figure 2.15 illustrates the configuration and dimensions of the glass and aluminum panels in the AD corner and presents an image of the front elevation.
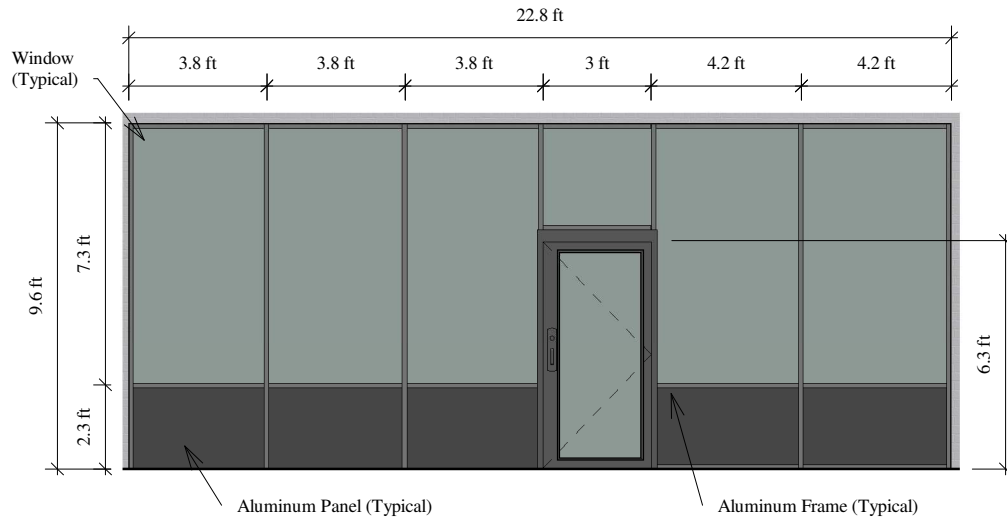
(a) Front Glass Illustration



(b) Front Elevation Photo

Figure 2.15: Image and dimensioned illustration for the front window wall of unit 1069–1071.

To limit fire spread to the side B exposure roof, the rubber membrane and foam insulation were removed over Unit 1067 and approximately 15 ft (4.6 m) of Unit 1069–1071 along the side B exposure. The area removed ran from the front parapet wall to the rear of the unit.

## 2.1.4  Unit 1067 - Experiments 5, 6, and 7

Unit 1067 was utilized as the fire unit for Experiments 5, 6, and 7. The unit was 70.0 ft (21.3 m) deep by 30.0 ft (9.1 m) wide. A floor plan of the unit, along with the ceiling heights, floor coverings, and the sizes and types of doors, appears in Figure 2.16. The roof deck was 15.0 ft (4.6 m) above the finished floor level. A layer of 1/4 in. cement board and a layer of 5/8 in. gypsum wall board were installed on the underside of the metal roof trusses in the large volume of the unit to harden it for multiple fire experiments. The rear rooms of the unit were isolated from the experimental volume by 5/8 in. gypsum wall board on 2x4 wood studs that ran to bottom side of the roof deck. This area is shaded gray in Figure 2.16. The side A, side B, and side C exterior walls were concrete block with wood furring strips covered with two layers of 3/8 in. gypsum wall board. The separation between unit 1067 and unit 1069–1071 on the side D was a metal stud wall with two layers of 1/2 in. gypsum wall board on each side. The interior walls were constructed using 2x4 wood studs, with two layers of 3/8 in. gypsum wall board on the side facing the large volume of the unit and one layer on all others. The floor was covered by carpet. Images from the interior of the unit are presented in Figure 2.17.
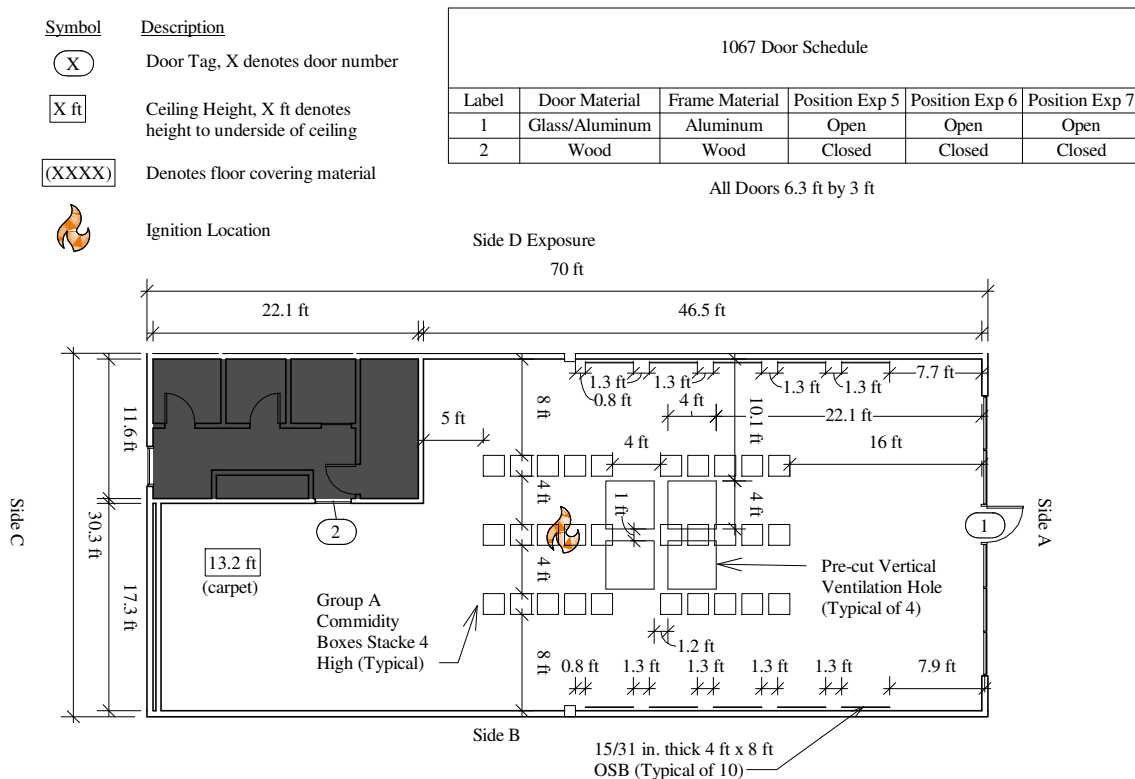


Figure 2.16: Floor plan of unit 1067 utilized for Experiments 5, 6, and 7. The dark gray shaded area was isolated from the experimental volume for these experiments.

The unit was furnished with 120 group A commodity boxes stacked four high, in rows of five stacks each, with a separation of 6 in. (15.2 cm) between stacks. The rows were configured to represent the aisles in side a retail-type occupancy with 4 ft (1.2 m) aisles between rows. The front three

rows started 16 ft (14.9 m) off the front wall. The rear three rows were separated from the front rows by a 4 ft (1.2 m) cross aisle. Ten sheets of 15/32 in. oriented strand board (OSB) were added for additional fuel. Five sheets each were secured to the side B and side D walls. The configuration of the fuel package is illustrated in Figure 2.16 and presented in Figure 2.17.



Figure 2.17: Interior images of unit 1067, looking toward side C from the front entry door (left), and toward side C from two-thirds of the way into the space (right).

The unit had two exterior access doors, one in the front and one in the rear. The front door was an aluminum/glass door in an aluminum frame. The rear door was a steel door in steel frame. The rear door was secured shut via its door latch during all three experiments.

The front wall had a series of double-pane glass windows and aluminum panels, both in aluminum frames. Figure 2.18 illustrates the configuration of the panels and presents an image of the front elevation.
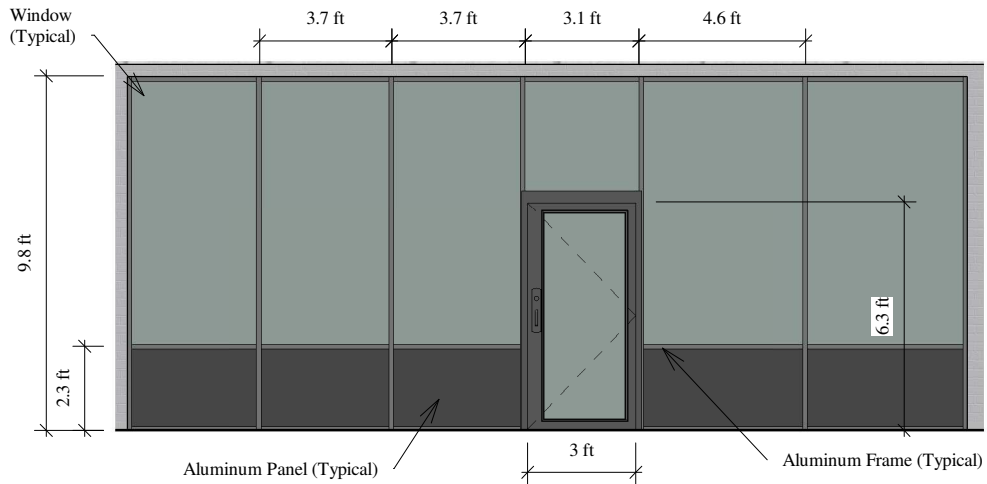
(a) Front Glass Illustration



(b) Front Elevation Photo

Figure 2.18: Image and dimensioned illustration for the front window wall of unit 1067.

Four vertical 4 ft by 4 ft (1.2 m by 1.2 m) roof vent holes were cut in the roof prior to any fire experiments. A vertical chimney was constructed for each hole that ran from the underside of the gypsum wall board ceiling up through the metal roof trusses, through the roof, and extended beyond the roof. The total height of each chimney was 4 ft 7 in. (1.4 m) from the underside of the ceiling to the top. The chimneys were lined with two layers of 1/2 in. cement board. The roof vents were capped with wood framed louvered caps, covered with 1/2 in. concrete board. To open the vents remotely from the ground, a pulley system was installed with metal cables running over the side B and side D walls. Figure 2.19 presents the roof vent holes from the underside and above.

(a) Underside of Roof Vents          (b) Top Side of Roof Vents

Figure 2.19: Images of the precut roof vents in unit 1067.

The roof of Unit 1067 was stripped of the foam insulation and rubber membrane, as shown in Figure 2.19b. The fuel was removed from the roof to limit the potential of flame spread to the roof because this unit was used for three experiments.

## 2.2 Instrumentation

The strip mall units in these experiments were instrumented to measure gas temperature, differential pressure, and gas velocity, while hoselines were instrumented to measure suppression flow rates. Instruments utilized during the experiments included thermocouples, pressure transducers, bi-directional probes, and water flow meters.

Gas temperatures were measured with 0.05 in. bare-bead, chromel-alumel (type K) thermocouples and 0.0625 in. inconel-sheathed thermocouples. Small-diameter thermocouples were used during these experiments to limit the impact of radiative heating and cooling. The total expanded uncertainty associated with the temperature measurements from these experiments is estimated to be ± 15% as reported by researchers at NIST [21, 22]. Thermocouples were installed throughout the units in specific spatial locations that can be found on the floor plans for each of the experiments discussed in Section 3. In each spatial location, thermocouples were installed as a vertical array. Unless otherwise noted, the array consisted of seven thermocouples with the top thermocouple in each array located 1 in. below the roof deck with the remaining seven thermocouples spaced at 2 ft intervals.

Pressure measurements were made using differential pressure sensors to determine changes relative to ambient pressure (outside the structure). Three, 1/4 in. copper pressure taps were installed 1 ft off the wall (at locations described in each structure instrumentation plan) and connected to one side of the differential transducer. The other side was exposed to ambient conditions. At each location, pressure was measured 1 ft, 7 ft, and 13 ft above the floor. The differential pressure

sensors had an operating range of ± 125 Pa. The total expanded uncertainty associated with pressure measurements obtained from the transducers is estimated as ± 10% [14].

Sheathed thermocouples were paired with pressure transducers connected to bi-directional probes to measure gas velocity. Sheathed thermocouples allowed the instrumentation to be placed in areas where suppression streams might impact the thermocouples in order to minimize the affect the water had on the measurement. The pressure measurements, as part of the velocity sensor package, were made using differential pressure sensors connected to each side of the bi-directional probe. A gas velocity measurement study examining flow through doorways in pre-flashover compartment fires yielded expanded uncertainties ranging from ± 14% to ± 22% for measurements from bi-directional probes similar to those used during this series of tests [23].

Hoseline water flow measurements were obtained from electromagnetic flow meters. A flow meter was installed downstream of the engine but upstream of the nozzle, at a coupling, to monitor the flow of water through the hoseline. A 2.5 in. flow meter was attached to the primary hoseline while a 1.5 in. flow meter was attached to the secondary hoseline, if one was used. Flow meters were used to verify flow rates as well as measure total volume. The standard uncertainty associated with water flow rate measurements is ± 11% [24].

Wind speed was measured with a balanced propeller driving a serrated disk, which generates pulses in an optical switch. Direction was measured with an optical resolver connected to a wind vane. Both sensors were contained in a single unit. The wind speed sensor has a manufacturer's stated range of 0 mph to 120 mph (0 m/s to 60 m/s) and an accuracy of ±1.0%. The direction sensor has a manufactured stated range of 360° with a resolution of 1.0°, and accuracy of ±1.0% [25].

All numerical data was recorded with a purpose-built data acquisition system with specifically programmed software. Raw voltage values were translated to quantities of interest through post-processing software specifically programmed for use with the system. Data were sampled at 1 Hz across all channels. Video cameras were installed inside the units to capture information about the fire dynamics of the experiments. Video cameras and firefighting IR cameras were also positioned outside of the units to monitor the flow of smoke, flames, and air at the exterior vents. To ensure video capture even if the cameras experienced thermal failure, the cameras were hardwired to a digital video recorder outside the structure.

## 2.3   Fuel Package

The fuel package for this project was selected to be representative of a fuel load potentially found in a strip mall, mercantile-type occupancy. Cartoned, non-expanded, Group A plastic commodity classification boxes designed for rack storage testing of automatic fire sprinklers were used as a representative high potential-energy fuel.

The commodity classification boxes were corrugated cardboard boxes measuring 21 in. by 21 in. by 20.5 in. (53 cm by 53 cm by 52 cm), filled with empty non-expanded polystyrene 16 oz (0.5 L)

cups. The cups are packaged upside down in a grid fashion with 25 cups per layer, separated by a single layer of corrugated cardboard between cups and between layers. Each box had five layers of cups, for a total of 125 per cups per box (Figure 2.20). The commodity boxes were purchased pre-packaged from a third-party vendor.



Figure 2.20: Image of the internal configuration of the plastics cups and cardboard in side a Group A plastic commodity box. The exterior cardboard has been cut away to reveal the internal structure.

The ignition package for the fuel was a 3 gal (11.4 L) plastic trash can filled with twenty-seven 9 oz (266.2 mL) wax paper cups and newspaper. The package was ignited by a match book with a nichrome wire running through the match heads connected to a 24V power supply (i.e., an electric match). A 1.0 in. (2.5 cm) hole was drilled in the bottom of the trashcan to pass the wire for the electric match into the can. The ignition package was placed adjacent to a row of commodity boxes as presented in Figure 2.21.

Figure 2.21: Image of the ignition source utilized in these experiments. The source consisted of wax paper cups and newspaper in a plastic trash can.

An analysis of the quantity of the fuel was conducted to assess the fuel load relative to whether post-flashover conditions could be achieved for the given ventilation conditions. Research conducted for the development of the "ALIVE" training tool examined the energy released from burning Group A plastic commodity boxes [26]. Consider Figure 2.22, which presents the rate of energy release, or heat release rate (HRR), versus time for a stack of three Group A plastic commodity boxes and two stacks of three Group A plastic commodity boxes spaced 6 in. (15 cm) apart. In the "ALIVE" experiments, the boxes were ignited using a smaller ignition source than the one described above which is approximately 40 kW to 50 kW, therefore the initial growth rates presented in Figure 2.22 can be considered conservative.
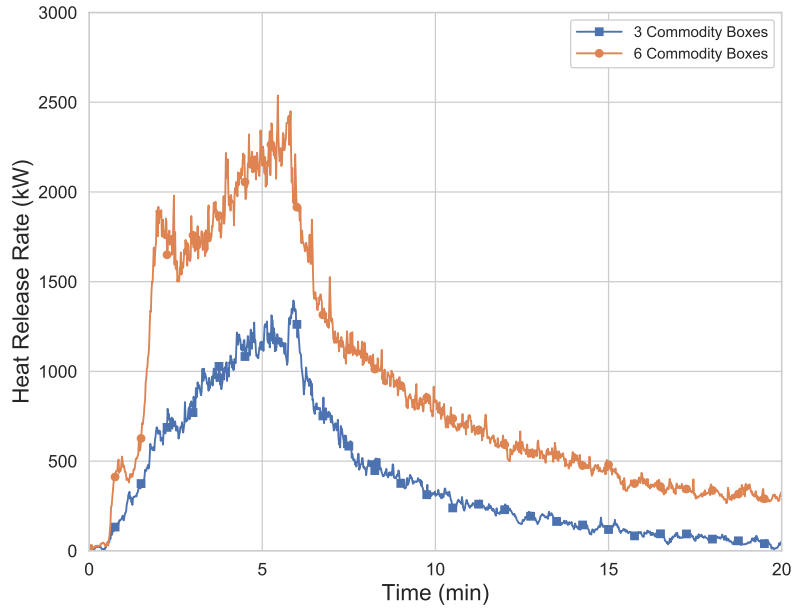
Figure 2.22: The growth rate of two commodity box configurations: a stack of 3 boxes and a two stacks of 3 boxes spaced 6 in. (15 cm) apart [26].

It is important to note the differences in HRR between the 3 commodity box arrangement and the 6 commodity box arrangement. Instead of following the same curve as the 3 box arrangement for a longer period of time, the peak HRR of the 6 box arrangement has a steeper initial growth ramp and peaks about 55% higher because the ignition occurred between the stacks. The ability of air and the associated oxygen to mix with the fuel gas combined with additional heat transfer between the elements of the fuel package due to the gap enabled the increase in HRR. Essentially, for the case of the two columns of stacked boxes, more of the energy from the fire is transferred back more efficiently, which results in more of the fuel burning at one time and a higher HRR.

The HRR necessary to transition the compartment to flashover can be estimated based on horizontal ventilation openings, a simplified but widely used analysis developed by Babrauskas is applied [27]:

$$\dot{Q} = 750A\sqrt{h} \tag{2.1}$$

where $\dot{Q}$ is the HRR in kW, $A$ is the area of the opening in m$^2$, and $h$ is the height of the opening in m. There are several conditions in these experiments which may impact these estimates such as the discrete vent openings (doors and windows), different sill heights between door and windows, and the large compartment volume of the strip mall unit. Despite these factors, the values presented in Table 2.1 were used as an initial guide to determine the total fuel load.

28

Table 2.1: Ventilation Areas in the Acquired Strip Mall Used to Estimate the Heat Release Rate (HRR) Necessary to Transition the Compartment to Flashover

| Ventilation | Area [m$^2$] | Height [m] | HRR [kW] |
|---|---|---|---|
| Door | 1.8 | 1.93 | 1900 |
| Window | 2.7 | 2.3 | 3000 |
| Door + Window | | | 4900 |
| Door + 3 Windows | | | 10900 |
| Door + 5 Windows | | | 16900 |

Based on the estimates from Table 2.1 and the experimental data from Figure 2.22, the fuel load range of between 90 total boxes to 260 total boxes for this experimental series was sufficient to develop ventilation-limited conditions, and to support flashover based on the ventilation provided.

To provide additional context on how the fuel package used these experiments compares to commonly used ignition sources (e.g., cigarette, candle, coffeemaker, small trash can) and residential fuels (e.g., upholstered chair and sofa) see Table 2.2. In these experiments, the primary fuel package consisted of commodity boxes stacked between 3 and 4 boxes high, with between 90-260 boxes in total. Two stacks of boxes aligns with common residential upholstered furniture with respect to peak HRR.

Table 2.2: Heat Release Rates (HRR) of Common Ignition Fuels, Residential Fuels and Group A Plastic Commodity Boxes

| Object | Peak HRR |
|---|---|
| Cigarette | 5 W [28] |
| Candle | 80 W [29] |
| Coffeemaker | 40 kW [30] |
| Small trash can | 40 kW to 300 kW [31, 32] |
| 3 commodity box stack | 1.4 MW [26] |
| Upholstered chair | 80 kW to 2.5 MW [33] |
| 6 commodity box (2x stack of 3) | 2.5 MW [26] |
| Upholstered sofa | 3 MW to 5 MW [33, 34] |

# 3  Results

To evaluate the impact of ventilation in a commercial structure, experiments were conducted in a multi-unit strip mall. A series of seven experiments were conducted to evaluate the impact of increased ventilation in four separate units as described in Section 2. To focus on the impact of ventilation, the fire service technical panel narrowed the tactical choices for the experiments into four broad categories: no ventilation, horizontal ventilation, vertical ventilation, and combined horizontal and vertical ventilation. Additionally, water usage was monitored during the experiments to capture suppression information.

The seven experiments are described in Table 3.1. The unit, ventilation, and major experiment notes are described in the table. To comply with regional and national regulations, asbestos abatement was performed in accordance with the authority having jurisdiction. In some units, asbestos prevented them from being able to be used as fire units. In these instances, the units were instrumented as exposure units or were not used in this series. For experimental consistency, some interior alterations were performed. Where necessary, walls were added to create similar unit sizes, exterior doors and windows were blocked, the drop ceiling was removed, and the unit hardened to allow for multiple experiments.

Table 3.1: Experiments Conducted

| Experiment | Ventilation | Notes |
|:---:|:---:|:---|
| 1 | No Fire Service Ventilation | Only natural leakage of the unit |
| 2 | Front Door & Windows | Windows taken in sequence |
| 3 | Front Door & Windows | Windows taken simultaneously |
| 4 | Front Door & Windows | Double volume, windows taken simultaneously |
| 5 | Front Door & Roof Vent | 32.0 ft$^2$ (3.0 m$^2$) roof vent simultaneous with suppression |
| 6 | Front Door & Roof Vent | 64.0 ft$^2$ (6.0 m$^2$) roof vent, suppression delayed until after ventilation impact |
| 7 | Front Door, Windows & Roof Vent | Windows taken simultaneously, 64.0 ft$^2$ (6.0 m$^2$) roof vent, suppression delayed until after ventilation impact |

Time series charts were developed from the data acquired for each experiment. Interventions and significant events were added to the charts as vertical lines. Water flow data from the primary hoseline for each experiment has been depicted as blue shaded areas indicating when water was flowing. Figure 3.1 provides an example of a typical time series plot with significant events and the water flow indication which can be found throughout this section.
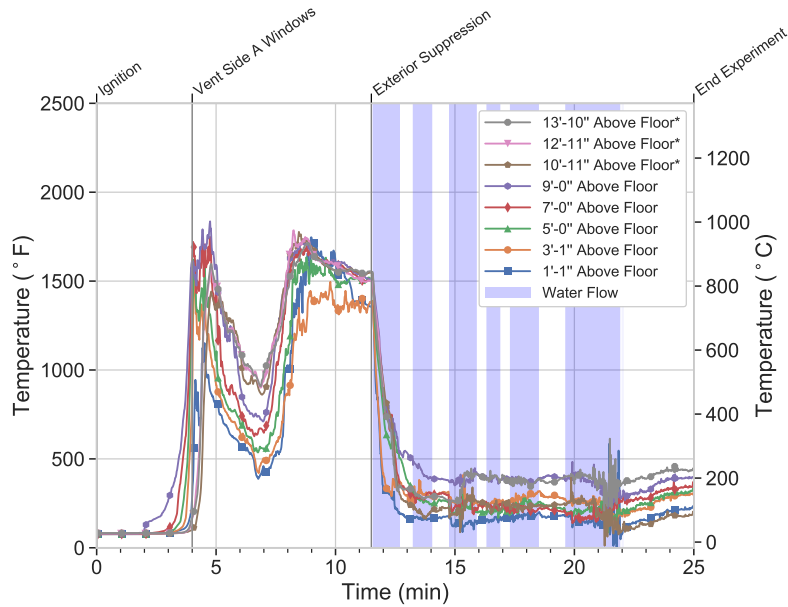


Figure 3.1: Example of a time series chart with interventions, significant events, and water flow. (Experiment 3)

## 3.1    Experiment 1 - No Fire Service Ventilation

Experiment 1 was designed to examine the impact of no additional ventilation on fire behavior in a 30 ft by 80 ft (9.1 m by 24.4 m) commercial unit. The fire was ignited in unit 1078, with units 1076 and 1080 as the side B and side D exposures, respectively. All exterior openings to the fire unit were closed. The front door to the side B and side D exposures were open.

The fire unit was instrumented to monitor the temperatures and pressures in the compartments, and flow velocity at the front door (see Figure 3.2). The thermocouple arrays contained seven thermocouples starting between 2 in. to 5 in. above the floor with a thermocouple every 2 ft (0.6 m), ending with the last thermocouple 1 in. (2.3 cm) below the metal roof deck. The differential pressure transducer arrays included pressure transducer taps at 1 ft (0.3 m), 7.5 ft (2.3 m), and 13 ft (4.0 m) above the floor that measured the differential pressure between the fire and exposure units. The bi-directional probe array in the front door included probes and thermocouples at 4.0 in. (10.2 cm), 22.0 in. (55.9 cm), 40 in. (101.6 cm), 58 in. (147.3 cm), and 76 in. (193.0 cm) above the floor.
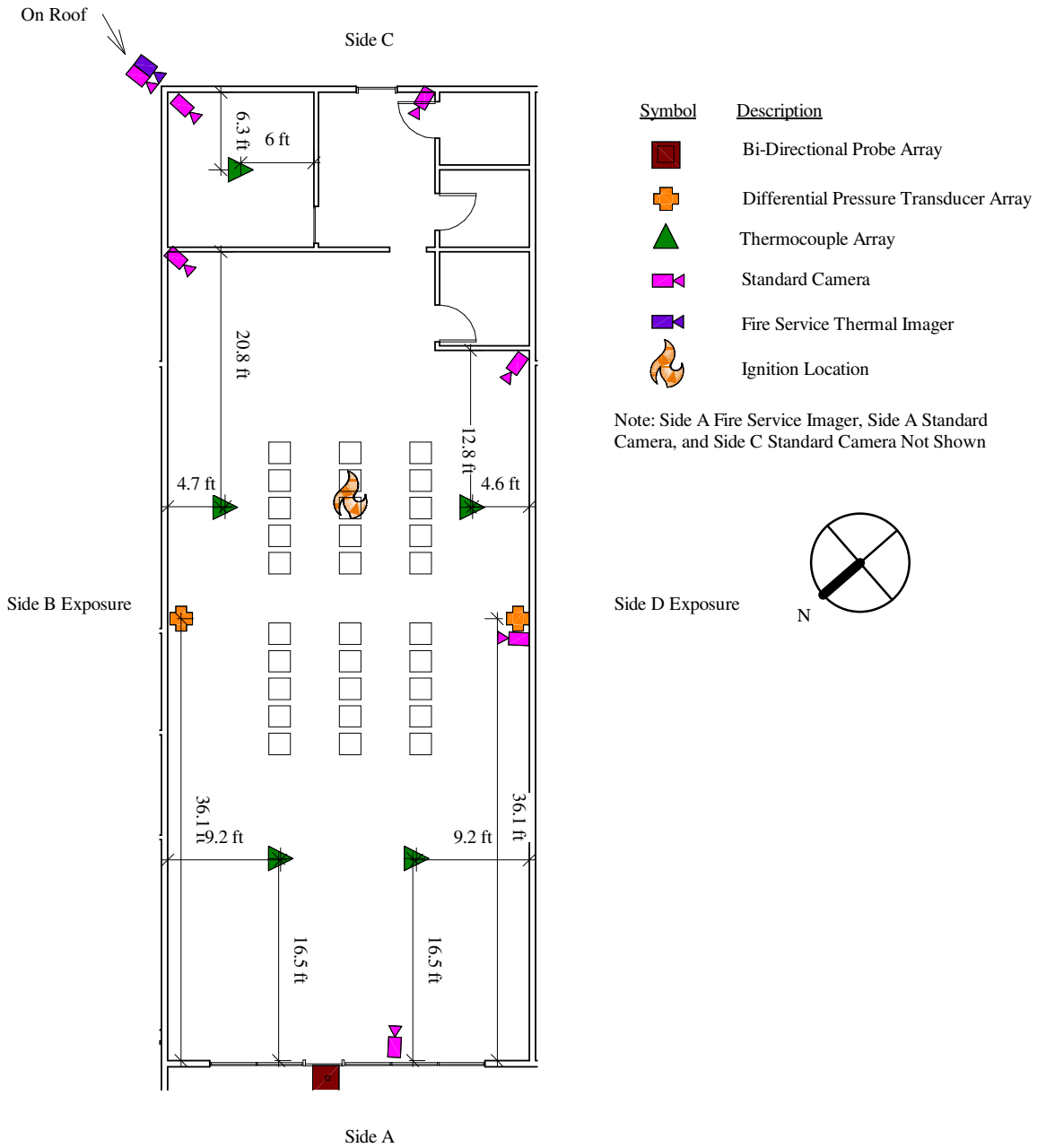
Figure 3.2: Instrumentation plan for unit 1078. Not shown are the locations where wind speed, wind direction, ambient temperature, and suppression water flow were recorded.

The experiment started with ignition (source described in Section 2.3) located between the second and third stacks of boxes from the rear, in the center rear row as shown on Figure 3.2. Table 3.2 lists the interventions and significant events from Experiment 1.

Table 3.2: Experiment 1 Sequence and Ventilation

| Timing (mm:ss) | Event | Opening(s) | Area ft$^2$ (m$^2$) |
|:---:|:---:|:---:|:---:|
| 00:00 | Ignition | None | - |
| 04:09 | Front Door Blew Open | Door | 19.0 (1.8) |
| 04:20 | Front Door Closed | None | - |
| 15:00 | Front Door Open | Door | 19.0 (1.8) |
| 19:17 | Suppression Crew Entered | - | - |
| 20:08 | Interior Suppression | - | - |
| 30:00 | End Experiment | - | - |

Flames were visible near the point of ignition 1 min into the experiment (see Figure 3.3b). The gas temperatures recorded in Experiment 1 are presented in Figure 3.4 as time resolved data starting at ignition and ending at the completion of the experiment. It took 1 min 30 s, for an increase in gas temperature to be recorded at the drop ceiling level in the main volume. The increase in temperature resulted in the expansion of gases. This expansion was recorded on the differential pressure transducers 2 min after ignition, as seen in Figure 3.5. At the time of the initial pressure increase, flames were impinging on the drop ceiling (see Figure 3.3c). The smoke layer can be seen reaching the top of the boxes 3 min after ignition (see Figure 3.3d), and visibility was completely obscured 5 min after ignition (see Figure 3.3f).

(a) Ignition

(b) 1 min

(c) 2 min

(d) 3 min
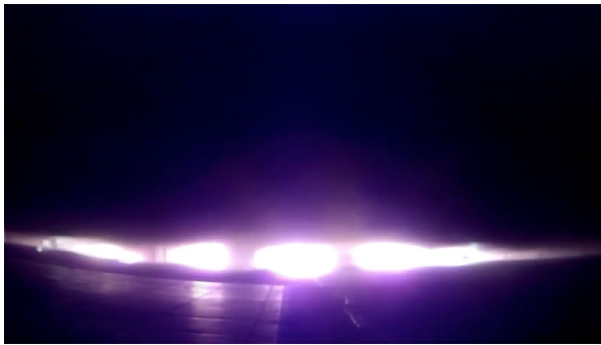
(e) 4 min

(f) 5 min

Figure 3.3: Sequential interior images during Experiment 1 looking toward side C from side A. The interior camera was lost after 5 min due to thermal damage from the fire.

(a) BC Quadrant Temperature

(b) CD Quadrant Temperature

(c) AB Quadrant Temperature

(d) AD Quadrant Temperature

* sensor was above the drop ceiling.
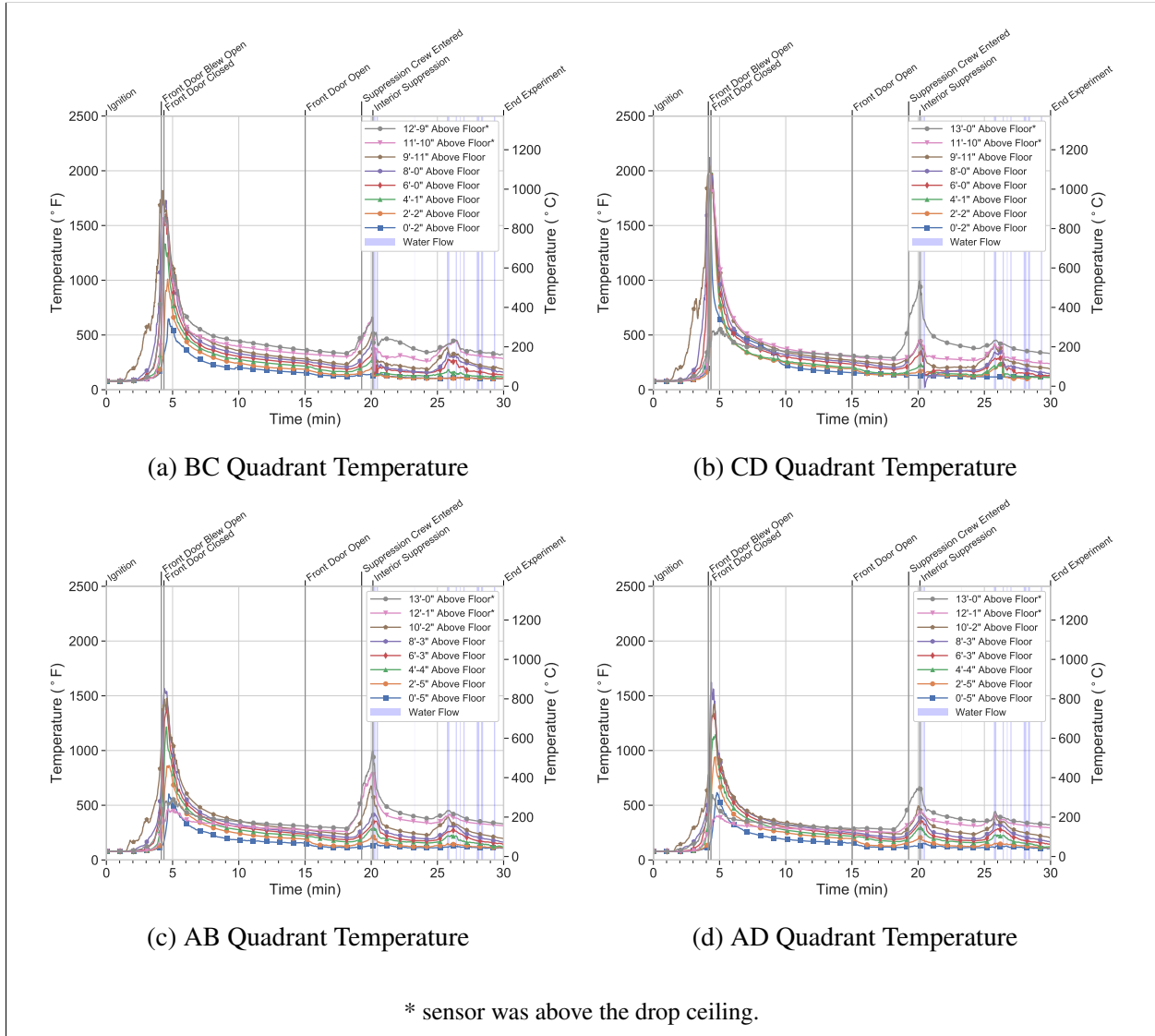
Side A

Figure 3.4: Fire compartment temperatures recorded during Experiment 1. Charts are arranged to correspond with the location of the thermocouple array in the unit. Side A is denoted outside the frame as a point of reference to the structure illustrated in Figure 3.2.
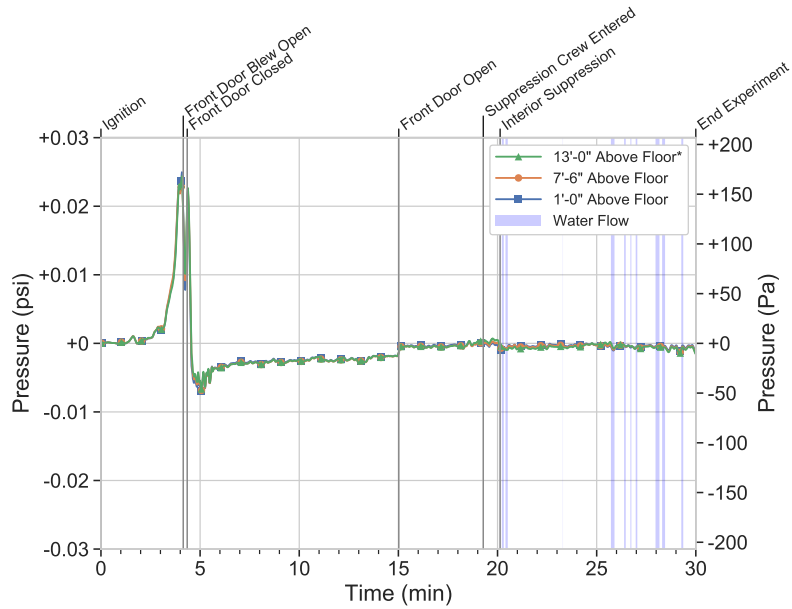
(a) Differential Pressure Side B Exposure
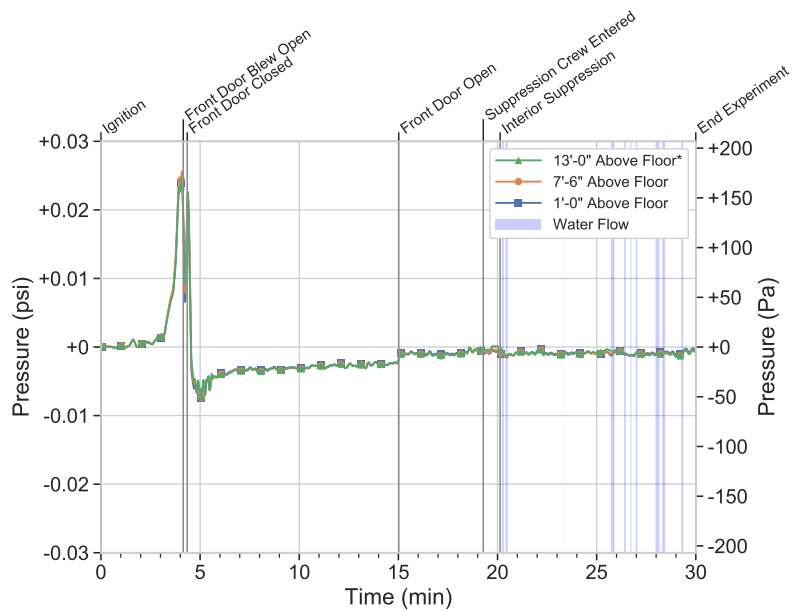


(b) Differential Pressure Side D Exposure

Figure 3.5: Pressures recorded during Experiment 1. Positive values indicate overpressure in the fire compartment compared to the exposure compartment.
* sensor was above the drop ceiling.

As gas temperatures continued to increase, expansion continued. With all the exterior doors and windows closed, pressure in the fire compartment volume exceeded 0.018 psi (124.4 Pa), the range of the pressure transducers (see Figure 3.5). The pressure forced the free-swinging front door open 4 min 9 s, after ignition, relieving some of the pressure. Based on the area of the door, 2,736 in.[2]

(1.765 m$^2$), and the pressure in the unit, 0.018 psi (124.4 Pa), at least 49 lbf (219 N) was exerted on the door before it opened (*Force = Pressure × Area*). The door was closed by the fire suppression crew within 11 s, and the pressure increased to previous levels. The front door velocity probes recorded flow in excess of 10 mph (4.5 m/s), (see Figure 3.6a), the temperatures in the doorway exceeded 350 °F (177 °C) (see Figure 3.6b), and flames were visible out the front door while the door was open (see Figure 3.7).
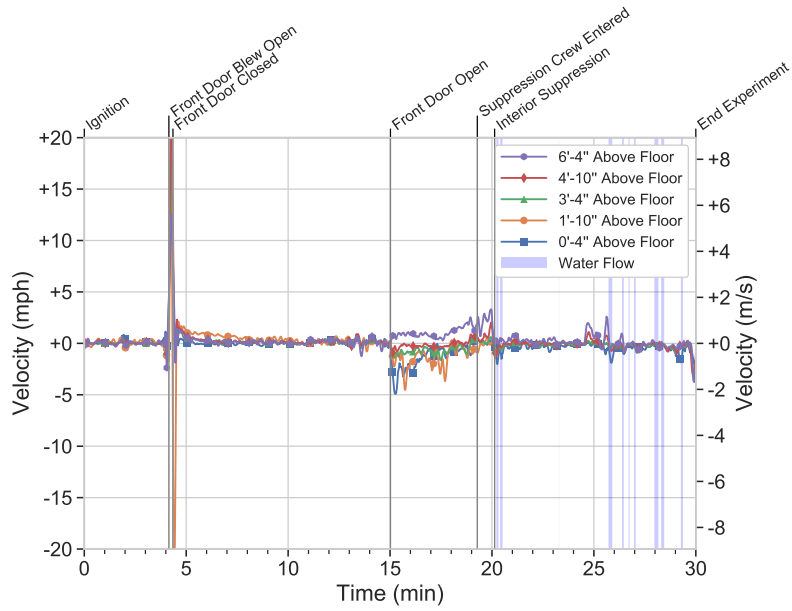
(a) Gas Velocities
Positive direction indicates flow out of the unit
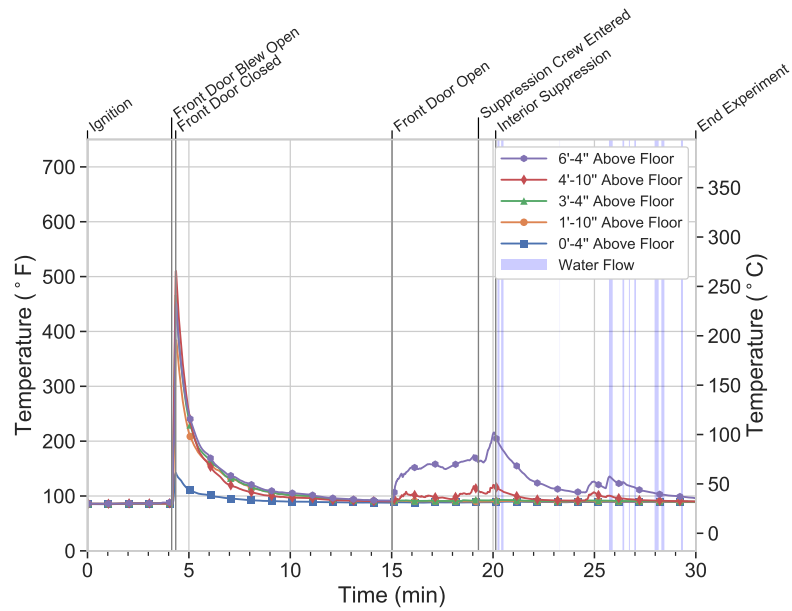


(b) Temperatures

Figure 3.6: Gas velocities (left) and temperatures (right) recorded in the front door during Experiment 1.

Figure 3.7: Flames exhausting from the front door captured by the helmet camera of the firefighter who closed the door during Experiment 1.

Temperatures peaked 4 min 30 s after ignition. The thermocouple array in the CD quadrant, the array nearest ignition, recorded the highest temperature at 2,000 °F (1,093 °C) at 2 ft (0.6 m) above the floor. Thermocouple arrays further from the ignition location recorded lower peaks between 1,500 °F to 1,750 °F (816 °C to 954 °C). Temperatures decreased following the peak, and by 8 min into the experiment they were below 500 °F (260 °C). The rate of decrease slowed and temperatures remained stratified between 150 °F to 350 °F (66 °C to 177 °C) for the next 7 min until the front door was opened 15 min after ignition.

As the gas temperatures decreased, the gases inside the unit contracted. The pressures dropped from the maximum the transducers could record to -0.008 psi (-55 Pa) in a 30 s time period. The minimum value was recorded 5 min after ignition (see Figure 3.5). With no open windows or doors, the pressure remained negative and increased slowly toward ambient levels due to the air leakage into the unit.

The room in the BC corner of the unit was isolated from the remainder of the volume by a closed doorway and a drop ceiling. The thermocouple array in that room recorded gas temperatures in excess of 140 °F (60 °C) above the drop ceiling, with the peak temperature occurring 4 min 30 s after ignition, the same time as the fire compartment (see Figure 3.8). Gas temperatures beneath the drop ceiling remained below 125 °F (52 °C). The gas temperatures recorded by the thermocouples lower in the room increased only after the peak value was recorded above the ceiling and continued to increase until the completion of the experiment. The maximum recorded values remained below 125 °F (52 °C). With the closed door and drop ceiling in-place, there was no method to dissipate the heat energy from that space. As a result, gas temperatures remained elevated.
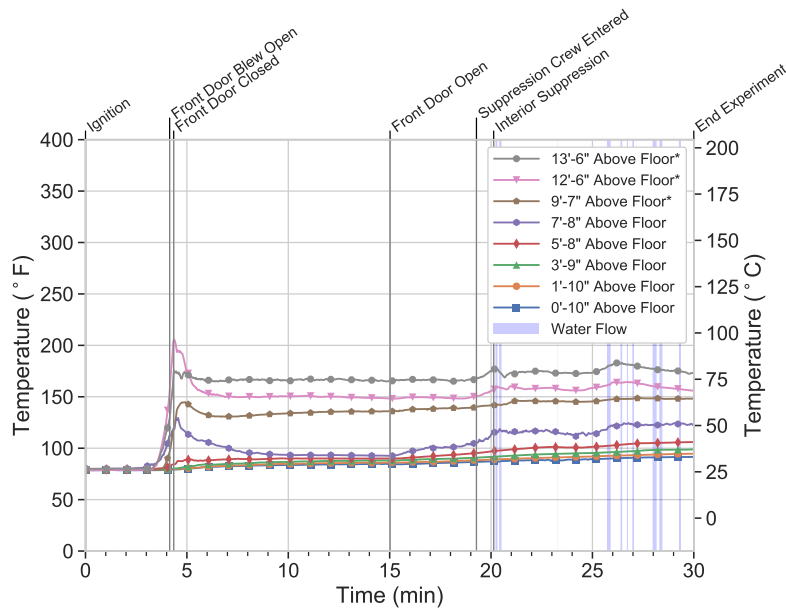
Figure 3.8: Temperatures recorded in the rear room with a closed door during Experiment 1.
* sensor was above the drop ceiling.

The front door was opened 15 min after ignition to assess conditions and access the fire for suppression. Pressure recovered to ambient values upon the front door being opened (see Figure 3.5). Opening the door resulted in bi-directional flow at the front door. The top probe recorded exhaust at 1 mph (0.4 m/s), and the bottom four probes recorded inflow in a range from 0.25 mph to 5 mph (0.1 m/s to 2.2 m/s) (see Figure 3.6a). The temperatures at the top of the doorway increased, exceeding 170 °F (77 °C) as hot gases were exhausted past the sensors. Temperatures lower in the door remained at ambient as cooler gases from the exterior were drawn past the sensors (see Figure 3.6b).

After 3 min, the gas temperatures just below the metal roof deck started to increase. The temperature increase can be attributed to the additional oxygen entering the front door and reaching the smoldering material and transitioning it to flaming combustion. The largest increase was recorded at the thermocouple array closest to the front door (AB quadrant), reaching a peak of 1,000 °F (538 °C). The velocity of the gases exiting the top of the door increased to 3 mph (1.3 m/s), and the temperatures recorded at the top of the door increased to over 200 °F (93 °C).

The suppression crew entered the structure 19 min 17 s after ignition and found flaming combustion in the remaining fuel. A 1 3/4 in. handline with a 7/8 in. smooth-bore tip that flowed 160 gpm was used to extinguish the flames. Water application occurred 20 min 8 s after ignition. The water flow rate from the handline in Figure 3.9 shows the line was utilized in short bursts. Water flow never reached 160 gpm and the total water used for suppression was 70 gal. Applying water caused gas temperatures to decrease in the fire compartment. The velocity and temperature of the gases exhausting out of the front door decreased after water application. Gas temperatures near the metal roof deck remained elevated even after all visible flames were extinguished (see Figure 3.4)

due to the insulated roof structure holding heat and/or heat transfer from the hot metal deck to the thermocouples. The experiment concluded 30 min after ignition.
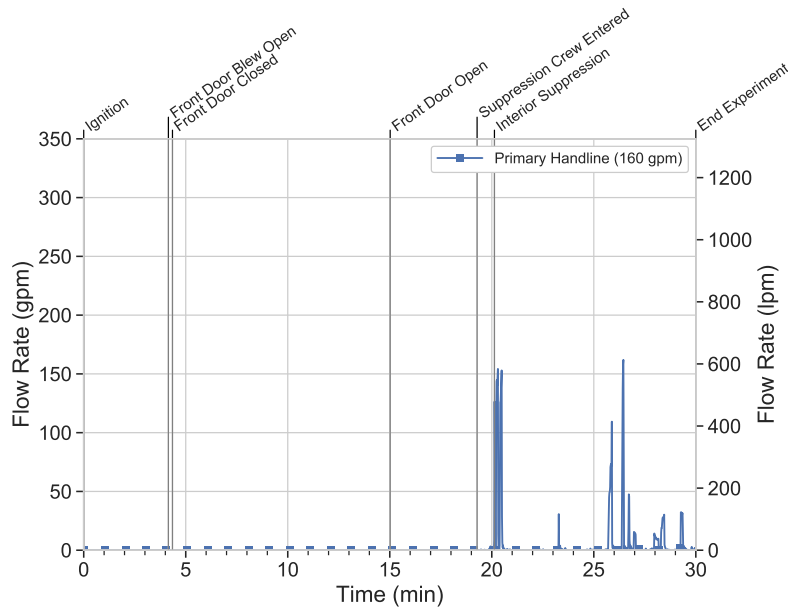


Figure 3.9: Water flows recorded in Experiment 1.

Plots of wind speed, ambient air temperature, and wind direction are presented in Figure 3.10 from ignition until the end of the experiment. The wind speed was between 3 mph to 14 mph (1 m/s to 6 m/s), blowing from the southwest toward the northeast, perpendicular to the front of the unit. The ambient air temperature was between 90 °F to 95 °F (32 °C to 35 °C) for the entire experiment. The elevated wind speed and flow across the front door of the unit may have had an impact on the magnitude of the flow at the front door after it was opened 15 min after ignition. The perpendicular flow could have limited the ability of the front door to efficiently exchange gases between the fire unit and the exterior.
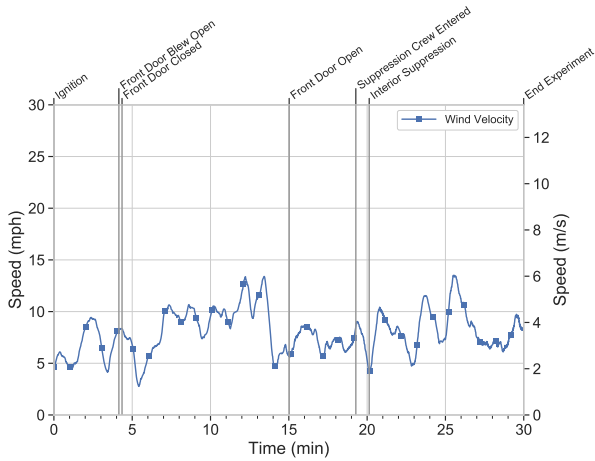
(a) Wind Speed
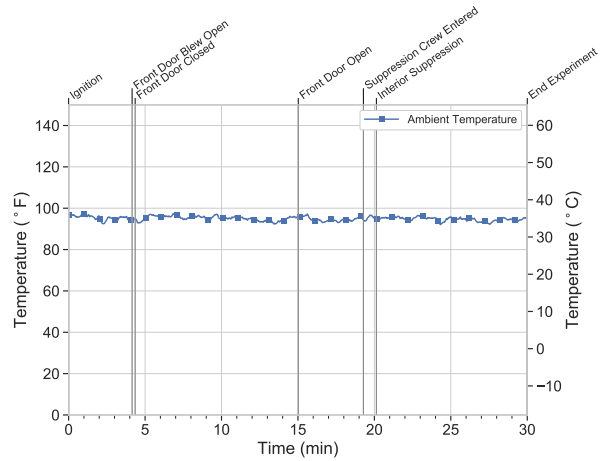


(b) Air Temperature
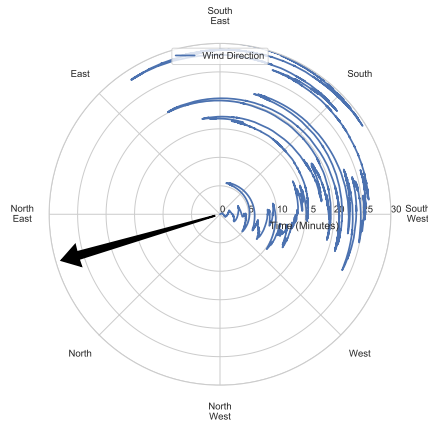


Side A

North on the chart is oriented to correspond with
North on the site layout (see Figure 2.4) and
corresponding instrument plan (see Figure 3.2), with
side A labeled for reference. The arrow indicates the
average direction the wind was blowing.

(c) Wind Direction

Figure 3.10: Weather conditions recorded during Experiment 1.

## 3.2 Experiment 2 - Horizontal Ventilation

Experiment 2 was designed to examine the impact of sequential horizontal ventilation in three stages: 1) a door, 2) a door and window, and 3) a door and multiple windows in a 30 ft (9.1 m) by 80 ft (24.4 m) commercial unit. The fire was ignited in unit 1078, with units 1076 and 1080 as the side B and side D exposures, respectively. The front doors to all three units were open.

The fire unit was instrumented to monitor the thermal conditions with thermocouple arrays, differential pressure sensor arrays between the unit and the exposures, and a bi-directional probe array in the front door, as illustrated in Figure 3.11. The thermocouple arrays contained seven thermocouples starting between 2 in. to 5 in. (2 cm to 13 cm) above the floor with a thermocouple every 2 ft (0.6 m), ending with the last thermocouple 1 in. (2.3 cm) below the metal roof deck. The differential pressure transducer arrays included pressure transducer taps at 1 ft (0.3 m), 7.5 ft (2.3 m), and 13 ft (4.0 m) above the floor measuring the differential pressure between the fire and exposure units. The bi-directional probe array in the front door included probes and thermocouples at 4.0 in. (10.2 cm), 22.0 in. (55.9 cm), 40 in. (101.6 cm), 58 in. (147.3 cm), and 76 in. (193.0 cm) above the floor level.
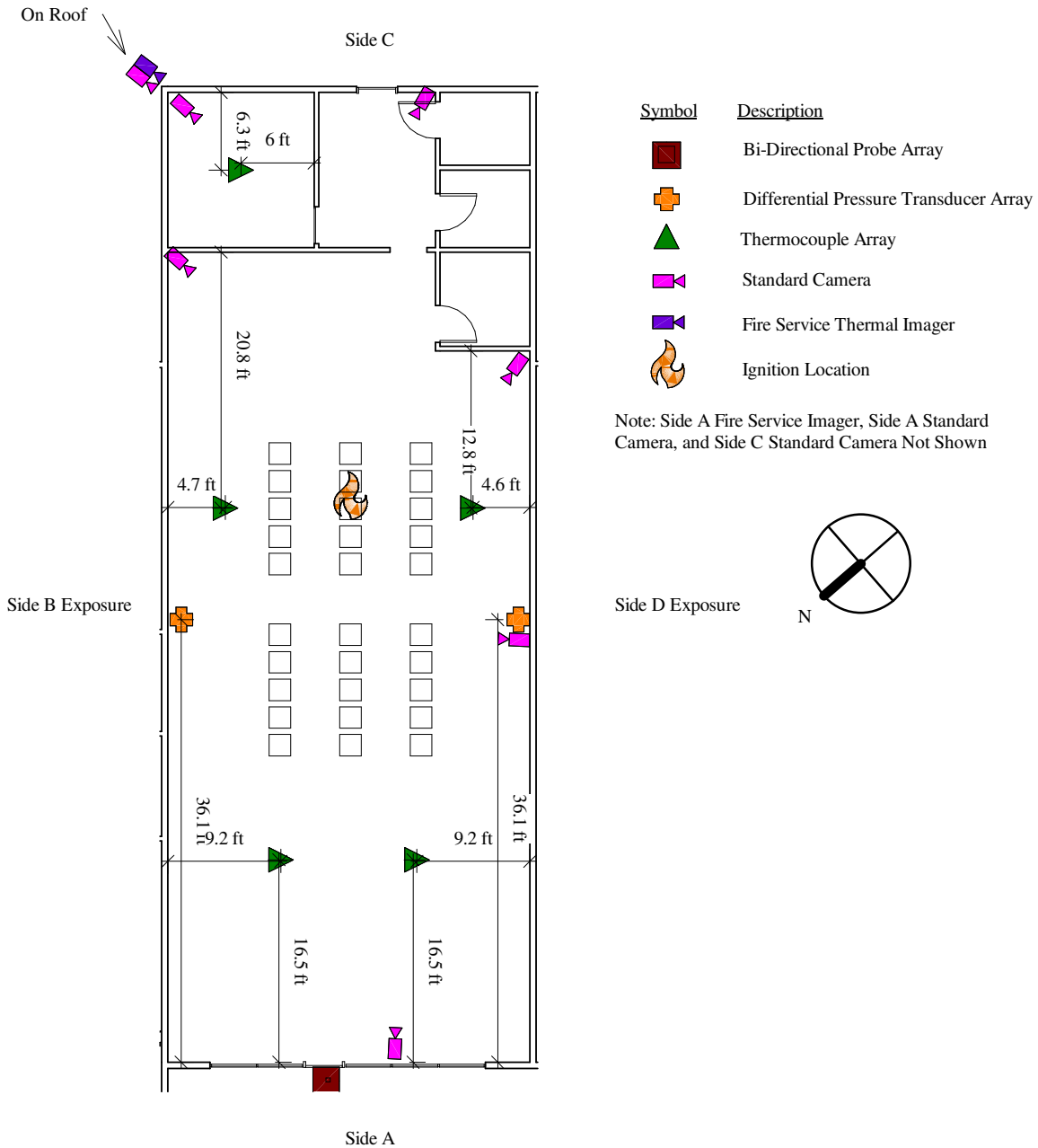
Figure 3.11: Instrumentation plan for unit 1078. Not shown are the locations where wind speed, wind direction, ambient temperature, and suppression water flow were recorded.

The experiment started with ignition (source described in Section 2.3) located between the second and third stacks of boxes from the rear in the center rear row as shown in Figure 3.11. Table 3.3 lists the interventions and significant events from Experiment 2. Figure 3.12 shows the window numbering used horizontal ventilation.

45

Table 3.3: Experiment 2 Sequence and Ventilation

| Timing (mm:ss) | Event | Opening(s) | Area ft$^2$ (m$^2$) |
|---|---|---|---|
| 00:00 | Ignition | Door | 19.0 (1.8) |
| 10:00 | Vent Window #5 | Door and Window | 47.8 (4.4) |
| 14:00 | Vent Window #3 and #4 | Door and Three Windows | 105.3 (9.8) |
| 18:55 | Exterior Suppression | - | - |
| 34:51 | Roof Collapse | - | - |
| 40:00 | End Experiment | - | - |



Figure 3.12: A schematic highlighting the window numbering for purposes of horizontal ventilation

The gas temperatures recorded in Experiment 2 are presented in Figure 3.13 starting at ignition and ending at the completion of the experiment. Following ignition, it took 1 min 30 s for an increase in gas temperature to be recorded at the thermocouples 13 ft (4.0 m) above the floor in the fire compartment. The damage to the ceiling grid from Experiment 1 allowed heat to penetrate the drop ceiling faster in Experiment 2. Flames were visible impinging on what was left of the drop ceiling 2 min after ignition (see Figure 3.14c).

(a) BC Quadrant Temperature

(b) CD Quadrant Temperature

(c) AB Quadrant Temperature

(d) AD Quadrant Temperature

* sensor was located above the drop ceiling.
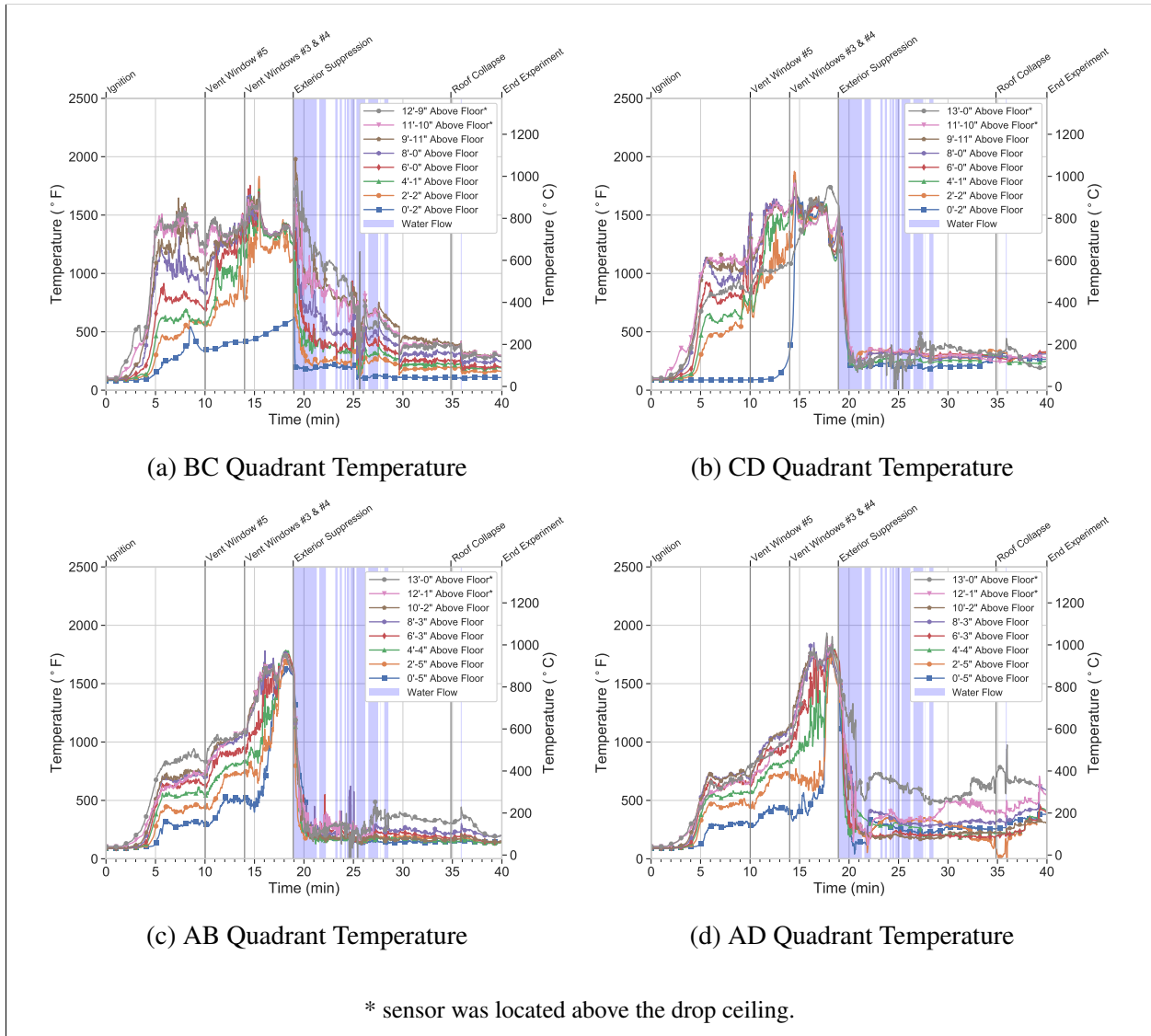
Side A

Figure 3.13: Fire compartment temperatures recorded during Experiment 2. Charts are arranged to correspond with the location of the thermocouple array in the unit. Side A is denoted outside the frame as a point of reference to the structure illustrated in Figure 3.11

(a) Ignition

(b) 1 min

(c) 2 min

(d) 3 min

(e) 4 min

(f) 5 min

(g) 6 min

Figure 3.14: Sequential interior images during Experiment 2 looking toward side C from the side A. The interior camera was lost after 6 min due to thermal damage from the fire.

The increase in temperature resulted in an expansion of the gases. This expansion was recorded on the differential pressure transducers as an increase in pressure above ambient 2 min 30 s after

ignition (see Figure 3.15), and as a uni-directional exhaust in the front door velocity probes 3 min after ignition (see Figure 3.16a). For the first 30 s, the exhaust was made up of the gases that were present in the compartment prior to ignition and the temperatures in the door remained near ambient. As the gases at the ceiling expanded, they forced out the gases lower in the space. At 3 min 30 s, temperatures in the door increased, indicating the gases being exhausted contained products of combustion (see Figure 3.16b).
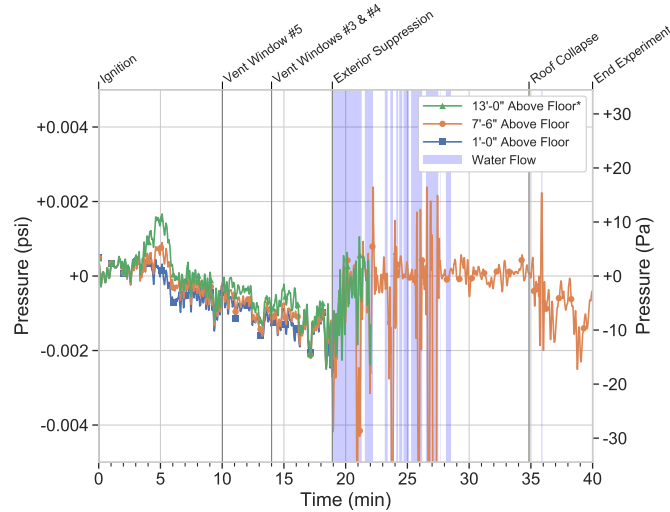


(a) Differential Pressure Side B Exposure
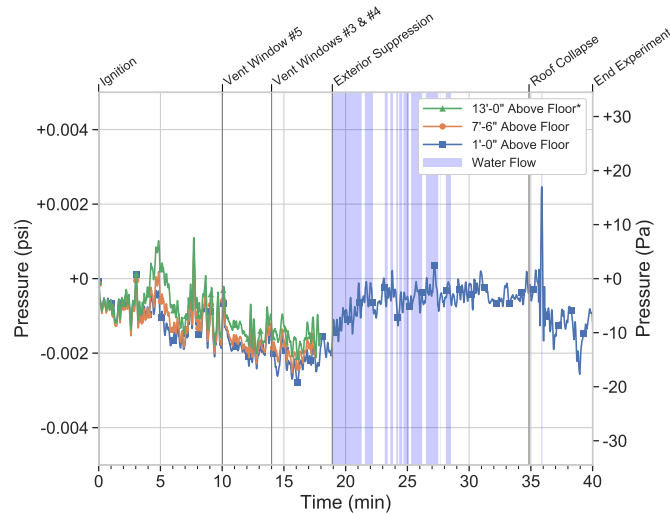


(b) Differential Pressure Side D Exposure

Figure 3.15: Pressures recorded during Experiment 2. Positive values indicate overpressure in the fire compartment compared to the exposure compartment.
* sensor was above the drop ceiling.

The smoke layer descended to the level of the second box in the fuel package stack at 4 min (see Figure 3.14e). The pressure was stratified with higher pressure above the drop ceiling and lower

pressure near the floor; all elevations recorded a positive pressure as the gases expanded. All front door velocities recorded unidirectional exhaust until 5 min after ignition with a peak exhaust of 1 mph (0.4 m/s) at the bottom and 5 mph (2.2 m/s) at the top.

At 5 min after ignition, the pressure peaked at 0.02 psi (11 Pa), lower than the peak in Experiment 1 due to the open front door. The front door became a bi-directional vent with exhaust at the top and inflow at the bottom. The maximum inflow recorded from 5 min to 10 min was −9 mph (−4 m/s) and the maximum exhaust was 11 mph (4.9 m/s). The smoke layer reached the floor at 6 min (see Figure 3.14g), completely obscuring the interior cameras. As the smoke layer reached the floor, temperatures stabilized ranging from 250 °F to 900 °F (121 °C to 482 °C) in the front of the fire compartment (see Figure 3.13c & 3.13d) and 100 °F to 1,500 °F (121 °C to 482 °C) in the rear of the fire compartment (see Figure 3.13a & 3.13b). Temperatures in the front door decreased at the lower three probes as cooler gases from the exterior were drawn past the sensors (see Figure 3.16b).
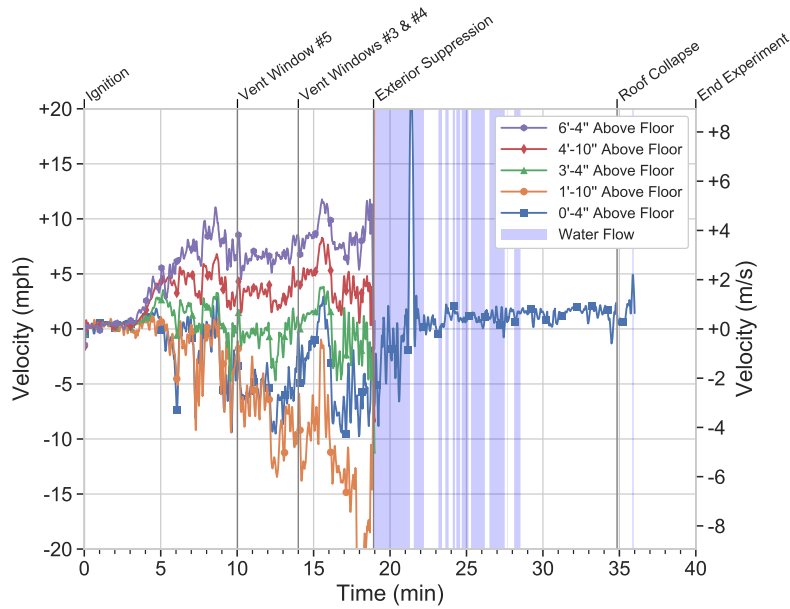
(a) Gas Velocities
Positive direction indicates flow out of the unit
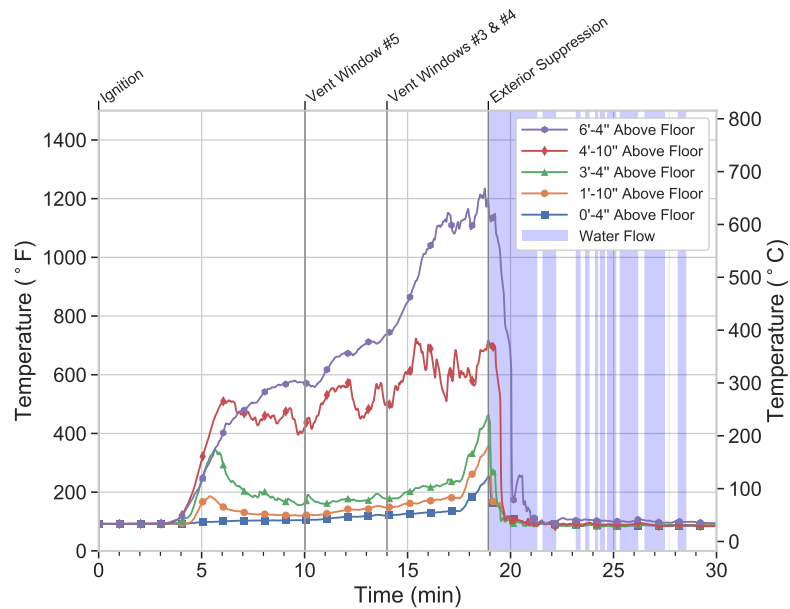


(b) Temperatures

Figure 3.16: Gas velocities and temperatures recorded in the front door during Experiment 2.

Throughout the experiment, the room in the BC corner was isolated from the remainder of the volume by a closed door and a drop ceiling. Although the previous experiment had damaged the drop ceiling in the fire compartment, no damage occurred in the rear, remote from the ignition. It took 2 min 30 s from ignition for the gas temperatures above the drop ceiling to record an increase

above ambient (see Figure 3.17). It was another 2 min until the temperatures increased below the drop ceiling 4 min after ignition. Temperatures increased steadily, reaching 300 °F (149 °C) above the drop ceiling at 10 min after ignition. The maximum temperature recorded below the ceiling during the same time period was 160 °F (71 °C) at the ceiling level. Temperatures below 4 ft (1.2 m) level remained below 125 °F (52 °C).
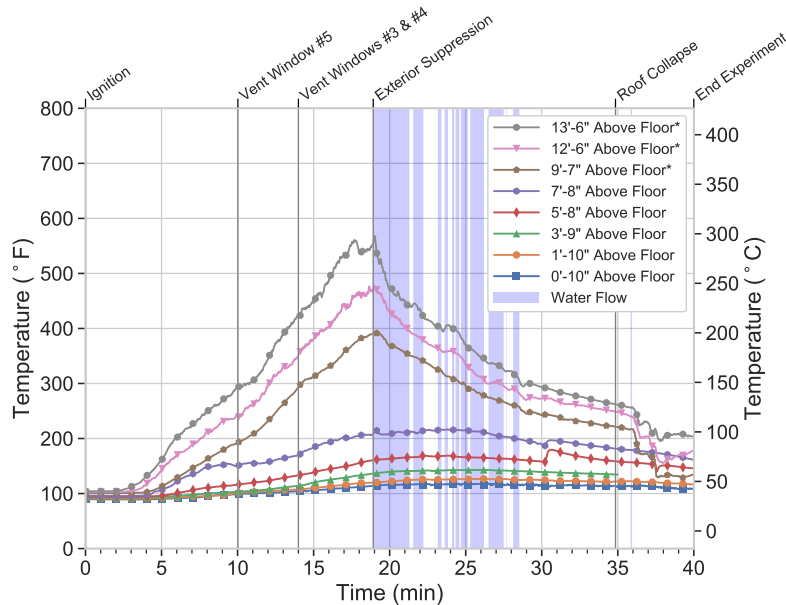


Figure 3.17: Temperatures recorded in the rear room with a closed door during Experiment 2.
* sensor was above the drop ceiling.

Ventilation of the front right window pane (window #5) resulted in temperature increases throughout the fire compartment, an indication that the fire size had increased. At 2 min after the ventilation (12 min after ignition), temperatures in the front of the unit ranged from 400 °F (204 °C) at the floor to 1,050 °F (566 °C) at the ceiling (see Figure 3.13c & 3.13d). Temperatures in the rear of the fire compartment above the 4 ft (1.2 m) level, exceeded 1,000 °F (538 °C) (see Figure 3.13a & 3.13b). The drop ceiling and closed door that separated the room in the BC corner from the fire compartment remained intact, effectively isolating the space. Temperatures just below the ceiling in that room were 190 °F (88 °C), and at 4 ft (1.2 m) above the floor they were below 130 °F (54 °C) .

After the initial single window pane ventilation, the magnitude of the average inflow at the bottom of the front door increased from -2.2 mph (-1 m/s) to -5.7 mph (-0.5 m/s), and the average exhaust at the top decreased from 7.6 mph (3.4 m/s) to 6.7 mph (3 m/s). The elevation of the window sill was 2 ft 4 in. (0.7 m) above the floor level, which limited the ability of the window to act as an inlet. The additional exhaust area, decreased the magnitude of the exhaust out the top of the front door. Although the magnitude of the exhaust flow at the door decreased, there was a net increase the total volume of the gases exhausted from the fire compartment due to the additional area. As a result, the magnitude of air intake at the bottom of the door increased. However, the inflow was

not sufficient to achieve equilibrium, and a decrease was recorded on the pressure transducers (see Figure 3.15). The values dropped below zero, indicating more volume was being exhausted than drawn in. Temperatures on the lower three probes remained under 200 °F (77 °C) while the upper two probes recorded an increase in temperature as the larger fire size increased the temperature of the products of combustion (see Figure 3.16b).

Two additional windows (windows #3 and #4) were ventilated 14 min after ignition. Three minutes afterwards, temperatures increased in the fire compartment to uniform floor to ceiling temperatures in excess of 1,200 °F (649 °C), conditions representative of flashover in all four quadrants (see Figure 3.4). Note the lowest thermocouple in the CD quadrant. This thermocouple was most likely in contact with the carpet as it increased from 250 °F (121 °C) to 1,600 °F (871 °C) as the carpet ignited during flashover. The second outlier was the lowest thermocouple located in the BC quadrant (see Figure 3.13a). This thermocouple was most likely in contact with the concrete below the carpet, because it remained below 600 °F (316 °C). The drop ceiling in the BC corner of the unit remained intact and, along with the closed door, continued to provide separation to the BC corner room. Temperatures above the drop ceiling exceeded 350 °F (177 °C). However, at 4 ft (1.2 m) above the floor, temperatures were below 140 °F (60 °C).

The additional exhaust area provided by the open windows decreased pressures further. Note the magnitude of the flows at the front door where the probe 1 ft 10 in. (0.6 m) recorded a peak inflow of −20 mph (8.9 m/s) and the top probe recorded a peak exhaust flow of 12 mph (5.4 m/s). After the ventilation of the AD left and center window panes, the probe 3 ft 4 in. (1 m) above the floor averaged a velocity of 0 mph (0 m/s), which indicates the neutral plane to be near that level (see Figure 3.16a). Temperatures recorded in the exhaust portion of the doorway continued to increase as the higher temperature products of combustion were exhausted past. Temperatures recorded in the inlet portion of the doorway also increased, but that was due to radiation from the hot gases above, not convected gases flowing past. (see Figure 3.16)

The ventilation area above the neutral plane was larger than the area below the neutral plane, with the end result being more exhaust flow than inflow (see Figure 3.18). The volume of gases being exhausted exceeded the volume of gases being drawn in, with the result being a decrease in pressure inside the unit.

53

Figure 3.18: Image and approximate location of the neutral plane in the openings on the front of Unit 1078 during Experiment 2 following the ventilation of the AD left and center window panes 18 min after ignition. The red line approximates the height of the neutral plane.

At 18 min after ignition, flames were visible on the exterior camera (see Figure 3.18). The flames increased the radiation on the lower three temperature senors in the inlet portion of the front door, which recorded the additional radiation as an increase in temperature (see Figure 3.16b).

The foam insulation and rubber membrane on the roof near the HVAC unit ignited 8 min 48 s after ignition. The flames spread to the majority of the main volume roof by 17 min 32 s (see Figure 3.19).



(a) 8 min 48 s

(b) 17 min 32 s

Figure 3.19: Images from the camera on the CD corner showing the ignition of the roofing material.

Exterior suppression occurred via a 1 3/4 in. handline with a 7/8 in. smooth-bore tip that flowed 160 gpm (606 lpm). The handline was directed through the side A windows and door, 18 min 55 s after ignition. The water flow is presented in Figure 3.20. The water stream impacted the probes for pressure and velocity, damaging some of the sensors. Temperatures in the front of the main volume decreased from 1,600 °F (871 °C) to below 500 °F (260 °C) 1 min after suppression started (see Figure 3.13c and Figure 3.13d and Figure 3.13b).

Temperature in the BC quadrant below 6 ft (1.8 m) dropped from 1,300 °F (704 °C) to below 500 °F (260 °C) in 2 min following the initial suppression action. Temperatures above 8 ft (2.4 m) briefly increased from 1,300 °F (704 °C) to a peak of 1,900 °F (1,037 °C) in the 15 s that followed suppression before dropping below 1,000 °F (537 °C) within 2 min of water application. The lack of visibility in the structure from the cameras makes it difficult to discern the exact cause of the temperature rise. A possibility is that the hose stream disrupted the local gas concentrations and the integrity of drop ceiling, allowing fresh air to mix with hot fuel gases that resulted in local flaming.
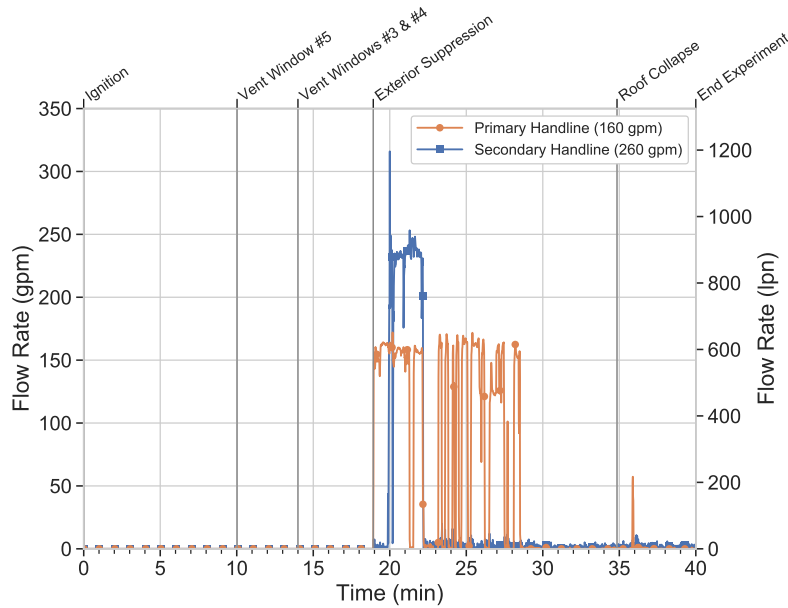


Figure 3.20: Water flows recorded during Experiment 2.

The one velocity probe that remained functional following suppression indicated the velocities began to return to pre-ignition conditions following the initial water application. Temperatures recorded in the front door decreased to under 200 °F (see Figure 3.16) within 1 min 30 s of the water application. The differential pressures returned to pre-ignition conditions following suppression.

A secondary, 2 1/2 in. handline with a 1 1/8 in. smooth bore tip that flowed 265 gpm (1,003 lpm), applied water on the combustible roof decking from side A starting at 20 min. All suppression occurred from the exterior and continued until all visible flames were extinguished. The total water used was 985 gal from the primary line and 542 gal from the secondary line for a total of 1,527 gal.

The roof collapsed in the front half of the unit at 34 min 51 s. As the roof joists in the unit heated they expanded, and pushed the front masonry wall toward side A. Once suppression had extinguished the fire, the joists cooled and retracted away from the front wall. No longer being supported by the wall, the front portion of the roof collapsed in a lean-to style collapse. Further discussion on the collapse mechanism is discussed in Section 4.3.

The experiment concluded at 40 min when the visible flames had been extinguished. Figure 3.21 shows images of the collapsed roof structure after the experiment concluded.



(a) Front Elevation        (b) From Adjacent Roof

Figure 3.21: Images of the lean-to front roof collapse that occurred during Experiment 2.

Plots of wind speed, ambient air temperature and wind direction are presented in Figure 3.22 from ignition until the end of the experiment. The wind speed was in the range of 5 mph to 24 mph (2.2 m/s to 10.8 m/s), blowing from the southwest toward the north east, perpendicular to the front of the unit. The ambient air temperature recorded was between 90 °F to 95 °F (32 °C to 35 °C) for the entire experiment. The wind blowing across the front of the unit may have impacted the ability of the open vents to effectively exchange air with the exterior by limiting the exhaust flow. Without a control experiment in a no-wind condition, it is difficult to determine how much of an impact this had on the experiment.
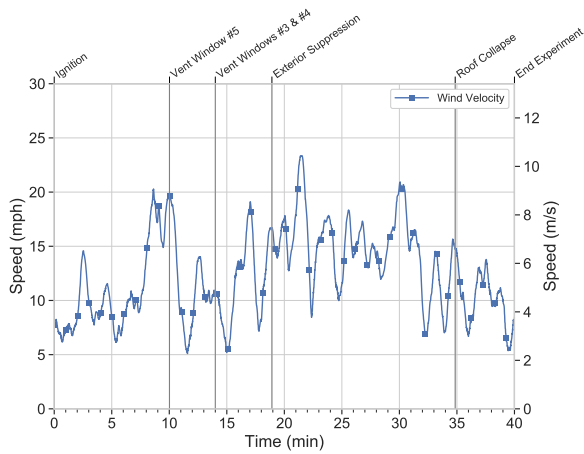
(a) Wind Speed
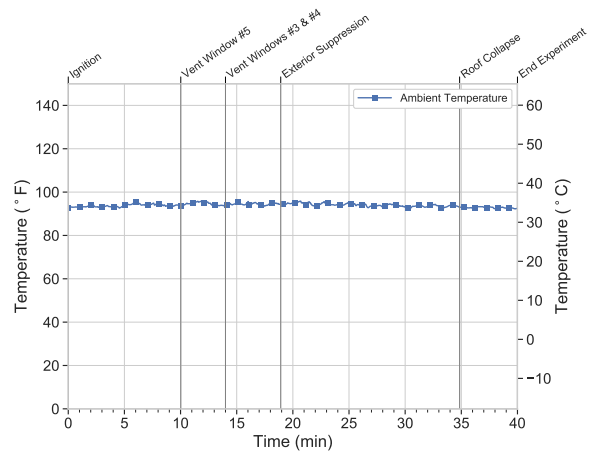
(b) Air Temperature
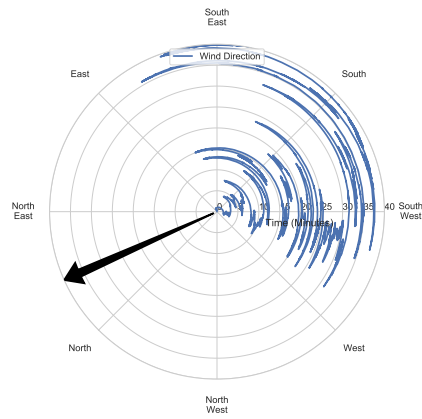


Side A

North on the chart is oriented to correspond with north on
the site layout (see Figure 2.4) and corresponding
instrument plan (see Figure 3.2), with side A labeled for
reference. The arrow indicates the average direction the
wind was blowing.

(c) Wind Direction

Figure 3.22: Weather conditions recorded during Experiment 2.

## 3.3 Experiment 3 - Horizontal Ventilation

Experiment 3 was conducted to examine the impact of horizontal ventilation. The horizontal ventilation scenario incorporated a similar ventilation area to Experiment 2, however the front windows were ventilated simultaneously in Experiment 3. Following ventilation, suppression was conducted on the post-flashover fire. Unit 1074 was the fire unit, with unit 1076 as the side D exposure. The front doors to both units were open when the experiment began.

The unit was instrumented to monitor the thermal conditions with thermocouple arrays, and a differential pressure sensor array between the unit and side D exposure as illustrated in Figure 3.23. The thermocouple arrays contained seven thermocouples starting between at 1 ft 1 in. (0.3 m) above the floor with a thermocouple every 2 ft (0.6 m), ending with the last thermocouple 1 in. (2.3 cm) below the metal roof deck. The differential pressure transducer array included pressure transducer taps at 1 ft (0.3 m), 7.5 ft (2.3 m) and 13 ft (4.0 m) above the floor measuring the differential pressure between the fire unit and side D exposure.
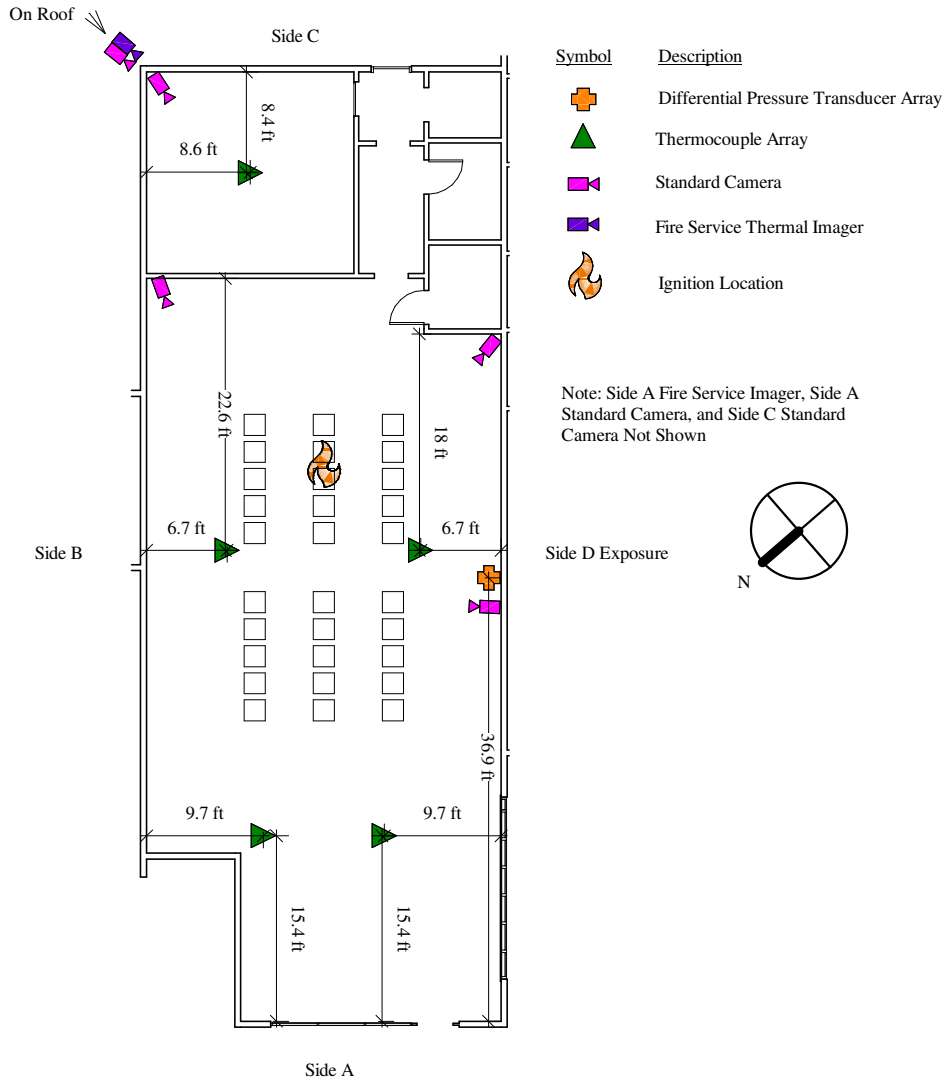
Figure 3.23: Instrumentation plan for unit 1074 utilized as the fire unit in Experiment 3. Not shown are the locations where wind speed, wind direction, ambient temperature, and suppression water flow were recorded.

The experiment started with ignition (source described in Section 2.3, located between the second and third stacks of boxes, from the rear, in the center rear row as shown in Figure 3.23. Table 3.4 lists the interventions and significant events from Experiment 3.

Table 3.4: Experiment 3 Sequence and Ventilation

| Timing (mm:ss) | Event | Opening(s) | Area ft$^2$ (m$^2$) |
|---|---|---|---|
| 00:00 | Ignition | Door | 19.0 (1.8) |
| 04:00 | Vent Side A Windows | Door and Three Windows | 97.3 (9.0) |
| 11:30 | Exterior Suppression | - | - |
| 25:00 | End Experiment | - | - |

The gas temperatures recorded in Experiment 3 are presented in Figure 3.24 starting at ignition and ending at the completion of the experiment. Following ignition, it took 1 min 45 s for an increase in gas temperature to be recorded on the first thermocouple below the drop ceiling (9 ft 11 in. above the floor), in the BC quadrant array. The other three arrays recorded gas temperature increase below the drop ceiling 2 min after ignition. Flames were visible impinging on the drop ceiling 2 min after ignition (see Figure 3.25c).

(a) BC Quadrant Temperature

(b) CD Quadrant Temperature

(c) AB Quadrant Temperature

(d) AD Quadrant Temperature

* sensor was located above the drop ceiling.
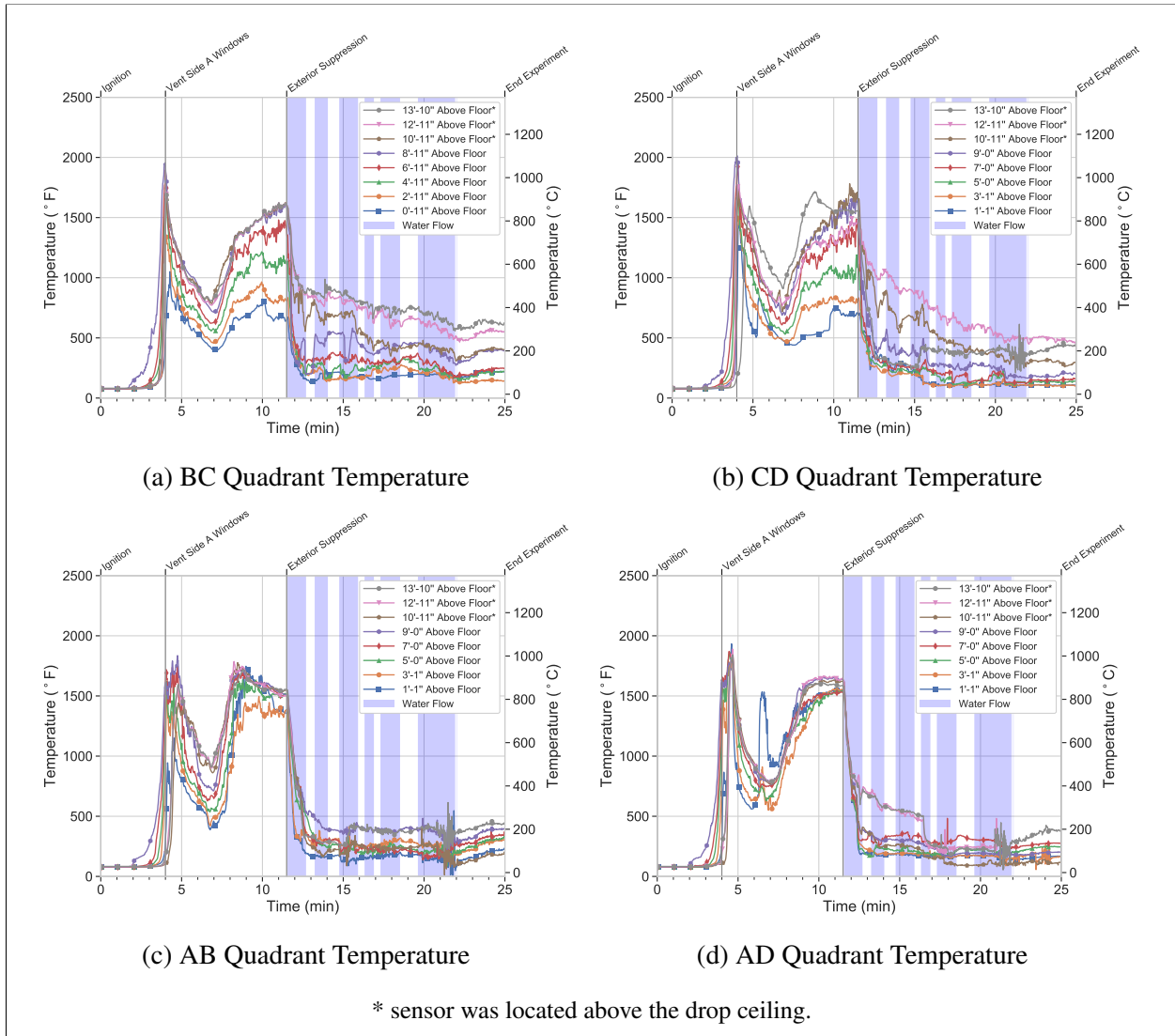
Side A

Figure 3.24: Fire compartment temperatures recorded during Experiment 3. Charts are arranged to correspond with the location of the thermocouple array in the unit. Side A is denoted outside the frame as a point of reference to the structure illustrated in Figure 3.23

61

(a) Ignition

(b) 1 min

(c) 2 min

(d) 3 min

(e) 4 min
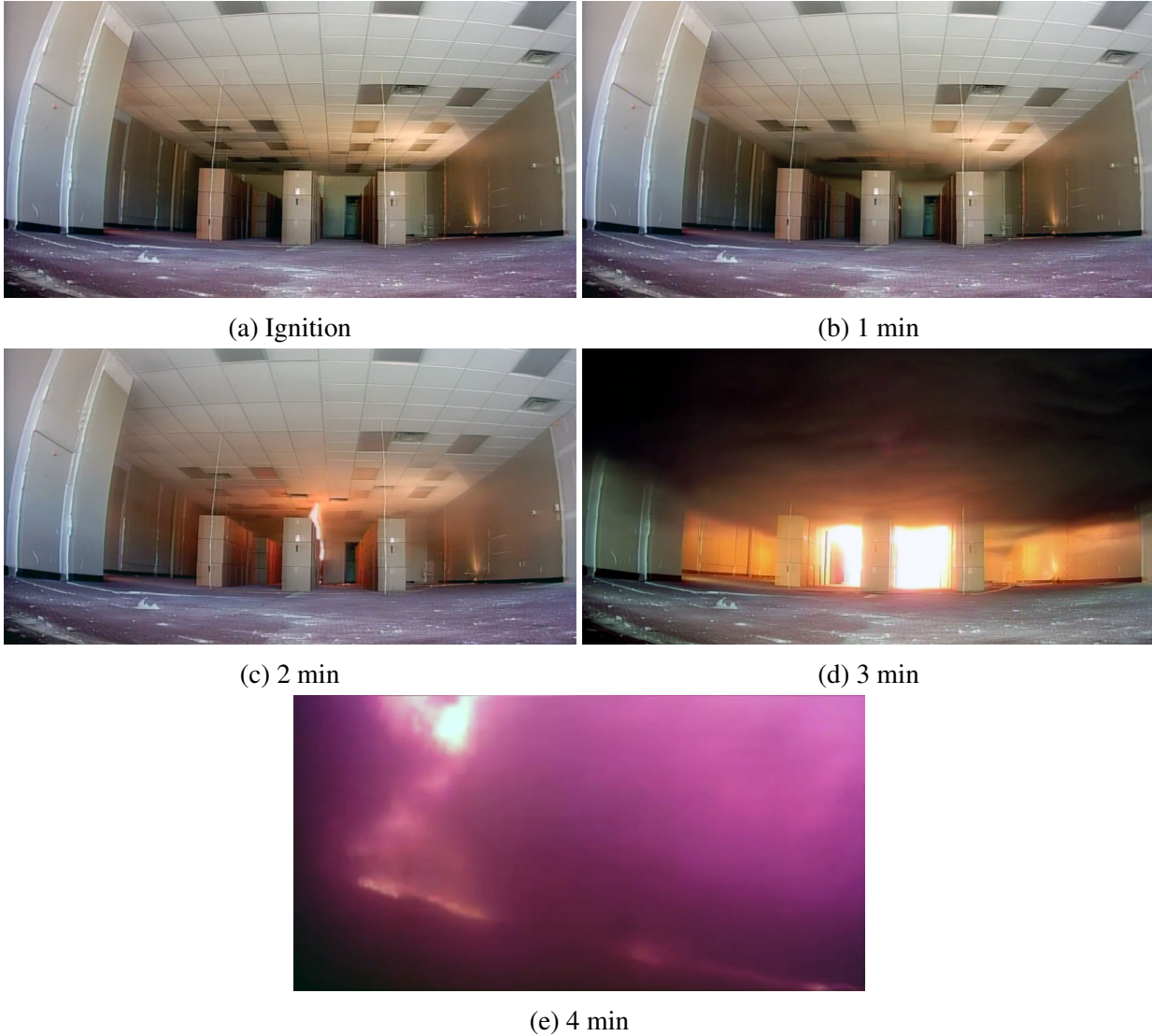
Figure 3.25: Sequential interior images during Experiment 3 looking toward the side C from the side A. The interior camera was lost after 4 min due to thermal damage from the fire.

The increase in temperature resulted in an expansion of the gases. This expansion was recorded on the differential pressure transducers as an increase in pressure above ambient 3 min after ignition (see Figure 3.26). The smoke layer descended to the top of the boxes at the same time as the initial pressure increase was recorded (see Figure 3.25d). With only the front door open, the pressure continued to increase resulting in a unidirectional exhaust of smoke and ambient gases out the front door starting 3 min 24 s after ignition and continuing until the the front windows were ventilated.
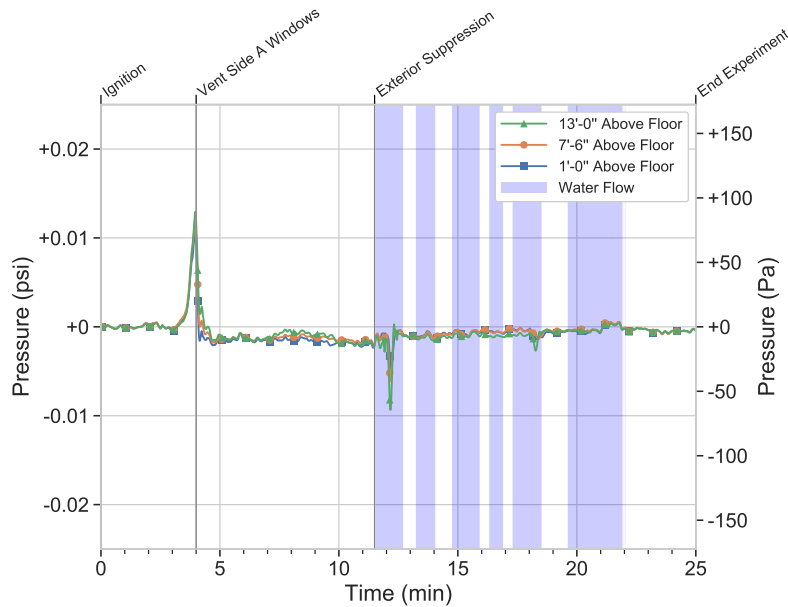
Figure 3.26: Differential pressures (fire compartment vs Side D exposure) recorded during Experiment 3. Positive values indicate overpressure in the fire compartment compared to the exposure compartment.
\* sensor was above the drop ceiling.

The ventilation of the front windows 4 min after ignition caused a series of fire dynamics changes and corresponding temperature changes throughout. At the same time the windows were ventilated, the carpet on the floor just inside the side A wall ignited (see Figure 3.25e). This occurred approximately the same time as the temperatures throughout the fire compartment exceeded 1,100 °F (593 °C) floor to ceiling, conditions representative of flashover. Flashover consumed the available oxygen in the rear of the fire compartment, and with no additional ventilation, that area became ventilation limited. Temperatures on the BC and CD quadrant thermocouple arrays decreased, indicating the lack of oxygen in that area was impacting the rate of combustion. As the temperatures in that area decreased, the amount of unburned fuel created from pyrolysis did as well.

The flow path created by the open front windows drew the flame-front forward in the unit. Within 30 s flames were visible exiting the front window on the exterior cameras (see Figure 3.27e). The thermocouple arrays in the AB and AD quadrants recorded a peak of approximately 1,800 °F (982 °C), 30 s after ventilation (4 min 30 s after ignition) occurred. At the same time, flames were visible in the upper gas layer exiting the top of the doorway (see Figure 3.27e). Flame spread along the carpet combined with radiation from flames in the upper layer led to the gases igniting at the side A vents 4 min 30 s after ignition, as seen in Figure 3.27f.

63

(a) 3 min 50 s    (b) 4 min 0 s (Vent)    (c) 4 min 10 s    (d) 4 min 20 s

(e) 4 min 30 s    (f) 4 min 40 s    (g) 4 min 50 s    (h) 5 min 0 s

(i) 5 min 30 s    (j) 6 min 0 s    (k) 6 min 30 s    (l) 7 min 0 s

(m) 7 min 30 s    (n) 8 min 0 s    (o) 8 min 30 s    (p) 9 min 0 s

Figure 3.27: Changes in visible fire from side A after horizontal ventilation of glass in Experiment 3. Rows 1 & 2 show rapid changes from 10 s before ventilation to 1 min after (3 min 50 s to 5 min). Rows 3 & 4 show the transition into a temporary decay phase and subsequent regrowth over the following 4 min.

The flames at the open front windows and door (see Figure 3.27g) consumed the available oxygen at the vent interface, preventing oxygen from entering further into the unit. The AB and AD quadrant thermocouple arrays, located over 15 ft (4.6 m) back into the unit, recorded a decrease, 1 min after ventilation (5 min after ignition) indicating a lack of oxygen available for combustion at that location. As temperatures decreased, the amount of unburned fuel being produced in that area also decreased.

The flaming combustion at the front windows lasted approximately 1 min until the carpet on the floor, and the unburned fuel in the upper gas layer was consumed (see Figure 3.27f-3.27j). With less pyrolysis occurring at the fuel located in the back two thirds of the unit, and no fuel (carpet) on the floor the flames at the front windows extinguished. This allowed the oxygen entering the windows to travel further back into the unit. Note the sharp temperature drop near the floor by the AB quadrant thermocouple array at 6 min 30 after ignition as cooler air reached that location. At the same time, temperatures briefly, though sharply, increased near the floor by the AD quadrant thermocouple array, likely due to additional oxygen reaching the smoldering fuels in that area, and transitioning them to flaming combustion.

As the fuel near the AB and AD quadrant thermocouple arrays transitioned from smoldering to flaming, the temperatures in those areas increased. By 8 min after ignition, 1 min 30 second after the temperature drop was recored, temperatures rebounded. Temperatures floor to ceiling exceed approximately 1,100 °F (593 °C), conditions representative of flashover. The localized flashover in that area consumed much of the available oxygen entering through the windows, limiting the amount which could travel further into the unit. Temperatures in the rear of the fire compartment, where the BC and CD thermocouple arrays were located, remained stratified and continued to increase until suppression.

Although the changes in fire dynamics resulted in temperature decreases where oxygen was not available, the temperatures remained above approximately 500 °F (232 °C), a critical temperature at which many components of firefighter personal protective equipment is tested [35], following ventilation.

The impact of the ventilation on temperatures in the room in the BC corner of the unit was less due to the isolation provided by the closed door and drop ceiling. Temperatures below the drop ceiling remained below 150 °F (66 °C), 5 ft (1.5 m) above the floor, approximately the head height of an average person (see Figure 3.28). These temperatures, however, remained steady as there was no direct water application or post-suppression ventilation of the space.
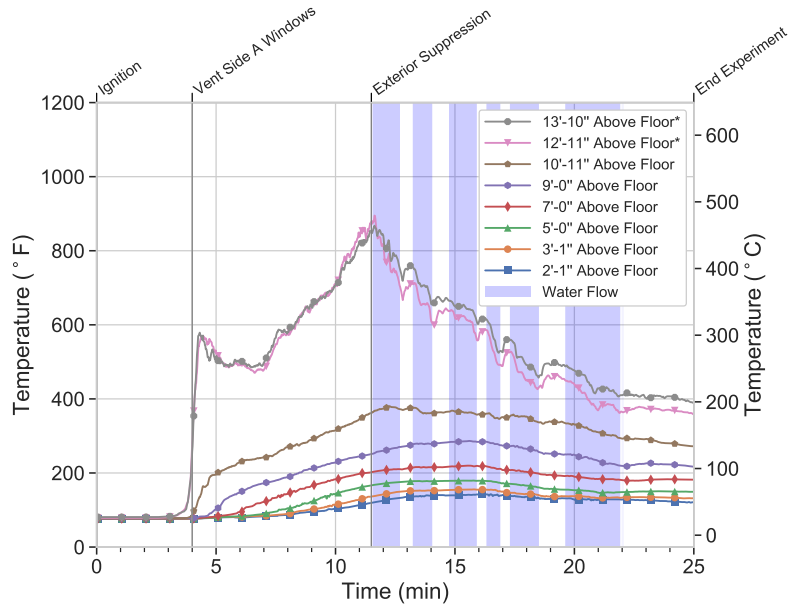
Figure 3.28: Temperatures recorded in the rear room with a closed door during Experiment 3.
\* sensor was above the drop ceiling.

The ventilation also impacted the differential pressure between the unit and the exterior. Immediately following the window ventilation, the pressure dropped from 0.013 psi (90 Pa) to a negative pressure (see Figure 3.26). The negative pressure can be attributed to the volume of exhaust exiting the unit exceeding the volume of gases entering the unit. The neutral plane was located approximately one third of the way up the windows (see Figure 3.29). The top two thirds of the window area was exhaust with the bottom third and the bottom half of the door as intake. The large exhaust area resulted in the volume of gases being exhausted exceeding the volume of gases being drawn in, and this a negative pressure was recorded on the pressure transducers.

Figure 3.29: View of the front of the unit from the exterior camera 4 min 30 s after ignition, 30 s after ventilation occurred, during Experiment 3. The red line illustrates the approximate location of the neutral plane.

Exterior suppression occurred via a 1 3/4 in. handline with a 7/8 in. smooth bore tip that flowed 160 gpm (606 lpm). The handline was directed through the side A windows and door 11 min 30 s after ignition. The water flow is presented in Figure 3.30. Heat was visible in the IR camera monitoring the roof 15 min after ignition, and a secondary 2 1/2 in. handline with a 1 1/8 in. smooth bore tip that flowed 265 gpm (1,003 lpm) applied water on the combustible roof decking from side A. All suppression occurred from the exterior and continued until all visible flames were extinguished. The total water used was 943 gal from the primary line and 455 gal from the secondary line for a total of 1,398 gal.
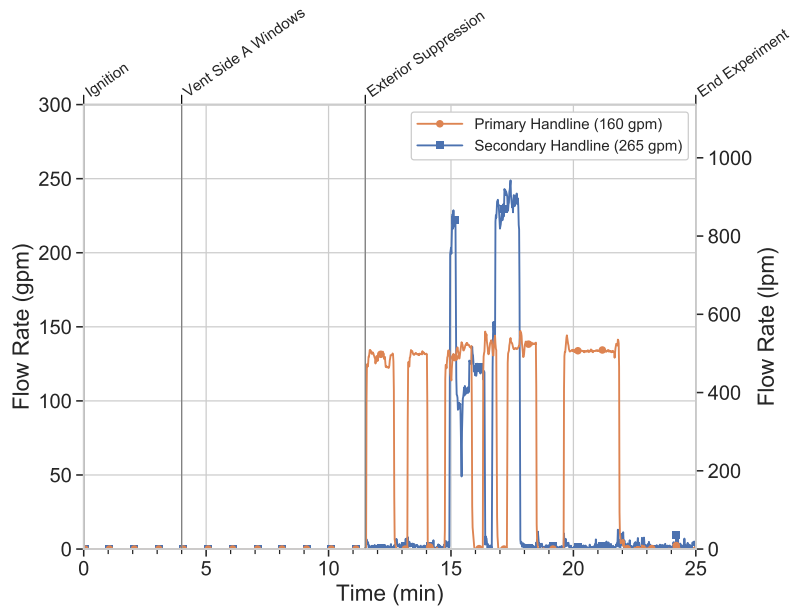
Figure 3.30: Water flows recorded during Experiment 3.

Temperatures in the rear of the unit at elevations below 9 ft (2.7 m) dropped under 500 °F (260 °C) within 1 min (see Figures 3.24a and 3.24b). The gas temperatures below 9 ft (2.7 m) dropped from 1,600 °F (871 °C) to under 500 °F (260 °C) within 1 min 30 s of suppression starting (see Figures 3.24c and 3.24d). Temperatures remained elevated (above 500 °F (260 °C)) above the 9 ft (2.7 m) measurement level throughout as heat was trapped in the upper portion of the unit, where no ventilation openings were present.

The isolated rear room gas temperatures above the drop ceiling remained elevated at levels similar to fire compartment. Below the drop ceiling the isolation of the ceiling and door trapped the heat and kept temperatures elevated near the levels recorded at the time of suppression.

Plots of wind speed and wind direction are presented in Figure 3.31 from ignition until the end of the experiment. The wind speed was in the range of 1 mph to 12 mph (0.4 m/s to 5.4 m/s), blowing from the southwest toward the northeast, perpendicular to the front of the unit. The ambient air temperature data acquisition malfunctioned during this experiment. Although the wind direction had the potential to make the ventilation openings at the front of the unit less efficient, the low wind speed made this less likely. Without a control experiment in a no-wind condition, it is difficult to determine how much of an impact this had on the experiment.
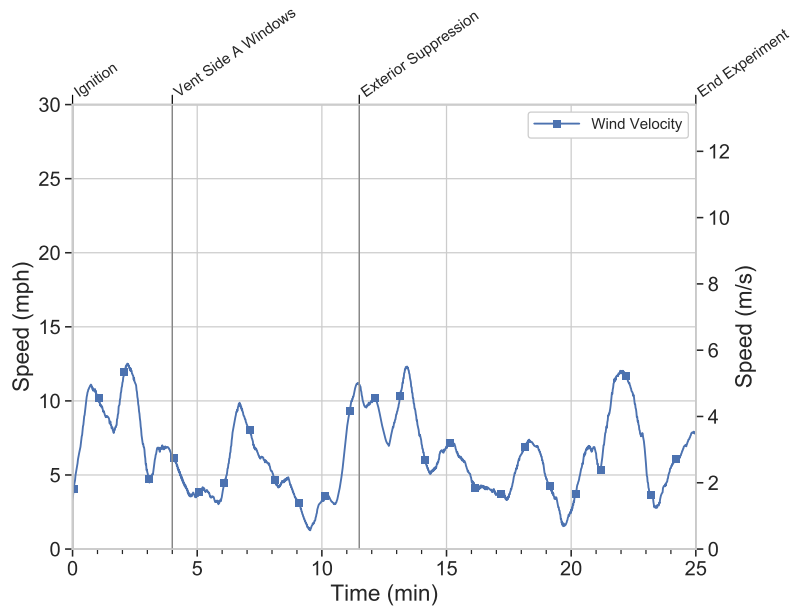
(a) Wind Speed
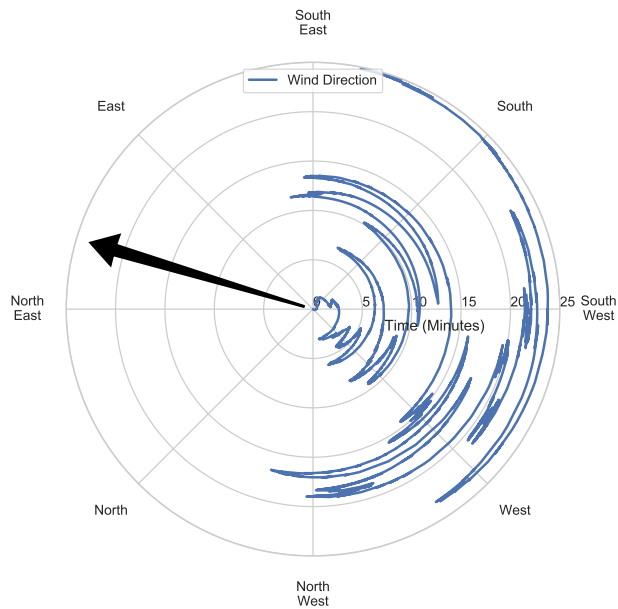


Side A

North on the chart is oriented to correspond with north on the site layout
(see Figure 2.4) and corresponding instrument plan (see Figure 3.23), with
side A labeled for reference. The arrow indicates the average direction the
wind was blowing.

(b) Wind Direction

Figure 3.31: Weather conditions recorded during Experiment 3.

## 3.4 Experiment 4 - Horizontal Ventilation

Experiment 4 was designed to examine the impact of horizontal ventilation, followed by suppression in a volume twice as large as other experiments. Unit 1069–1071 was the fire unit, with unit 1067 as the side B exposure. One front door to unit 1069–1071 was open at the beginning of the experiment.

The unit was instrumented to monitor the thermal conditions with thermocouple arrays, and differential pressure sensor arrays between the unit and the exterior as illustrated in Figure 3.32. The thermocouple arrays contained 7 thermocouples started at 2 ft 6 in. (0.8 m) above the floor with a thermocouple every 2 ft (0.6 m), ending with the last thermocouple 1 in. (2.3 cm) below the metal roof deck. The differential pressure transducer array included pressure transducer taps at 1 ft (0.3 m), 7.5 ft (2.3 m) and 14.5 ft (4.4 m) above the floor, measuring the differential pressure between the fire unit and the exterior.
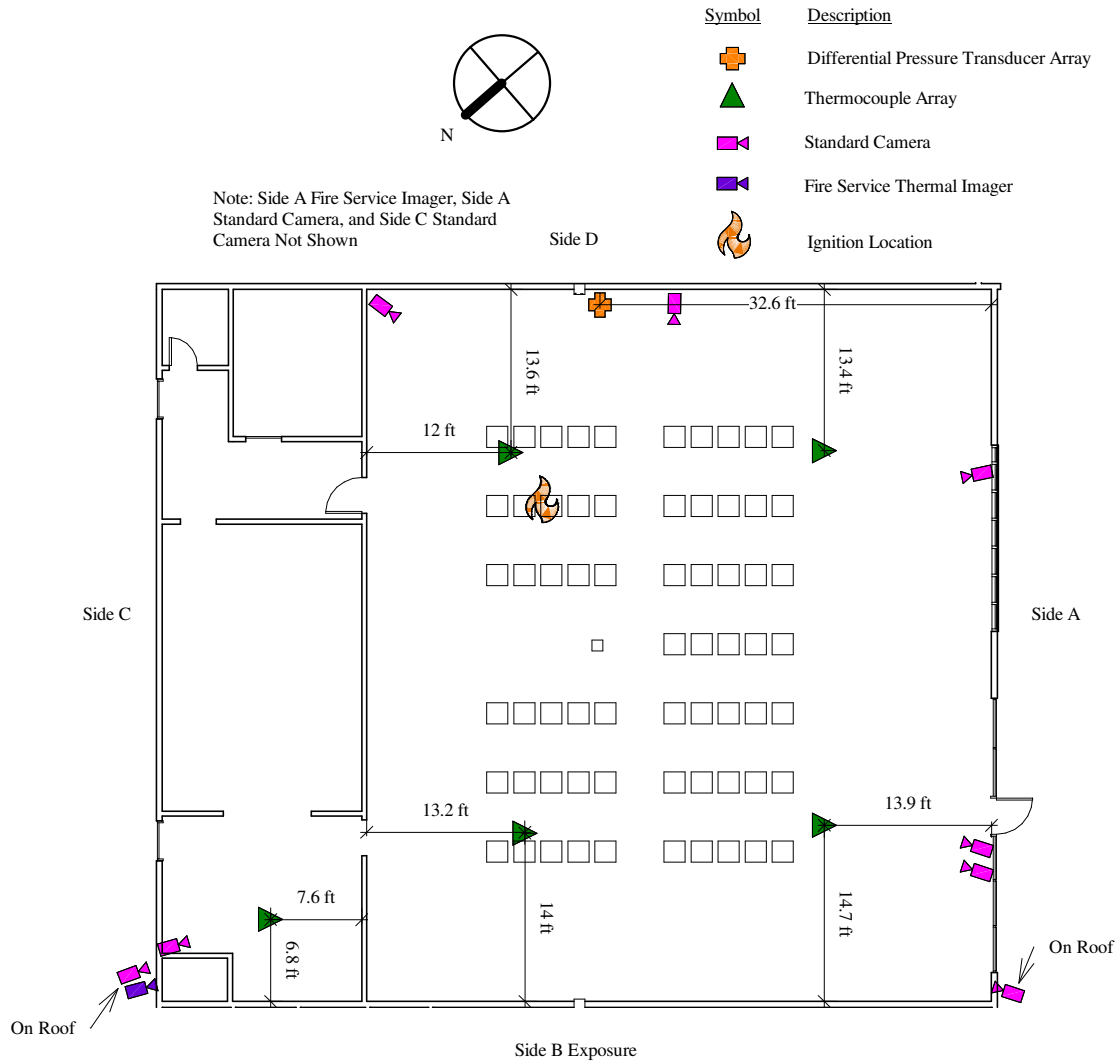
Figure 3.32: Instrument plan for unit 1069–1071. Not shown are the locations where wind speed, wind direction, ambient temperature and suppression water flow were recorded.

The experiment started with ignition (source described in Section 2.3) located between the second and third stacks of boxes from the rear, one row in from the side D wall as show in Figure 3.32. Table 3.5 lists the interventions from Experiment 4.

Table 3.5: Experiment 4 Sequence and Ventilation

| Timing (mm:ss) | Event | Opening(s) | Area ft$^2$ (m$^2$) |
|---|---|---|---|
| 00:00 | Ignition | Door | 19.0 (1.8) |
| 04:00 | Ventilation | Door and Five Windows | 162.8 (15.1) |
| 11:26 | Exterior Suppression 1 | - | - |
| 12:21 | Exterior Suppression 2 | - | - |
| 13:42 | Exterior Suppression 3 | - | - |
| 25:00 | End Experiment | - | - |

The gas temperatures recorded in Experiment 4 are presented in Figure 3.33 starting at ignition and ending at the completion of the experiment. Following ignition, it took 1 min for an increase in gas temperature to be recorded at the thermocouple array nearest ignition in the CD quadrant (see Figure 3.33a), followed by the array in the BC Quadrant at 1 min 30 s and the front two arrays in the AB and AD quadrants at 2 min. Flames were visible impinging on the drop ceiling at 2 min after ignition (see Figure 3.34c).

Side A

(a) CD Quadrant Temperature

(b) AD Quadrant Temperature

(c) BC Quadrant Temperature

(d) AB Quadrant Temperature

* sensor was above the drop ceiling.
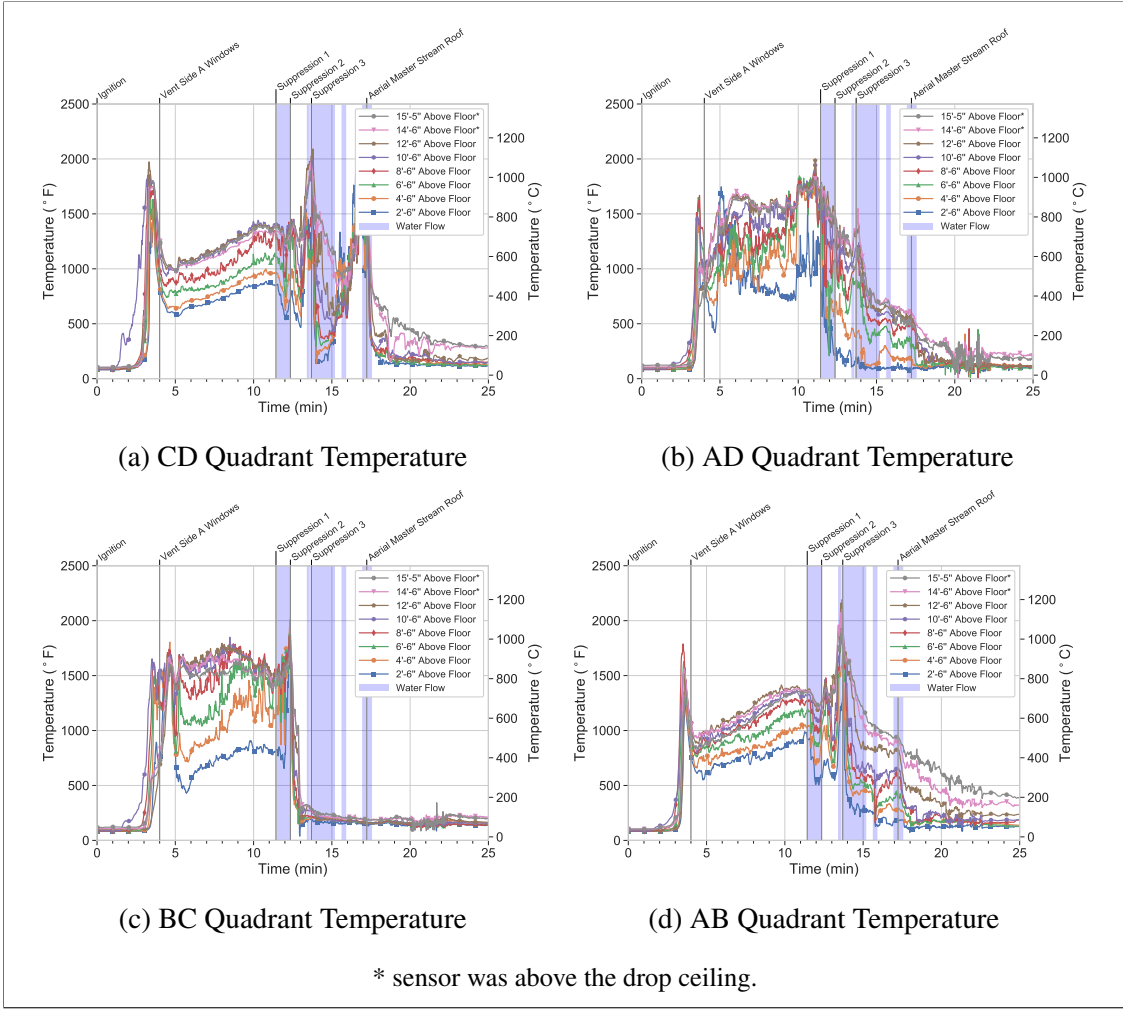
Figure 3.33: Fire compartment temperatures recorded during Experiment 4. Charts are arranged to correspond with the location of the thermocouple array in the unit. Side A is denoted outside the frame as a point of reference to the structure illustrated in Figure 3.32.

(a) Ignition

(b) 1 min

(c) 2 min

(d) 3 min

(e) 4 min
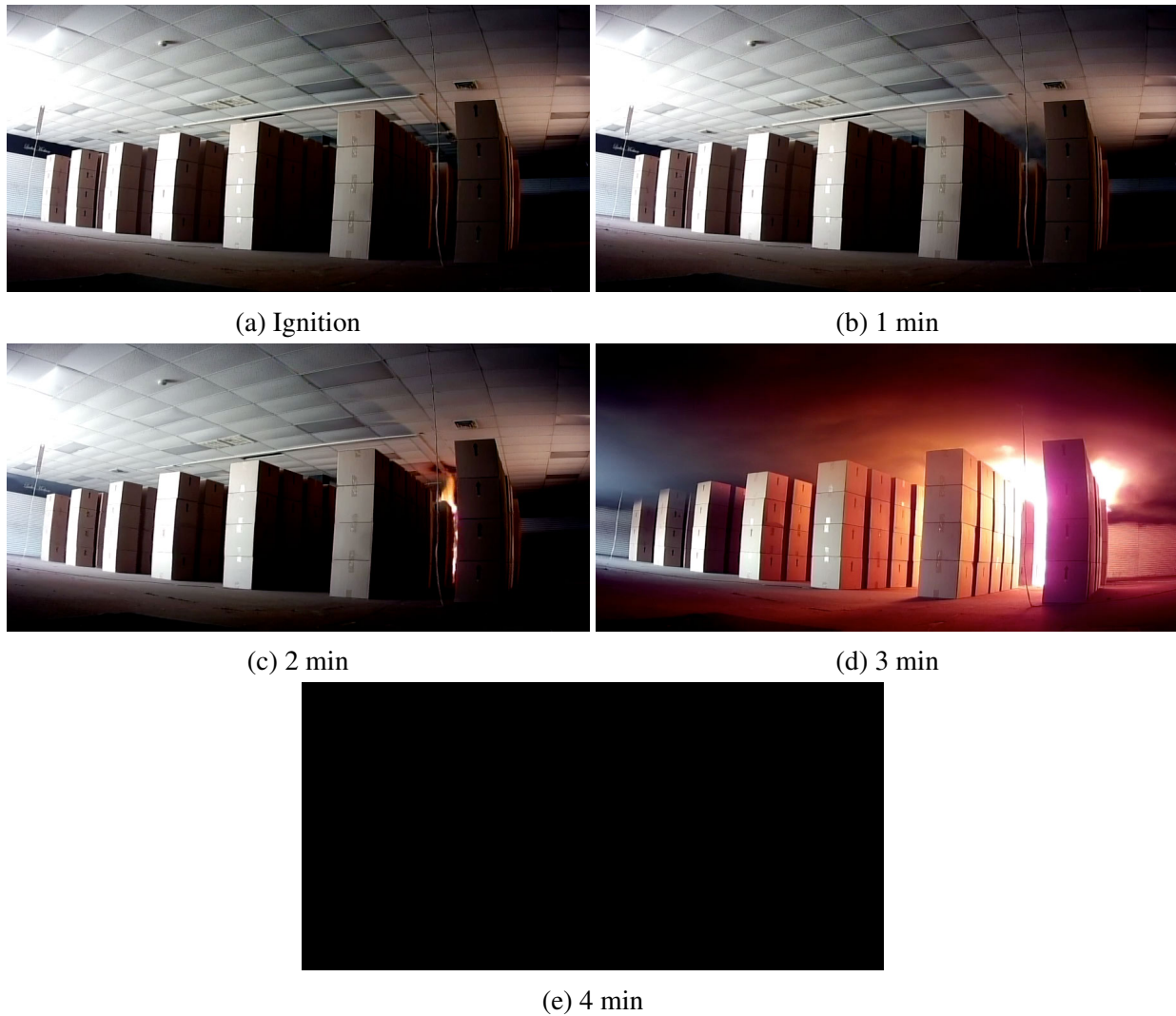
Figure 3.34: Sequential interior images during Experiment 4 looking toward the the B/C corner from side A. The interior camera was lost after 4 min due to the thermal damage from the fire.

The increase in temperature resulted in an expansion of the gases. This expansion was recorded on the differential pressure transducers as an increase in pressure above ambient at 3 min after ignition (see Figure 3.35). By 3 min the smoke layer had descended to the level of the top of the commodity boxes, with flaming combustion visible in the rows adjacent ignition. The pressure peaked 3 min 30 s after ignition, exceeding the maximum pressure the transducer was rated for 0.018 psi (124 Pa).
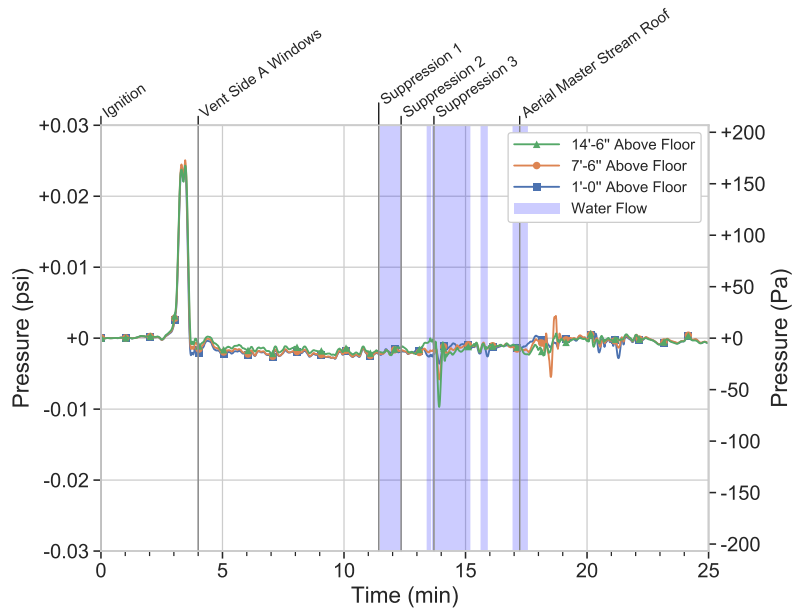
Figure 3.35: Differential Pressures recorded during Experiment 4. Positive values indicate increase of pressure in the fire compartment.
* sensor was above the drop ceiling.

With only the front door to the unit open and pressures in excess of 0.018 psi (124 Pa) a unidirectional exhaust was observed at the front door (see Figure 3.36). The exhaust started at the time the pressure increase was recorded at 3 min post ignition and continued until 3 min 35 s. The trailer on the right side of the image in Figure 3.36 was located in excess of 75 ft (22.9 m) from the front door of the unit (estimated based on the wire runs for instrumentation from the trailer to the front door). The exhaust can be seen extending to the side of trailer, indicating it extended a minimum of 75 ft (22.9 m).

75

|          |          |          |
|:--------:|:--------:|:--------:|
| (a) 2 min 50 s | (b) 3 min 0 s | (c) 3 min 10 s |
| (d) 3 min 20 s | (e) 3 min 30 s | (f) 3 min 40 s |
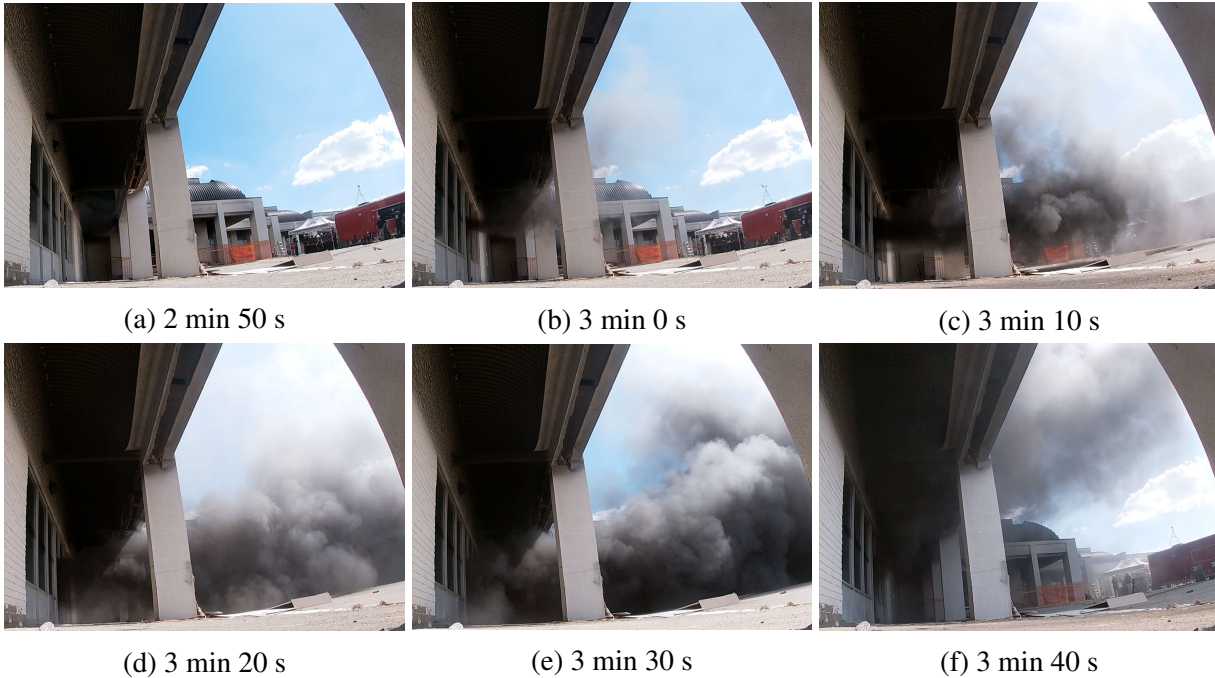
Figure 3.36: Sequential exterior images during Experiment 4 of front door exhaust from 2 min 50 s until 3 min 40 after ignition.

Temperatures in the fire compartment peaked at 3 min 30 s corresponding with the peak pressure. The AB, AD, and CD quadrant thermocouple arrays recorded uniform floor to ceiling temperatures in excess of 1,200 °F (649 °C), conditions representative of flashover, for 30 s. Temperatures in the BC quadrant, furthest from the door and the ignition, remained stratified with temperatures ranging from 800 °F (427 °C) at 2.5 ft above the floor to 1,200 °F (649 °C) at 1 in. (2.3 cm) below the roof deck. In the rear room, open to the fire compartment, temperatures above the drop ceiling were 500 °F (260 °C) with temperatures below the drop ceiling between 200 °F (93 °C) to 300 °F (149 °C) prior to side A window vent (see Figure 3.37).
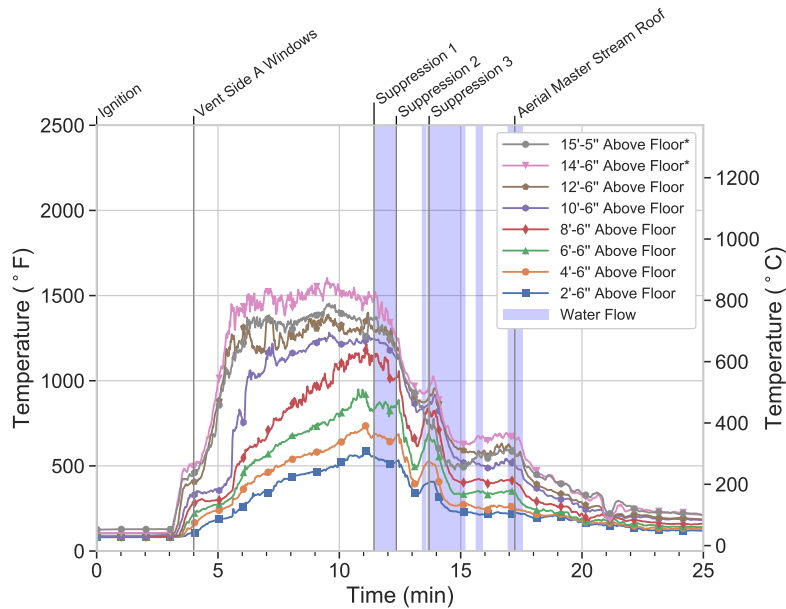
Figure 3.37: Temperatures recorded in the open rear room during Experiment 4.
* sensor was above the drop ceiling.

At 3 min 40 s after ignition, the uni-directional exhaust flow at the front door stopped and temperatures and pressures were decreased. The pressure dropped by 0.026 psi (180 Pa) in 15 s after the exhaust flow stopped and became negative. The drop in pressure was a result of contraction of the gases as they cooled from in excess of 1,750 °F (954 °C) to under 1,000 °F (538 °C), as well as the flow out the top of the doorway exceeding the air being drawn in the bottom. The end result was a value of −0.002 psi (−14 Pa) on the pressure transducers measuring differential pressure between the unit and the exterior and bi-directional flow at the front door.

Ventilation of the side A windows occurred at 4 min after ignition, and resulted in the additional exhaust of combustion products. Following ventilation, the thermocouple arrays in the AB, AD, and CD quadrants continued to decrease until temperatures again started to increase as oxygen reached the fuel, at 30 s after ventilation. The arrays in the AB, AD and CD quadrants recorded stratified temperatures at 500 °F (260 °C), 2.5 ft (0.8 m) above the floor, and greater than 1,000 °F (538 °C) at 1 in. (2.3 cm) below the metal deck. The thermocouple array in the AD quadrant recorded higher temperatures as it was located nearest the door where the air being drawn in had the most impact on conditions (see Figure 3.33d and 3.33b and 3.33a).

Temperatures steadily increased over the following 7 min 30 s. Peak temperatures prior to suppression were recored 1 in. (2.3 cm) below the metal roof deck, exceeding 1,750 °F (816 °C). During this time flames were present at all of the open vents where the hot fuel mixed with fresh air (oxygen) (see Figure 3.38a).

77

(a) Just prior to the initial suppression.　　　　(b) 30 s after the initial suppression started.

Figure 3.38: Conditions from the viewpoint of the nozzle firefighter at 11 min 30 s just prior to the initial suppression and 30 s later in Experiment 4.

Exterior suppression occurred via a 2 1/2 in. handline with a 1 1/8 in. smooth bore tip that flowed 265 gpm (1,003 lpm). The handline was directed through the side A windows and door, from the AB corner toward the CD corner (see Figure 3.39 position 1), at 11 min 30 s after ignition. The water flow rate from the suppression handlines is presented in Figure 3.40.
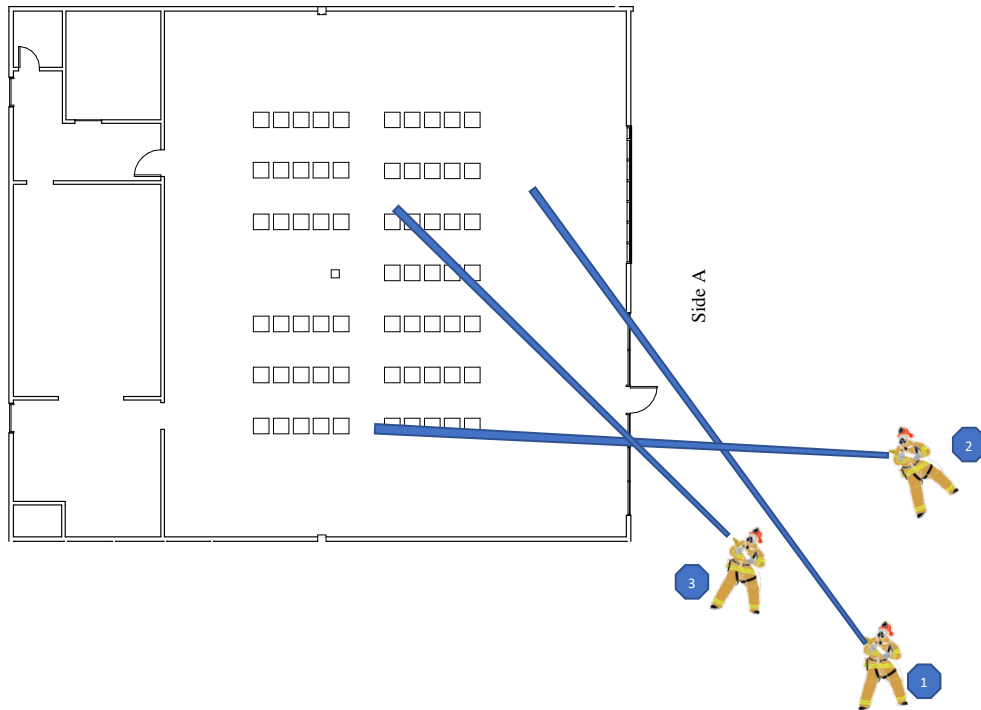


Figure 3.39: Graphic representation of water application locations and general direction during Experiment 4.
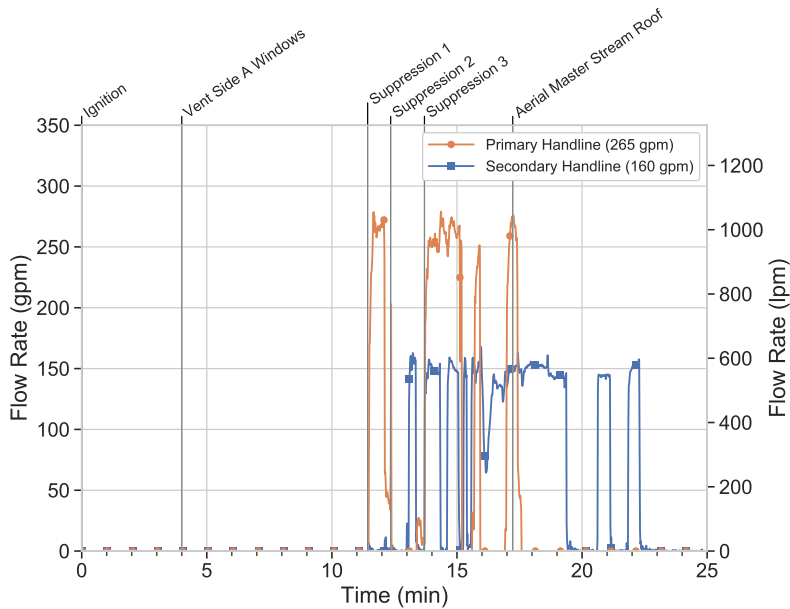
Note: signal for primary hand line lost between 12 min 21 s and 13 min 20 s.

Figure 3.40: Water flows recorded during Experiment 4.

The water application extinguished the flames at the ventilation openings (see Figure 3.38b), but only had a limited impact on temperatures in the AD quadrant where the line was directed. Temperatures near the floor where the water was directed decreased by approximately 750 °F (417 °C) (see Figure 3.33b). The AB, BC, and CD quadrant thermocouple arrays recorded decreases on the order of 250 °F (139 °C) until the line was shut down. The line flowed for 45 s. After the line was shut down, temperatures increased to levels above what was recorded prior to suppression. Extinguishing the flames at the front of the unit allowed the oxygen entering the front to travel further into the compartment before being consumed. This resulted in an increase in the rate of combustion near the AB, BC, and CD thermocouple arrays.

The primary handline was repositioned to be perpendicular with side A, and water was applied 12 min 21 s after ignition (see Figure 3.39 position 2). When the line was repositioned for suppression, it impacted the data collection from the flow meter and thus this water application is not represented as flow on Figure 3.40. The water was directed toward the BC quadrant, traveling through the AB quadrant. This flow had a limited impact on the temperatures measured in the AB quadrant. Temperatures recorded on the BC quadrant thermocouple array, where the water from the handline hit the floor, decreased from 1,750 °F (954 °C) to 250 °F (121 °C) in 30 s.

The handline flowed for approximately 50 s at position 2 until 13 min 15 s after ignition. After the line was shut down, temperatures recorded on the AD quadrant thermocouple array increased to more than 1,250 °F (677 °C) floor to ceiling, conditions representative of a localized flashover. The increase was the result of additional oxygen entering the front windows, reaching that area, and fueling fire growth because there was no direct application of water to the fuel in that area.

79

When the second water application appeared to have had the desired impact (see Figure 3.41), the suppression crew repositioned the handline to position 3 in Figure 3.39, closer to the unit than position 1. Temperatures in the AB and CD quadrants, where the line was now able to reach, dropped from in excess of 1,500 °F (816 °C) to under 500 °F (260 °C) during the 1 min 30 s the line was flowed (see Figure 3.33a). The drop in temperature caused gas contraction, and the differential pressure dropped below ambient to −0.1 psi (−69 Pa) and then returned to near ambient (see Figure 3.35).



(a) Just prior to the second suppression.

(b) 30 s after the second suppression started.

Figure 3.41: Conditions from the viewpoint of the nozzle firefighter at 12 min 21 s, just prior to initiating the second exterior water application, along with 30 s later (Experiment 4).

A secondary 1 3/4 in. handline with a 7/8 in. smooth-bore tip, that flowed 160 gpm was used to apply water on the front facade and roof decking, which had visible fire 13 min after ignition. The line was operated on and off, suppressing exterior fire until 21 min 30 s after ignition.

Temperatures started to increase again in the CD quadrant 15 min after ignition. The stability of the roof structure was in question, necessitating the use of an aerial master stream to reach the area where the handlines could not. The master stream was directed through a hole that had opened in the roof due to the fire at 17 min 14 s, and was operated for 1 min 39 s. All suppression occurred from the exterior and continued until all visible flames were extinguished.

The primary attack line utilized 938 gal and the secondary line utilized 904 gal for a total of 1,842 gal. The water flow rate from the aerial master stream was not recorded. Repositioning of the primary handline was required so the water could impact the entire unit. Had the line location been maintained, more water flow may have been required to achieve the same result.

Plots of wind speed, ambient air temperature, and wind direction are presented in Figure 3.42 from ignition until the end of the experiment. The wind speed ranged from 0 mph to 15 mph (0 m/s to 6.7 m/s), blowing from the north to the south, from the BC corner toward the AD corner of the unit. Although the wind speed was in the range that could have impacted the fire dynamics of the experiment, the direction was not across or into any of the ventilation openings and thus most likely had limited impact on the experiment.

The ambient air temperature sensor was impacted by the unidirectional exhaust at 3 min 30 s, recording a 45 °F (25 °C) increase. The exhaust can be seen extending out to the location of the ambient temperature sensor, located on the exterior of the red instrumentation trailer in Figure 3.36. Outside the impact of the unidirectional exhaust, the ambient temperature remained in the range of 75 °F to 80 °F (24 °C to 27 °C) during the experiment.
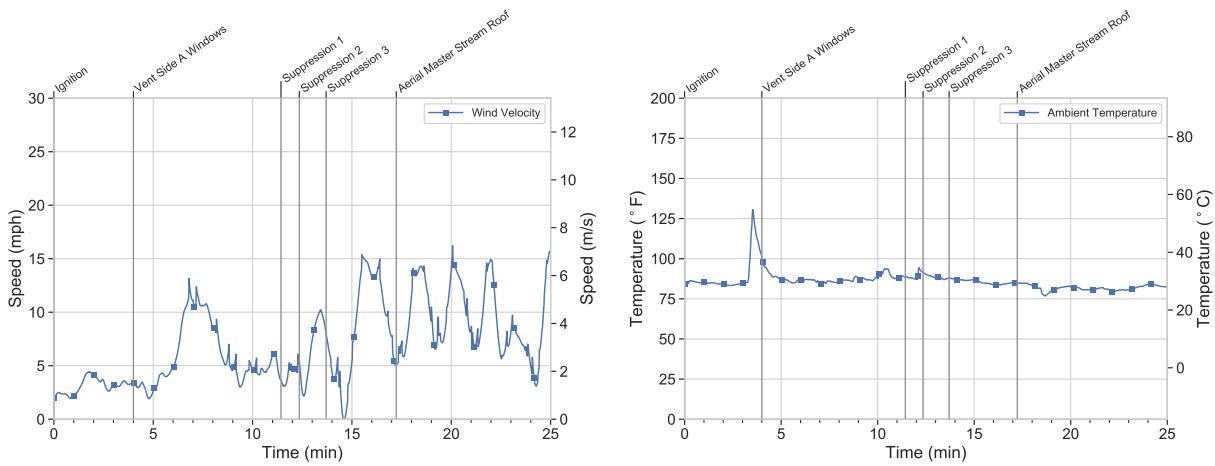


(a) Wind Speed
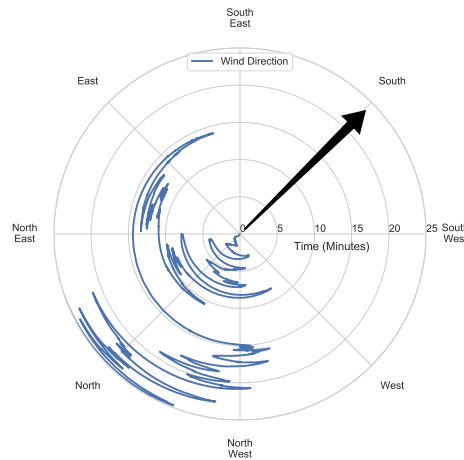
(b) Air Temperature



North on the chart is oriented to correspond with north on the site layout (see Figure 2.4) and corresponding instrument plan (see Figure 3.32). The arrow indicates the average direction the wind was blowing.

Figure 3.42: Weather conditions recorded during Experiment 4.

81

## 3.5 Experiment 5 - Horizontal and Vertical Ventilation

Experiment 5 was designed to evaluate the impact of vertical ventilation with coordinated suppression in a 30 ft (9.1 m) by 70 ft (21.3 m) commercial unit. Unit 1067 was the fire unit, with unit 1069–1071 as the side D exposure. The front door to unit 1067 was open at the beginning of the experiment. All exterior doors in unit 1069–1071 remained closed throughout the experiment.

The unit was instrumented to monitor the thermal conditions with thermocouple arrays, differential pressure sensor arrays between the unit and the exterior, and bi-directional probes in the chimneys leading to the roof vents and the front door as illustrated in Figure 3.43. The thermocouple arrays contained seven thermocouples starting 1 ft 2 in. (0.4 m) above the floor with a thermocouple every 2 ft (0.6 m), ending with the last thermocouple 1 in. (2.3 cm) below the gypsum wallboard ceiling. The differential pressure transducer array included pressure transducer taps at 1 ft (0.3 m), 7.5 ft (2.3 m) and 12.2 ft (3.7 m) measuring the differential pressure between the fire unit and the exterior. The bi-directional probe array in the front door included probes and thermocouples 4.0 in. (10.2 cm), 22.0 in. (55.9 cm), 40 in. (101.6 cm), and 76 in. (193.0 cm) above the floor level. Each chimney (recall Figure 2.19) had an array of three bi-directional probes and thermocouples centered in the opening from front to rear. The probe array started 12.0 in. (30.5 cm) from the side B vent wall, and the probes and thermocouples were spaced 12.0 in. (30.5 cm) apart. The array was vertically located 28.0 in. (71.1 cm) above the ceiling.



Figure 3.43: Instrumentation plan for unit 1067. Not shown are the locations where wind speed, wind direction, ambient temperature, and suppression water flow were recorded. The dark gray shaded area was isolated from the experimental volume for these experiments.

The experiment started with ignition (source described in Section 2.3) located between the second and third stacks of boxes from the rear in the center row as shown in Figure 3.43. The ventilation and suppression occurred as indicated in Table 3.6.

Table 3.6: Experiment 5 Sequence and Ventilation

| Timing (mm:ss) | Event | Opening(s) | Horizontal Area ft$^2$ (m$^2$) | Vertical Area ft$^2$ (m$^2$) |
|---|---|---|---|---|
| 00:00 | Ignition | Door | 19.0 (1.8) | |
| 05:00 | Exterior Suppression & Ventilation 1 | Door and Roof Vent | 19.0 (1.8) | 16.0 (1.5) |
| 05:30 | Ventilation 2 | Door and Two Roof Vents | 19.0 (1.8) | 32.0 (3.0) |
| 06:14 | Exterior Suppression 2 | - | | - |
| 06:45 | Interior Suppression | - | | - |
| 15:00 | End Experiment | - | | - |

The gas temperatures proximal to the fuel recorded in Experiment 5 are presented in Figure 3.44, starting at ignition and ending at the completion of the experiment. Following ignition, it took 1 min 30 s for an increase in gas temperature to be recorded at the thermocouples 14 ft (4.3 m) above the floor in the main volume. Flames were visible impinging on the gypsum board ceiling 2 min after ignition (see Figure 3.45c). The increase in temperature resulted in gas expansion, which was captured as unidirectional flow out the front door 2 min 30 s after ignition (see Figure 3.46a), and an increase in pressure on the differential pressure transducers 3 min after ignition (see Figure 3.47). For the first 30 s, the exhaust was made up of the gases in the compartment prior to ignition, and the temperatures in the door remained near ambient. As the gases at the ceiling expanded, they forced out the gases lower in the space. At 3 min, temperatures in the door increased, indicating the gases being exhausted contained products of combustion (see Figure 3.46b).
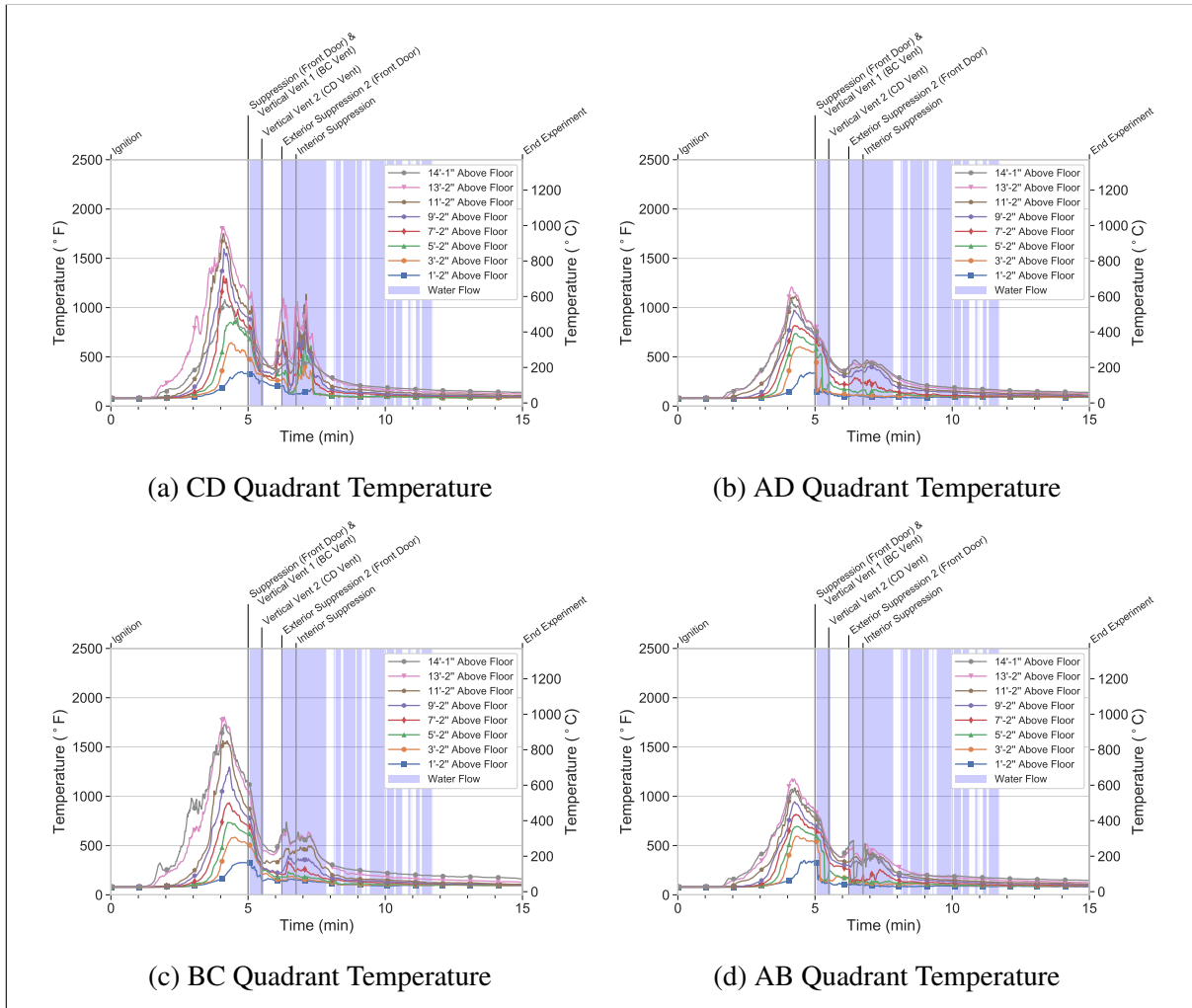
Figure 3.44: Fire Compartment temperatures recorded during Experiment 5. Charts are arranged to correspond with the location of the thermocouple array in the unit. Side A is denoted outside the frame as a point of reference to the structure illustrated in Figure 3.43.

(a) Ignition

(b) 1 min

(c) 2 min

(d) 3 min

(e) 4 min

(f) 5 min

(g) 6 min

(h) 7 min

(i) 8 min

(j) 9 min

(k) 10 min

(l) 11 min

(m) 12 min

(n) 13 min

(o) 14 min

Figure 3.45: Sequential interior images during Experiment 5 looking toward side C from side A.
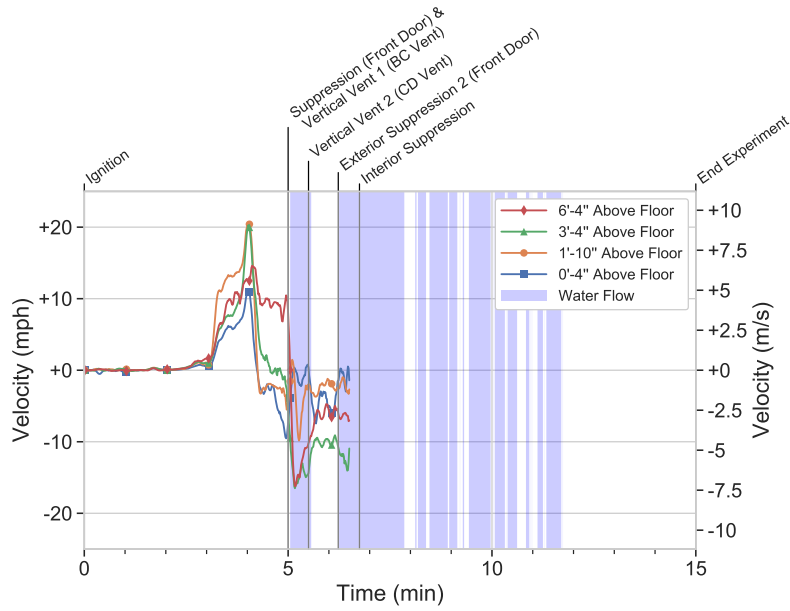
(a) Gas Velocities
Positive direction indicates flow out of the unit.
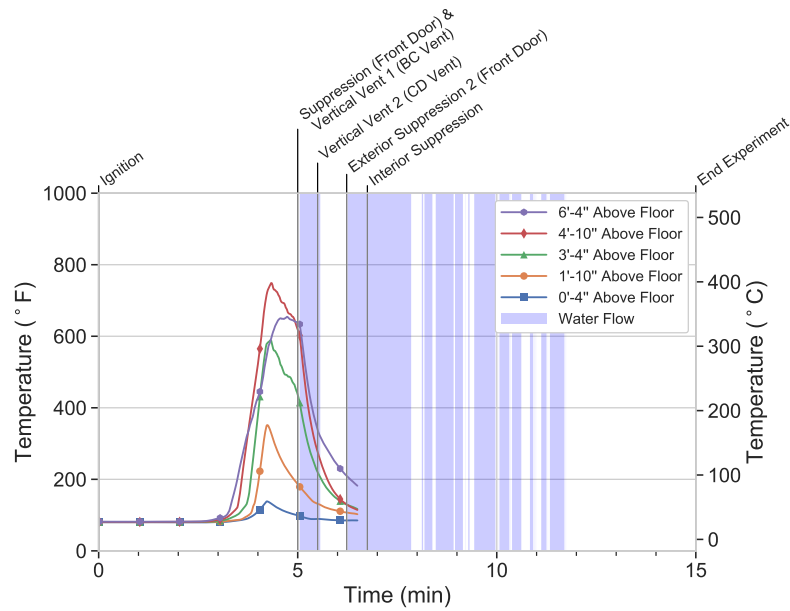


(b) Temperatures

Figure 3.46: Gas velocities and temperatures recorded in the front door during Experiment 5. The velocity probe array was moved at 6 min 30 s to allow the suppression crew access for interior suppression, stopping data collection on the sensor array.
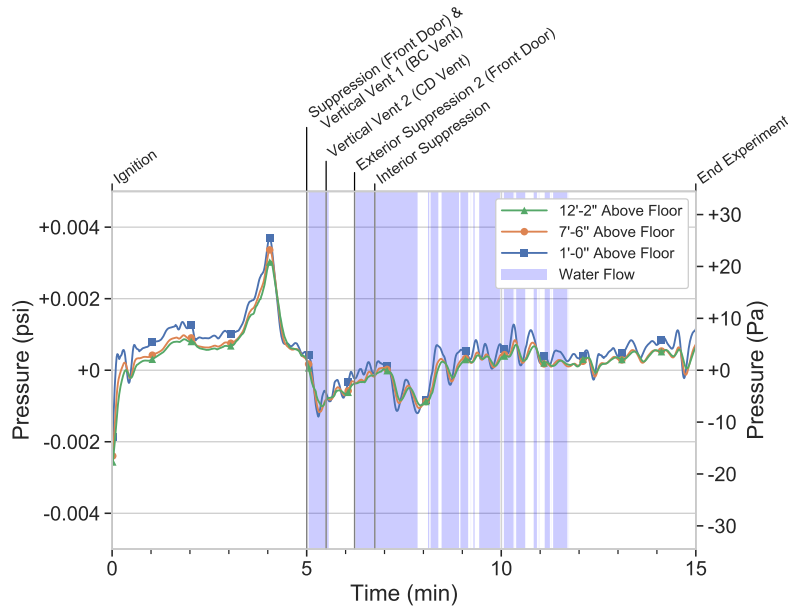
Figure 3.47: Differential pressures recorded during Experiment 5. Positive values indicate an a pressure rise in the fire compartment.

The smoke layer descended to the top of the boxes 3 min (see Figure 3.45d) after ignition and visibility was obscured by 5 min after ignition (see Figure 3.45f). Temperatures in all quadrants increased to a peak 4 min after ignition. The highest temperatures (1,750 °F (954 °C)) were recorded on the BC and CD thermocouple arrays, which were closest to ignition. The AB, AD, and rear (see Figure 3.48) thermocouple arrays recorded peak temperatures of 1,250 °F (677 °C) near the ceiling. Temperatures 1 ft (0.3 m) above the floor in all quadrants remained under 450 °F (232 °C). The front door exhaust peaked 4 min after ignition at 20 mph (8.9 m/s) on the middle probes and 10 mph (4.5 m/s) on the top and bottom probes. The pressure peaked at 0.004 psi (28 Pa), which corresponded with the peak temperatures and peak exhaust flows from the front door.
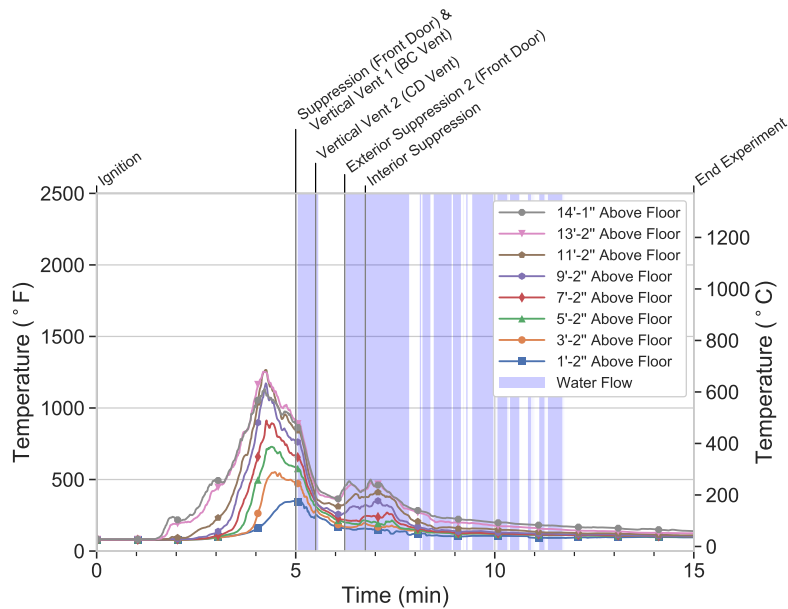
Figure 3.48: Rear temperatures recorded during Experiment 5.

After the fire had consumed the available oxygen within the unit, the fire entered a ventilation-limited state. This caused temperatures to decrease. Peak temperatures dropped from 1,750 °F (954 °C) to 1,250 °F (677 °C) in the 30 s after the fire became ventilation limited. This decrease in temperature corresponded with gas contraction, and combined with the exhaust flow out the unit, resulted in a decrease in the differential pressure. Pressures dropped by 0.003 psi (24 Pa) in the same time period the temperatures had decreased. The pressure decrease caused the front door to become a bi-directional vent, with a 10 mph (4.5 m/s) exhaust at the top and −2 mph (0.9 m/s) inflow at the bottom 4 min 30 s after ignition.

At 5 min post-ignition, coordinated vertical ventilation and suppression occurred. The 4 ft x 4 ft (1.2 m x 1.2 m) BC roof vent was opened for vertical ventilation. At the same time, the suppression crew directed a 1 3/4 in. handline with a 7/8 in. smooth-bore tip that flowed 160 gpm through the front door. Flow-rate data for the handline is presented in Figure 3.49.
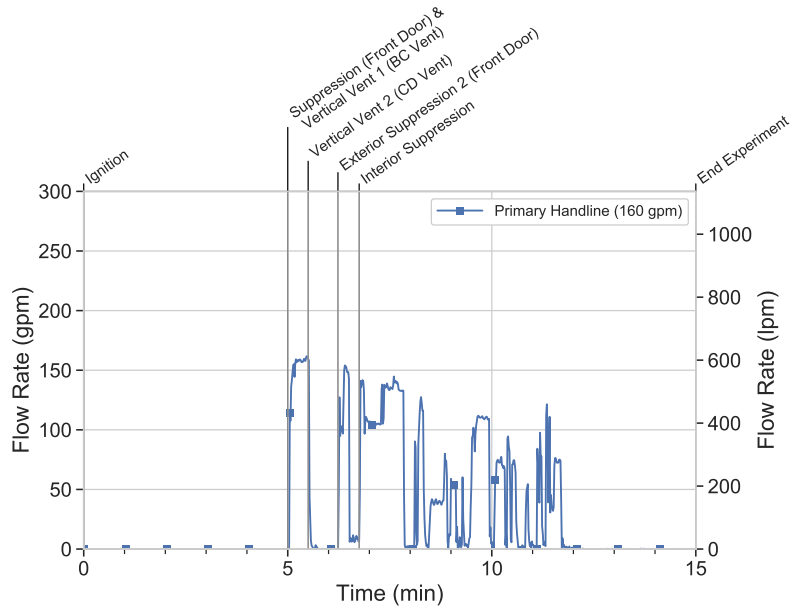
Figure 3.49: Water flows recorded during Experiment 5.

The vertical ventilation established a uni-directional flow path. Ambient air entered the front door at 15 mph (6.7 m/s), see Figure 3.46a, and products of combustion exited out of the open roof vent at 15 mph (6.7 m/s), see Figure 3.50.



(a) BC Roof Vent
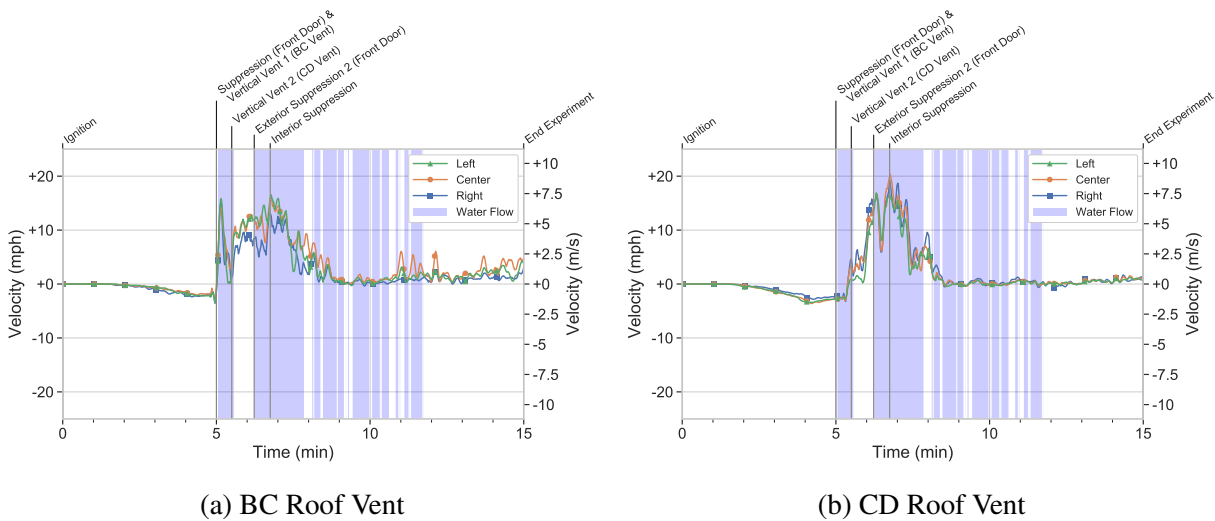
(b) CD Roof Vent

Figure 3.50: Gas velocities in the exhaust vents recorded during Experiment 5. Positive direction indicates flow out of the unit.

With the roof vents included in the exhaust portion of the flow path, the temperatures recorded in the roof vents increased. The increase only lasted for 15 s and did not exceed the previous peak of 750 °F (399 °C), recorded before firefighter intervention occurred (see Figure 3.51).

(a) BC Roof Vent



(b) CD Roof Vent
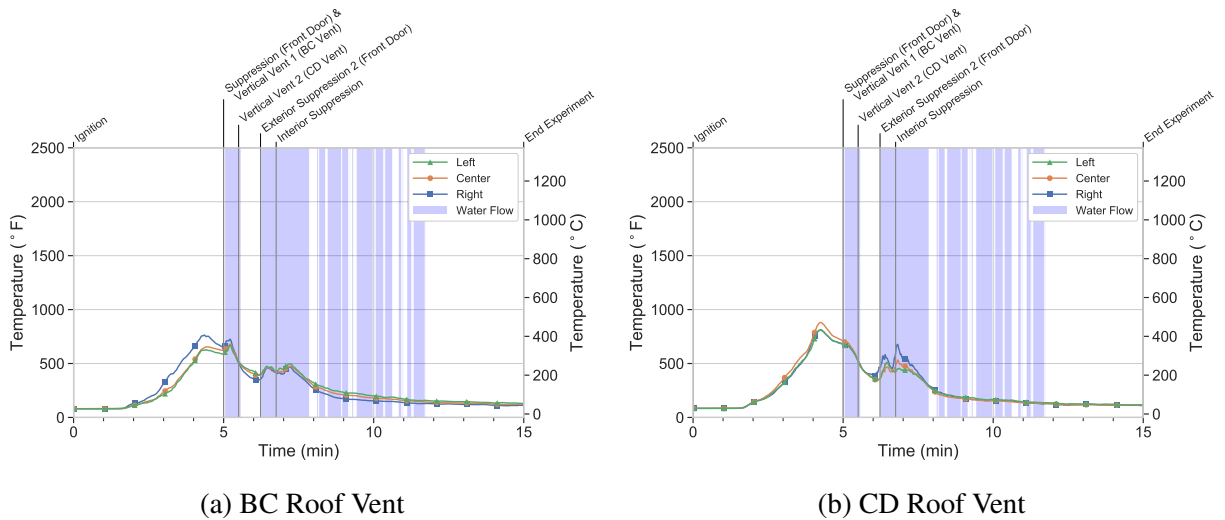
Figure 3.51: Temperatures in the exhaust vents recorded during Experiment 5.

The water application from the handline cooled the gases and the fuel. The simultaneous actions of ventilation and suppression dropped peak temperatures from 1,100 °F (593 °C) to under 500 °F (260 °C) during the 30 s the line flowed water. Pressures inside the unit dropped from 0.0004 psi (3 Pa) to −0.001 psi (−10 Pa) through a combination of gas contraction and more gas being exhausted out of the open roof vent compared to the gas being drawn in the front door. The temperature of the gases exhausted out of the open roof vents decreased from 750 °F (399 °C) to 500 °F (260 °C).

A second 4 ft x 4 ft (1.2 m x 1.2 m) roof vent was opened at the time the handline was shut down, 5 min 30 s post-ignition. Temperatures in the AB, AD, and BC quadrants (see Figure 3.44) and rear arrays (see Figure 3.48) below the 5 ft (1.5 m) level continued to decrease, with the thermocouples recording values under 150 °F (66 °C). Near the ignition point in the CD quadrant, temperatures were 250 °F (121 °C) 5 ft (0.3 m) above the floor. The temperatures of the gases exiting out of the open roof vents decreased.

As water was applied into the compartment, the environment cooled, reducing the buoyant flow out of the open roof vents. Following the additional ventilation opening and initial water application, the exhaust in the BC roof vent was 10 mph (4.5 m/s), while the exhaust in the CD roof vent was 15 mph (6.7 m/s). The front door remained a uni-directional inflow with peak inflow of −10 mph (4.5 m/s). Temperatures in the front door decreased to under 200 °F (93 °C) as the cooler gases flowed past all the sensors.

As products of combustion were exhausted out of the roof vent, they were replaced by clean air through the front door. This clean air provided oxygen to the smoldering combustion near the CD thermocouple array, which resulted in a transition to flaming combustion. The rekindle caused temperatures near the ceiling to increase 6 min after ignition. The gas temperatures in the open vents increased as some of the additional heat was exhausted out of the open vents. Temperatures reached 1,000 °F (538 °C) in the CD quadrant prior to a second water application from the exterior,

which occurred at 6 min 14 s. The additional water application decreased temperatures throughout, but once the line was shut down after 15 s, temperatures increased again. This regrowth was an indication the exterior position of the line could not reach all of the fuel to fully extinguish the fire. The crew repositioned the line to the interior for a final suppression at 6 min 30 s. The front door velocity probes were moved to allow access to the interior, ending data collection on those sensors. Interior suppression reduced temperatures to under 250 °F (121 °C) in all areas 1 min 30 s after water application occurred. As the interior environment cooled, the temperatures in the open vents decreased. With a lower temperature differential between the interior and the exterior, less of a buoyant force existed, and the flow out of the open vents decreased (see Figure 3.50).

The visibility on the interior began to clear 8 min after ignition (see Figure 3.45i), 3 min after the initial intervention. The stacks of boxes were visible 9 min after ignition (see Figure 3.45j). As the temperature dropped, the buoyancy of the gases decreased and the velocity of the gases out of the roof vents decreased. At 9 min after ignition, 2 min 15 s after interior suppression started, the velocity recorded in both vents was approximately 1 mph (0.5 m/s). The roof vents were visible on the interior camera 12 min after ignition, which was 7 min after the simultaneous ventilation and suppression operations started (see Figure 3.45m).

The experiment ended once all visible fire had been extinguished and conditions returned to approximately ambient 15 min after ignition. A total of 413 gal of water was utilized for suppression operations.

Plots of wind speed, ambient air temperature, and wind direction are presented in Figure 3.52 from ignition until the end of the experiment. The wind speed ranged from 0 mph to 10 mph (0 m/s to 4.5 m/s), blowing from the northeast toward the southwest, from side C of the unit toward side A. The ambient air temperature was 80 °F (27 °C) for the entire experiment. Due to the wind direction relative to openings in the structure and low speed, it most likely had a limited impact on the experimental results.
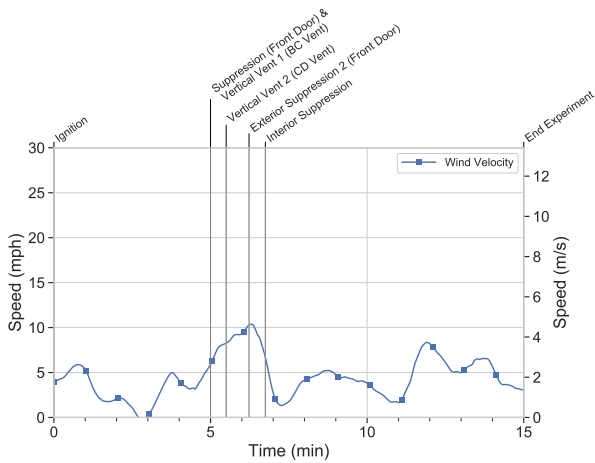
(a) Wind Speed
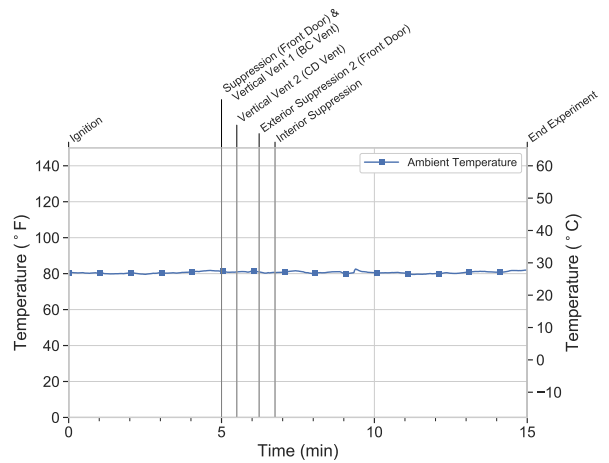


(b) Air Temperature
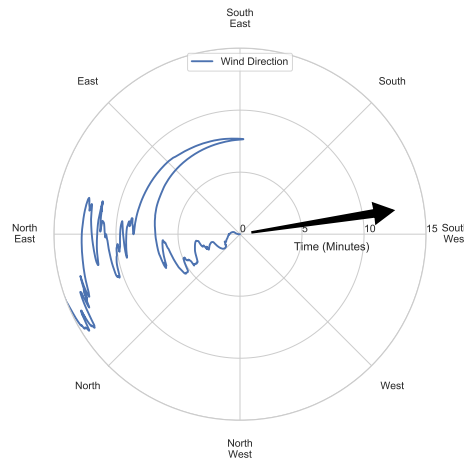


North on the chart is oriented to correspond with north on
the site layout (see Figure 2.4) and corresponding
instrument plan (see Figure 3.43). The arrow indicates
the average direction the wind was blowing.

(c) Wind Direction

Figure 3.52: Weather conditions recorded during Experiment 5.

## 3.6 Experiment 6 - Horizontal and Vertical Ventilation

Experiment 6 was designed to examine the impact of an increasing vertical ventilation area followed by water application in a 30 ft (9.1 m) by 70 ft (21.3 m) commercial unit. Unit 1067 was the fire unit, with unit 1069–1071 as the side D exposure. The front door to unit 1067 was open at the beginning of the experiment. All exterior doors in unit 1069–1071 remained closed throughout the experiment.

The unit was instrumented to monitor the thermal conditions with thermocouple arrays, differential pressure sensor arrays between the unit and the exterior, and bi-directional probes in the chimneys leading to the roof vents and the front door as illustrated in Figure 3.53. The thermocouple arrays contained seven thermocouples starting 1 ft 2 in. (0.4 m) above the floor with a thermocouple every 2 ft (0.6 m), ending with the last thermocouple 1 in. (2.3 cm) below the gypsum wallboard ceiling. The differential pressure transducer array included pressure transducer taps 1 ft (0.3 m), 7.5 ft (2.3 m), and 12.2 ft (3.7 m) measuring the differential pressure between the fire unit and the exterior. The bi-directional probe array in the front door included probes and thermocouples 4.0 in. (10.2 cm), 22.0 in. (55.9 cm), 40 in. (101.6 cm), and 76 in. (193.0 cm) above the floor. Each chimney (recall Figure 2.19) had an array of three bi-directional probes and thermocouples, centered in the opening from front to rear. The probe array started from side B of the vent 12.0 in. (30.5 cm) from the side wall, and the probes and thermocouples were spaced 12.0 in. (30.5 cm) apart. The array was vertically located 28.0 in. (71.1 cm) above the ceiling.
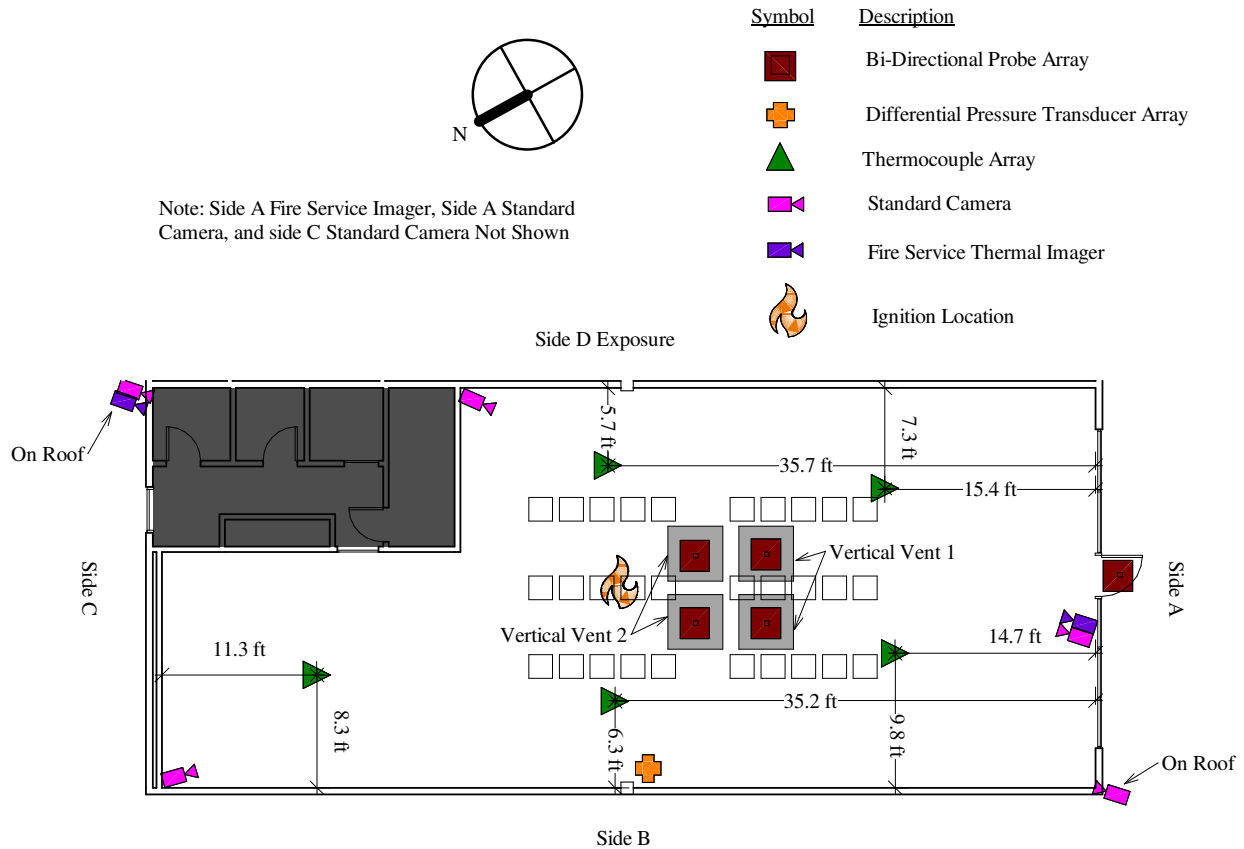
Figure 3.53: Instrumentation plan for unit 1067, Experiment 6. Not shown are the locations where wind speed, wind direction, ambient temperature, and suppression water flow were recorded. The dark gray shaded area was isolated from the experimental volume for these experiments.

The experiment started with ignition (source described in Section 2.3) located between the second and third stacks of boxes from the rear in the center row as shown in Figure 3.53. The ventilation and suppression occurred as indicated in Table 3.7.

Table 3.7: Experiment 6 Sequence and Ventilation

| Timing (min:s) | Event | Opening(s) | Horizontal Area ft$^2$ (m$^2$) | Vertical Area ft$^2$ (m$^2$) |
|---|---|---|---|---|
| 00:00 | Ignition | Door | 19.0 (1.8) | - |
| 05:30 | Ventilation 1 | Door & Two Roof Vents | 19.0 (1.8) | 32.0 (3.0) |
| 07:30 | Ventilation 2 | Door & Four Roof Vents | 19.0 (1.8) | 64.0 (6.0) |
| 09:23 | Exterior Suppression 1 | - | - | - |
| 09:40 | Exterior Suppression 2 | - | - | - |
| 14:33 | Interior Suppression | - | - | - |
| 20:00 | End Experiment | - | - | - |

The gas temperatures recorded in Experiment 6 are presented in Figure 3.54 and 3.55 starting at ignition and ending at the completion of the experiment. Following ignition, it took 1 min 30 s for an increase in gas temperature to be recorded at the thermocouples 14 ft (4.3 m) above the floor in the fire compartment. Flames were visible impinging on the gypsum ceiling 2 min after ignition (see Figure 3.56c).



(a) CD Quadrant Temperature

(b) AD Quadrant Temperature

(c) BC Quadrant Temperature

(d) AB Quadrant Temperature
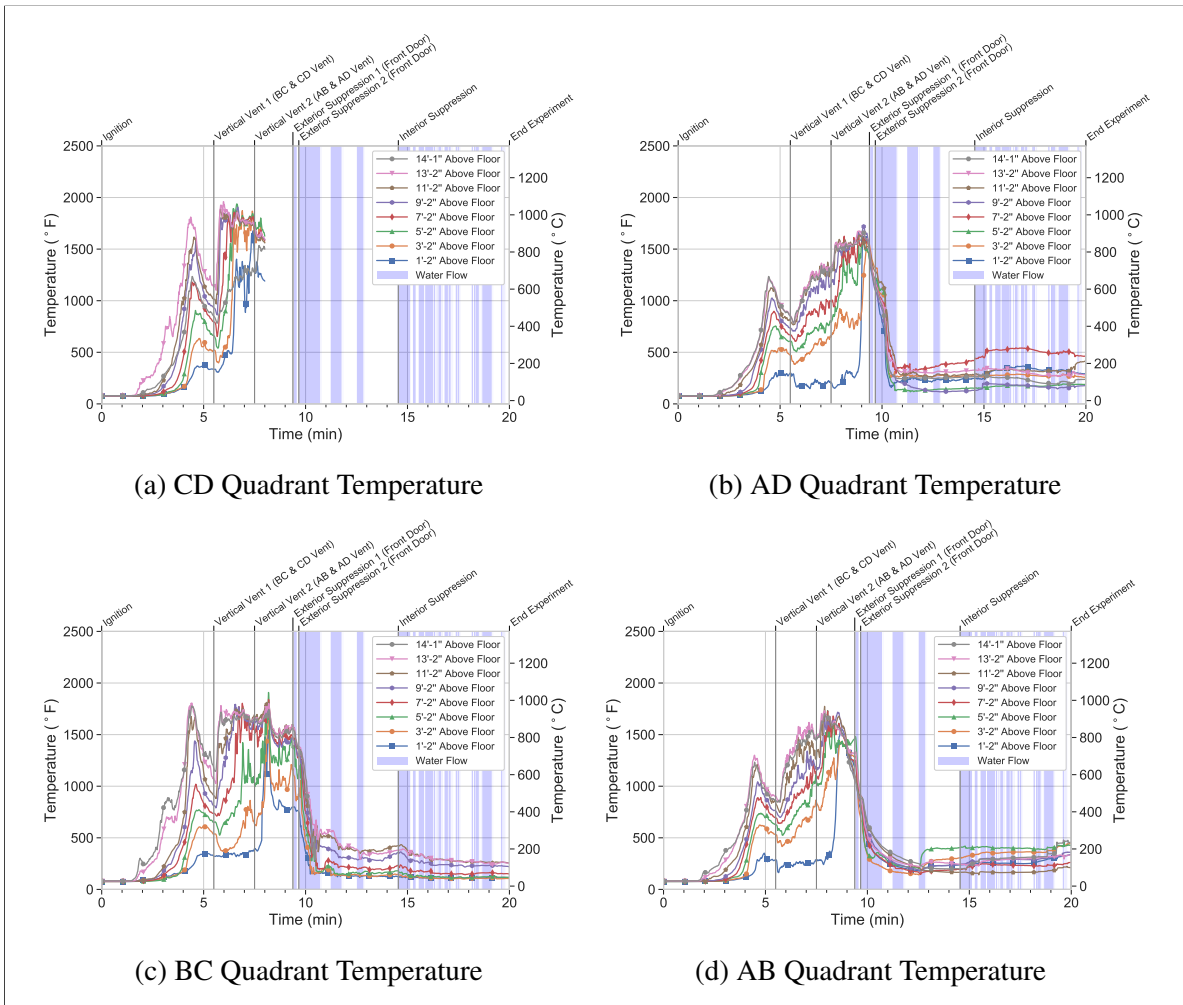
Side A

Figure 3.54: Temperatures recorded in the fire compartment during Experiment 6. Charts are arranged to correspond with the location of the thermocouple array in the unit. The thermocouple array in the CD quadrant was damaged during the experiment, therefore the data are cut at 8 min. Side A is denoted outside the frame as a point of reference to the structure illustrated in Figure 3.53.
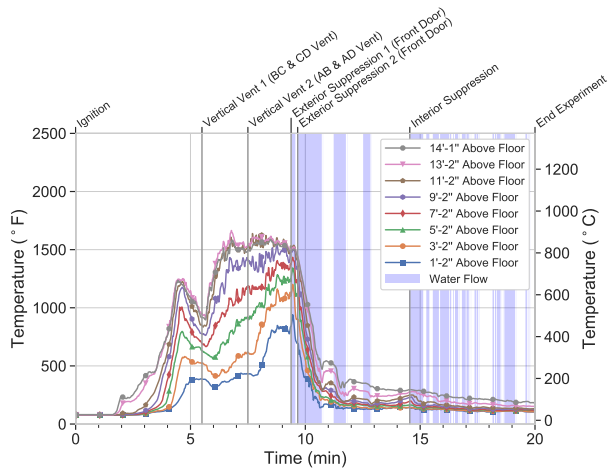
Figure 3.55: Temperatures in the rear, open to the fire compartment, during Experiment 6.



(a) Ignition

(b) 1 min

(c) 2 min

(d) 3 min

(e) 4 min

(f) 5 min
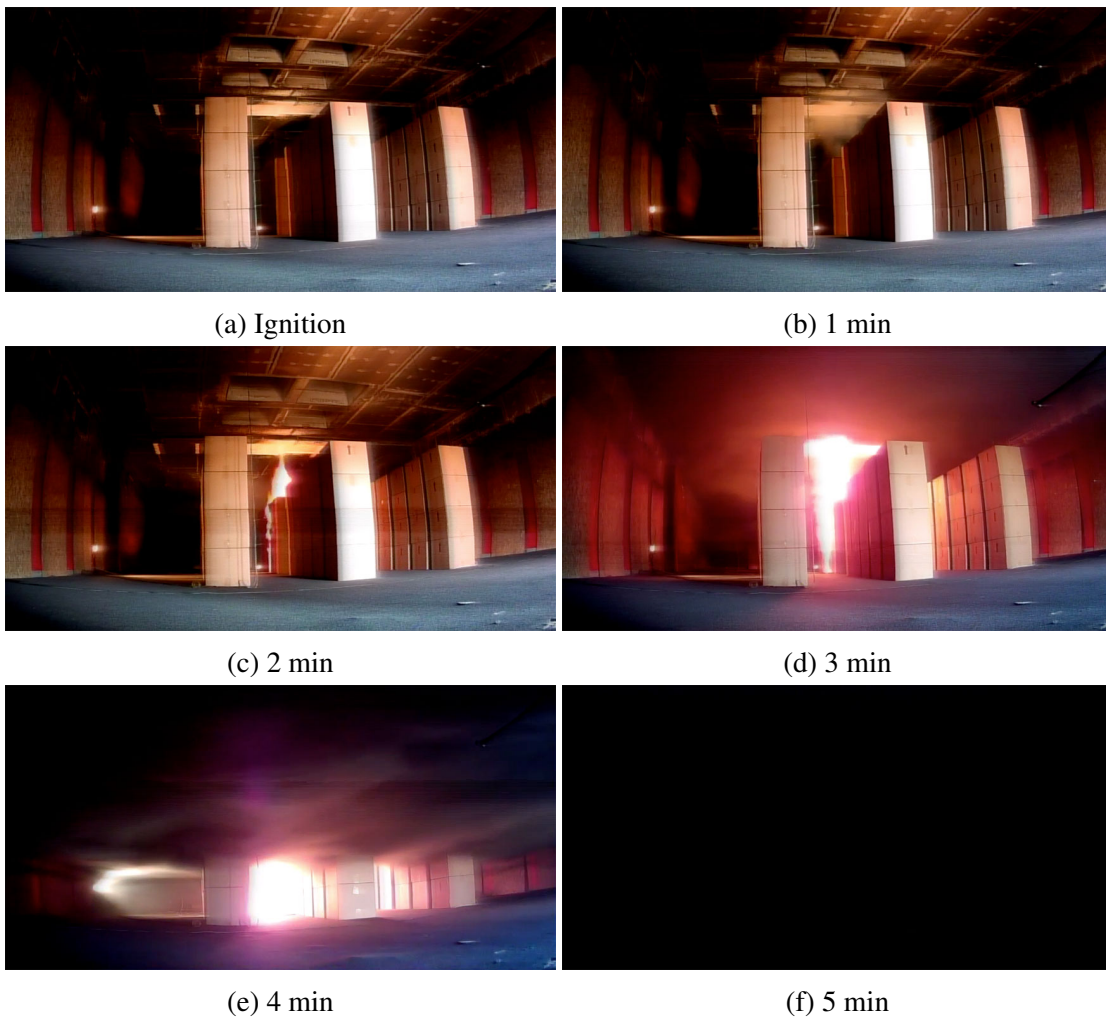
Figure 3.56: Sequential interior images during Experiment 6 looking toward the B/C corner from the A/D corner. The interior camera was lost after 5 min due to thermal damage from the fire.

The increase in temperature resulted in gas expansion. This expansion was recorded on the differential pressure transducers as an increase in pressure above ambient (see Figure 3.57), and as uni-directional exhaust from the front door 3 min after ignition (see Figure 3.58a). Pressure peaked at 0.0025 psi (18 Pa), 4 min after ignition. The gas velocities at the front door were unidirectional exhaust from 3 min to 4 min 30 s, with a peak exhaust of 10 mph (4.5 m/s) at the bottom and 20 mph (8.9 m/s) at the top. For the first 30 s, the exhaust was made up of the gases in the compartment prior to ignition, and the temperatures in the door remained near ambient. As the gases at the ceiling expanded, they forced out the gases lower in the space. At 3 min 30 s, temperatures in the door increased, indicating the exhaust contained products of combustion (see Figure 3.58b).
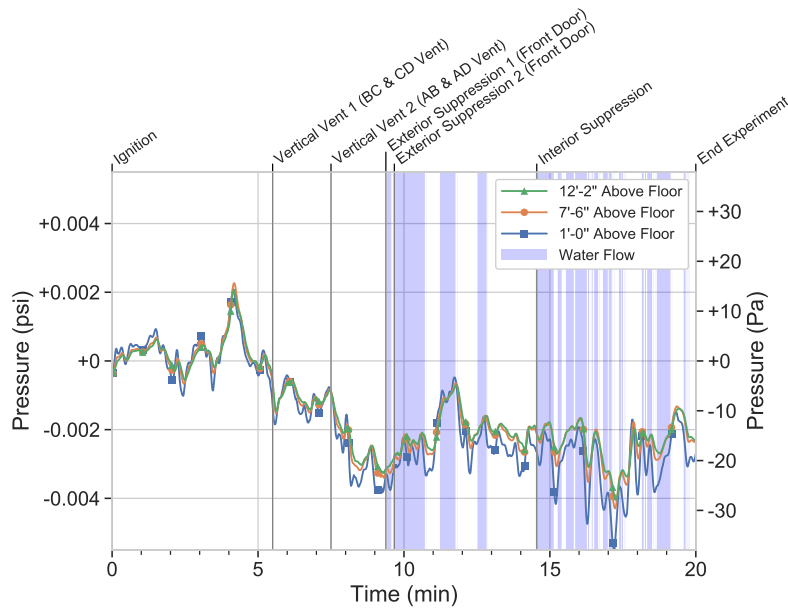


Figure 3.57: Differential pressures recorded during Experiment 6. Positive values indicate pressure rise in the fire compartment.
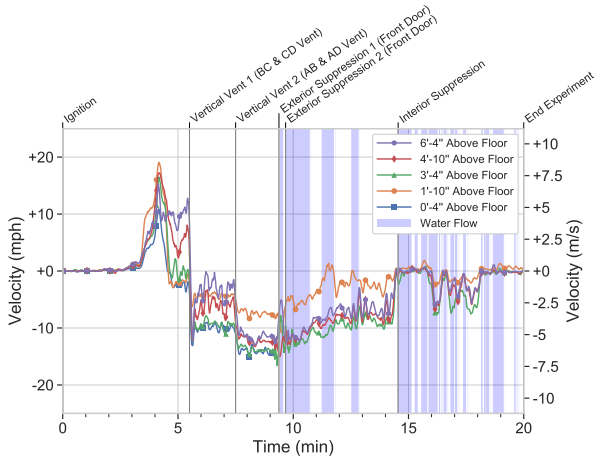
(a) Gas Velocities

(b) Temperatures

Positive direction indicates flow out of the unit
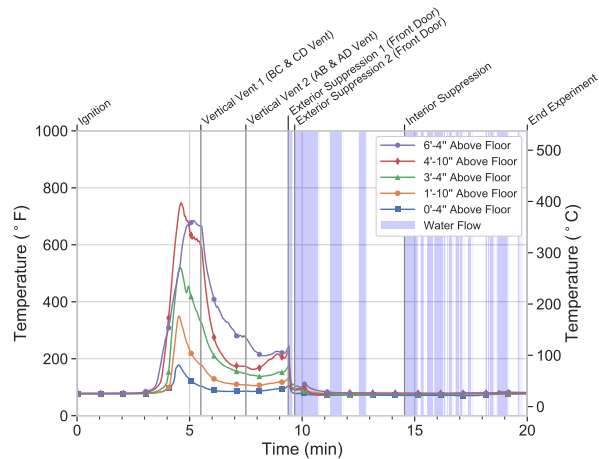
Figure 3.58: Gas velocities and temperatures recorded in the front door during Experiment 6. Probes moved at 14 min 30 s for interior suppression and returned to original position at 16 min 21 s.

The smoke layer descended to 7 ft (2.1 m) above the floor, the level of the top box, at 3 min (see Figure 3.56d), and to approximately 2.6 ft (0.8 m) at 4 min (see Figure 3.56e). Temperatures peaked prior to the fire becoming ventilation limited. Peak temperatures reached 1,750 °F (954 °C) at the ceiling and then decreased approximately 500 °F (277 °C) over the next 30 s. The decrease in temperature resulted in gas contraction, and pressures decreased from 0.002 psi (13 Pa) to near ambient. As the differential pressure between the unit and the exterior decreased, the front door became a bi-directional vent with exhaust (10 mph or 4.5 m/s) at the top, and inflow (−2 mph or −0.9 m/s) at the bottom. Temperatures at the top of the door remained elevated while the lower sensors decreased as cooler gases were drawn in past the sensors from outside the structure.

Vertical ventilation occurred when two 4 ft x 4 ft (1.2 m x 1.2 m) roof vents (the BC and CD vents) were opened 5 min 30 s after ignition. Opening the vents established a uni-directional flow path within the structure. The front door became the intake (ranging from −2 mph to −10 mph (−0.9 m/s to −4.5 m/s) with the highest velocity on the middle probes), and the open roof vents became the exhaust, exceeding 35 mph (15.6 m/s (see Figure 3.60). The volume of the exhaust gases exiting the vertical vents was more than the intake volume at the front door, resulting in an average pressure of −0.018 psi (−12 Pa) on the inside of the unit (see Figure 3.57).

After vertical ventilation, the temperatures in the front door decreased as the temperature sensors were cooled by the gases flowing into the structure from the exterior. Due to the radiation from the hot gas layer, the upper temperature remained elevated, while the bottom temperature returned to ambient. The bottom probe was further from the hot gas layer, received the least amount of radiation, and thus remained low (see Figure 3.58b).

The temperatures in the open vents (at the BC and CD locations) exceeded 1,500 °F (816 °C) as the

hot gases exhausted through the vent. Temperatures in the closed vents (the AB and AD locations) remained below 1,100 °F (593 °C) because the sensors were not located within the flow path (see Figure 3.59).



(a) AB Roof Vent

(b) AD Roof Vent

(c) BC Roof Vent
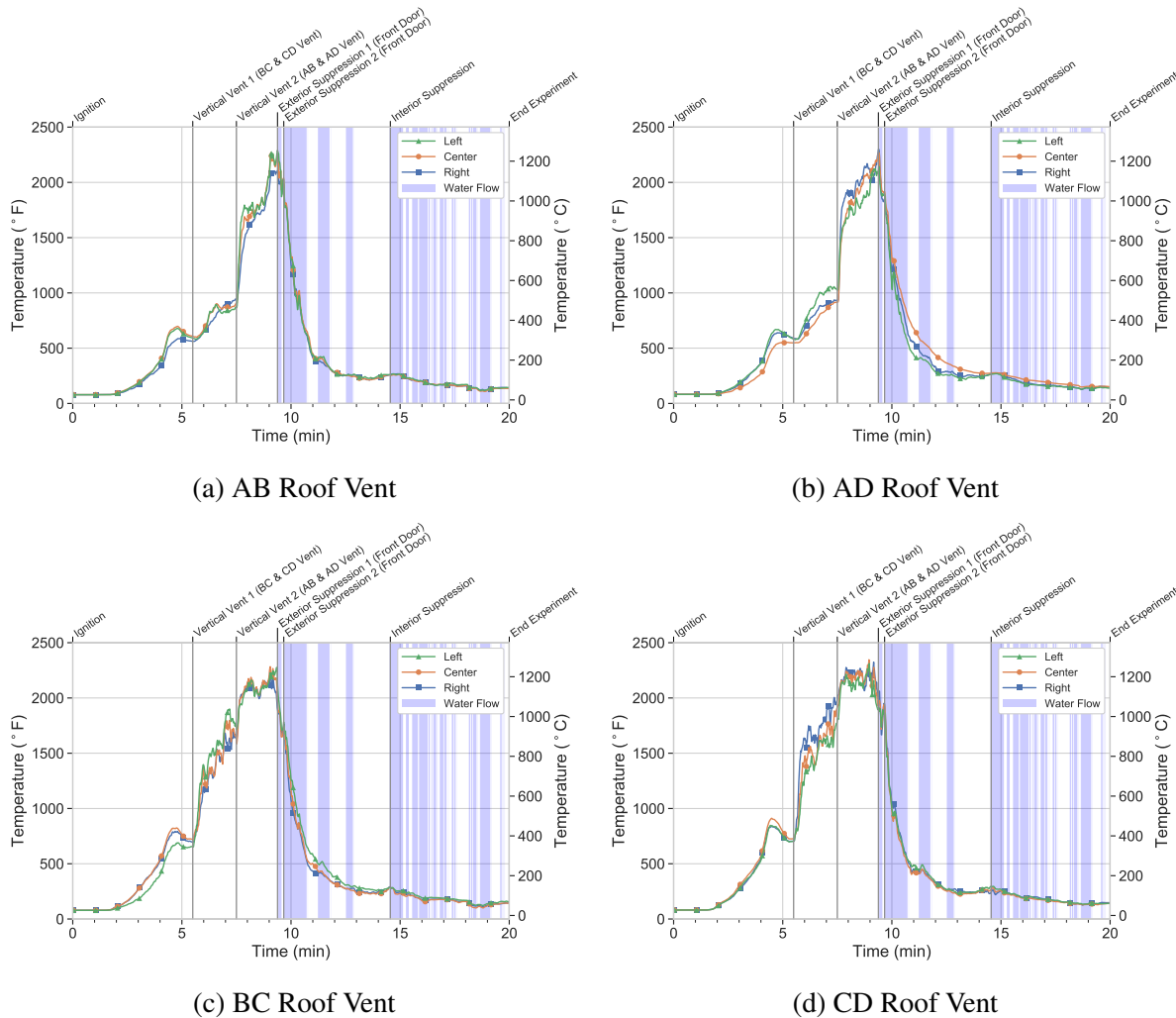
(d) CD Roof Vent

Figure 3.59: Temperatures recorded in the roof vents during Experiment 6.

The increase in flow in the front door allowed more oxygen to enter, which increased the size of the fire. Temperatures increased throughout the unit within 5 s of ventilation. Temperatures recorded on the CD quadrant thermocouple array exceeded 1,250 °F (677 °C), conditions representative of a localized flashover, 1 min after ventilation. Temperatures recorded in the other areas remained stratified, indicating combustion in those areas was limited by the available oxygen.

Additional vertical ventilation was provided via two 4 ft x 4 ft (1.2 m x 1.2 m) roof vents (the AB and AD vents) 7 min 30 s after ignition. The additional ventilation area increased the velocity of the intake gases at the front door and the total volumetric flow rate of the exhaust gases at the roof vents. The velocity probes at the front door recorded a peak inflow of −17 mph (−8 m/s). Each of the velocity probes in the roof vent measured approximately 35 mph (16 m/s) (see Figure 3.60).

99
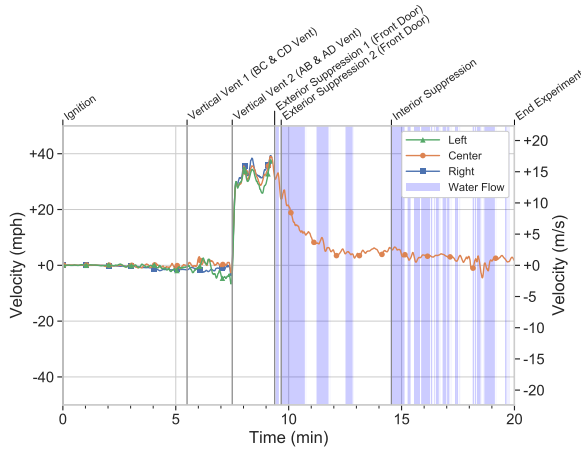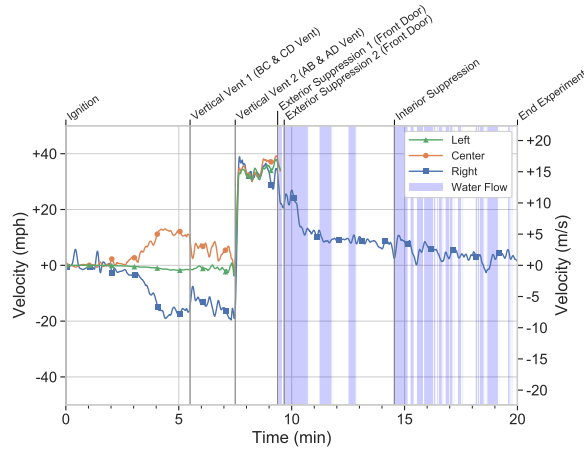
(a) AB Roof Vent
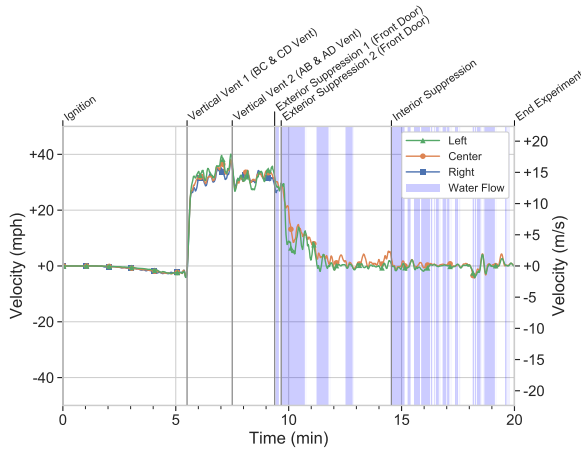


(b) AD Roof Vent
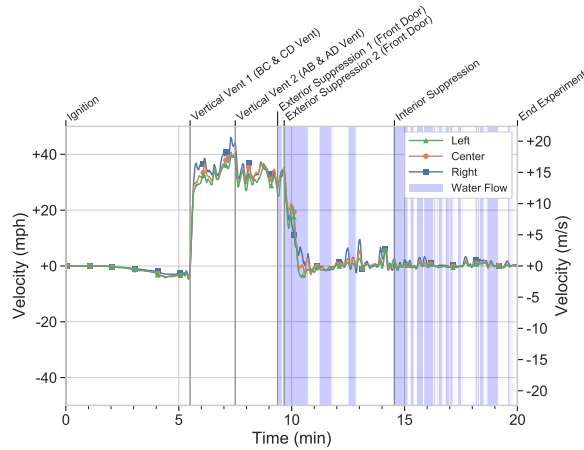


(c) BC Roof Vent



(d) CD Roof Vent

Figure 3.60: Gas velocities recorded in the roof vents during Experiment 6. Positive direction indicates flow out of unit.

Adding exhaust area allowed more oxygen to enter through the front door and increased the size of the fire. The AB, AD, and BC quadrant thermocouple arrays recorded temperatures exceeding 1,250 °F (677 °C) floor to ceiling, conditions representative of localized flashover in those areas, 1 min 30 s after the ventilation occurred. Temperatures in the rear remained stratified with 1,500 °F (816 °C) at the ceiling and 1,000 °F (538 °C) at 1 ft (0.3 m) above the flow, an indication that combustion in that area was limited by the available oxygen. The thermocouple array in the CD quadrant was damaged by the extended exposure to flashover and data collection ended on that sensor array.

As the gas temperatures in the unit increased, the sensors in the front door received more heat energy from radiation. Due to their proximity to the hot gases, the highest two probes recorded temperatures over 200 °F (93 °C). The lower three probes were further from the hot gases and thus received less radiation. With less radiation, the temperatures recorded on the lower three probes

remained below 150 °F (66 °C). At 9 min 10 s, the gases at the front door ignited. The flames provided additional radiation (see Figure 3.61), which was recorded on the temperature sensors at the front door as an increase in temperature, see Figure 3.58b.



Figure 3.61: Flames at the front door 14 s prior to suppression (9 min 10 s after ignition) in Experiment 6.

The larger fire size on the interior resulted in higher temperatures in the roof vents. Temperatures recorded in all four vents exceeded 2,000 °F (1,093 °C). As the hot smoke exhausted out of the open vents, it mixed with the oxygen on the exterior and flaming combustion occurred. Flames were visible from all four vents (see Figure 3.62).

Figure 3.62: A drone image of the roof vents, looking from the BC corner toward the AD corner 10 s prior to suppression (9 min 14 s after ignition) in Experiment 6.

Matt Sortman, Fairborn Police Department

Exterior suppression occurred via a 1 3/4 in. handline with a 7/8 in. smooth-bore tip that flowed 160 gpm (606 lpm). The line was directed through the side A door, toward side C, 9 min 22 s after ignition and flowed for 8 s. The handline was repositioned closer to the doorway and a second exterior water application through the front door occurred 9 min 40 s after ignition that lasted 1 min. The water flow rate is presented in Figure 3.63.
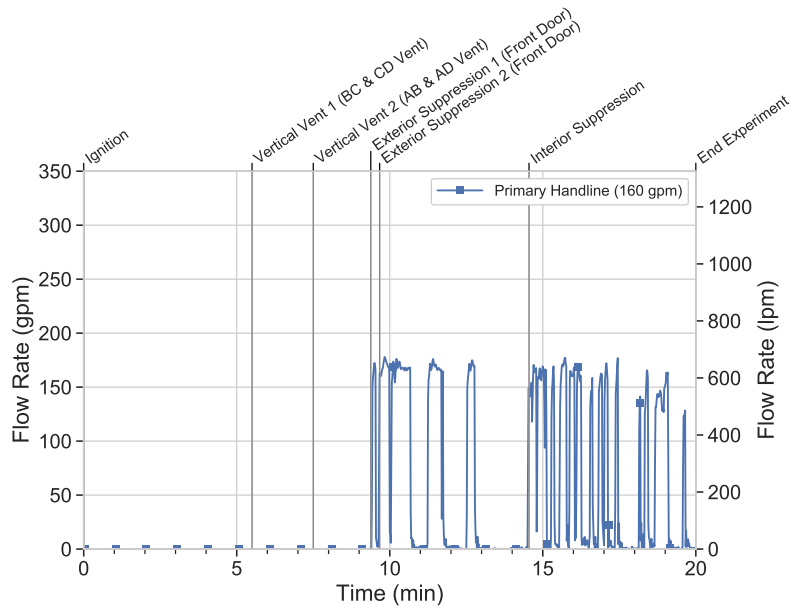
Figure 3.63: Water flows recorded during Experiment 6.

Temperatures decreased from in excess of 1,500 °F (816 °C) to under 500 °F (260 °C) within 2 min of the water application (11 min 30 s after ignition). The cooling of the gas temperatures on the interior reduced buoyancy, and the velocities at the front door and vertical vents decreased. The velocity of gases out of the roof vent slowed to a range of 5 mph to 10 mph (2.2 m/s to 4.5 m/s). The front door inflow decreased to a range of −5 mph to −10 mph (2.2 m/s to 4.5 m/s).

Suppression extinguished the flames in the gases at the front door and temperatures decreased (see Figure 3.58b). Flames were no longer visible from the roof vents 30 s after the initial suppression (9 min 54 s), and temperatures in the roof vents decreased (see Figure 3.64). The temperatures in the roof vents dropped from in excess of 2,000 °F (1,093 °C) to under 500 °F (260 °C) within 2 min 30 s of the initial suppression (see Figure 3.59).

Figure 3.64: A drone image of the roof vents looking from the CD corner toward the AB corner 30 s after the initial suppression (9 min 54 s after ignition) in Experiment 6.

Although temperatures decreased, flames were visible on the interior from the front door 11 min 30 s after ignition because the exterior location of the line limited the ability of the water to fully extinguish the fire. The suppression crew repositioned the line to the interior and applied water from the interior 11 min 47 s after ignition. Interior suppression continued until all visible flames were extinguished. The suppression crew utilized a total of 670 gal. The experiment concluded at 20 min when the visible flames had been extinguished.

Plots of wind speed, ambient air temperature, and wind direction are presented in Figure 3.65 from ignition until the end of the experiment. The wind speed ranged from 0 mph to 10 mph (0 m/s to 4.5 m/s), blowing from the northeast toward the southwest (from side C of the unit toward side A). The ambient air temperature was in the range of 75 °F to 80 °F (24 °C to 27 °C) for the entire experiment. Due to the wind direction relative to the orientation of the structure and low speed, there was minimal impact to the results of the experiment.
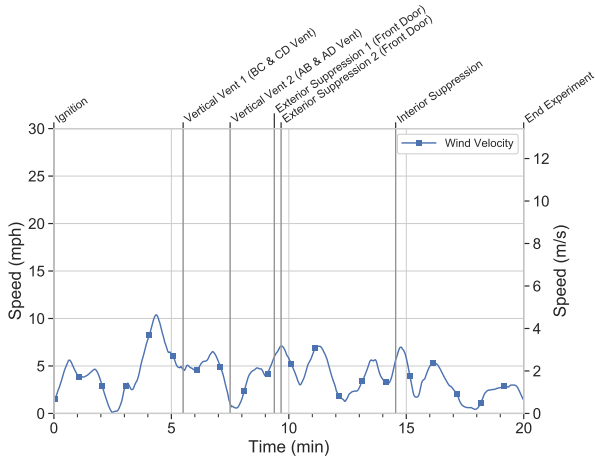
(a) Wind Speed
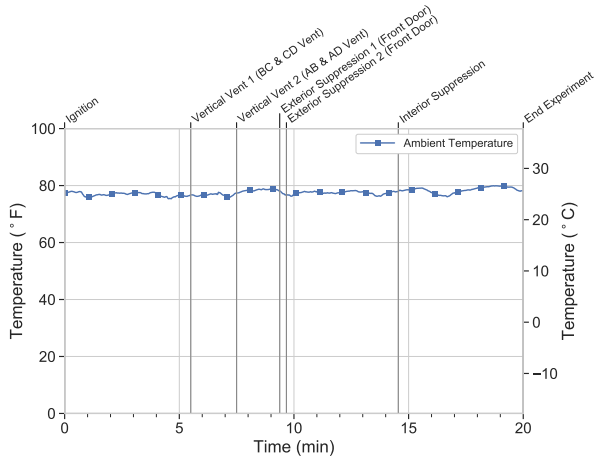
(b) Air Temperature
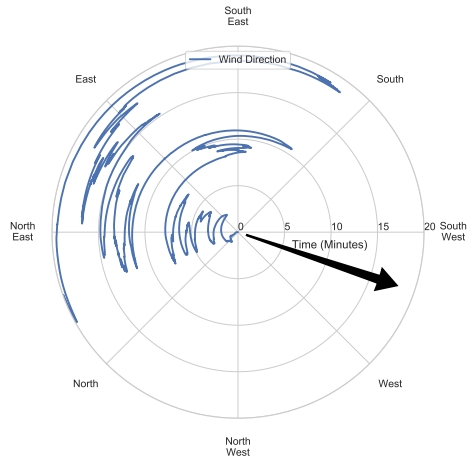


North on the chart is oriented to correspond with north on
the site layout (see Figure 2.4) and corresponding
instrument plan (see Figure 3.43). The arrow indicates
the average direction the wind was blowing.

(c) Wind Direction

Figure 3.65: Weather conditions recorded during Experiment 6.

## 3.7 Experiment 7 - Horizontal and Vertical Ventilation

Experiment 7 was designed to examine the impact of combined horizontal and vertical ventilation, followed by water application, in a 30 ft (9.1 m) by 70 ft (21.3 m) commercial unit. Unit 1067 was the fire unit, with unit 1069–1071 as the side D exposure. The front door to unit 1067 was open at the beginning of the experiment. Unit 1069–1071 had been used for a previous experiment and its front glass windows, door and portions of the roof were open throughout the experiment.

The unit was instrumented to monitor the thermal conditions with thermocouple arrays, bi-directional probes in the chimneys leading to the roof vents and bi-directional probes in the front door (as illustrated in Figure 3.66). The thermocouple arrays contained seven thermocouples starting 1 ft 2 in. (0.4 m) above the floor with a thermocouple every 2 ft (0.6 m), ending with the last thermocouple 1 in. (2.3 cm) below the gypsum wallboard ceiling. The bi-directional probe array in the front door included probes and thermocouples 4.0 in. (10.2 cm), 22.0 in. (55.9 cm), 40 in. (101.6 cm), and 76 in. (193.0 cm) above the floor level. Each chimney (recall Figure 2.19) had an array of three bi-directional probes and thermocouples centered in the opening from front to rear. The probe array started 12.0 in. (30.5 cm) from the side B vent wall, and the probes and thermocouples were spaced 12.0 in. (30.5 cm) apart. The array was vertically located 28.0 in. (71.1 cm) above the ceiling.
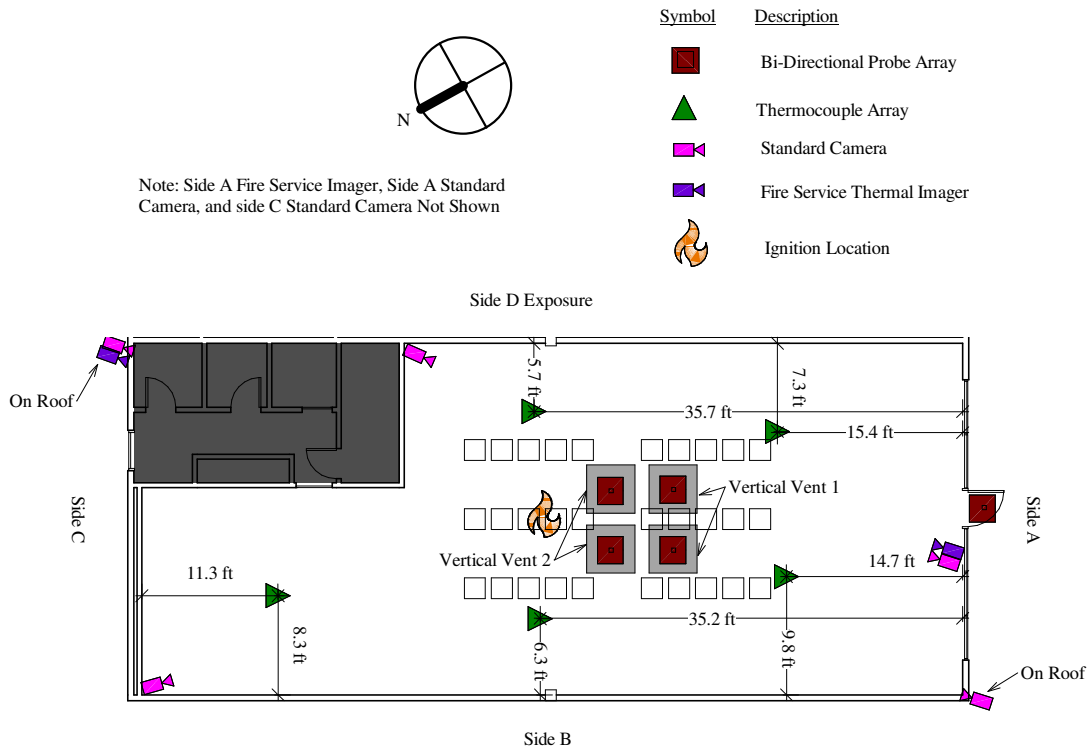


Figure 3.66: Instrumentation plan for unit 1067 utilized for Experiment 7. Not shown are the locations where wind speed, wind direction, ambient temperature, and suppression water flow were recorded. The dark gray shaded area was isolated from the experimental volume for these experiments.

The experiment started with ignition (source described in Section 2.3) located between the second and third stacks of boxes from the rear in the center row as shown in Figure 3.66. The ventilation and suppression occurred as indicated in Table 3.8.

Table 3.8: Experiment 7 Sequence and Ventilation

| Timing (min:s) | Event | Opening(s) | Horizontal Area ft$^2$ (m$^2$) | Vertical Area ft$^2$ (m$^2$) |
|---|---|---|---|---|
| 00:00 | Ignition | Door | 19.0 (1.8) | - |
| 04:00 | Vent Front Windows | Door and Front Windows | 81.5 (7.6) | - |
| 05:30 | Vent BC and CD Roof Vents | Door, Windows and Two Roof Vents | 81.5 (7.6) | 32.0 (3.0) |
| 07:30 | Vent AB and AD Roof Vents | Door, Windows and Four Roof Vents | 81.5 (7.6) | 64.0 (6.0) |
| 09:10 | Exterior Suppression 1 | - | | - |
| 10:03 | Exterior Suppression 2 | - | | - |
| 12:30 | Exterior Suppression 3 | - | | - |
| 20:00 | End Experiment | - | | - |

The gas temperatures recorded in Experiment 7 are presented in Figure 3.67 and 3.68 starting at ignition and ending at the completion of the experiment. Following ignition, it took 1 min 30 s for an increase in gas temperature to be recorded at the thermocouples 14 ft (4.3 m) above the floor in the fire compartment. The increase in temperature resulted in gas expansion, which was captured as unidirectional flow out of the front door 3 min after ignition (see Figure 3.69a). For the first 15 s, the exhaust was made up of the gases in the compartment prior to ignition, and the temperatures in the door remained near ambient. As the gases at the ceiling expanded, they forced out the gases lower in the space. At 3 min 15 s, temperatures in the door increased, indicating the exhaust contained products of combustion (see Figure 3.69b).
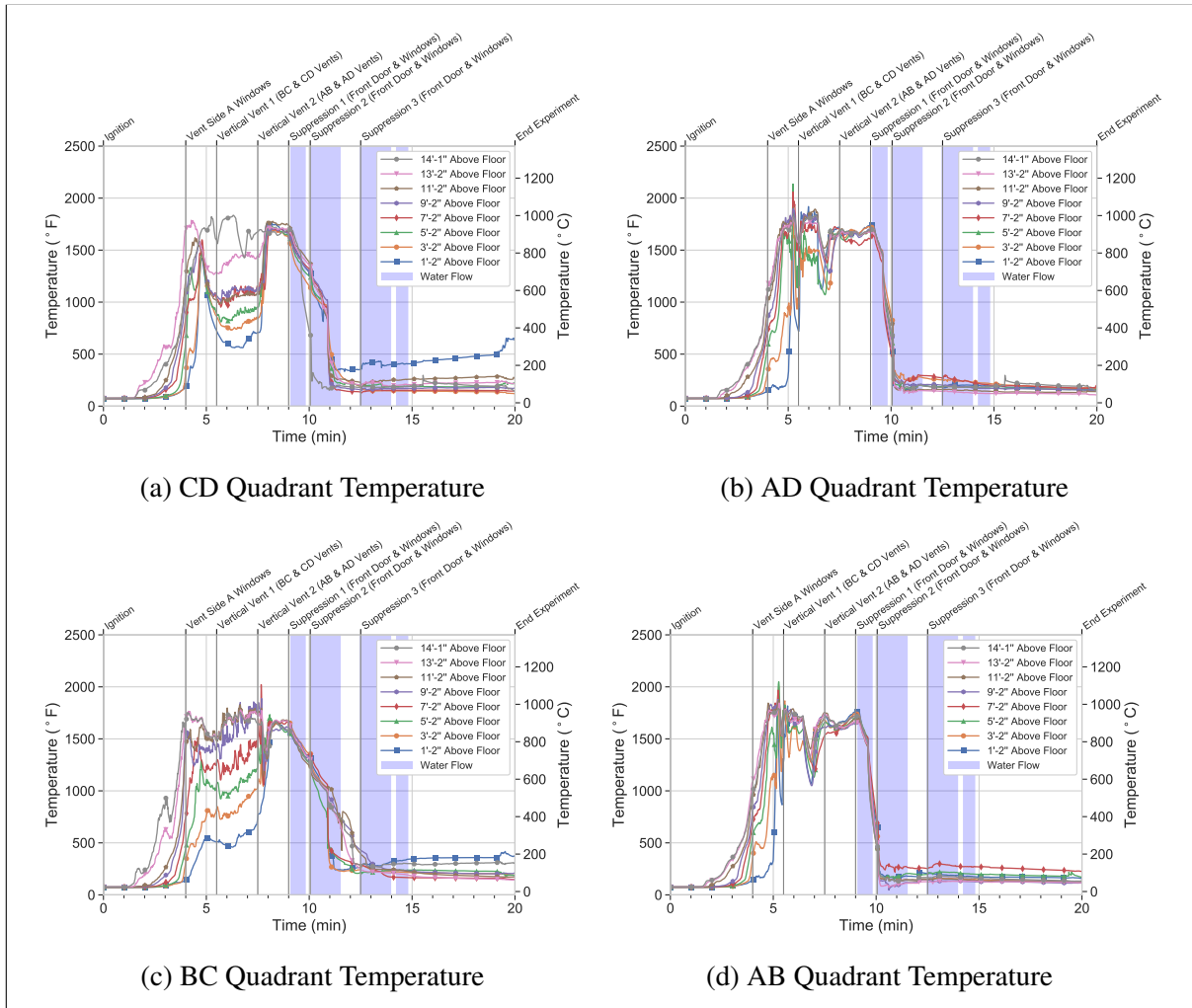
Figure 3.67: Temperatures recorded in the fire compartment during Experiment 7. Charts are arranged to correspond with the location of the thermocouple array in the unit. Side A is denoted outside the frame as a point of reference to the structure illustrated in Figure 3.66.
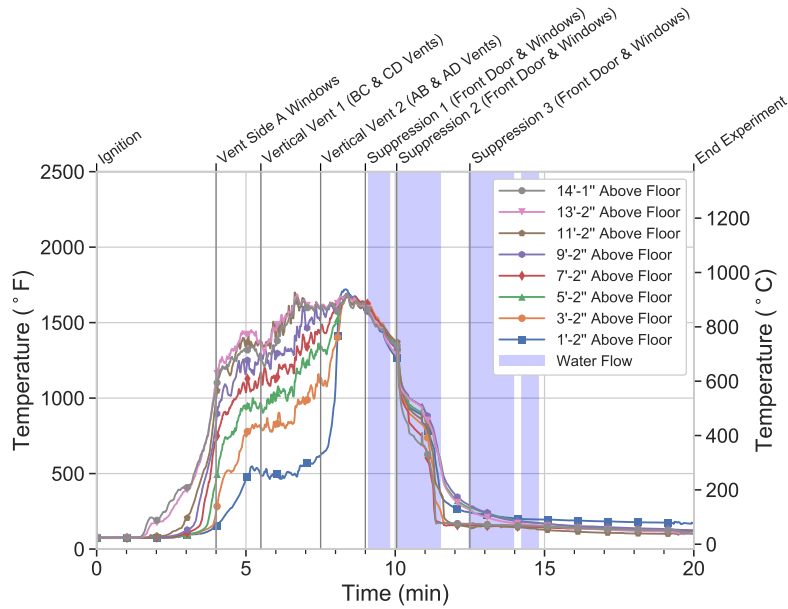
Figure 3.68: Temperatures recorded in the rear area open to the main area during Experiment 7.
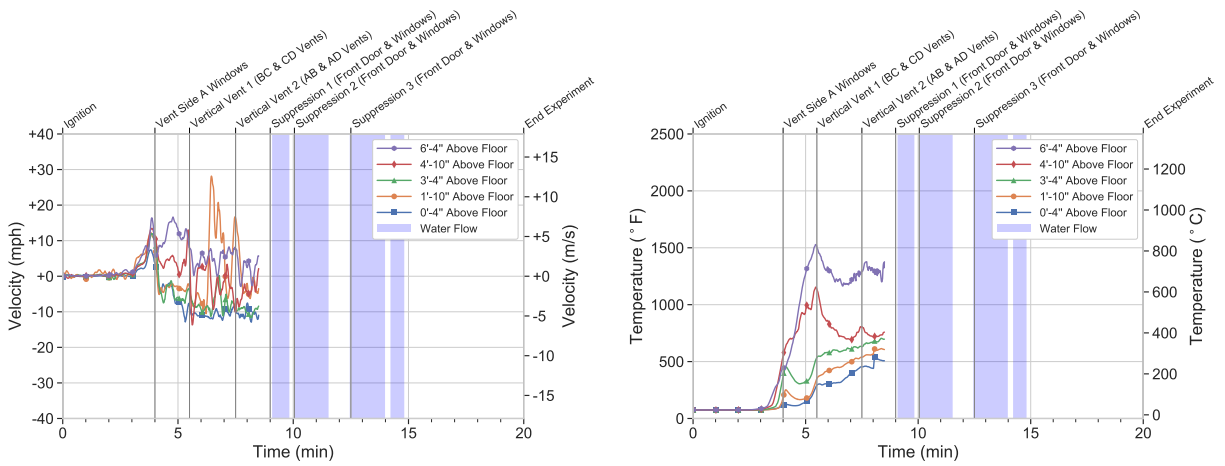


(a) Gas Velocities

(b) Temperatures

Positive direction indicates flow out of the unit.

Figure 3.69: Gas velocities (left) and temperatures (right) recorded in the front door during Experiment 7. The sensor array was damaged by the fire 8 min 30 s after ignition, ending data collection on the sensors.

The smoke layer descended to 7 ft (2.1 m) above the floor, the level of the top of the boxes, 3 min (see Figure 3.70d) after ignition. At 4 min after ignition, the smoke layer was just above the floor (see Figure 3.70e). Temperatures peaked at 1,750 °F (954 °C) at the ceiling in the BC and CD quadrants, 1,250 °F (677 °C) at the ceiling in the rear, and 1,000 °F (538 °C) at the ceiling in the front AB and AD quadrants 4 min after ignition.

(a) Ignition        (b) 1 min

(c) 2 min        (d) 3 min

(e) 4 min        (f) 5 min

(g) 6 min
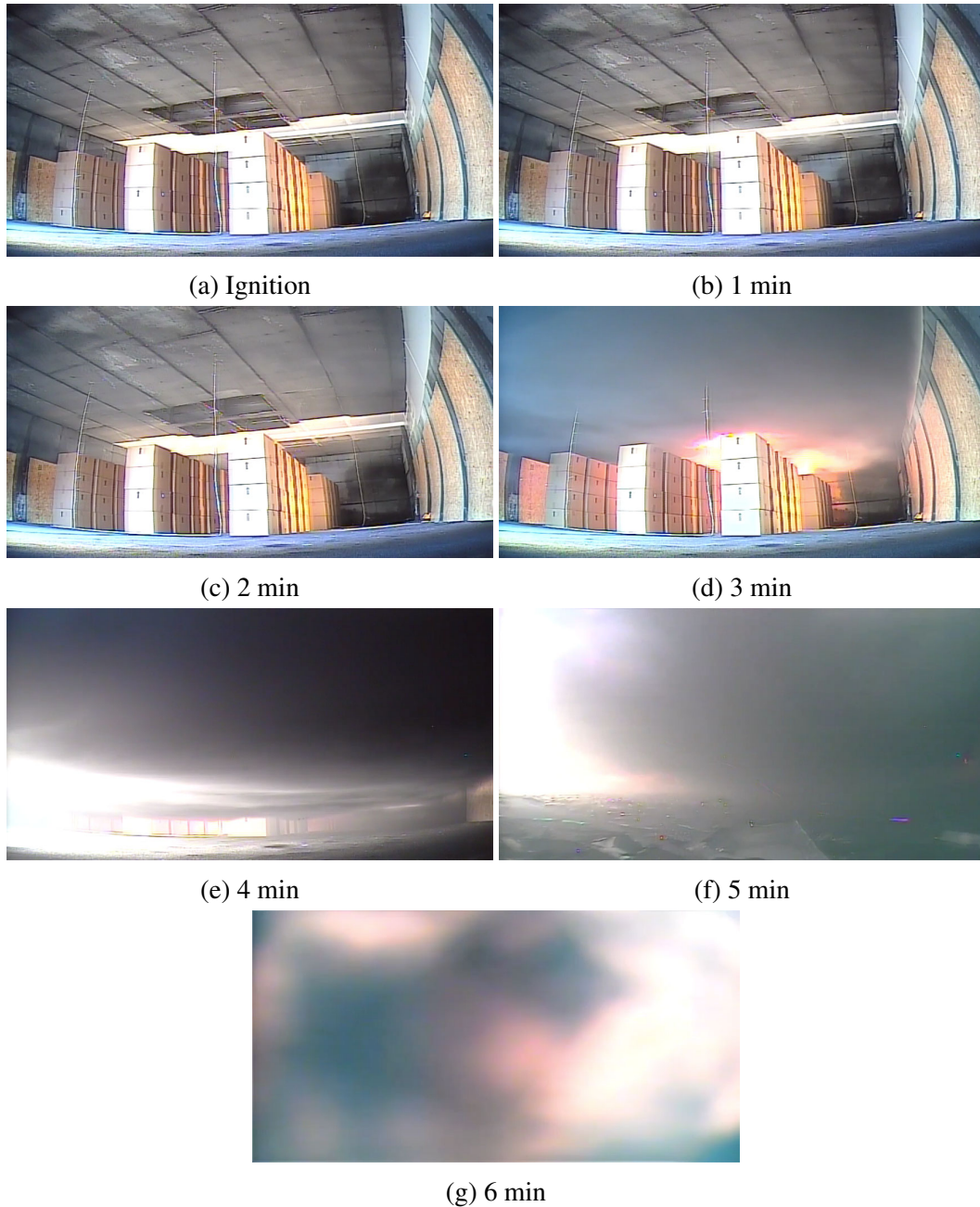
Figure 3.70: Sequential interior images during Experiment 7 looking toward the BC corner from the AD corner.

The front windows of the unit were ventilated 4 min after ignition. As a result, built-up heated products of combustion exhausted from the unit. The additional horizontal ventilation relieved the pressure within the structure that had built due to the gas expansion from increasing temperatures. Flow at the front door became bi-directional. The exhaust at the top of the door peaked at 18 mph (8 m/s) while the inflow at the bottom peaked at −13 mph (6 m/s). As the hot gases exhausted out the top of the door, temperatures on the top two sensors recorded over 1,000 °F (538 °C). The

cooler gases entering the bottom of the door lowered the temperature at the bottom two sensors (see Figure 3.69b).

The exhaust of the built-up heated air and products of combustion temporarily slowed the rate of temperature growth in the structure, but the additional ventilation allowed more oxygen to enter, increasing the size of the fire within 30 s. The increased fire size corresponded with rises in measured temperatures in all quadrants. Peak temperatures were in excess of 1,500 °F (816 °C) 1 min after the window ventilation. The rapid growth of the fire consumed the available oxygen in the compartment. With the front door and windows as the only source of oxygen, the combustion in the BC and CD quadrants was limited by the available oxygen, and temperatures decreased. The rear area filled with combustion gases, which resulted in temperature increases. However, temperatures remained below 1,500 °F (816 °C) at the ceiling because of a lack of oxygen. Due to the open front windows and door, more oxygen was available in the front of the unit and the temperatures in the AB and AD quadrants continued to increase. Temperatures exceeded 1,100 °F (593 °C) floor to ceiling, conditions representative of a localized flashover. This localized flashover was recorded on the interior camera with flames at the floor level 5 min after ignition (see Figure 3.70f).

The temperature of the hot gases exhausted past the top two thermocouples in the front door increased. Temperatures recorded on the lower probes in the doorway also increased, but that was due to radiation from the hot gases above, not the cooler gases flowing past the sensors from the exterior. The lowest sensor received the least radiation, because it was furthest from the hot gases (see Figure 3.69b).

Vertical ventilation was provided by opening two 4 ft x 4 ft (1.2 m x 1.2 m) roof vents (the BC and CD vents) 5 min 30 s after ignition, resulting in a flow path with intake through the open front door and front windows, and exhaust out of the roof vents. The exhaust out of the roof vents ranged from 45 mph to 50 mph (20 m/s to 22 m/s, see Figure 3.71). Temperatures recorded in the exhaust vents exceeded 2,000 °F (1,093 °C) because the vents were now part of the exhaust portion of the flow path (see Figure 3.72). Flames were visible in the exhaust from the open roof vents 30 s after ventilation occurred as the fuel rich products of combustion mixed with oxygen and resulted in flaming combustion (see Figure 3.73).
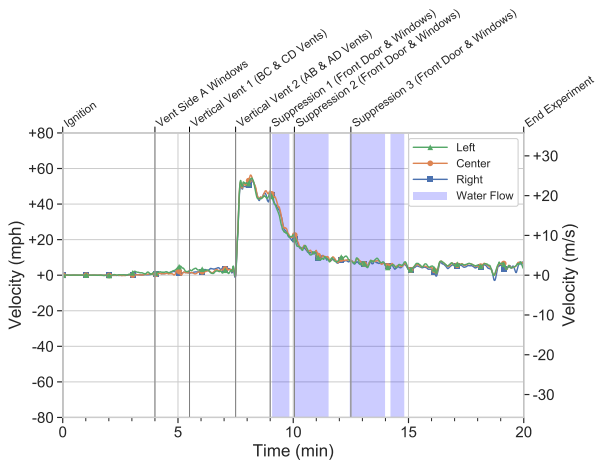
(a) AB Roof Vent
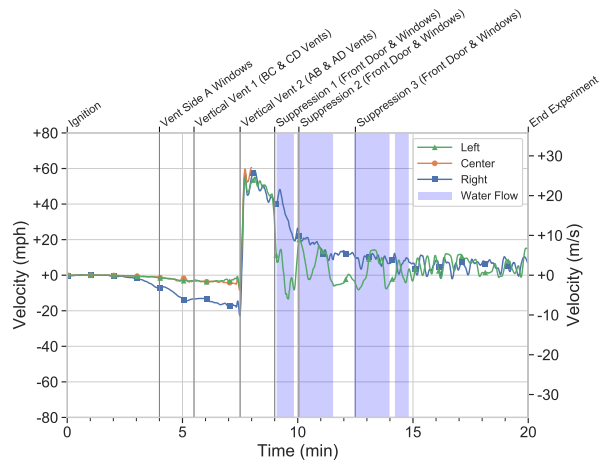
(b) AD Roof Vent
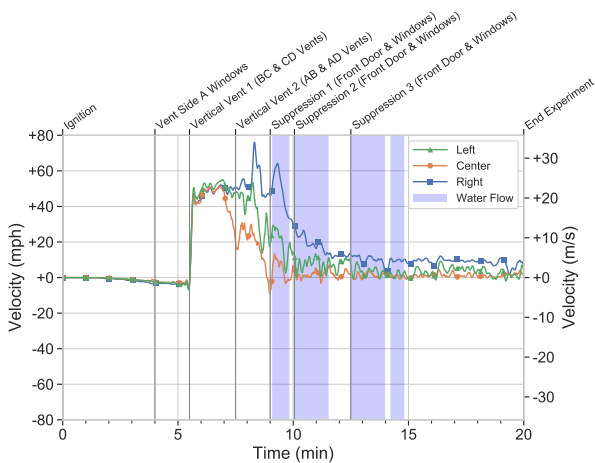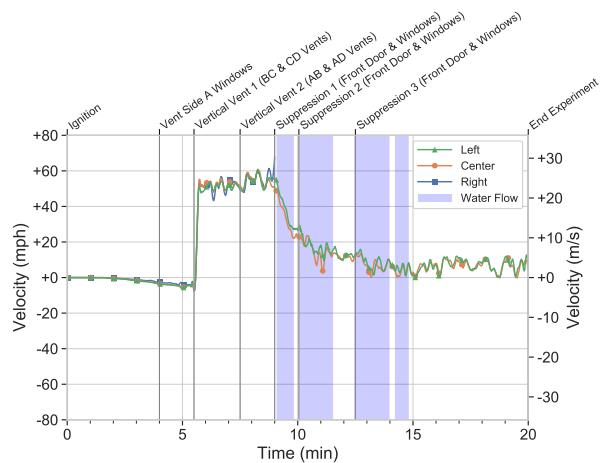
(c) BC Roof Vent

(d) CD Roof Vent

Figure 3.71: Gas velocities recorded in the roof vents during Experiment 7. Positive direction indicates flow out of the unit.
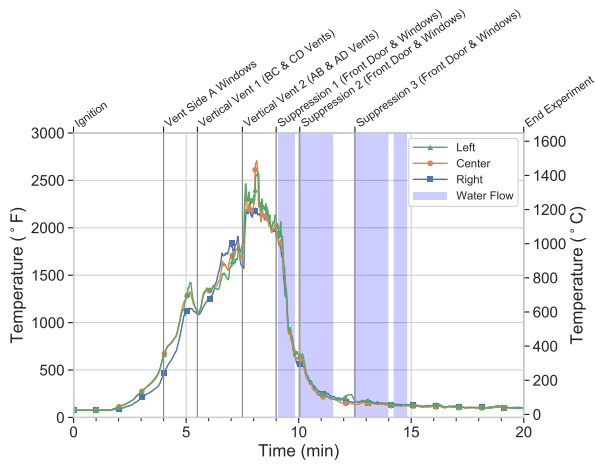
(a) AB Roof Vent
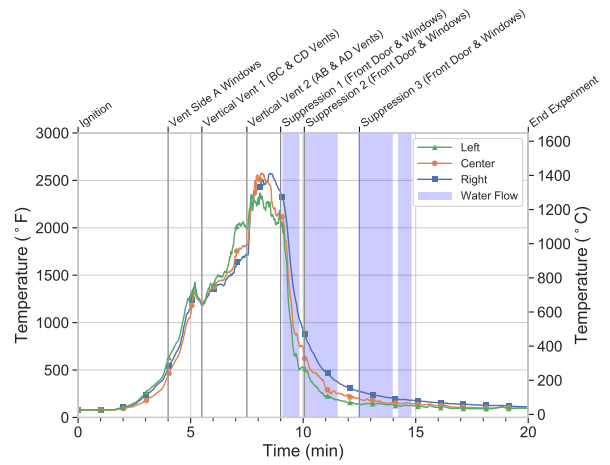
(b) AD Roof Vent
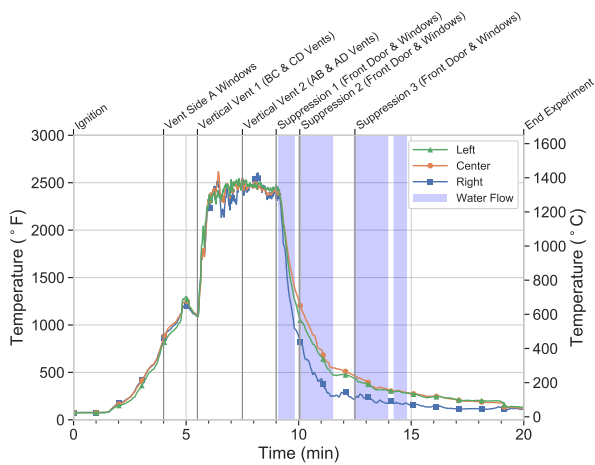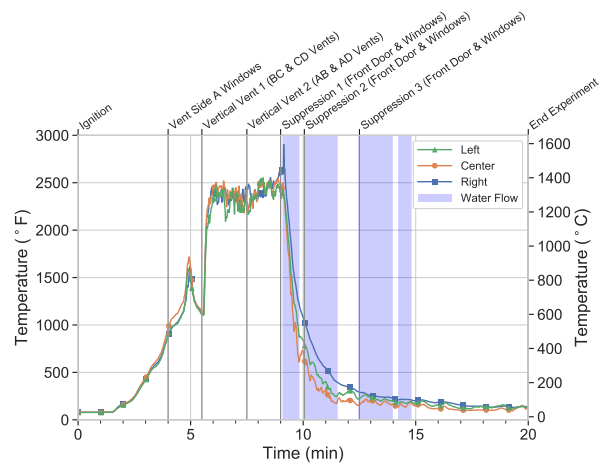
(c) BC Roof Vent

(d) CD Roof Vent

Figure 3.72: Temperatures recorded in the roof vents during Experiment 7.

Figure 3.73: Image of the open BC and CD roof vents 30 s after ventilation occurred (6 min after ignition) during Experiment 7. The image was taken from the AB corner looking toward the CD corner.

The exhaust capacity of the roof vents was not sufficient to develop a uni-directional flow path, so the front door and windows remained bi-directional vents. The velocity of inflow near the bottom of the front door increased to −13 mph (−6 m/s), and the exhaust velocity at the top of the front door decreased to 5 mph (2 m/s) (see Figure 3.69a).

The inflow of air through the front door and windows and exhaust of combustion gases out of the roof vents provided additional oxygen in the AB and AD quadrants, where temperatures exceeded 1,500 °F (816 °C) floor to ceiling. Temperatures in the BC, CD, and rear increased but remained stratified, ranging from 750 °F (399 °C) 1 ft (0.3 m) above the floor to 1,750 °F (954 °C) at the ceiling, an indication the combustion was limited by the available oxygen. Temperatures in the front door increased as the fire grew (see Figure 3.69b).

Two additional 4 ft x 4 ft (1.2 m x 1.2 m) roof vents (the AB and AD vents) were opened 7 min 30 s after ignition, providing additional vertical ventilation. All four open vents recorded uni-directional exhaust with velocities exceeding 50 mph (22 m/s, see Figure 3.71). Temperatures recorded in the roof vents exceeded 2,250 °F (1,232 °C) (see Figure 3.72). Flames were visible in the exhaust from the open roof vents 10 s following ventilation (see Figure 3.74). The additional exhaust provided was borderline in creating a uni-directional vent at the front door and widows. Although the velocity decreased, the top probe in the front door measured velocities that fluctuated

between −2 mph to 5 mph (−0.9 m/s to 2.2 m/s). The sensor array in the front door was damaged by fire 8 min 30 s after ignition, and data collection ended on those sensors.



Figure 3.74: An image of the roof vents 10 s after ventilation occurred (7 min 40 s after ignition) during Experiment 7. Image was taken from the AB corner looking toward the CD corner.

The additional air entering the front door and windows provided oxygen further into the unit and increased the size of the fire. Thermocouple arrays in all areas recorded temperatures exceeded 1,500 °F (816 °C) floor to ceiling, conditions representative of flashover throughout the entire unit, 8 min after ignition, 30 s after the additional roof ventilation occurred.

Exterior suppression occurred via a 2 1/2 in. handline with a 1 1/8 in. smooth-bore tip that flowed 265 gpm. The line was directed through the side A door and windows 9 min 10 s after ignition, and flowed for 50 s. The water flow rate is presented in Figure 3.75.
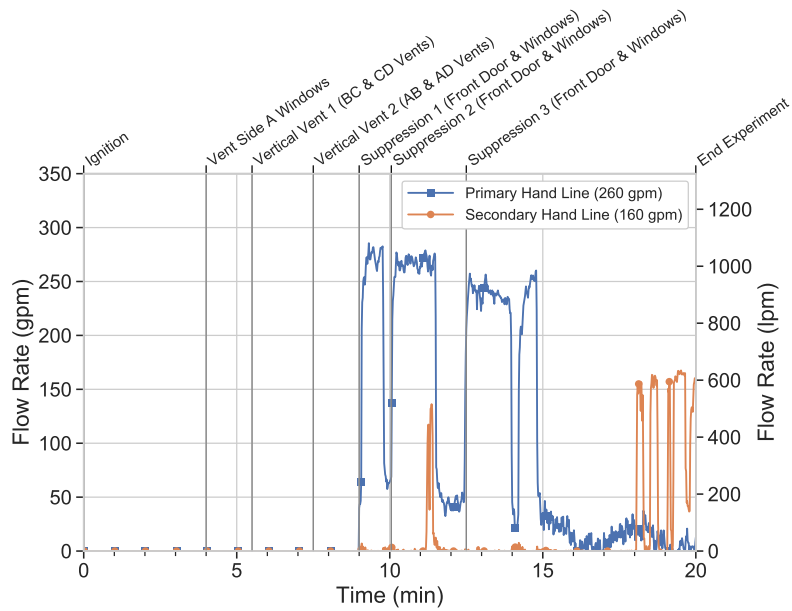
Figure 3.75: Water flows recorded during Experiment 7.

Temperatures decreased once suppression began through the rest of the scenario, from in excess of 1,500 °F (816 °C) to under 500 °F (260 °C) within 1 min in the AB and AD quadrants, where the water from the line could reach. The line was repositioned for additional suppression at 10 min 3 s and 12 min 30 s to allow water to reach the fuel further into the unit. After the third suppression, temperatures were under 500 °F (260 °C) throughout the fire compartment.

As temperatures decreased, the buoyancy of the products of combustion decreased, which resulted in a decrease in the velocity of the gases exhausted out of the open roof vents. Temperatures recorded in the roof vents decreased from over 2,250 °F (1,232 °C) to under 500 °F (260 °C) within 3 min of suppression. The flames in the roof vents were no longer visible within 30 s of the initial water application (see Figure 3.76). Once temperatures on the interior were under 500 °F (260 °C), the velocity of gases flowing out of the vents ranged from 0 mph to 10 mph (0 m/s to 4.5 m/s).

Figure 3.76: An image of the roof vents 30 s after suppression started (9 min 40 s after ignition) during Experiment 7. The image was taken from the AB corner looking toward the CD corner.

A secondary 1 3/4 in. handline with a 7/8 in. smooth-bore tip that flowed 160 gpm was directed on the front facade to suppress visible fire. The experiment concluded at 20 min after all visible flames had been extinguished. The primary handline utilized 1,212 gal, and the secondary handline utilized 208 gal for a total of 1,220 gal.

Plots of wind speed, ambient air temperature, and wind direction are presented in Figure 3.52 from ignition until the end of the experiment. The wind speed ranged from 0 mph to 7 mph (0 m/s to 3.1 m/s), blowing from the northwest toward the southeast, from side D of the unit toward side B. The ambient air temperature recorded ranged from 80 °F to 85 °F (26 °C to 29 °C) for the entire experiment. Due to the wind direction relative to the orientation of the structure and low speed, there was minimal impact to the results of the experiment.
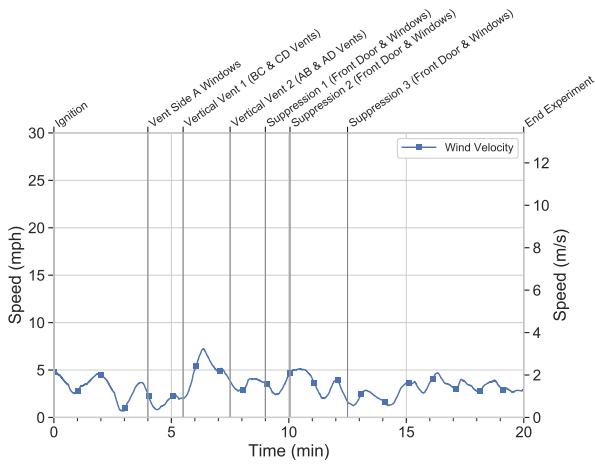
(a) Wind Speed
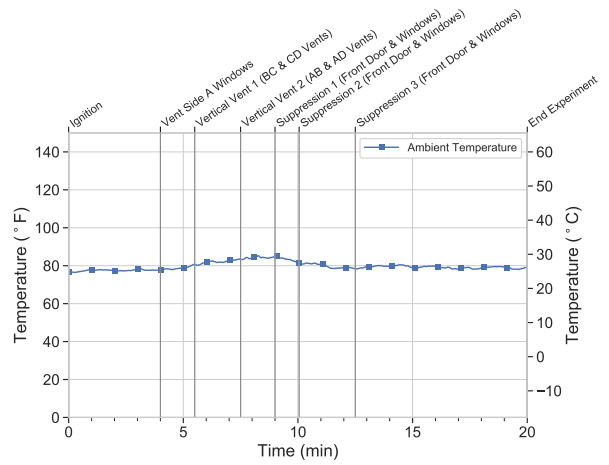
(b) Air Temperature
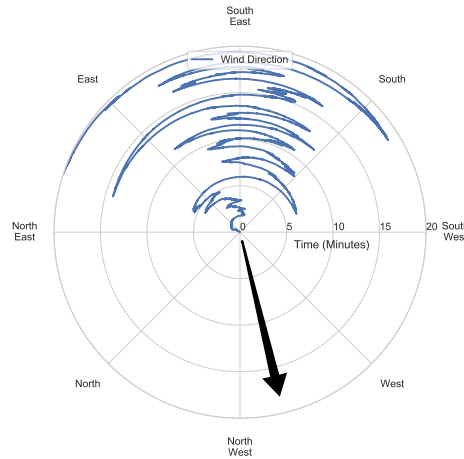


North on the chart is oriented to correspond with north on
the site layout (see Figure 2.4) and corresponding
instrument plan (see Figure 3.43). The arrow indicates
the average direction the wind was blowing.

(c) Wind Direction

Figure 3.77: Weather conditions recorded during Experiment 7.

# 4 Discussion

## 4.1 Impact of Ventilation

Buildings exchange air between the inside and the outside through ventilation. Ventilation can occur through leakage in and around construction systems, through an opening such as a window or door, or through the building heating, ventilation, and air conditioning (HVAC) system. During a fire, ventilation exchanges the products of combustion that have accumulated inside the building with air and thus oxygen from the outside. To evaluate the impact of ventilation on fire dynamics in a commercial structure, experiments were conducted that progressively increased the area of openings. Table 4.1 lists the types of ventilation and openings provided during each of the experiments.

Table 4.1: Ventilation Experiments

| Experiment | Ventilation Type | Openings |
|:---:|:---:|:---:|
| 1 | No Fire Service Ventilation | No Open Doors or Windows |
| 2 | Horizontal | Front Door and Windows (Sequential) |
| 3 | Horizontal | Front Door and Windows (Simultaneous) |
| 6 | Vertical and Horizontal | Front Door and Roof Vents |
| 7 | Vertical and Horizontal | Front Door, Front Windows and Roof Vents |

Note: During all experiments, leakage existed in and around construction systems.

### No Fire Service Ventilation

Consider the no fire service ventilation case (Experiment 1), meaning all doors and windows were closed. Figure 4.1 illustrates temperatures near the front door and in the rear of the unit. Following ignition, the temperatures increased as the fire grew, reached a peak at 4 min 30 s, and subsequently decreased as the fire entered a decay stage.
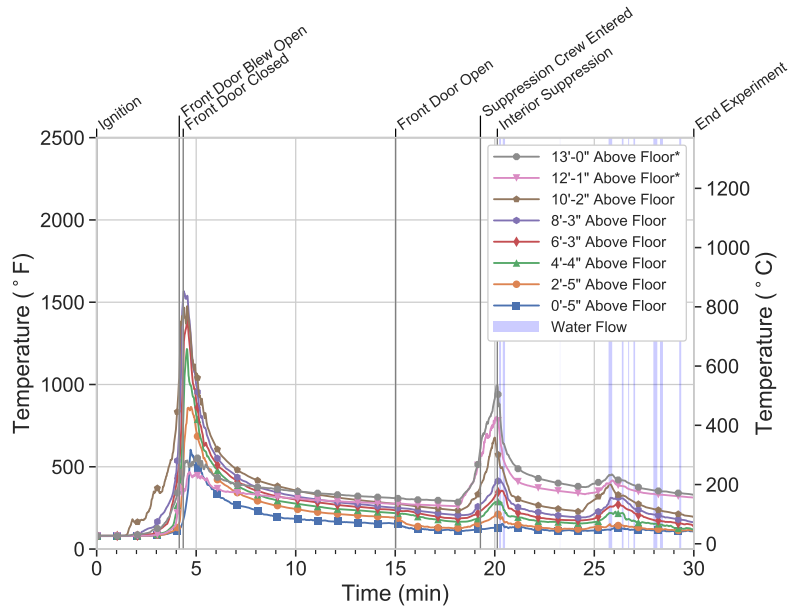
(a) AB Temperatures (Front Near Door)
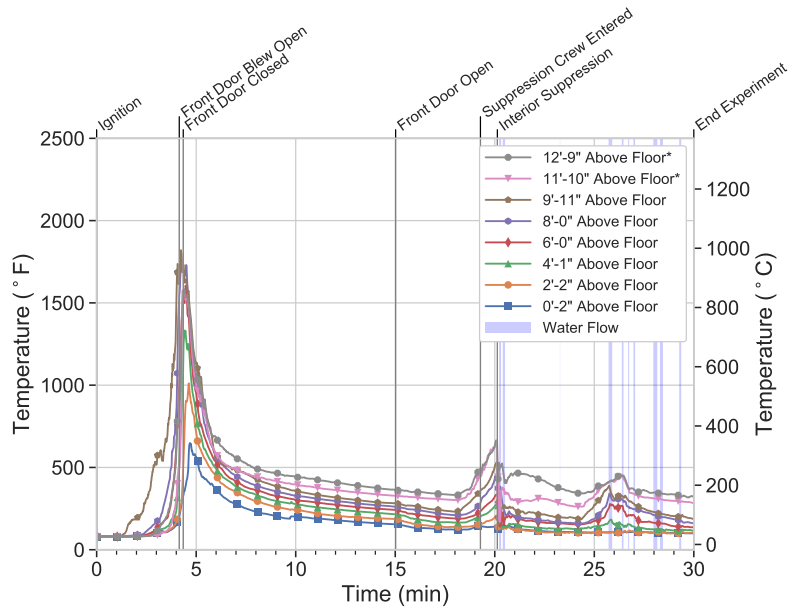


(b) BC Temperatures (Rear Near Ignition)

Figure 4.1: Temperatures near the door (AB) and in the rear near ignition (BC), when no ventilation was provided (Experiment 1). Blue shaded areas indicate time and duration of water flow.

Following suppression, fuel remained (see Figure 4.2), indicating the decay stage was due to a lack of oxygen, not the lack of fuel. A visual estimation of the fuel remaining indicated approximately 40% had been consumed. The lack of oxygen limited the fire size, which resulted in a ventilation-limited fire. This was consistent with earlier research in commercial buildings [10] and furnished residential structures [1–4, 12, 13]. With no open windows or doors, the fires became ventilation

limited, entering a decay state. In Experiment 1, when the front door was opened at 15 min to access and suppress the fire, it provided ventilation. The ventilation allowed additional oxygen into the compartment and the fire transitioned into a growth stage.



(a) Prior to Ignition                    (b) After Suppression

Figure 4.2: Images of fuel package prior to ignition and after suppression (Experiment 1).

## Horizontal Ventilation

When the front door was open prior to ignition and remained open throughout the duration of the experiment (Experiment 2), providing 19 ft$^2$ (1.8 m$^2$) of horizontal area (see Figure 4.3), it took longer for ventilation-limited decay to occur. Temperatures increased following ignition, and at 5 min 30 s the fire reached a ventilation-limited steady state as fresh air flowed in through the front door and provided a steady source of oxygen. Conditions were monitored for any sign of ventilation-limited decay, at which time additional horizontal ventilation was provided.
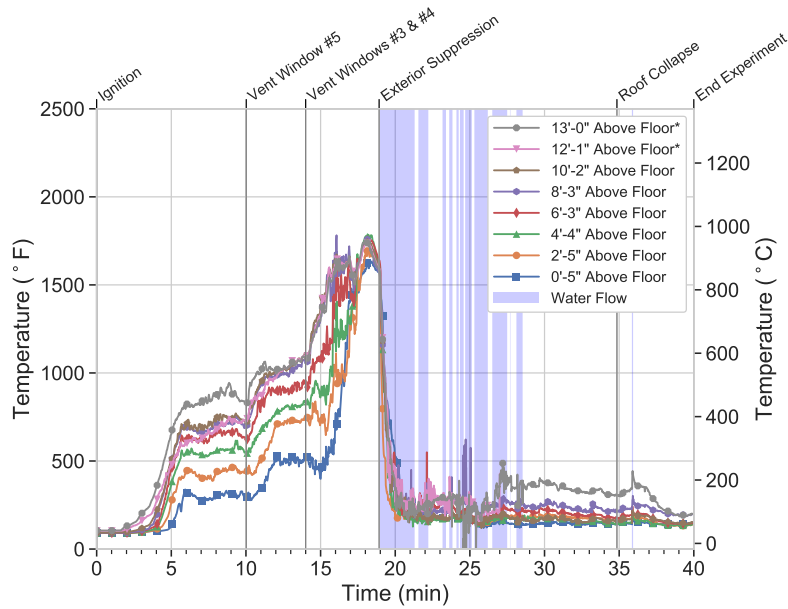
(a) AB Temperature (Front Near Door)
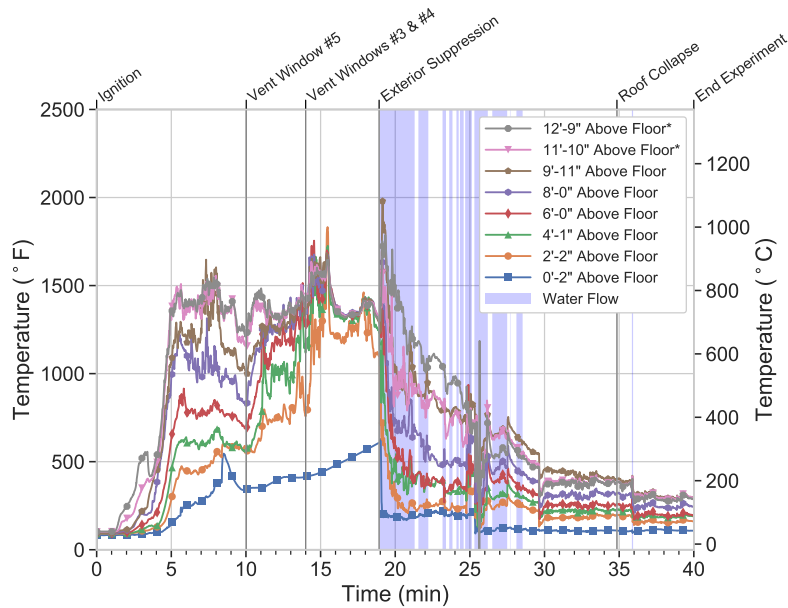


(b) BC Temperature (Rear Near Ignition)

Figure 4.3: Temperatures near the door (AB), and in the rear near ignition (BC), when the front door was opened throughout and additional ventilation provided (Experiment 2). Blue shaded areas indicate time and duration of water flow.

Additional horizontal ventilation was performed, with the ventilation of a 28.8 ft$^2$ (2.6 m$^2$) window (see Figure 3.12 – window #5) 10 min after ignition. The open window allowed products of combustion to exit and additional oxygen to be drawn in through the front door and windows. The heat release rate (HRR) of the fire increased and temperatures increased throughout. Following the

additional ventilation, the fire reached a new ventilation-limited steady state 12 min after ignition (see Figure 4.3).

Further horizontal ventilation was added when two more windows were opened (see Figure 3.12 – windows #3 and #4) 14 min after ignition. The second set of windows brought the total horizontal ventilation area to 105.8 ft$^2$ (9.8 m$^2$). The openings provided oxygen to the ventilation limited fire and temperatures increased within 2 min, indicating conditions representative of a post flashover fire in the front of the unit between the open vents and the ignition point. Temperatures in the rear decreased (see Figure 4.3). Note the temperature nearest the floor in the BC quadrant – this sensor was most likely in contact with the concrete below the carpet because it remained below 600 °F (316 °C). Flames were visible exiting the open windows and door (see Figure 4.4).



Figure 4.4: An image of flames venting out of the open front windows and door 18 min after ignition (Experiment 2).

Performing the horizontal ventilation all at once versus sequentially reduced the time to flashover. In Experiment 3, the front door was open at ignition, and all of the front glass windows were ventilated during the initial growth of the fire, 4 min after ignition. The open windows brought the total horizontal ventilation area to 97.3 ft$^2$ (7.2 m$^2$). Following ventilation, temperatures dropped by approximately 200 °F (93 °C) in the front as products of combustion were exhausted. After 30 s, temperatures in the front of the compartment increased, an indication of fire growth (see Figure 4.5a), and flames were visible out the front of the unit (see Figure 4.6). Temperatures in the rear of the unit decreased because the flames consumed the oxygen near the front of the unit, limiting how much oxygen could reach the rear of the unit (see Figure 4.5b).
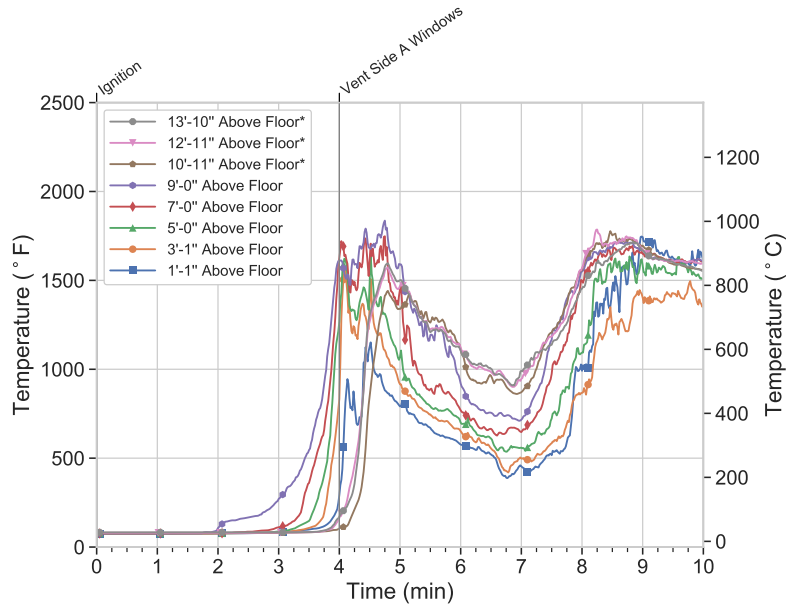
(a) AB Temperatures (Front Near Door)
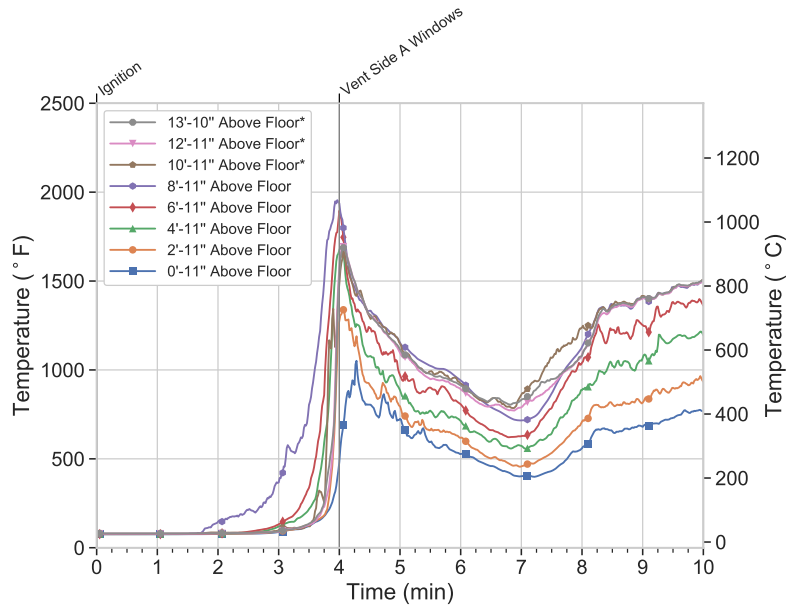


(b) BC Temperatures (Rear Near Ignition)

Figure 4.5: Temperatures for the first 10 min near the front door (AB) and near ignition (BC) when the front windows were vented all at once (Experiment 3).

(a) 30 s Post Vent



(b) 40 s Post Vent



(c) 50 s Post Vent



(d) 60 s Post Vent

Figure 4.6: Sequential images showing the front of the unit starting 30 s after the ventilation of the front windows in Experiment 3. Images continue until 60 s after window ventilation had occurred.

Table 4.2 lists the peak temperatures following the different horizontal ventilation actions that occurred in these experiments along with the total horizontal ventilation area. The more horizontal ventilation area provided, the higher the peak temperatures following ventilation.

Table 4.2: Maximum Temperatures Measured at AD Thermocouple Array Following Horizontal Ventilation

| Exp. | Openings | Ventilation Area $ft^2$ | Peak Temp. °F | Time After Ignition (min s) |
|---|---|---|---|---|
| 1 | No Openings | 0 | 285 | 15 min 0 s |
| 1 | Front Door | 19 | 670* | 20 min 0 s |
| 2 | Front Door | 19 | 740 | 9 min 0 s |
| 2 | Front Door + Window #5 | 47.8 | 1145 | 14 min 0 s |
| 2 | Front Door + Windows #3 & #4 | 105.3 | 1935 | 18 min 0 s |
| 3 | Front Door + Side A Windows | 97.3 | 1935 | 4 min 30 s |

* Regrowth after initial decay; fire was extinguished 5 min after door was opened.

This trend is consistent with previous research in furnished residential structures and commercial buildings with ventilation-limited fires, where adding horizontal ventilation increased the HRR of the fire [1–4, 10, 12, 13].

## Vertical Ventilation

When vertical ventilation was conducted in combination with horizontal ventilation (open front door) without simultaneous suppression as was the case for Experiment 6, the impact on the fire dynamics was similar to the additional horizontal ventilation experiments. After ignition, temperatures increased, reached a peak as the available oxygen in the unit was consumed, then decreased as the fire entered a ventilation-limited decay stage (see Figure 4.7). Even with the front door open, the fire transitioned from a fuel-limited fire to a ventilation limited steady state where the fire size was limited by the oxygen available through the open front-door. The only flow path was between the front door and the seat of the fire with the bottom of the doorway serving as the intake and the top of the doorway as the exhaust.
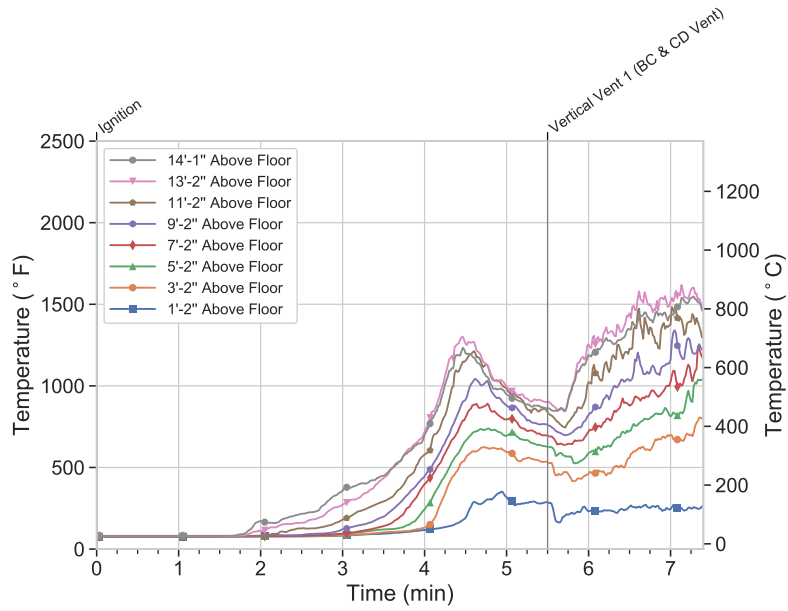
(a) AB Temperatures (Front Near Door)
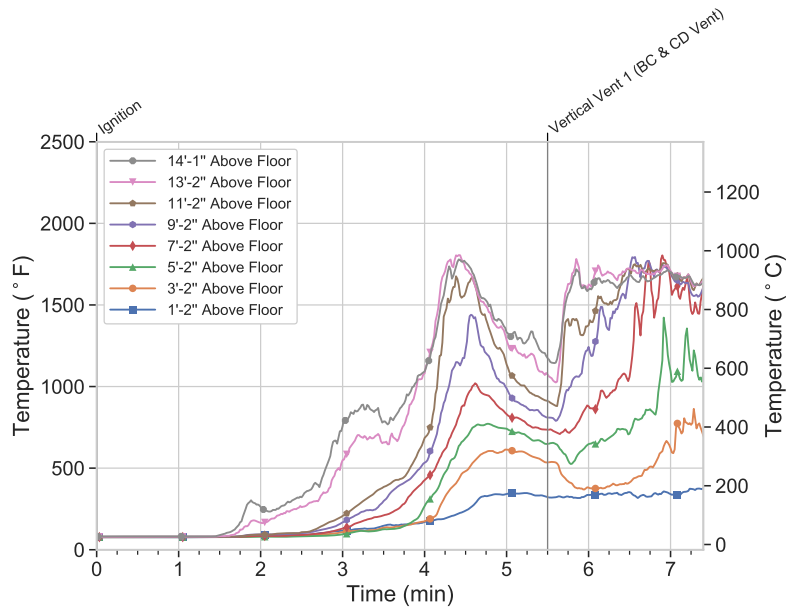


(b) BC Temperatures (Rear Near Ignition)

Figure 4.7: Temperatures in the front (AB) and rear (BC) of the unit following the initial vertical ventilation with 19 ft$^2$ (1.8 m$^2$) of intake and 32 ft$^2$ (3.0 m$^2$) of exhaust (Experiment 6).

At 5 min 30 s after ignition, a 32 ft$^2$ (3.0 m$^2$) vertical ventilation area was opened (Vertical Vent 1). The open vents created a flow path from the front door, which then became a unidirectional intake (see Figure 4.8a), to the roof vent, the unidirectional exhaust (see Figure 4.8b). Images from drone footage during the experiment captured the change in the flow path (see Figure 4.9).
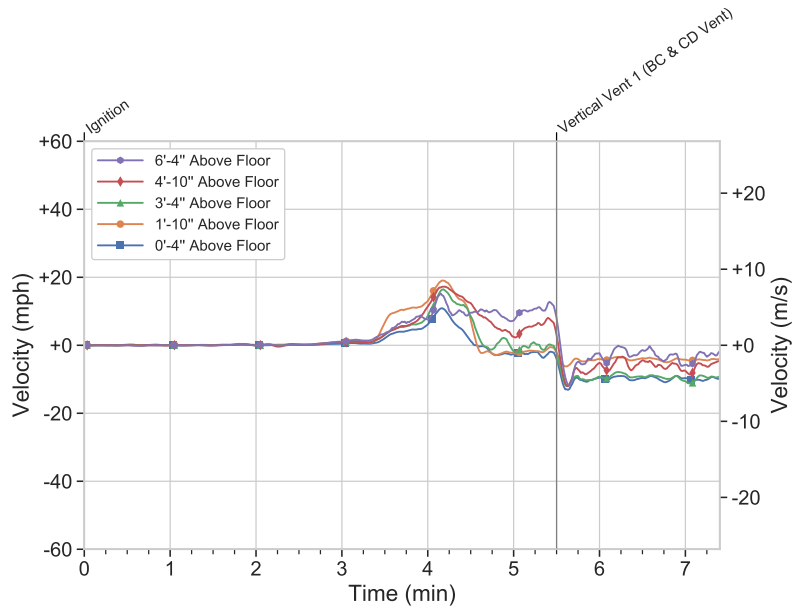


(a) Velocity - Front Door
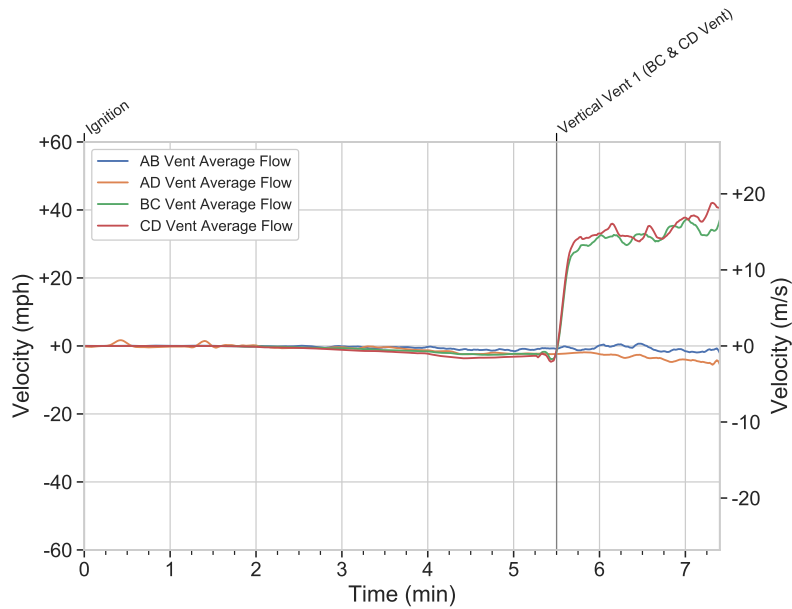


(b) Average Velocity - Vertical Vents

Figure 4.8: Gas velocity at front door and roof openings following the initial vertical ventilation with 19 ft$^2$ (1.8 m$^2$) of intake and 32 ft$^2$ (3.0 m$^2$) of exhaust (Experiment 6).

(a) 10 s Pre-Vent  (b) 0 s Vent  (c) 10 s Post Vent

(d) 20 s Post Vent  (e) 30 s Post Vent  (f) 40 s Post Vent
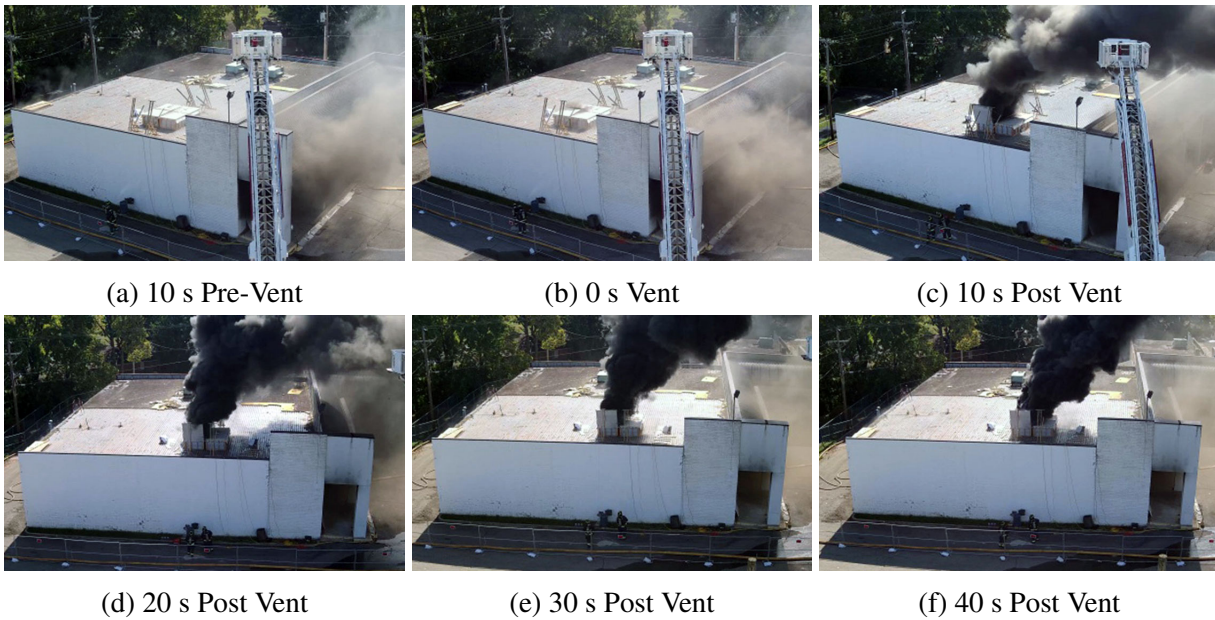
Figure 4.9: Changes in visible smoke conditions after vertical ventilation via an aerial drone view from 10 s before ventilation to 60 s after ventilation with 19 ft$^2$ (1.8 m$^2$) of intake and 32 ft$^2$ (3.0 m$^2$) of exhaust (Experiment 6).

Matt Sortman, Fairborn Police Department

The new flow path increased the oxygen entering the front door (see Figure 4.8b), and within 2 min temperatures increased, indicating the HRR of the fire had increased (see Figure 4.7).

Vertical ventilation 2 included an additional 32 ft$^2$ (3.0 m$^2$) area of roof ventilation, opened 7.5 min after ignition. The total size of the vertical ventilation area after the second ventilation was 64 ft$^2$ (6.0 m$^2$). Temperatures increased following the creation of the second vertical ventilation opening (see Figure 4.10). In approximately 1 min, temperatures represented a localized flashover in the front of the unit. The additional vertical ventilation area increased the intake at the front door (see Figure 4.11a) and the total exhaust flow (see Figure 4.11b), which increased the oxygen available for combustion and thus the HRR of the fire.
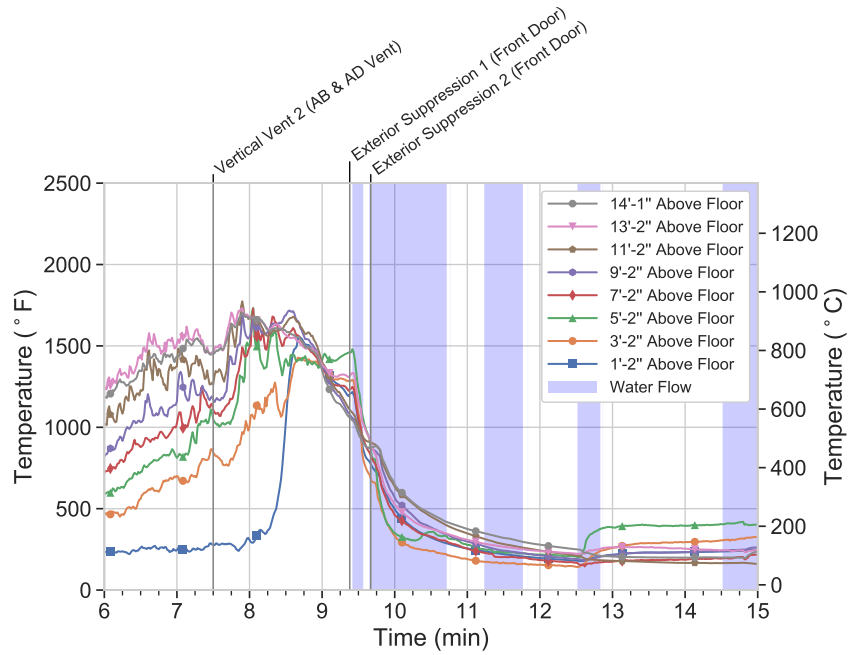
(a) AB Temperatures (Front Near Door)
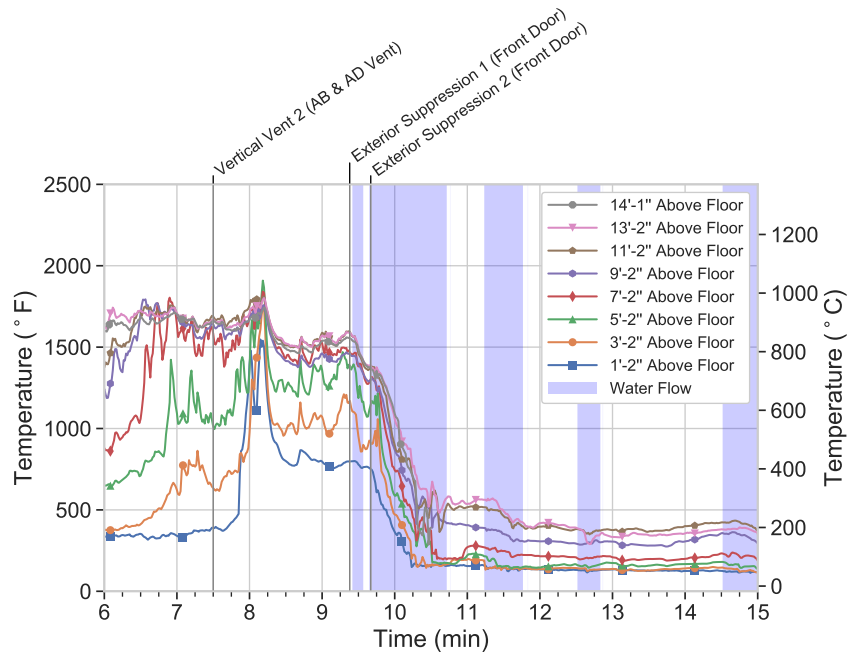


(b) BC Temperatures (Rear Near Ignition)

Figure 4.10: Temperatures following the creation of the second vertical ventilation opening with 19 ft$^2$ (1.8 m$^2$) of intake and 64 ft$^2$ (6.0 m$^2$) of exhaust (Experiment 6). Blue shaded areas indicate time and duration of water flow.
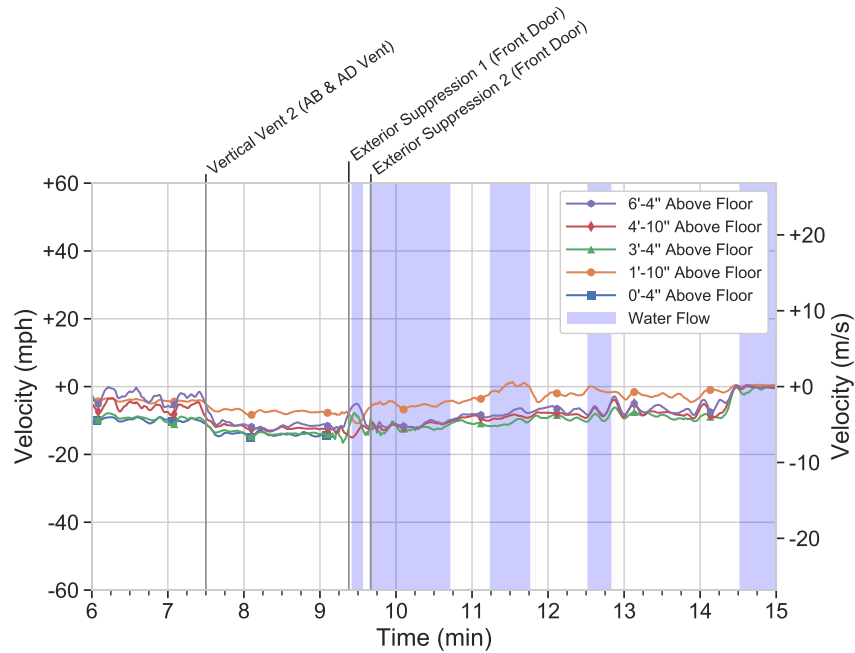
(a) Velocity - Front Door
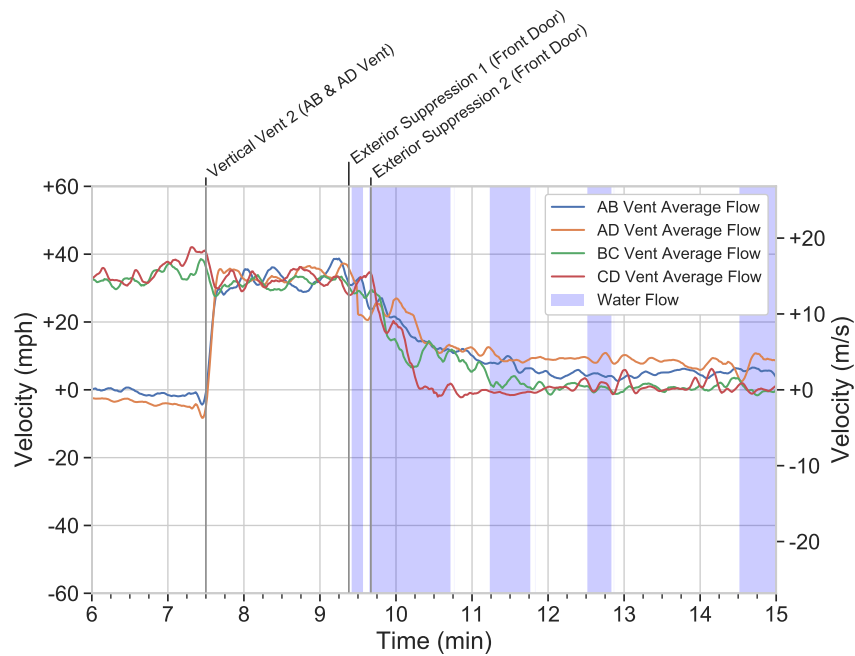


(b) Average Velocity - Vertical Vents

Figure 4.11: Gas velocity at front door and vertical ventilation openings following the initial tactical vertical ventilation with 19 ft$^2$ (1.8 m$^2$) of intake and 64 ft$^2$ (6.0 m$^2$) of exhaust (Experiment 6). Blue shaded areas indicate time and duration of water flow.

Flames were visible at the roof vents 10 s after the second ventilation action as the hot fuel-rich products of combustion mixed with oxygen on the exterior (see Figure 4.12).



(a) 10 s Pre Vent

(b) 0 s Vent

(c) 10 s Post Vent

(d) 20 s Post Vent

(e) 30 s Post Vent

(f) 40 s Post Vent
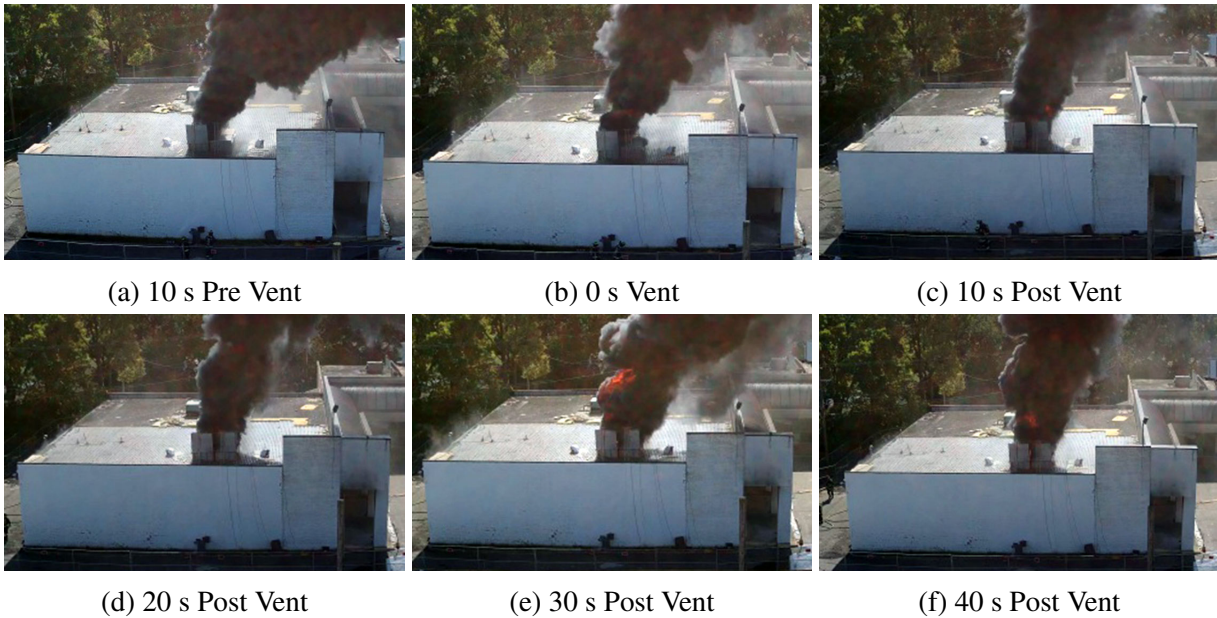
Figure 4.12: Changes in visible fire conditions after opening the second set of vertical vents via drone from 10 s before ventilation to 40 s after ventilation with 19 ft$^2$ 1.8 m$^2$ of intake and 64 ft$^2$ (6.0 m$^2$) of exhaust. (Experiment 6).

Matt Sortman, Fairborn Police Department

Table 4.3 lists the peak and 3 ft above-floor peak temperatures recorded near the front door (AB temperatures) prior to first vertical ventilation action, prior to the second vertical ventilation action, and 1 min after the second vertical ventilation action in Experiment 6. The 3 ft peak temperature highlights the impact vertical ventilation could have had on a crawling firefighter at that location. Similar to horizontal ventilation, the increased vertical ventilation area resulted in higher steady-state air temperatures. Although the additional ventilation exhausted more products of combustion, it also allowed more oxygen to enter the compartment and lead to an increased HRR.

Table 4.3: Peak Temperatures (AB Thermocouple Array) Experiment 6

| Exp. | Openings | Ventilation Area ft$^2$ | | Peak Temp. °F | 3ft Peak Temp. °F | Time After Ignition min s |
| | | Intake | Exhaust | | | |
|---|---|---|---|---|---|---|
| 6 | Front Door | 10* | 9* | 1861 | 568 | 5 min 30 s |
| 6 | Front Door + BC & CD Vents | 19 | 32 | 1960 | 865 | 7 min 30 s |
| 6 | Front Door + All 4 Vents | 19 | 64 | 1805 | 1430 | 8 min 30 s |

* Area estimated via bi-directional probe data from front door.

Consider the smoke and fire conditions at the front door as function of increased vertical ventilation as shown in Figure 4.13. Prior to the first vertical vent action (see Figure 4.13a), there was bi-directional flow at the front door as shown in both Figure 4.8a and Table 4.3. As the vertical ventilation area increased (see Figure 4.13b–4.13d), the velocity profile at the door became unidirectional intake (see Figure 4.11a) and temperatures inside the front door rose (see Table 4.3) with minimal changes in visibility at the front door. At 2 min after the second set of vertical ventilation vents were opened, flames were visible at the front door.

(a) Prior to Vertical Vents (5:30)



(b) 60 s Post Vent 1 (6:30)



(c) Prior to Vertical Vent 2 (7:30)



(d) 60 s Post Vent 2 (8:30)



(e) 120 s Post Vent 2 (9:30)

Figure 4.13: Changes in visible smoke and fire conditions at the front door after changes in vertical ventilation (Experiment 6).

To assess if the front door limited the intake and prevented additional cooling during vertical ventilation, Experiment 7 was conducted with additional horizontal ventilation area combined with the same total area of roof vents. With the front door open, the fire was ignited and temperatures increased as the fire spread through the fuel package near the point of ignition (see Figure 4.14).

(a) AB Temperatures (Front Near Door)

(b) BC Temperatures (Rear Near Ignition)
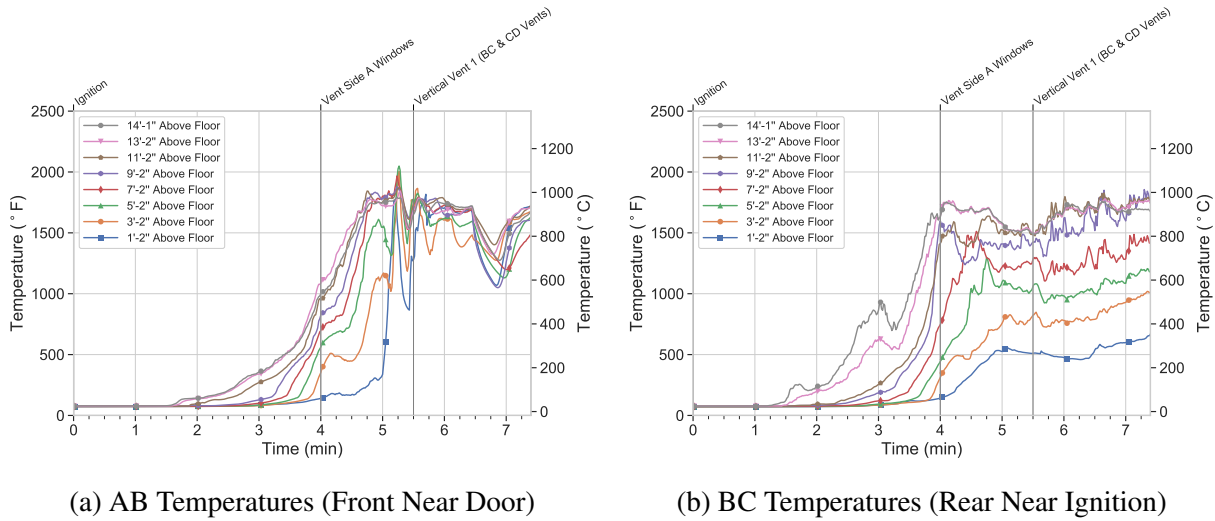
Figure 4.14: Temperature response during Experiment 7 to horizontal ventilation and initial vertical ventilation (BC & CD vents) with total vertical vent area of 32 ft$^2$ (3.0 m$^2$) and the horizontal ventilation area of 81.5 ft$^2$ (7.6 m$^2$).

In the beginning stages of this scenario (Experiments 5, 6, and 7), a flow path was established between the open front door and the seat of the fire. The flow path began and ended at the front door, with the bottom of the door as the intake and the top of the door as the exhaust. Intake flows circulated as far back as the group of boxes near ignition. Consider Figure 4.15, which depicts a cutaway of the unit generated from a computational fire model [36] with representative flows that developed as a result of the open front door. The blue arrows denote intake air flow, red arrows denote exhaust flow of combustion gases, and purple arrows denote a mixture of air and combustion gases. The depth of travel for the intake air decreases as the compartment becomes more ventilation-limited and the flame front moves toward the open vent consuming the oxygen. Also note the area of recirculation in the rear of the unit in Figure 4.15. Before the oxygen available for combustion in the rear is completely consumed, it mixes with the gases produced by the fire (creating the purple arrows) and becomes an inefficient supply for combustion.
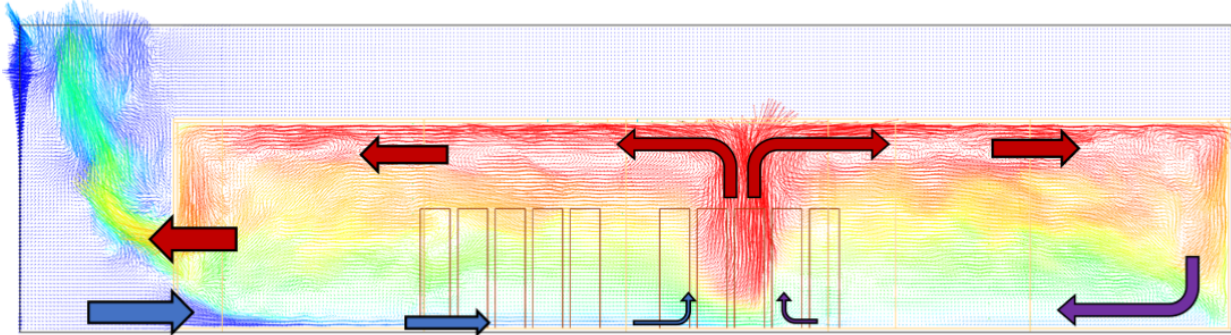
Figure 4.15: A representation of flow (intake and exhaust) within the unit for Experiment 7 following horizontal ventilation generated using a computational fire model [36]. The blue arrows denote intake air flow, red arrows denote exhaust flow of combustion gases, and purple arrows denote a mixture of air and combustion gases.

In Experiment 7, the front windows were vented 4 min after ignition, providing 62.5 ft$^2$ (5.8 m$^2$) of additional horizontal ventilation area. The total horizontal vent area following the opening of the windows was 81.5 ft$^2$ (7.6 m$^2$). After the windows were opened, the rate of temperature rise slowed in the front of the compartment, then returned to previous conditions (see Figure 4.14). Flames were visible pushing out of the open front windows and front door 1 min after the horizontal ventilation occurred (see Figure 4.16). The flow path increased in width as it now included the bottom of the door and windows as the intake, and the top of the door and windows as the exhaust.



Figure 4.16: An image of flames venting out of the open front windows and door 1 min after horizontal ventilation, 5 min after ignition (Experiment 7).

A roof vent 32 ft$^2$ (3.0 m$^2$) in area was opened 5 min 30 s after ignition. Following the vertical ventilation, an additional flow path was established. The initial flow path that started and ended at the front door and windows was supplemented by a flow path between the horizontal opening on the front and the open roof vents. The velocity of the gases exiting the top of the horizontal opening on the front decreased (see Figure 4.17a) as the open vertical vents exhausted products of combustion through the roof vents (see Figure 4.17b). Flames were visible both at the front opening and the open roof vents (see Figure 4.18).
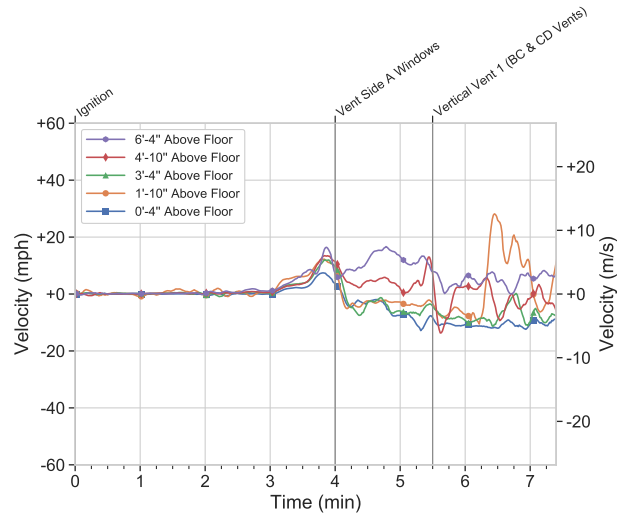


(a) Velocity - Front Door
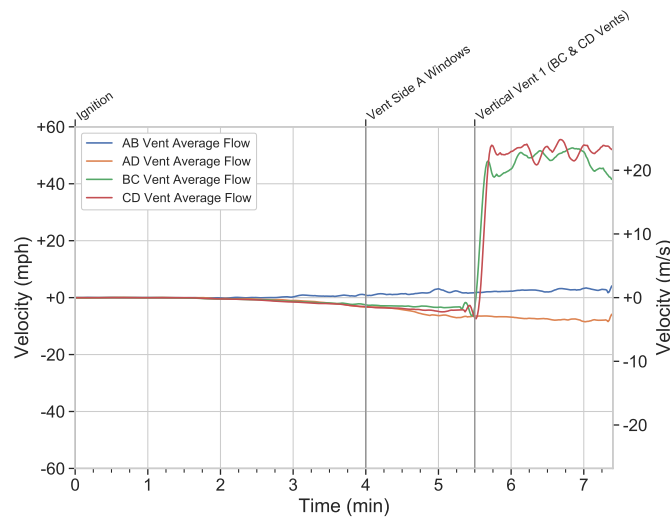


(b) Average Velocity - Vertical Vents

Figure 4.17: Gas velocity response to the first vertical ventilation for Experiment 7 when the vertical ventilation was 32 ft$^2$ (3.0 m$^2$) and the horizontal ventilation area was 81.5 ft$^2$ (7.6 m$^2$).

(a) 10 s Pre Vent



(b) 0 s Vent



(c) 10 s Post Vent



(d) 20 s Post Vent

Figure 4.18: Smoke and fire conditions associated with the first vertical ventilation on conditions at the front of the unit (left column) and roof (right column) from 10 s before vertical ventilation to 20 s after. The vertical openings combined for a total of 32 ft$^2$ (3.0 m$^2$), and the horizontal opening was 81.5 ft$^2$ (7.6 m$^2$) (Experiment 7).

Temperatures in both the front (AB) and rear (BC) increased following the vertical ventilation. The additional oxygen provided by the additional exhaust opening, increased the heat release rate of the fire (see Figure 4.14).

An additional 32 ft$^2$ (3.0 m$^2$) of vertical ventilation was provided at 7 min 30 s after ignition. The total size of the vent areas was 81.5 ft$^2$ (7.6 m$^2$) of horizontal area and 64 ft$^2$ (6.0 m$^2$) of vertical area. The additional ventilation increased the flow between the front openings and the roof vents (see Figure 4.19). Following the additional vertical vents, flames retracted into the unit in the front, and flames were visible from all four roof vents (see Figure 4.20).
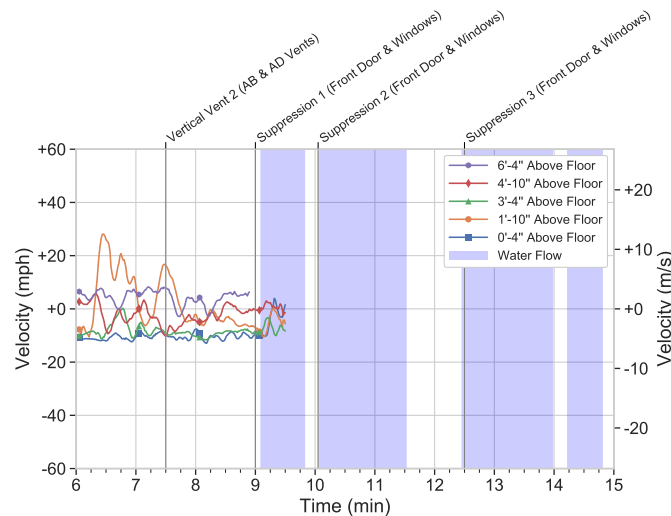


(a) Velocity - Front Door
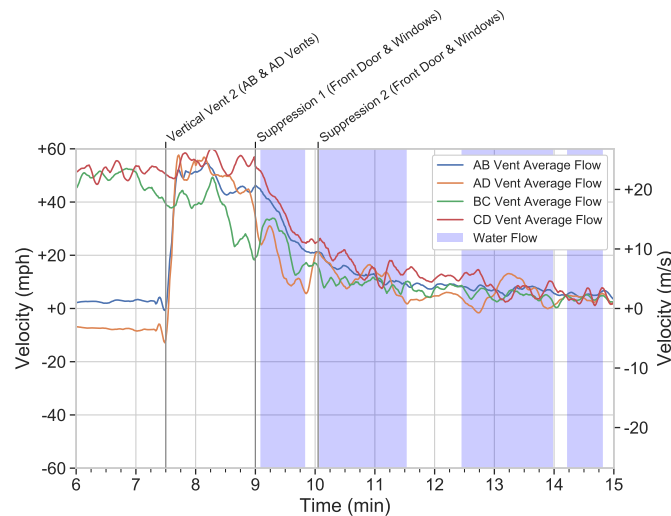


(b) Average Velocity - Vertical Vents

Figure 4.19: Gas velocity in Experiment 7, focused on the second vertical ventilation action when the vertical ventilation was 64 ft$^2$ (6.0 m$^2$) and the horizontal ventilation area was 81.5 ft$^2$ (7.6 m$^2$). Blue shaded areas indicate time and duration of water flow.

(a) 10 s Pre Vent



(b) 0 s Vent



(c) 10 s Post Vent



(d) 20 s Post Vent

Figure 4.20: Smoke and fire conditions associated with the second vertical ventilation for Experiment 7 on conditions at the front of the unit (left column) and roof (right column) from 10 s before ventilation to 20 s after ventilation. The vertical vent area was 64 ft$^2$ (6.0 m$^2$), and the horizontal vent area was 81.5 ft$^2$ (7.6 m$^2$).

Compared to Experiment 6, the additional horizontal vents in the front in Experiment 7 not pro-
vided provided more make up air for the vertical vents, they also provided more oxygen to a
ventilation limited fire and increased the heat release rate of the fire. This is indicated by the
higher temperatures recorded in the vertical vents during Experiment 7 (see Figure 4.21b) versus
Experiment 6 (see Figure 4.21a).
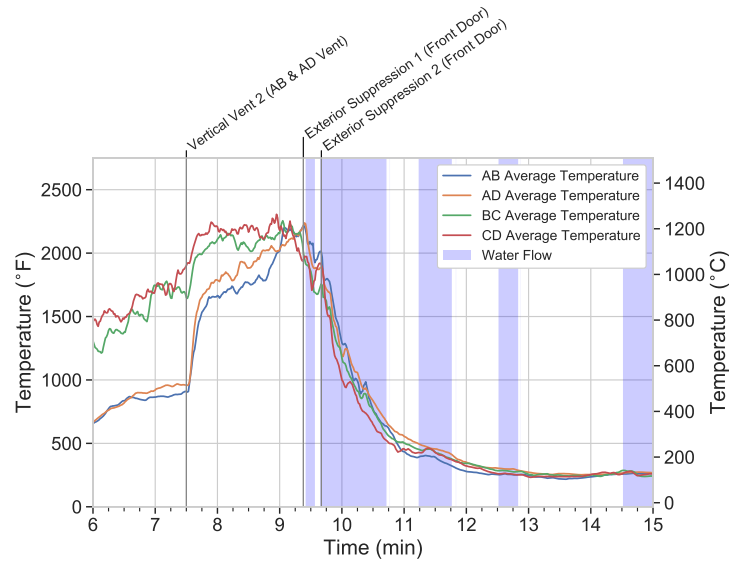


(a) Experiment 6
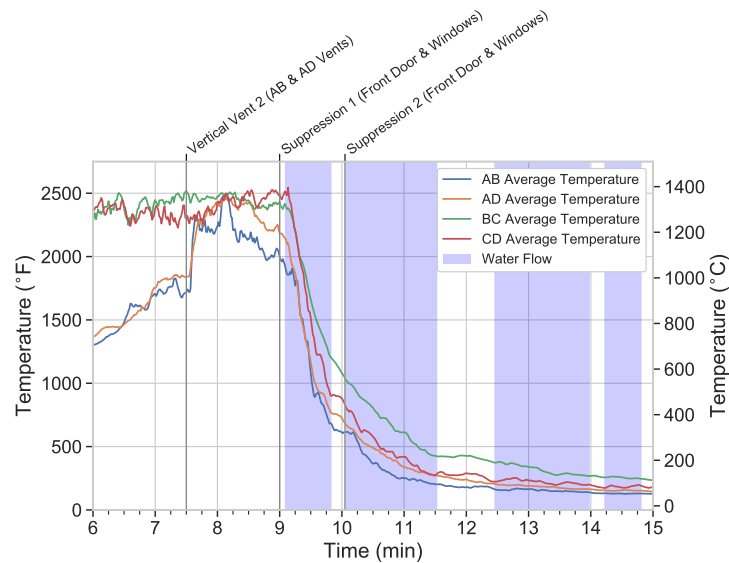


(b) Experiment 7

Figure 4.21: Temperature changes associated with the second ventilation when the vertical venti-
lation was 64 ft$^2$ (6.0 m$^2$) and the horizontal ventilation area was 81.5 ft$^2$ (7.6 m$^2$). Blue shaded
areas indicate time and duration of water flow.

Additionally, in Experiment 7, temperatures on the interior further increased after subsequent vertical vent area was opened. Uniform floor to ceiling temperatures were recorded in both the front and the rear, an indication of flashover conditions throughout (see Figure 4.22). The additional vertical ventilation exhausted more products of combustion and allowed more air to enter the front of the unit, increasing the heat release rate inside and outside the structure.
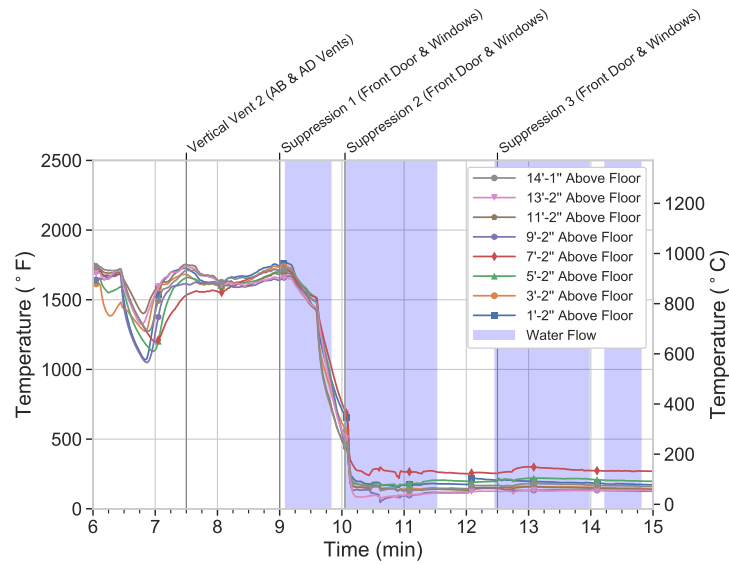


(a) AB Temperature (Front Near Door)
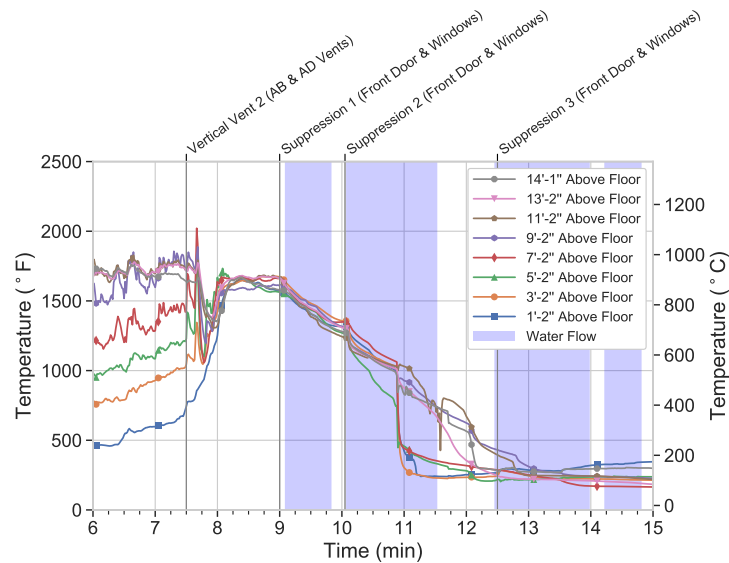


(b) BC Temperature (Rear Near Ignition)

Figure 4.22: Temperature changes associated with the second vertical ventilation action for Experiment 7 when the vertical ventilation was 64 ft$^2$ (6.0 m$^2$) and the horizontal ventilation area was 81.5 ft$^2$ (7.6 m$^2$). Blue shaded areas indicate time and duration of water flow.

Figure 4.23 provides a representation of the flows within the unit with front door and windows open and all of the vertical vents open generated with a computational fire model [36]. The blue arrows denote intake air flow, red arrows denote exhaust flow of combustion gases, and purple arrows denote a mixture of air and combustion gases. In this figure, the addition of the vertical vents transitioned the front of the structure from a bi-directional flow to a unidirectional intake as the vertical vents were unidirectional exhausts. Note the decreasing magnitude of intake with elevation. This is similar to Experiment 7 where the top probe showed fluctuations between intake and exhaust.
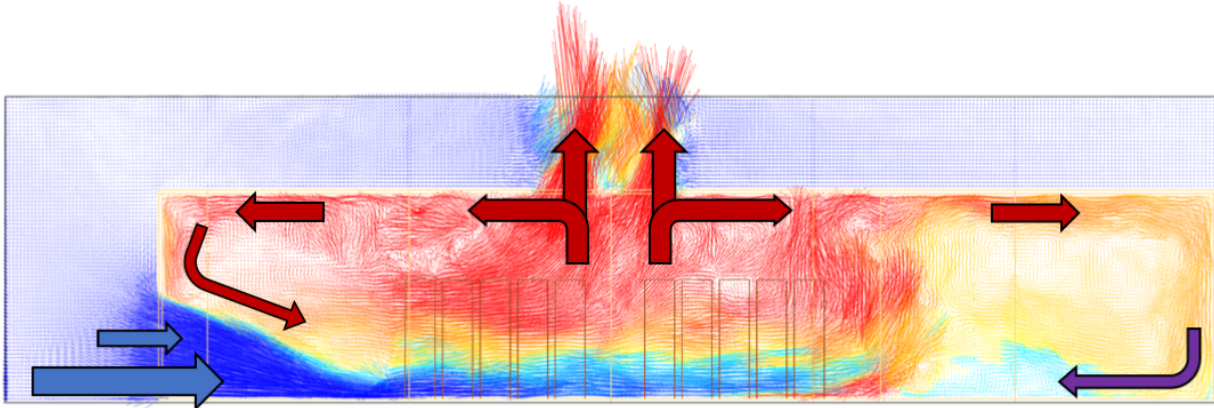


Figure 4.23: A representation of flow (intake and exhaust) within the unit for Experiment 7 following the second vertical ventilation action generated using a computational fire model [36]. The blue arrows denote intake air flow, red arrows denote exhaust flow of combustion gases, and purple arrows denote a mixture of air and combustion gases.

In each scenario examined, when the additional ventilation area (vertical or horizontal) increased the exhaust of combustion products, it also caused additional air to enter the unit. The additional air added oxygen to a ventilation-limited fire, and the temperatures increased. Although flames were visible in Experiments 6 and 7 at the open vertical vents, this was not an indication that all of the heat was being exhausted. It is important to note that the total horizontal ventilation area was constrained by the physical building and the maximum vertical ventilation area was determined prior to the experiments through consensus discussion with the project technical panel. The results from these experiments (Experiments 1-4, 6, and 7) are consistent with prior research into furnished residential structures with ventilation-limited fires where ventilation without coordinated suppression lead to an increase in the heat release rate of the fire [2, 12, 37]. In Experiment 5, the simultaneous suppression with vertical ventilation showed a reduction in temperatures and resultant fire HRR, similar to the results of prior research on coordinated suppression of residential fires [24].

## 4.2 Pressure

The relationship between pressure and temperature in a constant volume and a fixed mass is known as Gay-Lussac's Law [38]. When the temperature of constant volume gas is increased, the gas expands, and the pressure increases proportionally. This phenomenon is important to understand in compartment fires. As the fire creates heat, that heat is transferred to the surrounding gases and expansion occurs, resulting in increased pressure within the compartment. Consider Experiment 1 where all windows and doors were closed at ignition. The fire was ignited and gas temperatures increased (see Figured 4.24a). As the gas temperatures increased, the gas expanded and the pressure transducers recorded a pressure increase (see Figure 4.24b). While some leakage did exist in the structure and reality does not match the 'ideal' case perfectly, the phenomenon is adequately described by the above relationship.
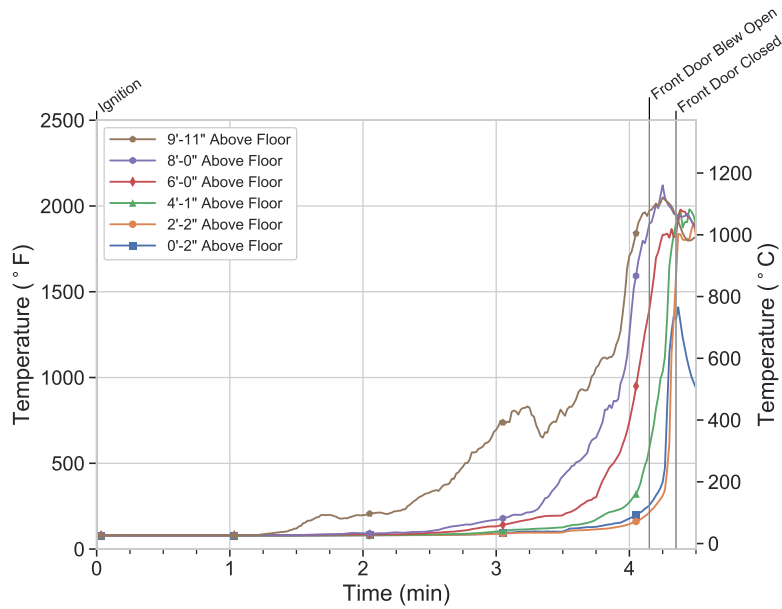
(a) CD Temperatures
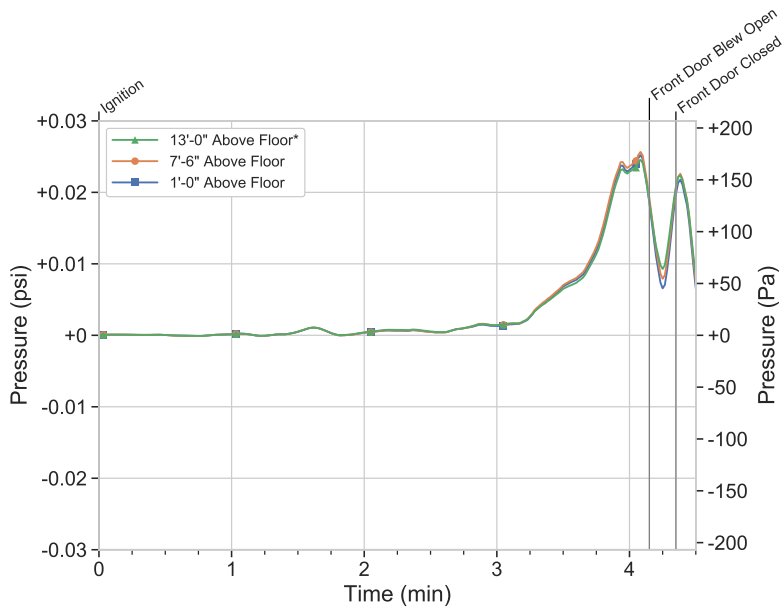


(b) Side D Pressure

Figure 4.24: CD temperature and side D pressure recorded during the first 4 min 30 s of Experiment 1. Positive values indicate a pressure rise in the fire compartment.

Conversely, when the temperature of constant volume gas is decreased, the gas contracts, and the pressure decreases proportionally. For example, in Experiment 1, all the doors and windows were closed. As the fire consumed the available oxygen, it entered into a ventilation-limited decay state at 4 min 20 s. The lack of oxygen decreased the heat release rate and gas temperatures decreased (see Figure 4.25a).
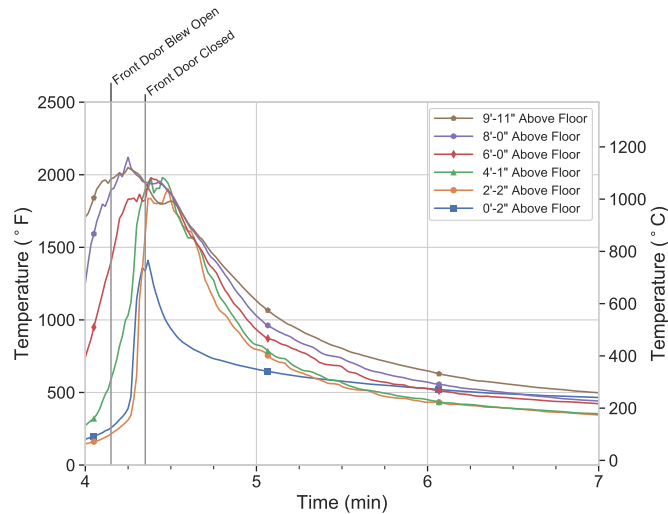
(a) CD Temperatures
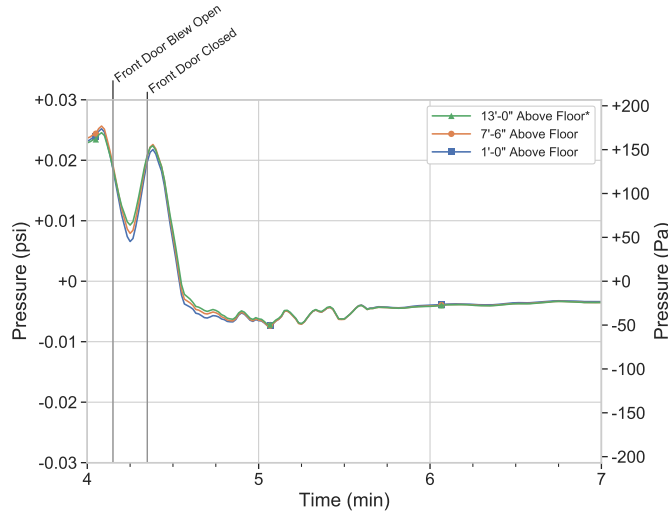


(b) Side D Pressure

Figure 4.25: CD temperature and side D pressure recorded from 4 min to 7 min during Experiment 1. Positive values indicate a pressure rise in the fire compartment.

The decrease in temperature caused contraction of gases in the compartment. With all doors and windows closed, the contraction resulted in a decrease in pressure. Because the door opened due to the pressure generated during gas expansion, some of the gases were exhausted. High-pressure gases inside the unit flowed out of the building to the low-pressure ambient air on the exterior. When the door was closed, the pressure recovered to the levels slightly below those recorded before the door opened. This is due to the volume of gas that exhausted under pressure when the quasi-constant volume constraint was removed (i.e., door opened). As the gas temperatures cooled, the gas contracted, and the pressure dropped below the initial ambient value and became negative (see Figure 4.25b).

In addition to the expansion and contraction of gases, flow can also impact measured pressure. Consider the unidirectional flow path between the front door (intake) and the open roof vents (exhaust) in Experiment 6 (see Figure 4.26).
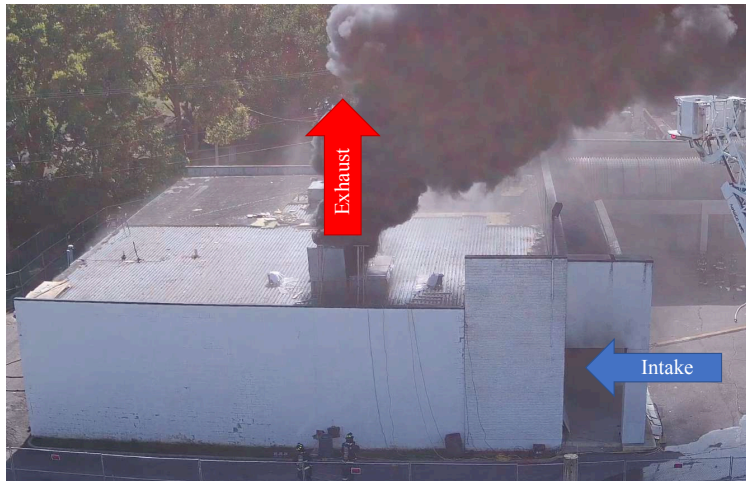


Figure 4.26: Flow path after initial vertical ventilation during Experiment 6 with the front door as a unidirectional intake and the open two roof vents as a unidirectional exhaust.

Matt Sortman, Fairborn Police Department

For Experiment 6, the pressure sensors located in the side B wall measured the differential pressure between the unit interior (flow) and the unit exterior (no-flow). With only the front door open at ignition, a bi-directional flow was recorded on the front door velocity probes. Gases were exhausted at the top and air was drawn in at the bottom (see Figure 4.27a from 5 min to 5 min 30 s). At 5 min 30 s, two roof vents were opened, which created a unidirectional flow path through the front door and out of the open roof vents (see Figures 4.27a and 4.27b). The gases flowing through the interior volume created a zone of low pressure in which the interior pressure was less than the exterior, and therefore negative (see Figure 4.27c). Recall pressures were recorded as gauge pressure, or pressure relative to the atmospheric pressure (or ambient pressure outside of the structure). On the graphs, atmospheric pressure is represented as 0 psi (0 Pa), with positive values representing pressures above atmospheric and negative values representative of pressures below atmospheric.
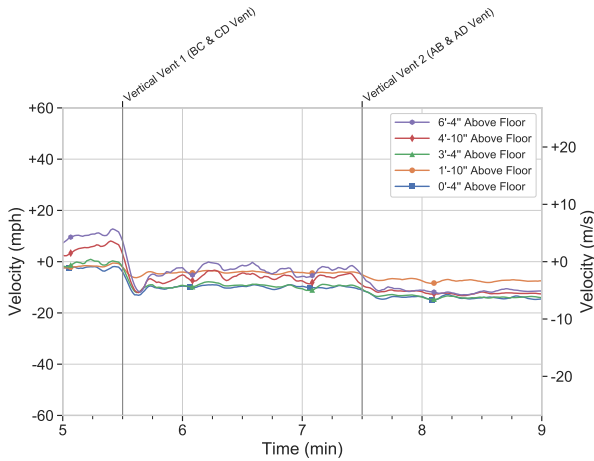
(a) Front Door Gas Velocities
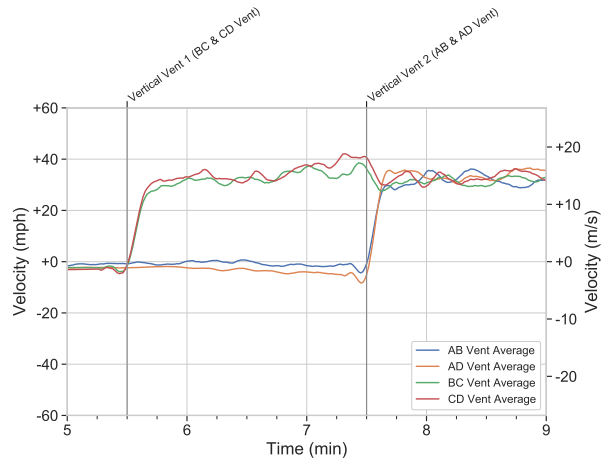


(b) Roof Vent Gas Velocities
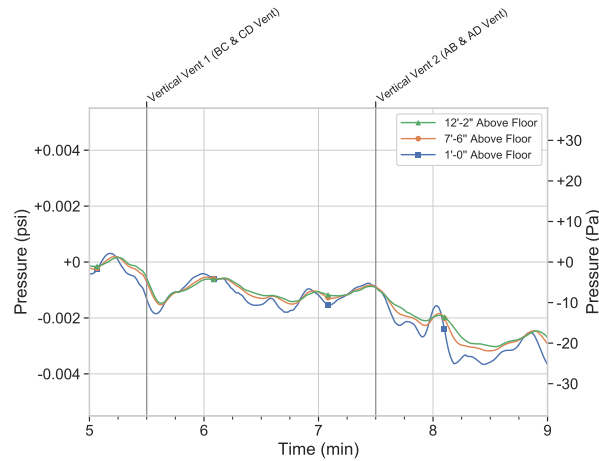


(c) Side B Pressure

Figure 4.27: Gas velocities in the open front door, gas velocities in the roof vents, and differential pressure in Experiment 6 from 5 min to 9 min. The gases flowing in through the front door (negative values at front door) and exhausting through the roof vents (position values at roof vents) created a zone of low pressure which is shown via the side B pressure data.

At 7 min 30 s, two additional roof vents were opened. The additional exhaust area increased the inflow at the front door (see Figure 4.27a), which resulted in an additional pressure decrease (see Figure 4.27c). Although the fire created pressure through gas expansion, the pressure decrease due to the flow was greater than the pressure rise from expansion, and the values remained negative.

Gas flow out of ventilation openings in a compartment fire are driven by the pressure profile across the opening. The heat energy released from the fire increases the temperature of the gases and causes expansion, which increases the pressure in the compartment and translates to flow out of any available openings. Karlsson et. al. discusses this phase of fire growth in *Enclosure Fire Dynamics* as lasting only a few seconds after the hot gases first flow out the top of any open vent [39]. After this period of exhaust, the mass flow out is balanced by a mass flow in, and the

148

pressure profile across the opening transitions to exhaust at the top and intake at the bottom [39].

During all of the experiments in which the front door was open at ignition (Experiments 2–7), a unidirectional exhaust from the open doorway was observed prior to 5 min into the experiment. This unidirectional outflow of smoke continued beyond the hot gas layer reaching the top of the open doorway. No additional openings, beyond natural structure leakage, were present at the time of the unidirectional exhaust.

For Experiment 1, where the front door was closed prior to ignition, pressure magnitudes similar to Experiment 4 and exhaust velocities similar to Experiments 5 and 6 were measured in the 30 s window around the door being blown open. Consider the series of images taken in the second prior to the door opening as shown in Figure 4.28. Notice the concavity change of the reflection in window (highlighted by the red circle) in the first three images prior to the door opening (see Figures 4.28a–4.28c) compared to after the door was opened (see Figure 4.28d). While it may be difficult to see from the set of images, the reflection bowing outward before it flattens out is an indication of the pressure build up and subsequent relief following the open door.

(a) 1 s Prior to Door Open



(b) 0.75 s Prior to Door Open



(c) 0.5 s Prior to Door Open



(d) Door Open

Figure 4.28: A series of images that show the pressure rise in Experiment 1 from 1 s prior to the door opening to the door opening. The reflection in three images prior to the door open show an outward bow of the glass, an indication of built-up pressure in the unit. Following the door opening, the reflection flattened out as the pressure inside the unit dropped.

Prior to the door opening in Experiment 1, pressures exceeded 0.023 psi (160 Pa) (see Figure 4.29a) and following the door being opening exhaust velocities ranged from 11 mph to 22 mph (5 m/s to 9.8 m/s). Despite the door being closed prior to ignition, there was still sufficient oxygen available for combustion in the unit during Experiment 1 to support fire growth that approached flashover as temperatures in the fire compartment above 2 ft and below the drop ceiling reached 1,000 °F (537 °C). The rapid fire growth led to a increase in pressure. The pressure increase was sufficient

to force open the door. A unidirectional exhaust flow was then established at the front door until the door was closed as the high pressure gases in the unit flowed to the low pressure ambient conditions outside of the unit.
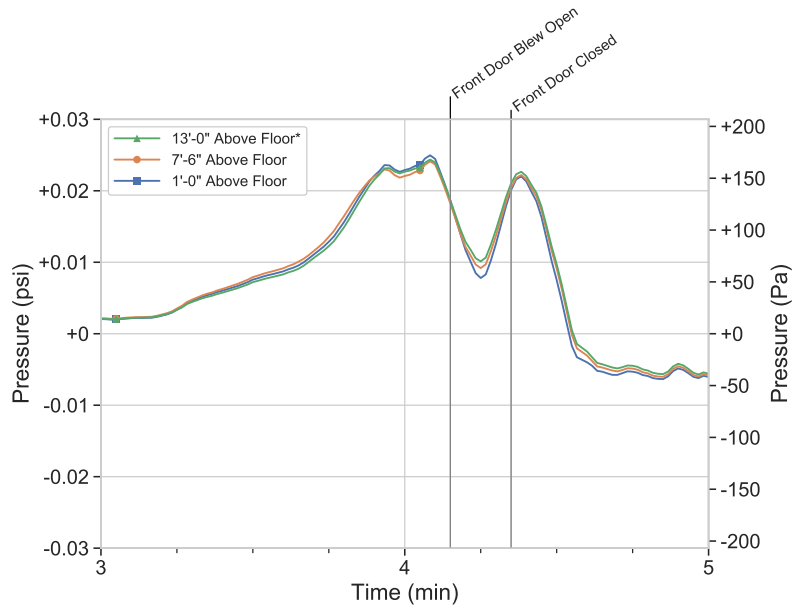


(a) Side B Pressure
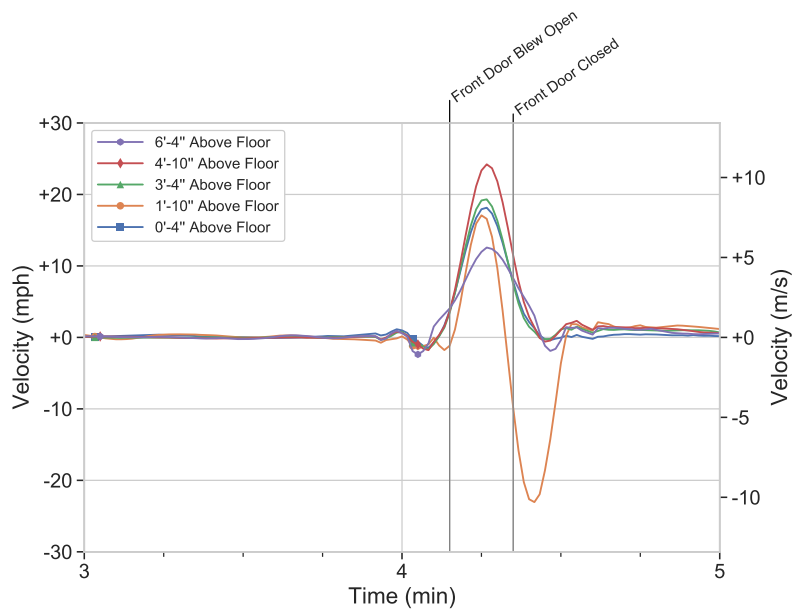


(b) Front Door Velocity

Figure 4.29: The pressure and velocity for Experiment 1 that show the development of unidirectional exhaust. Positive pressure values indicate a rise in pressure in the fire compartment and positive velocity values indicates exhaust flow. Note, from video analysis the 1 ft 10 in. probe was knocked out of alignment when the door was opened.

The most pronounced example of the exhaust flow for experiments with an open door occurred during Experiment 4, as seen in Figure 4.30 and 4.31. The exhaust flow extended over 75 ft (22.9 m) out the front door of the unit and lasted for 45 s.



(a) Exhaust Start 0 s        (b) 10 s        (c) 20 s

(d) 30 s        (e) 40 s        (f) 45 s
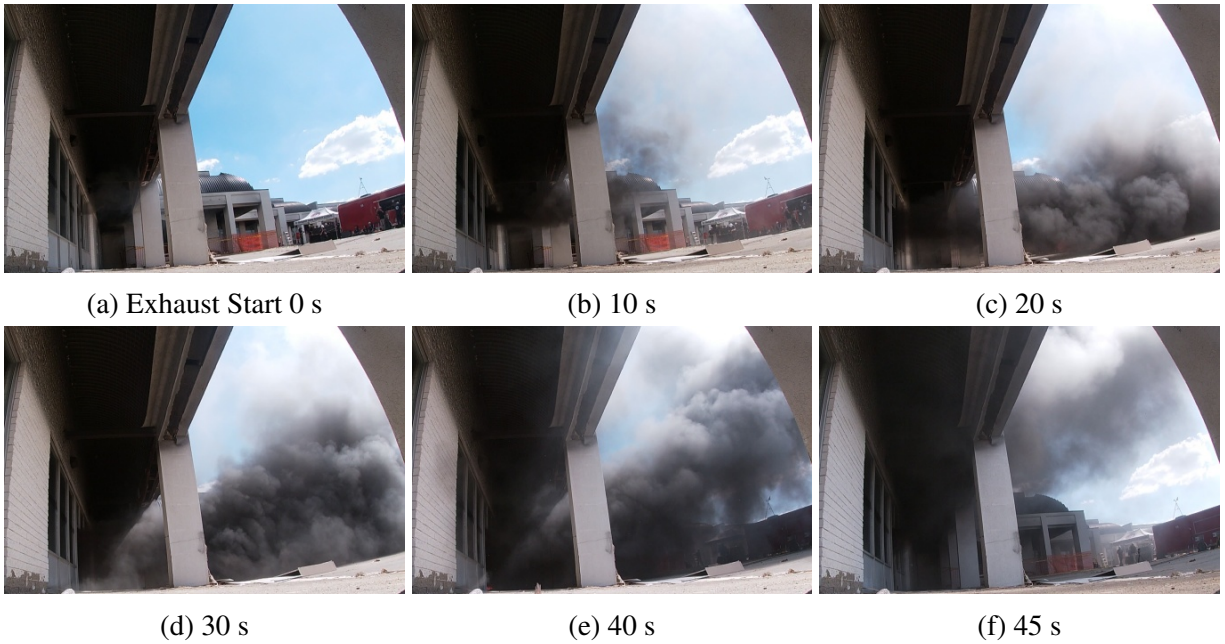
Figure 4.30: Images of the smoke exhaust from Experiment 4. Time 0 s represents the start of the flow, which occurred 2 min 55 s into the experiment.



Figure 4.31: A drone image shows the peak of the smoke exhaust during Experiment 4.

Matt Sortman, Fairborn Police Department

Although velocity was not recorded at the front door, the pressure increase due to expansion was recorded on the pressure transducer in the side D wall of the unit, shown in Figure 4.32. The peak flow corresponded with the peak pressure on the pressure transducer. For additional insight into the relationship between pressure and velocity see Appendix A which presents a simplified analysis using the Bernoulli Principle.
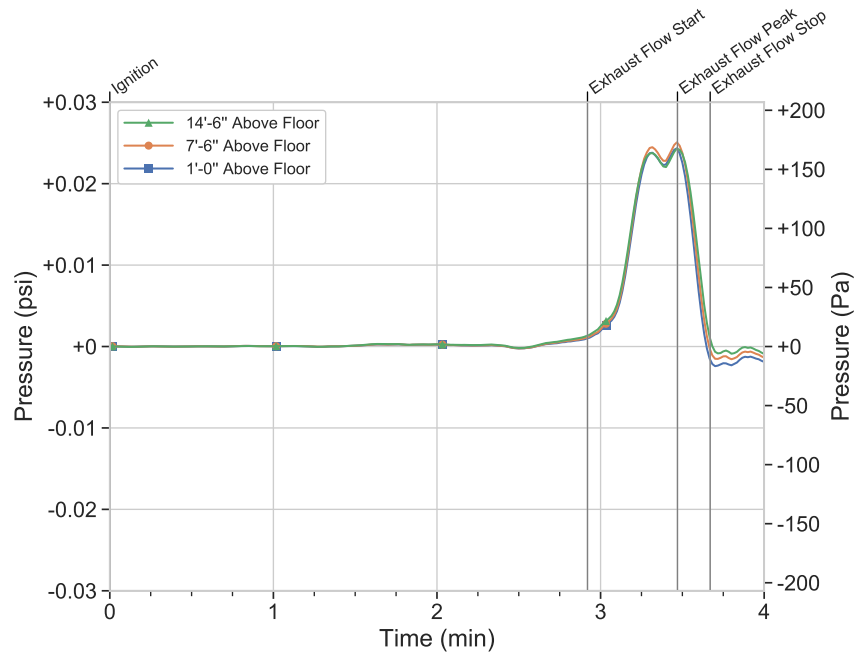


Figure 4.32: Pressure recorded in Experiment 4 during the initial growth of the fire, from ignition until 4 min. Positive values indicate a pressure rise in the fire compartment.

In the experiments conducted with an open side A door, exhaust flow continued beyond the hot gas layer reaching the top of the open doorway. Table 4.4 lists the start, stop, and duration for the unidirectional exhaust captured during these experiments.

Table 4.4: Periods of Overpressure Smoke Exhaust from the Front Door

| Experiment | Exhaust Start (min:s) | Exhaust Stop (min:s) | Duration (min:s) |
|:---:|:---:|:---:|:---:|
| 2 | 3:37 | 4:58 | 1:21 |
| 3** | 3:24 | 4:00* | 0:36 |
| 4** | 2:55 | 3:40 | 0:45 |
| 5 | 2:40 | 4:13 | 1:31 |
| 6 | 3:01 | 4:31 | 1:28 |
| 7 | 3:07 | 4:04* | 0:58 |

\* Exhaust stopped at the time horizontal ventilation was performed.

\** Timing obtained from video analysis. Start time contains significant variability
 because early exhaust did not contain distinguishable amounts of particulate and
 was thus difficult to visually identify.

In all of the open door experiments, the unidirectional exhaust flow corresponded to a temperature and pressure rise. Although the front door was open, the rapid rise in temperature happened over a period of less than 90 s and the doorway could not exhaust the expanding gases fast enough to equilibrate pressure. The best quantified example of the unidirectional exhaust flow from these experiments where velocity, temperature, and pressure were recorded was in Experiment 5. Images from the unidirectional exhaust period are shown in Figure 4.33.



(a) 0 s  (b) 15 s  (c) 30 s  (d) 45 s

(e) 60 s  (f) 75 s  (g) 90 s  (h) 105 s
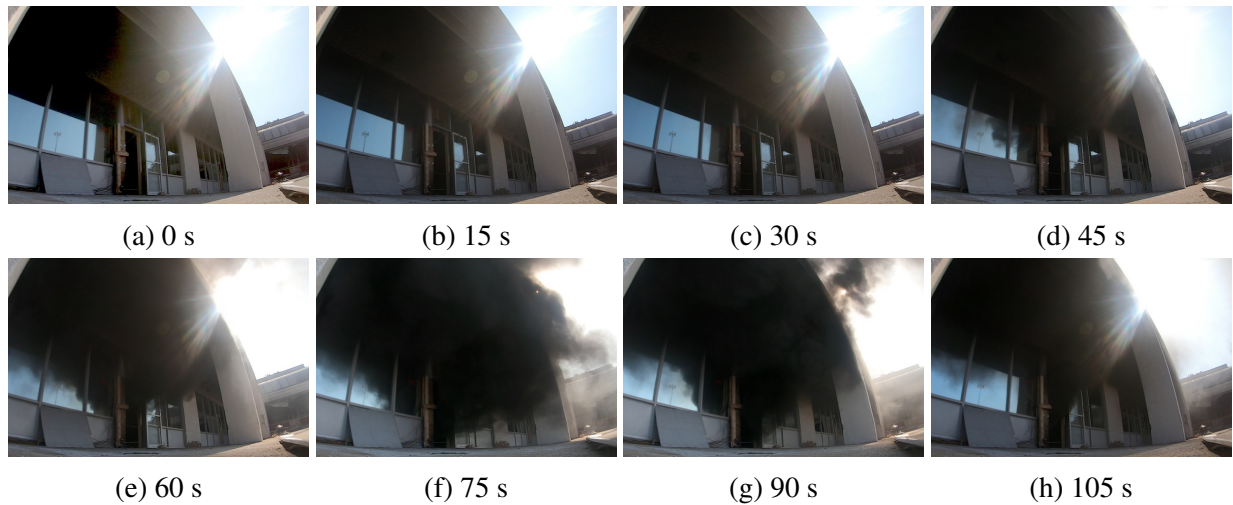
Figure 4.33: Images of the front door during Experiment 5 from the start of the unidirectional exhaust. Time 0 s represents the start of the flow, which occurred 2 min 40 s into the experiment.

The temperature rise on the interior of the unit corresponded with an increase in pressure and a unidirectional exhaust on the bi-directional probes in the open door. The temperature, pressure, front door temperature, and front door velocity are shown in Figure 4.34 where the orange shaded area illustrates where the unidirectional exhaust out of the open front door exceeded 0.5 mph (0.22 m/s).

The temperatures recorded in the front door opening during the exhaust exceeded 500 °F (260 °C), a common test temperature used for evaluating many firefighter personal protective equipment components [35].



(a) AB Temperature (Near Door)

(b) Side B Pressure

(c) Front Door Temperatures

(d) Front Door Gas Velocities
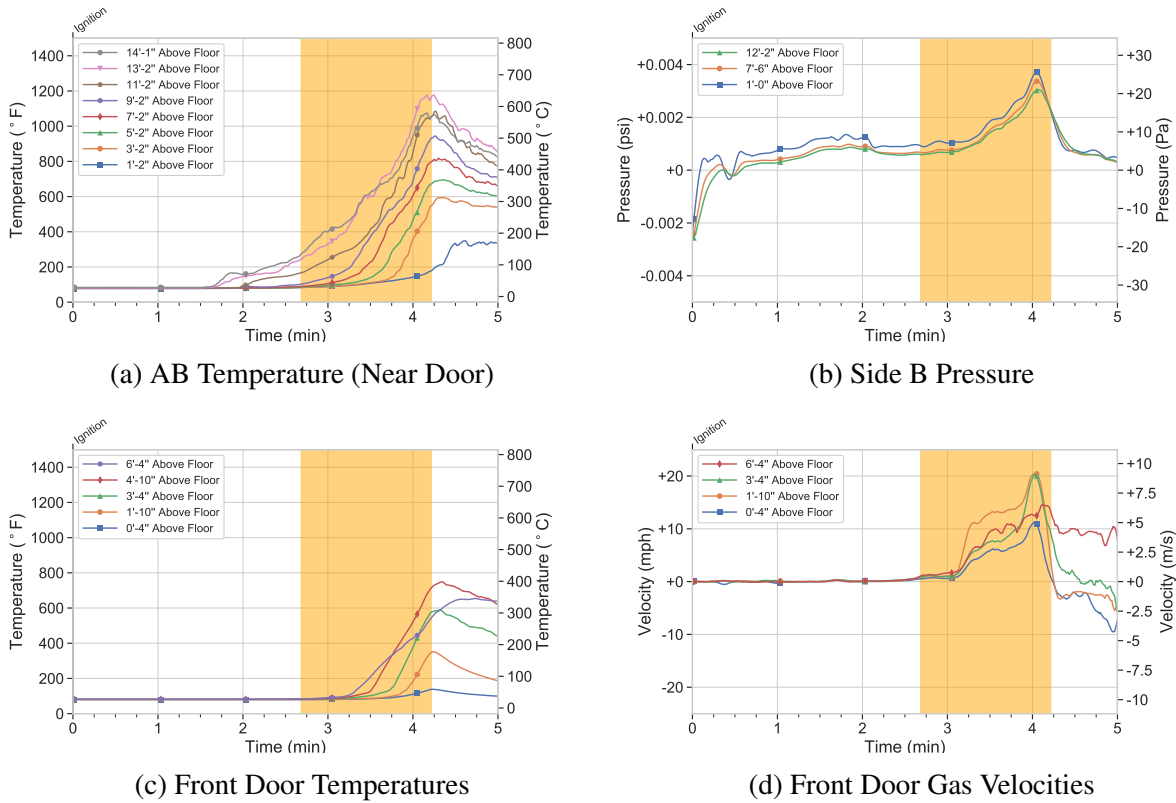
Figure 4.34: Temperatures near the door, differential pressure between the interior and exterior, gas velocities in the doorway, and the front door temperatures from ignition until 5 min during Experiment 5. The orange shaded area represents a unidirectional flow out of the open front door in excess of 0.5 mph (0.22 m/s). Positive pressure values represent a rise in pressure in the fire compartment and positive velocity values indicate exhaust flow.

There are a number of factors that likely contribute to the unidirectional exhaust flows observed during a fire in a large-volume compartment such as a unit in a strip mall. A strip mall unit has more oxygen available for combustion before needing to draw from ventilation openings, relative to a smaller compartment such as in a typical residential structure. With more available oxygen, the heat release rate can increase which leads to an increase in gas temperature and corresponding gas expansion. This will create pressure. Gases will flow from areas of higher pressure to lower pressure. Like all flows, the pressure difference between the interior of the unit and exterior of the unit is the driver of the unidirectional exhaust seen in these experiments. The magnitude and duration of the exhaust would be impacted by the rate at which the heat release rate increases, the pressure compared to the available intake and exhaust area, and the vent locations. Additional factors that can influence the exhaust flow include the energy density and pyrolysis rate of the fuel, the height of the unit relative to the door soffit which allows the accumulation of more unburnt fuel

prior to venting compared to a typical residential compartment, and that a localized flashover can occur within the unit. Further research is needed to fully understand when/where exhaust events such as these can be expected, and to quantify exactly how much compartment volume, fuel burn rate, and geometry impact pressure development (see Section 6).

## 4.3 Structural Stability

Understanding the structural stability of metal truss roofs was not a specific goal of this project, but a collapse occurred in Experiment 2. The mechanism of collapse was similar to incidents in which firefighter LODDs have occurred [9, 40], and the type of construction has been documented as a hazard to firefighters [18].

The roof structure for the units in this project incorporated a corrugated metal deck covered with foam insulation and a rubber membrane, and supported by open web steel bar joists. Two distinct roof areas, one in the front and one in the rear, were separated by a wide flange steel beam supported on either end by wide flange steel columns. The open web steel bar joists ran from front to back of the unit, with an array of them making up the support assembly in the front of the unit and an array making up the support assembly in the rear of the unit. The open web steel bar joists rested on the wide flanged beam in the center of the unit, and on the front or rear load-bearing walls on the opposite end. Figure 4.35 illustrates the structure but is not intended to provide the specifics that would be needed to conduct a structural analysis.
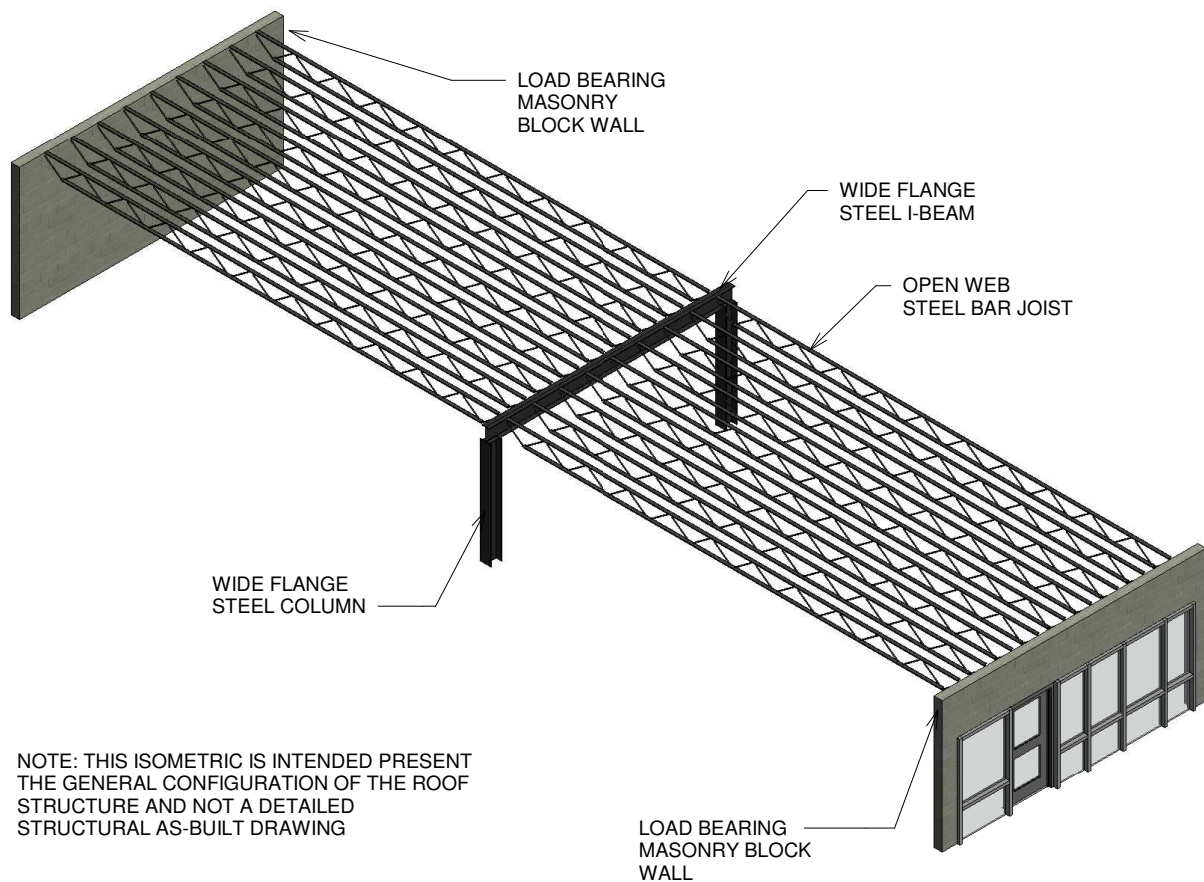
Figure 4.35: A schematic of the roof support system found in the strip mall.

During the experiments in which the open web steel bar joists were left unprotected (Experiment 1–4), damage to the front and rear load-bearing masonry walls was observed. The heat from the fire caused both expansion and deformation of the open web bar joists. The expansion pushed out the front and rear load bearing masonry walls. Cracks formed where the load-bearing masonry walls intersected with the non-load bearing separation walls. Figure 4.36 presents an example of the damage from Experiment 3 (Unit 1074).



(a) Front

(b) Rear
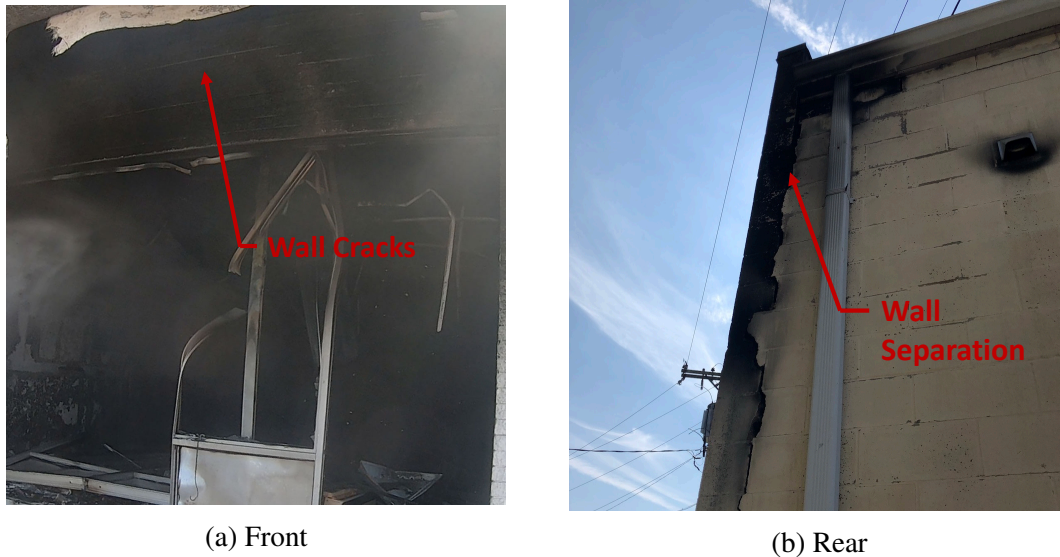
Figure 4.36: Images of the front and rear wall damage noted after Experiment 3.

In addition to the wall damage, deformation of the joists occurred as they were heated and sagged under the weight of the roof. Figure 4.37 shows the damage from Experiment 3 (Unit 1074) and Experiment 4 (Unit 1067–1069) where the open web steel bar joists sagged.



(a) Experiment 3 - Unit 1074

(b) Experiment 4 - Unit 1067-1069
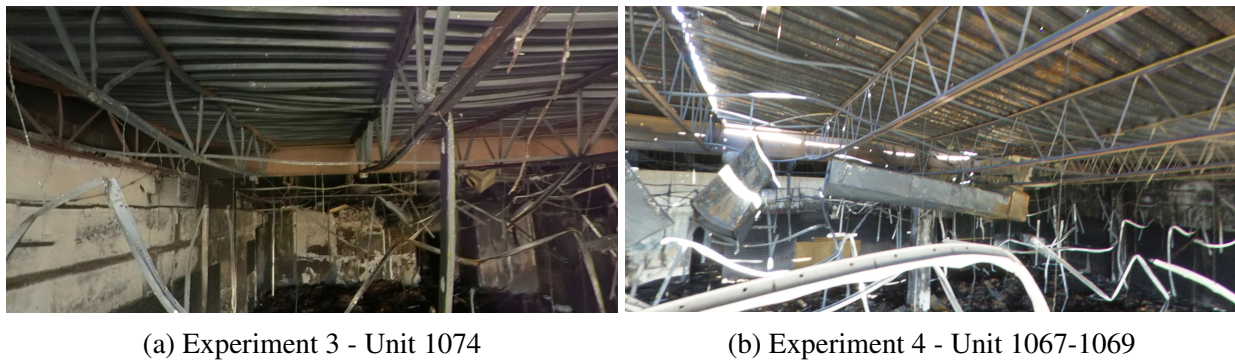
Figure 4.37: Images of open web joist deformation from Experiment 3 and Experiment 4 after the fire had been suppressed.

In Experiment 2, this damage resulted in a significant lean-to roof collapse during the overhaul phase 34 min 51 s after ignition. As water was directed from the exterior onto the open web steel

bar joists from below, the front section of the roof separated from the front masonry load-bearing wall and collapsed. Figure 4.38 presents images of the roof structure and masonry load-bearing wall after the collapse had occurred.



(a) Front Elevation        (b) From Adjacent Roof

Figure 4.38: Images of the lean-to front roof collapse that occurred in Experiment 2.

The late-stage collapse was most likely a result of both the deformation as well as contraction of the open web steel bar joists following fire exposure and cooling via water application. The front wall had been forced out from the expansion, and once the deformation and contraction pulled the joists away from the wall, the collapse occurred. The mechanisms of collapse observed indicate the state of the fire (i.e., growth, post-flashover, decay, overhaul) should not be the only indicator for a potential collapse. Further research is needed to better understand the operational time frame firefighters have when working in and around these types of roof structures (see Section 6).

# 5  Tactical Considerations

A tactical consideration is "an evidence-based concept for the fire service to consider implementing to enhance efficiency and effectiveness, and to increase knowledge to accomplish their mission [41]." The following considerations are meant to inform, not replace local standard operating procedures. Each situation is unique, requiring different tactical choices to achieve the incident priorities. They are titled considerations because the local fire service – crew, station, battalion, department – needs to determine how and when to implement the information.

Although the fuel package, the geometry and construction of available units, and the number of experiments conducted limit definitive conclusions from these experiments, data were collected that can be used to develop a few tactical considerations for strip mall fires. The fuel package was selected because it could produce a repeatable, fast-growing fire, and the strip mall units could be realistically loaded to ensure ventilation-limited conditions based on estimates of ventilation available for combustion. At the same time, the commodity boxes were centrally concentrated within each unit, there were no obstructions (e.g., shelves, furniture, etc.) that would impact the hose stream, and the boxes could be displaced by a hose stream, therefore no suppression specific conclusions could be made.

## 5.1  Timeline of Coordination - Strip Malls

Research in residential structures has shown the amount of fuel relative to the volume of the structure often leads to a ventilation-limited fire. When ventilation was provided by opening the front door for access, or by conducting horizontal or vertical ventilation, and the suppression was delayed, the ventilation led to an increase in the oxygen available for combustion. When additional oxygen was provided to a vent-limited fire, the heat release rate of the fire increased [1, 2]. These experiments demonstrated that this concept was similarly applicable to structures with a larger volume. Although the main compartment volumes in these experiments were up to three times larger than the residential compartment volumes from previous research, the ratio of fuel to oxygen available for combustion still resulted in a ventilation limited fire[1]. Figure 5.1 shows an example of the temperatures in a strip mall fire (Experiment 1) where all exterior doors and windows were closed at the time of ignition. Within 5 min, sufficient oxygen was consumed to impact the heat release rate of the fire and reduce temperatures. After the front door was opened at 15 min, it allowed additional oxygen to enter, and by 18 min the temperatures began to increase. This was an indication the fire was limited by the available oxygen.

---

[1]For reference: The smallest strip mall unit was approximately 28,000 ft$^3$ and the largest unit was approximately 58,000 ft$^3$. The 2-story, open floor plan colonial style residential structure used in prior research was approximately 20,000 ft$^3$.
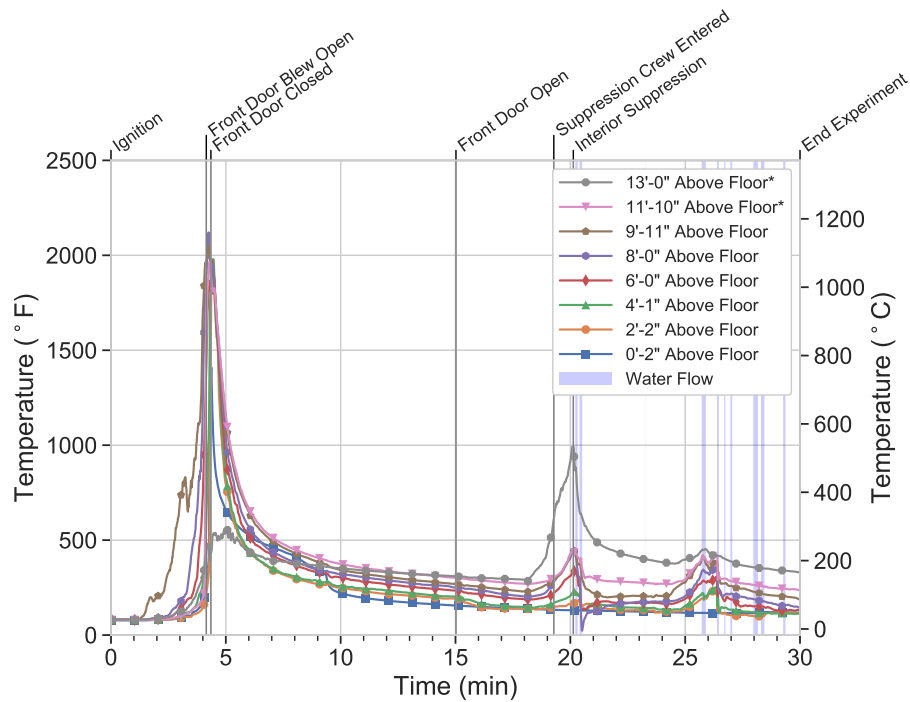
Figure 5.1: An example of temperatures near ignition (CD temperatures) when no additional ventilation beyond natural leakage was provided during a strip mall fire (Experiment 1). Blue shaded areas indicate time and duration of water flow.

For these experiments, when ventilation was provided to a ventilation-limited fire without simultaneous suppression (regardless of ventilation type), the result was an increase in temperature. Figure 5.2 shows examples of ventilation that was added without suppression. Providing additional horizontal ventilation (see Figure 5.2a) via the front windows resulted in fire growth and localized flashover conditions. Opening the the entire front window wall resulted in fire out the front of the unit (see Figure 5.3). Similarly, vertical ventilation of the roof (see Figure 5.2b) lead to an increase in temperature throughout. Opening the equivalent of a 64 ft$^2$ (3.0 m$^2$) roof vent, resulted in flashover. The increase in temperature following both horizontal and vertical ventilation indicated an increase in the heat release rate of the fires.

161
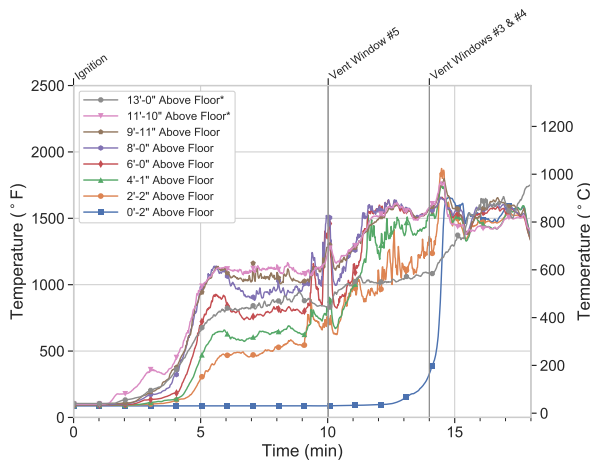
(a) Impact of Horizontal Ventilation (CD Temperatures) Near Ignition (Experiment 2)
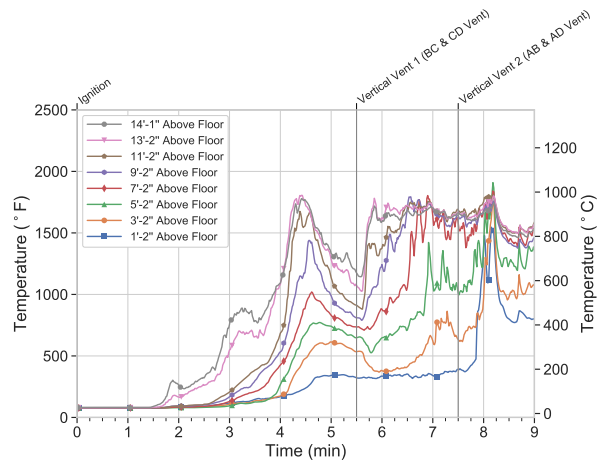
(b) Impact of Vertical Ventilation (BC Temperatures) Near Ignition (Experiment 6)

Figure 5.2: The impact of horizontal ventilation and vertical ventilation on temperatures within a strip mall fire.



Figure 5.3: An image from Experiment 3 after all of the front windows were opened during the initial growth of the fire.

When vertical ventilation was simultaneous with suppression, the response was an immediate temperature decrease. Figure 5.4 shows the temperature response to coordinated vertical ventilation and suppression. The initial exterior suppression cooled the environment but could not fully extinguish the fire. Interior suppression was required to provide complete extinguishment.
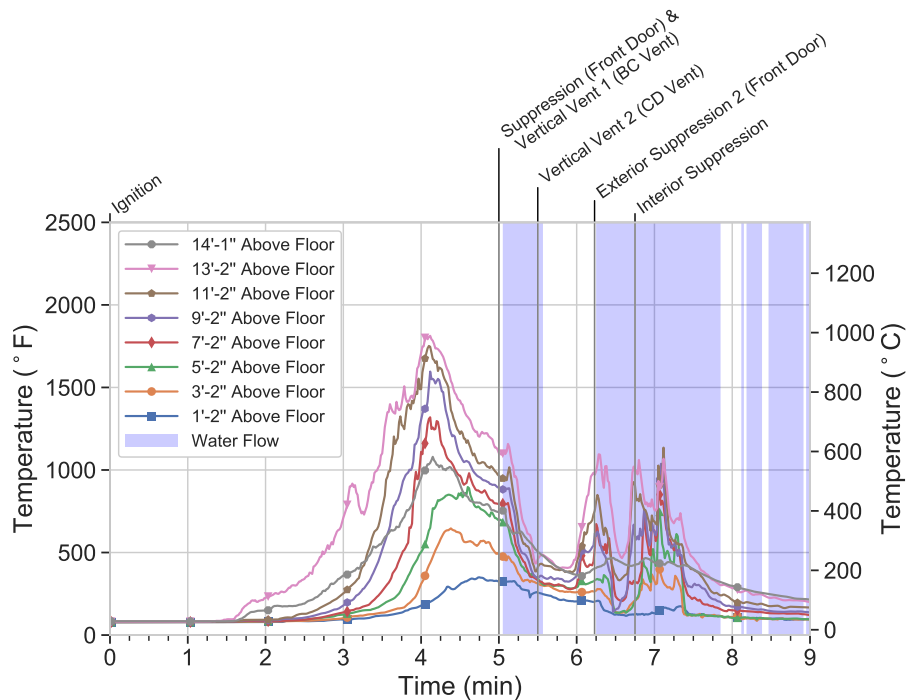
Figure 5.4: The impact of conducting suppression simultaneous with vertical ventilation on temperatures (CD temperatures) near ignition within a strip mall fire (Experiment 5). Blue shaded areas indicate time and duration of water flow.

According to Mittendorf and Dodson, "Classic building fire attack (interior attack supported by rooftop ventilation) can no longer be the default. Prefire planning, building familiarization, and developed skills in reading a building as essential to fireground decision making [42]." When confronted with a fire in a strip mall, consideration should be given to the time it will take to apply water before any opening in the compartment is made. If water is applied immediately following an opening being made, the removal of heat prior to the renewed source of oxygen reaching the combustibles that are still pyrolyzing can positively impact the thermal conditions within the structure. If suppression is delayed, keeping the fire compartment closed can limit the heat release rate of the fire, limiting the potential thermal damage.

There are additional factors that can impact the timeline of changes in fire behavior in response to ventilation. These factors include but are not limited to the growth rate of the fuel (i.e., how fast the fuel pyrolzes and how fast flames spread), the amount of fuel in the unit, weather conditions (especially wind speed and direction), the size of the fire unit, and the amount of compartmentation that exists within the unit. Due to the hazards associated with fires in large commercial structures, it is also important to be mindful of available resources when considering tactics, especially whether tasks can be completed simultaneously versus sequentially.

## 5.2 Size-up and Initial Fire Growth

Each experiment conducted was instrumented with sensors and video cameras to specifically capture information regarding the fire dynamics in the fire unit and in adjacent exposure units, effectively providing a real-time scene assessment. Equivalently, a size-up of the critical factors is a must on every fireground. As Mittendorf and Dodson state in their book, *The Art of Reading Buildings*, "Conducting a relevant building size-up has become challenging due to evolving technology and the vast differences, methodologies, and materials that have been used in building construction since the founding of this country [42]." In terms of commercial strip-mall fires key elements of a size-up would include building geometry (roof type, roof loads, joist direction, skylights, etc.), construction type, fire location and potential extension into exposure units, presence and location of fire walls, potential areas of collapse including side A facades/parapets/awnings, existing ventilation (including soffit and sill heights of horizontal openings), and potential compartmentalization of the unit(s). An appropriate size-up may likely require 'eyes on the roof' to best inform the incident commander.

One of the hazards highlighted for strip mall fires is the large open compartment compared to the typical residential occupancy [16, 18]. Initially, the large open compartment adds the potential for more fuel. However in compartment fires, the oxygen available for combustion often limits the size of the fire more so than the fuel. The large open compartment in strip malls has more oxygen available for combustion than a typical residential compartments would.

The potential fire size based on the oxygen available for combustion can be estimated using Equation 5.1 in which $PE$ is the estimated potential energy from the oxygen, $P_{O_2}$ is the percentage of the volume that is oxygen available for combustion, $\rho$ is the density of oxygen at standard temperature and pressure (1.33 kg/m$^3$), $V$ is the volume of the unit (m$^3$), and $\Delta H_c$ is the approximate energy released per unit mass of oxygen (13.1 MJ/kg). Research on the use of oxygen reduction systems for fire protection has shown flames may self extinguish when the oxygen concentration reaches 13.6–15% [43] by volume.

$$PE = P_{O_2}\rho V \Delta H_c \qquad (5.1)$$

For this analysis, the 15% threshold is considered the point at which the heat release of the fire begins to be affected by the oxygen available for combustion. Consider the estimated potential fire size based on the oxygen available for combustion in four potential structure fires, a single story ranch, a two story colonial, a small strip mall unit, and a large strip mall unit. If all exterior doors and windows are closed, $P_{O_2}$ is 6% based on the 21% ambient level minus 15%. This estimation assumes the atmosphere in the fire compartment is a homogeneous mixture and can be considered conservative as it does not account for the volume the fuel load would occupy. The fuel would displace air volume, therefore lowering $V$ in Equation 5.1. This could result in a ventilation-limited fire prior to reaching the estimated potential energy shown in Figure 5.5. Figure 5.5 illustrates a comparison of the potential energy (i.e., the amount of heat) these four structures can theoretically support before the declining oxygen levels impact the energy release of the fire. While this estimate

does not account for any additional ventilation, fuel load density, fuel burning rate, or time, the intent is to show the impact of increasing compartment volume on initial potential energy.
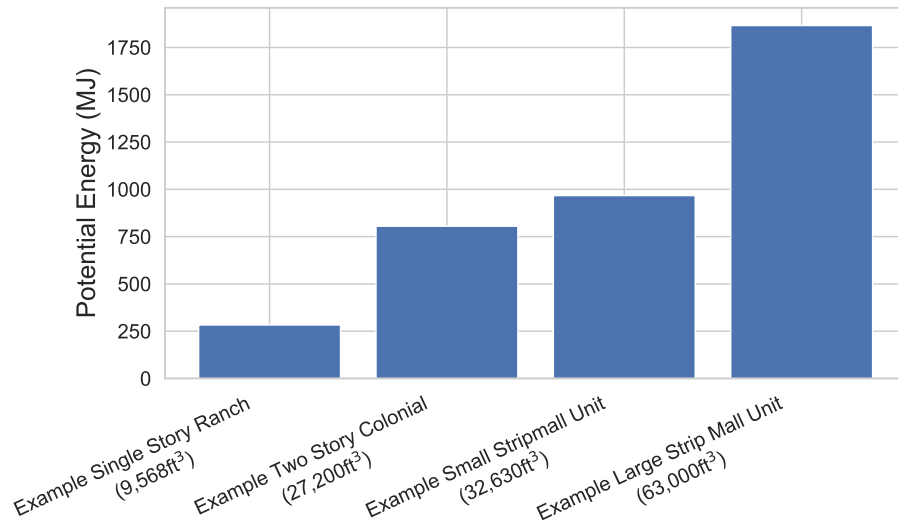


Figure 5.5: An estimation of the potential energy release for various size volumes when no exterior openings are present before the oxygen level decreases to 15%.

The larger the compartment sizes studied in these experiments resulted in high heat release rate fires, even with just a single door open compared to a typical residential compartment fire. Consider Experiment 4, the largest volume utilized, where the highest peak temperature prior to any additional ventilation was recorded. Figure 5.6 illustrates the temperatures during the initial growth of the fire. As the fire developed, temperatures throughout the unit briefly exceed 1,200 °F (648 °C) floor to ceiling (conditions representative of flashover) before decreasing. The front door was open at ignition. Therefore, the fire size was initially based on the oxygen available for combustion in the unit, plus the oxygen available for combustion entering the front door.
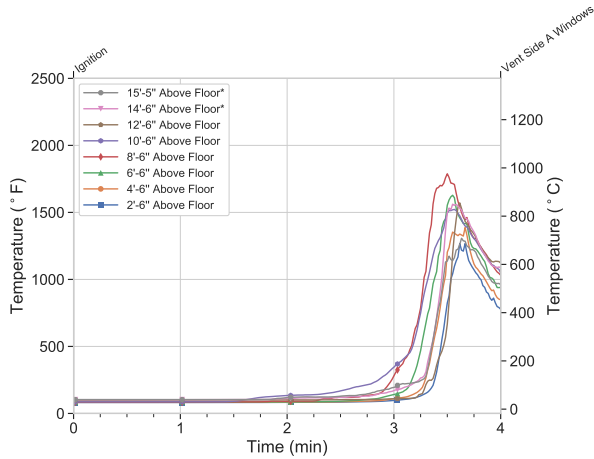
(a) AB Temperatures (Front Near Door)
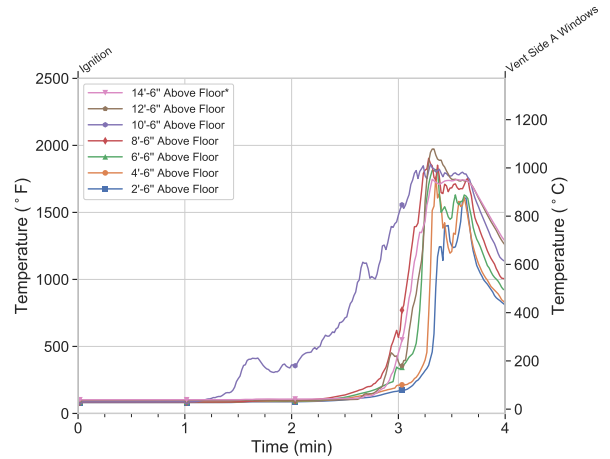


(b) CD Temperatures (Rear Near Ignition)

Figure 5.6: Temperatures in the front near the door (the AB temperatures) and in the rear near ignition (CD temperatures) for Experiment 4, show initial fire growth in a 63,000 ft$^3$ volume with the front door open at ignition.

The temperature rise caused gas expansion, which increased the pressure in the unit. With only the front door open, the pressure increased and resulted in a unidirectional exhaust out the front door. Initially as the gases in the upper portion of the volume expanded, they forced out the gases lower in the volume. As the expansion continued, the exhaust began to include products of combustion. The smoke exhausted for 45 s and extended in excess of 75 ft horizontally from the open door as shown in Figure 5.7.

|  |  |  |
|---|---|---|
| (a) Exhaust Start 0 s | (b) 10 s | (c) 20 s |
| (d) 30 s | (e) 40 s | (f) 45 s |
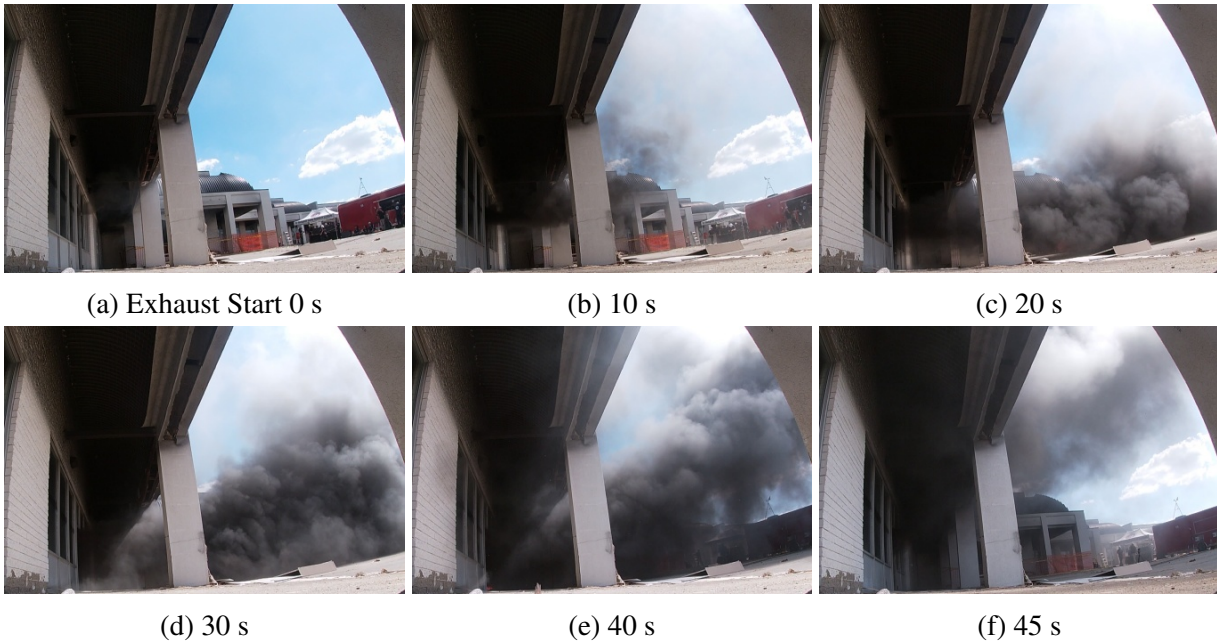
Figure 5.7: Evolution of the unidirectional exhaust from Experiment 4. Time 0 s represents the start of the flow, which occurred 2 min 55 s into the experiment.

A similar, though less dramatic, unidirectional exhaust was observed in each experiment with an open front door, lasting between 45 s and 91 s. In strip malls, the large compartment size encloses more oxygen, and thus the heat release rate can increase to higher levels before it is impacted by the lack of oxygen available for combustion. A higher heat release rate will result in increased temperature rise, and more gas expansion. The more expansion, the more pressure. With limited ventilation, the pressure increase can result in unidirectional exhaust out any available openings.

Tactical choices for addressing the unidirectional exhaust may be limited. Although conducting ventilation during the event can release the pressure, it also provides additional oxygen to the ventilation-limited fire leading to a higher heat release rate. This may result in a pressure increase depending upon the size of the vent. Figure 5.8 illustrates the pressure (see Figure 5.8a) and temperature (see Figure 5.8b) in Experiment 3, where horizontal ventilation was added during the smoke exhaust event. Although the pressure was relieved, the additional ventilation resulted in fire out the front of the unit (see Figures 5.8c and 5.8d). The increase in flaming combustion is likely due to a combination of the increased heat release rate in the unit and under-ventilated hot gases mixing with fresh air at the opening in the front of the unit.
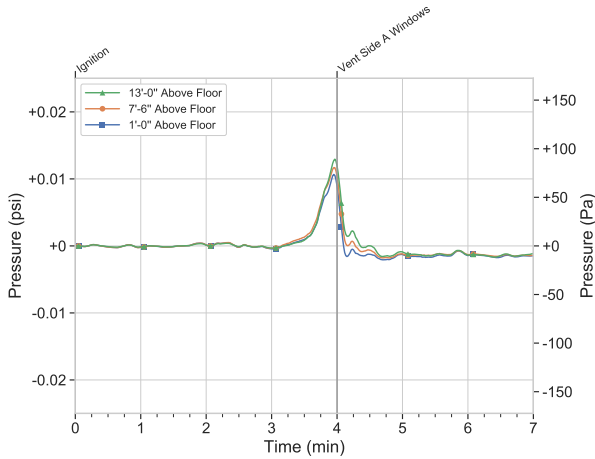
(a) Differential Pressure (Fire Unit & D Exposure)
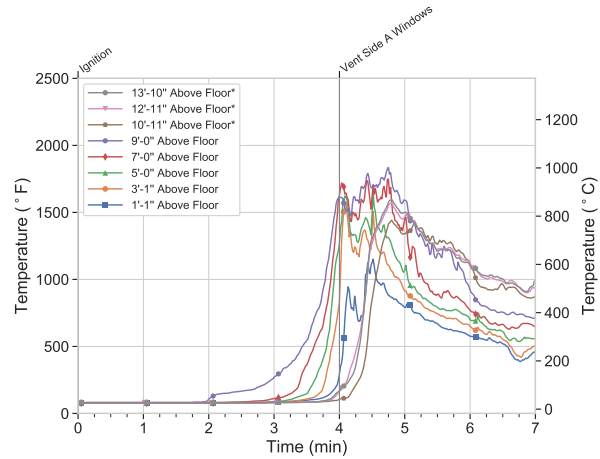


(b) Temperatures Near Doorway (Front)



(c) Front Image Prior To Ventilation



(d) Front Image 30 s Post Ventilation

Figure 5.8: The impact of additional horizontal ventilation during the overpressure smoke exhaust event on pressure and temperature; images show the visual fire development (Experiment 3). Positive pressure values represent a rise in pressure in the fire compartment.

If water can be applied into the unit from a safe distance (it is important to recognize the potential for a side A collapse of a facade, canopy, or parapet wall), previous research has shown rapidly cooling an environment can lead to gas contraction [4], which could counteract the pressure increase, while at the same time cooling and suppressing the fire. If water application is delayed, the most effective and possibly the safest method to deal with this increase in pressure and smoke exhaust event may be to wait for the event to finish before conducting additional ventilation, or attempting to access the building.

Similar events have been documented during fire department operations (see Figure 5.9). A fire in a bowling ally in Troy, NY, resulted in a significant smoke and fire exhaust during fire department operations. With the limited viewpoint, it is difficult to determine exactly what caused this event,

but the exhaust out of the open vents is similar to what was observed in the above experiments. Unlike the events from these experiments, this fire resulted in flames out an opening during the unidirectional exhaust as the hot products of combustion mixed with oxygen on the exterior.



(a) 0 s        (b) 5 s        (c) 10 s

(d) 30 s        (e) 35 s

Figure 5.9: Images taken from a video of a fire in Troy, NY at the Alpha Lanes Bowling Ally on May 8, 2019. These time-lapse images are separated by varying time intervals avoid obstructed views from the by-standers [44].

Regardless of what causes the exhaust event, note that rapid changes in pressure are occurring on the interior. More research is needed to fully understand what causes the rapid change in pressure, but understanding that the potential exists and may occur during the growth of a fire can aid firefighters in conducting an effective ongoing size-up.

## 5.3 Unprotected Metal Roof Collapse

The collapse danger from an unprotected metal truss roof during a fire is well documented in fire service training materials [16, 45]. Two modes of failure were noted by Brannigan in his book "Building Construction for the Fire Service [46]," one where steel roof joists elongate and push out masonry load-bearing walls, and one where steel roof joists are weakened when heated in excess of 1,000 °F (538 °C). Both modes of failure were noted in this project. Figure 5.10 shows the damage to the exterior masonry walls from the elongating of the open web steel bar joists, and Figure 5.11 shows their deformation.



(a) Front

(b) Rear
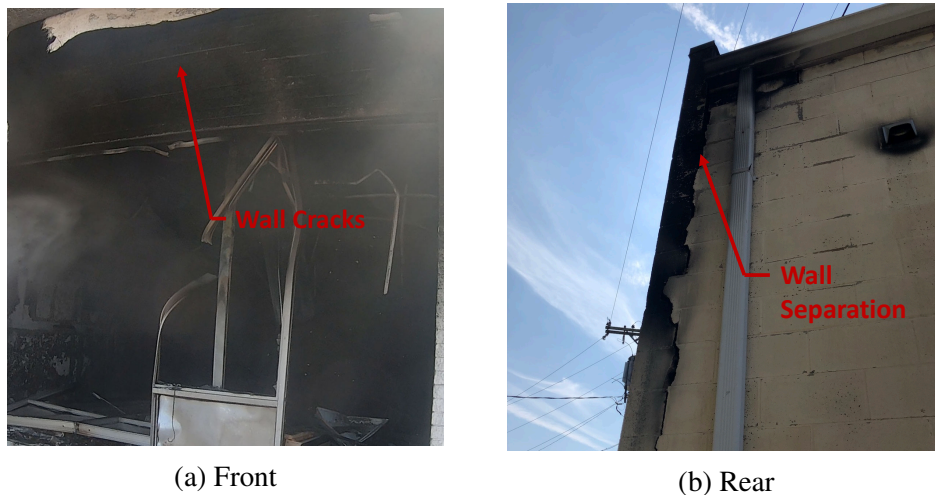
Figure 5.10: Images of front and rear structural wall damage from Experiment 3.



(a) Experiment 3 - Unit 1074

(b) Experiment 4 - Unit 1067-1069
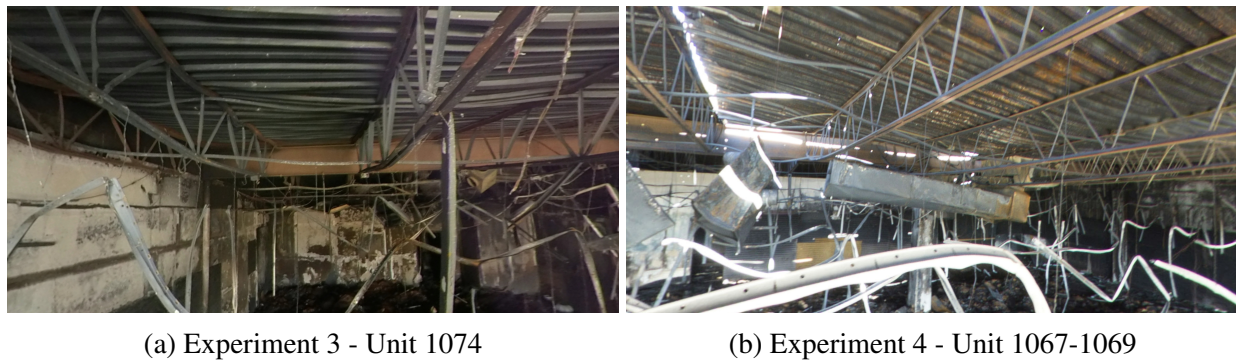
Figure 5.11: Post fire images from Experiment 3 and Experiment 4 where deformation of the open web steel bar joists occurred.

Late in Experiment 2, a lean-to collapse occurred, potentially due to the contraction of the open web steel bar joists as they cooled and retracted from the supporting masonry wall (see Figure 5.12). This collapse occurred after the fire had been placed under control, and the crews were

170

extinguishing hot spots more than 30 min after the fire started. The open web steel bar joists were deformed prior to the collapse, providing an indication they were compromised.



(a) Front Elevation



(b) From Adjacent Roof

Figure 5.12: Images of lean-to front roof collapse from Experiment 2.

Collapse of unprotected open web steel bar joists is a hazard not only under a fire exposure, but also late in the incident, after the fire has been knocked down. The mechanisms of collapse observed indicate the state of the fire (growth, post-flashover, decay, overhaul) should not be the only indicator for a potential collapse. When presented with a fire in a building with unprotected open web steel bar joists and masonry load bearing walls, consider limiting the operations inside the unit to those necessary for the successful stabilization of the incident.

# 6  Future Research

Additional research is needed to better understand the impact of coordinated suppression and ventilation tactics on fire dynamics in large compartments common in commercial occupancies such as strip malls. Construction practices as well as fuel loads continue to evolve, which further amplifies the need to conduct research to effectively reduce the hazards from fire.

Several topics emerged during these experiments that could potentially expand the tactical considerations in Section 5, once additional research is completed. Those topics include fire dynamics in large volumes, suppression tactics including water usage, and the collapse mechanisms in roofs exposed to fire. Each of these research questions would benefit from data collection in additional strip malls as well as in even larger volumes such as big box stores (e.g., open concept department store) and open-concept office buildings.

Fire development in large volumes documented during these experiments highlights the need to further explore the impact of compartment volume and geometry on fire dynamics. Compartment height, floor area, ceiling height to vent height (i.e., volume above the highest vent where gases can accumulate prior to release from the structure), and the ratio of length to width can impact fire development. Additional construction components that can influence fire dynamics and resulting tactics include common attics/cocklofts across units, types of roof construction, and potential fuel loads incorporated into the construction. Several of these factors have been evaluated in residential-size compartments, but research projects specifically focused on fire development in large volumes could aid in understanding the challenges presented as fuel load and compartment volume increase.

During several experiments in this series, an overpressure occurred during fire growth in a large volume where ventilation was minimal. This transient event appeared to occur as portions of the large compartment were transitioning to flashover. Examining the event itself and how the transition of the space to flashover relates to the pressure increase and smoke exhaust would help the fire service better understand overpressure events.

Further work on the mechanisms of collapse in large-volume structures may allow for the development of collapse indicators. Additional efforts to identify how the hazard evolves during the stages of a fire could provide the data needed to develop effective mitigation strategies when buildings of this size are exposed to fire.

Finally, the current experiments provided the opportunity to collect new data on water usage to complete successful suppression operations and the use of positive pressure fans to protect exposure units in strip malls. The data collected was not sufficient to develop tactical considerations, but it can be used as the foundation for future studies. The sections below present an overview of those topics.

## 6.1　Water Usage

For decades, the fire service has worked to understand the quantity and flow rate of water required to effectively extinguish structure fires. Currently, necessary flow rates are estimated by experience-based models or the analysis of incident data comparing the area of fire involvement to the flow utilized [47–53]. A limitation of the work conducted here was the fuel choice and placement of fuel within the unit. To have a repeatable and representative fuel load, this fuel package was designed to produce a fast-growing fire, and the units were sufficiently loaded so that fire would become ventilation-limited based on the initial oxygen available for combustion. However, the commodity boxes were centrally concentrated within each unit, there were no obstructions (e.g., shelves, furniture, etc.) that would impact the hose stream, and the boxes could be displaced by a hose stream. Therefore, the data presented below should be considered exploratory.

Table 6.1 shows the fire area, compartment volume, and flow rate used for each of the units in these experiments.

Table 6.1: Unit Areas and Volumes

| Unit Number | Fire Area | Fire Compartment Volume | Flow Rate |
|:-----------:|:---------:|:-----------------------:|:---------:|
| 1067 | 1,736 ft$^2$ | 27,430 ft$^3$ | 160 gpm/265 gpm |
| 1067-1071 | 3,941 ft$^2$ | 63,000 ft$^3$ | 265 gpm |
| 1074 | 1,917 ft$^2$ | 31,090 ft$^3$ | 160 gpm |
| 1078 | 2,170 ft$^2$ | 32,630 ft$^3$ | 160 gpm |

Table 6.2 shows the impact of suppression streams on temperatures nearest the entry door (AB temperature). In all instances, the application of water reduced temperatures within a 30 s to 60 s period of time.

Table 6.2: Temperature Reduction Due to Water Application

| | AB Temperature 5 ft Above Floor °F (°C) | |
|:----------:|:-------------------------:|:-------------------------:|
| Experiment | 5 s Prior to Suppression | 30 s Post Suppression |
| 2 | 1633 (889) | 557 (291) |
| 3 | 1514 (823) | 873 (467) |
| 4 | 1613 (878) | 345 (173) |
| 5 | 459 (237) | 137 (58) |
| 6 | 1477 (802) | 986 (530) |
| 7 | 1715 (935) | 689 (365)* |

\* - 60 s Post Suppression

In addition to flow rate, the total amount (volume) of water is also an important measurement for understanding the ability of water to extinguish a fire. Table 6.3 illustrates the total volume

of water used. As a reminder, the experiments were concluded when all visible flame had been extinguished.

Table 6.3: Water Used for Suppression Operations

| Experiment | Primary Hoseline (gal) | Secondary Hoseline (gal) | Total Used (gal) |
|---|---|---|---|
| 1 | 70 | 0 | 70 |
| 2 | 985 | 542 | 1527 |
| 3 | 942 | 455 | 1398 |
| 4 | 937 | 904 | 1842 |
| 5 | 413 | 0 | 413 |
| 6 | 670 | 0 | 670 |
| 7 | 1212 | 208 | 1420 |

Note: Water usage measurement stopped after all visible flames were extinguished.

For these experiments and fuel packages, the fire was controlled with less than 1,850 gal of water. In the experiments where all front windows were ventilated (Experiments 2-4 and 7), the amount of water utilized was similar (approximately 1400-1850 gallons). Although Experiment 4 included a fire area that was more than twice that of the other experiments, the horizontal ventilation area was similar to other units and thus the amount of water utilized was of similar magnitude. In Experiment 1 where the amount of additional ventilation was limited to only the front door (and that occurred after reaching vent limited conditions), the least amount of water was used. Further research is needed on to understand the relationship between the ventilation area and the coordination between suppression and ventilation actions on the amount of water needed to control a fire.

Research focusing on the suppression capabilities of current fire service handlines compared to compartment volume, ventilation area, and fuel load can provide the fire service with the data to aid in further developing tactical considerations for necessary water flow rates (i.e., rate of water getting to a specific area or water flux, gal/min/ft$^2$) to extinguish many different types of fires. Additional research needs include studies that focus on the impact of heat on a hose stream (i.e., is stream length impacted when flowing through large open spaces with elevated temperatures?) and the impact of flowing water on smoke in large volumes with respect to localized gas cooling and gas contraction.

## 6.2   Exposure Protection via Positive Pressure Ventilation

Fire service positive pressure fans have been recommended in some texts for limiting horizontal fire spread between units in a strip mall, by increasing the pressure in adjacent units and preventing smoke and fire infiltration from the fire unit. The fan is positioned at the front of the unit and

ventilation is limited to the inlet where the fan is positioned, with the intent of maintaining the pressure in the exposure above the adjacent fire unit [54].

In this study, limitations in fan capabilities, wind conditions, and the measurement uncertainty of the pressure transducers prevented conclusive findings. Future work utilizing larger fans in a more controlled environment is needed to determine the effectiveness of utilizing a positive pressure fan for exposure protection in strip malls.

# 7 Summary

Seven experiments were conducted in four different units in an acquired, commercial strip mall to quantify the impact of horizontal and vertical ventilation on fire dynamics. A baseline experiment with no additional ventilation (only natural leakage) was conducted to quantify fire behavior. Specifically, the decay in temperature and pressure that resulted from ventilation-limited conditions for a fire in a large open volume was examined. Successive experiments increased horizontal ventilation (via front doors and front windows) and combined horizontal and vertical ventilation (via front doors, front windows, and roof vents).

While the largest fire compartment in these strip mall experiments was approximately three times the size of the open volume in the two-story colonial residential compartment used in prior research [33], the amount fuel and oxygen available for combustion still resulted in a ventilation-limited fire. Without coordinated suppression (Experiment 5), additional ventilation (Experiments 2-4, 6, 7) increased the exhaust of combustion products and caused additional air to enter the unit. The additional air added oxygen to a ventilation-limited fire, and the temperatures increased. For a fire in a strip mall occupancy, consider keeping the fire ventilation-limited until water can be applied. This consideration is consistent with a previous study in single-family homes [24].

During several experiments in this series, an overpressure occurred during fire growth as the fire transitioned to flashover, which resulted in a unidirectional exhaust flow from the fire unit. This exhaust involved gases in excess of 500 °F (260 °C). Following the unidirectional exhaust, the fire remained ventilation-limited. It is important to recognize the role pressure plays in fire development and gas flow on the fireground, especially as it pertains to large volume compartments.

Damage to open web steel bar joists was noted in these experiments. For one experiment, that damage resulted to a collapse late in the experiment. The structural damage noted in these experiments highlights the potential collapse hazards found in open web metal truss roof construction when exposed to fire.

When firefighters are confronted with a fire in a strip mall, consideration should be given to the impact ventilation without suppression will have on the heat release rate, the impact the compartment size has on fire development, and the collapse hazards associated with open web steel bar joist truss roof construction.

# References

[1] S. Kerber. Summary - Impact of Ventilation on Fire Behavior. Underwriters Laboratories, Northbrook, Illinois, December 2010.

[2] S. Kerber. Study of the Effectiveness of Fire Service Vertical Ventilation and Suppression Tactics in Single Family Homes. UL Firefighter Safety Research Institute, Northbrook, Illinois, June 2013.

[3] R. Zevotek and S. Kerber. Study of the Effectiveness of Fire Service Positive Pressure Ventilation During Fire Attack in Single Family Homes Incorporating Modern Construction Practices. UL Firefighter Safety Research Institute, Columbia, MD, May 2016.

[4] R. Zevotek, K. Stakes, and J. Willi. Impact of Fire Attack Utilizing Interior and Exterior Streams on Firefighter Safety and Occupant Survival: Full-Scale Experiments. UL Firefighter Safety Research Institute, Columbia, Maryland, January 2018.

[5] F. Washenitz and T and Mezzonotte. Supermarket Fire Claims the Life of One Career Fire Fighter and Critically Injures Another Career Fire Fighter – Arizona. NIOSH F2001-13, NIOSH Fire Fighter Fatality Investigation and Prevention Program, 2002.

[6] T. Merinar and R. Braddee. Career Fire Fighter Dies and Chief is Injured When Struck by 130-Foot Awning that Collapses during a Commercial Building Fire – Texas. NIOSH F2007-01, NIOSH Fire Fighter Fatality Investigation and Prevention Program, 2007.

[7] T. Merinar, M. Bowyer, and K. Kline. Career Fire Fighter Dies and Another is Seriously Burned Fighting Arson Fire at a Commercial Strip Mall – Texas. NIOSH F2017-14, NIOSH Fire Fighter Fatality Investigation and Prevention Program, 2018.

[8] T. Merinar, M. Bowyer, and M. Loflin. Volunteer Fire Fighter Dies After Running Out of Air and Becoming Disoriented in Retail Store in Strip Mall Fire – North Carolina. NIOSH F2016-07, NIOSH Fire Fighter Fatality Investigation and Prevention Program, 2017.

[9] S. Miles and J. Tarley. Career Probationary Fire Fighter Runs Out of Air and Dies in Commercial Structure Fire – Michigan. NIOSH F2013-14, NIOSH Fire Fighter Fatality Investigation and Prevention Program, 2016.

[10] D. Stroup, D. Madrzykowski, W. Walton, and W. Twilley. Structural Collapse Fire Tests: Single Story, Ordinary Construction Warehouse. Technical Report NISTIR 6959, National Institute of Standards and Technology, Gaithersburg, MD, May 2003.

[11] D. Stroup and N. Bryner. Structural Collapse Research at NIST. In *Proceedings of the Eleventh International Interflam Conference*. Interscience Communications, London, 2007.

[12] S. Kerber and R. Zevotek. Study of Residential Attic Fire Mitigation Tactics and Exterior Fire Spread Hazards on Fire Fighter Safety. UL Firefighter Safety Research Institute, Columbia, Maryland, November 2014.

[13] D. Madrzykowski and C. Weinschenk. Understanding and Fighting Basement Fires. UL Firefighter Safety Research Institute, Columbia, Maryland, March 2018.

[14] S. Kerber and D. Madrzykowski. Evaluating Positive Pressure Ventilation in Large Structures: School Pressure and Fire Experiments. Technical Report NIST Technical Note 1498, National Institute of Standards and Technology, Gaithersburg, MD, July 2008.

[15] S. Kerber and D. Madrzkowski. Go with the Flow NIST Study proves PPV can save lives & improve safety. *FireRescue Magazine*, pages 36–38, November 2009.

[16] J. Norman. *Fire Officer's Handbook of Tactics*. PennWell Corporation, Tulsa, OK, 5 edition, 2019.

[17] B.J. Klaene and R.E. Sanders. *Structural Fire Fighting*. National Fire Protection Association, Quincy, MA, 2000.

[18] J Silvernail. *Suburban Fire Tactics*. PennWell Corporation, Tulsa, OK, 2013.

[19] J Smith. *Strategic & Tactical Considerations on the Fire Ground*. Pearson Education, Inc., Upper Saddle River, NJ, 3rd edition, 2012.

[20] Google Maps. Satellite Image - Skyway Shopping Plaza, Fairborn, OH, October 2019.

[21] L.G. Blevins. Behavior of bare and aspirated thermocouples in compartment fires. In *National Heat Transfer Conference, 33rd Proceedings*, pages 15–17, 1999.

[22] W.M. Pitts, E. Braun, R. Peacock, H. Mitler, E. Johnson, P. Reneke, and L.G. Blevins. Temperature uncertainties for bare-bead and aspirated thermocouple measurements in fire environments. *ASTM Special Technical Publication*, 1427:3–15, 2003.

[23] R.A. Bryant. A comparison of gas velocity measurements in a full-scale enclosure fire. *Fire Safety Journal*, 44:793–800, 2009.

[24] J. Regan, J. Bryant, and C. Weinschenk. Analysis of the Coordination of Suppression and Ventilation in Single-Family Homes. UL Firefighter Safety Research Institute, Columbia, Maryland, March 2020.

[25] RainWise, Inc., Bar Harbor, Maine. *The RainWise AerVane for measuring Wind Speed and Direction*, 2019.

[26] New Training Tool Helps Firefighters Stay ALIVE, October 2013. Accessed 02-20-2020, https://fire.engineering.nyu.edu/home/alive.html.

[27] V. Babrauskas. Estimating Room Dlashover Potential. *Fire Technology*, 16(2):94–103, 1980.

[28] V. Babrauskas and J. Krasny. Fire Behavior of Upholstered Furniture. *Final Report National Bureau of Standards*, 1985.

[29] A. Hamins, M. Bundy, and S.E. Dillon. Characterization of Candle Flames. *Journal of Fire Protection Engineering*, 15(4):265–285, 2005.

[30] D. Madrzykowski, A. Hamins, and S. Mehta. Residential Kitchen Fire Suppression Research Needs: Workshop Proceedings. NIST Special Publication 1066, National Institute of Standards and Technology, Gaithersburg, Maryland, 2007.

[31] D. Madrzykowski and S. Kerber. Fire Fighting Tactics Under Wind Driven Conditions: Laboratory Experiments. NIST Technical Note 1618, National Institute of Standards and Technology, Fire Research Division Engineering Laboratory, 2009.

[32] DW Stroup and D Madrzykowski. Heat Release Rate Tests of Plastic Trash Containers. Report of Test FR4018, National Institute of Standards and Technology, Gaithersburg, Maryland, 2003.

[33] D. Madrzykowski and C. Weinschenk. Impact of Fixed Ventilation on Fire Damage Patterns in Full-Scale Structures. UL Firefighter Safety Research Institute, Columbia, Maryland, April 2019.

[34] C. Weinschenk, D. Madrzykowski, and P. Courtney. Impact of Flashover Fire Conditions on Exposed Energized Electrical Cords/Cables. *Fire Technology*, pages 1–33, 2019.

[35] NFPA 1971. *Standard on Protective Ensembles for Structural Fire Fighting and Proximity Fire Fighting*. National Fire Protection Association, Quincy, Massachusetts, 2018.

[36] K. McGrattan, S. Hostikka, J. Floyd, R. McDermott, and M. Vanella. *Fire Dynamics Simulator, User's Guide*. National Institute of Standards and Technology, Gaithersburg, Maryland, USA, and VTT Technical Research Centre of Finland, Espoo, Finland, sixth edition, September 2019.

[37] Stephen Kerber. Impact of Ventilation on Fire Behavior in Legacy and Contemporary Residential Construction. Underwriters Laboratories, Northbrook, Illinois, December 2012.

[38] NASA Glenn Research Center. Charles and Gay-Lassac's Law. Accessed 03-05-2020 https://www.grc.nasa.gov/WWW/k-12/airplane/glussac.html.

[39] B. Karlsson and J. Quintiere. *Enclosure Fire Dynamics*. CRC Press LLC, Boca Raton, FL, 2000.

[40] J. Tarley, S. Berardinelli, M. McFall, and T. Merinar. Partial Roof Collapse in Commercial Structure Fire Claims the Lives of Two Career Fire Fighters – Tennessee. NIOSH F2003-18, NIOSH Fire Fighter Fatality Investigation and Prevention Program, 2004.

[41] C. Weinschenk. Tactical Considerations Web Series: Ep. 1 - There Is No Substitute For Knowledge, May 2018. Accessed 12-12-2019 https://ulfirefightersafety.org/posts/tactical-considerations-web-series.html.

[42] J. Mittendorf and D. Dodson. *The Art of Reading Buildings*. PennWell Corporation, Tulsa, OK, 2015.

[43] X. Zhou and Y. Xin. Evaluation of Oxygen Reduction System (ORS) in Large-Scale Fire Tests. FM Global, Norwood, MA, January 2018.

[44] B. Goldfeder, May 2019. Accessed 12-15-2019, https://twitter.com/billygoldfeder/status/1126198950782996480?lang=en.

[45] International Fire Service Training Association. *Essentials of Fire Fighting and Fire Department Operations*. Fire Protection Publications, Stillwater, OK, 7th edition, 2019.

[46] G. Corbett and F. Brannigan. *Brannigan's Building Construction for the Fire Service*. National Fire Protection Association, Quincy, MA, 5th edition, 2019.

[47] P.H. Thomas. Use of Water in the Extinction of Large Fires. *The Institution of Fire Engineers Quarterly*, 35:130–132, 1959.

[48] R. Baldwin. Use of water in the extinction of fires by brigades. *The Institution of Fire Engineers Quarterly*, 82:163–168, 1972.

[49] S. Särdqvist. Real Fire Data, Fires In Non-Residential Premises in London 1994-1997. Technical Report 7003, Department of Fire Safety Engineering, Lund University, Sweden, 1998.

[50] W. Labes. Fire Department Operations Analysis - Final Report. Technical Report NRDL-TRC-68-26, Illinois Institute of Technology, Research Institute, 1968.

[51] P. Grimwood, E. Hartin, J. McDonough, and S. Raffel. *3D Fire Fighting - Training, Techniques, and Tactics*. Fire Protection Publications, Oklahoma State University, 2005.

[52] *Student Manual - Preparing for Incident Command*. Federal Emergency Management Agency - National Fire Academy - National Emergency Training Center, August 1984.

[53] K. Royer and F.W. Nelson. Water for Fire Fighting. Iowa State University Bulletin. Iowa State University, Ames, Iowa.

[54] K. Garcia, R. Kauffmann, and R. Schelble. *Positive Pressure Attack for Ventilation & Firefighting*. PennWell Corporation, Tulsa, OK, 2006.

# Appendix A    Example of Using Bernoulli Principle for Pressure-Induced Flow

To show how pressure can drive flow, consider a simplified model of an experimental unit without a fire. Here, the unit has some initial pressure ($p_0$) and initial velocity ($v_0$) with the cross-sectional area of $A_0$. The outlet of the unit has pressure ($p_1$), velocity ($v_1$) and a cross-sectional area of $A_1$. See Figure A.1 for a representation of these parameters.
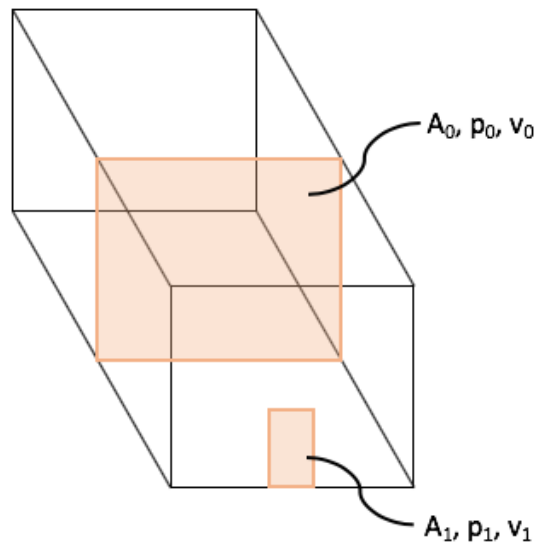


Figure A.1: An example schematic for a Bernoulli Principle application that shows the initial state (subscript 0) and final state (subscript 1) of pressure, velocity, and area.

For the purposes of this simplified example, consider the unit to be at a uniform pressure. The Bernoulli Equation used for this analysis is included here:

$$p_0 + \frac{1}{2}\rho_0 v_0^2 + \rho g z_0 = p_1 + \frac{1}{2}\rho_1 v_1^2 + \rho g z_1 \tag{A.1}$$

where $\rho$ is density and $z_0$, $z_1$ are elevations within the unit.

Assuming position 0 and position 1 have similar elevations ($z_1 \approx z_2$) then any difference in the exhaust elevation is negligible. Additionally, the density is the same at both locations. Then, Equation A.1 can be simplified to:

$$p_0 + \frac{1}{2}\rho v_0^2 = p_1 + \frac{1}{2}\rho v_1^2 \tag{A.2}$$

Equation A.2 can be rearranged to have pressure on one side and velocity on the other:

$$\frac{2(p_0 - p_1)}{\rho} = v_1^2 - v_0^2 \tag{A.3}$$

Equation A.3 shows, for this simplified example, the relationship between velocity ($v_1^2 - v_0^2$) and pressure ($p_0 - p_1$). For constant density, an increase in pressure inside the compartment (state 0) corresponds to a larger velocity difference at the doorway.